For more information, please contact:

World Meteorological Organization

Research Department

Atmospheric Research and Environment Branch

7 bis, avenue de la Paix – P.O. Box 2300 – CH 1211 Geneva 2 – Switzerland

Tel.: +41 (0) 22 730 83 14 – Fax: +41 (0) 22 730 80 27

E-mail: cpa@wmo.int – Website: http://www.wmo.int/pages/prog/arep/index_en.html

WMO/TD - No. 1541

WWRP 2010 - 2

1st WMO International Conference on Indian Ocean Tropical Cyclones and Climate Change, Muscat, Sultanate of Oman, 8-11 March 2009

Chairperson, Publications Board
World Meteorological Organization (WMO)
7 bis, avenue de la Paix
P.O. Box 2300
CH-1211 Geneva 2, Switzerland

Tel.: +41 (0) 22 730 84 03
Fax: +41 (0) 22 730 80 40
E-mail: Publications@wmo.int

WORLD METEOROLOGICAL ORGANIZATION

WORLD WEATHER RESEARCH PROGRAMME

WWRP 2010 - 2

1st WMO INTERNATIONAL CONFERENCE ON TROPICAL CYCLONES AND CLIMATE CHANGE

Muscat, Sultanate of Oman, 8 – 11 March 2009

Edited by:
Salim Al-Hatrushi and Yassine Charabi

Department of Geography
Sultan Qaboos University, Muscat, Sultanate of Oman

WMO/TD-No.1541

TABLE OF CONTENTS

INTER-ANNUAL VARIATION OF FREQUENCY OF CYCLONIC DISTURBANCES LANDFALLING OVER WMO/ESCAP PANEL MEMBER COUNTRIES

Ajit Tyagi, M.Mohapatra, B.K. Bandyopadhyay and Naresh Kumar
India Meteorological Department, Mausam Bhavan, Lodi Road, New Delhi-110003

Abstract

A study is undertaken to find out characteristics of interannual variation like coefficient of variation, trends and periodicities etc. in the annual frequencies of different categories of disturbances such as depressions, cyclonic storms, severe cyclonic storms, total cyclonic storms and total cyclonic disturbances landfalling over different coastal states of India and other member countries of World Meteorological Organisation (WMO) / Economic and Social Cooperation for Asia and the Pacific (ESCAP) Panel based on the data of 115 years (1891-2005). Considering different coastal states of India, about 68% of the disturbances developing over the Bay of Bengal have landfall over east coast and about 30% of the disturbances developing over the Arabian Sea have landfall over west coast. Out of total disturbances having landfall over east and west coasts of India, about 85% and 44% cross Orissa and Gujarat coasts respectively. While the frequency of severe cyclonic storms crossing Andhra Pradesh coast shows significant increasing trend, the frequencies of cyclonic storms crossing Orissa, West Bengal and Gujarat coasts show significant decreasing trends. The sixth order polynomial trends could be well fitted to the frequencies of different categories of disturbances crossing the coasts during this period. The quasi-biennial oscillation (QBO) is significantly observed in the frequency of cyclonic storms crossing Orissa coast. The cyclonic storms crossing Andhra Pradesh and Tamil Nadu coasts show significant cycles of 5-6 years. The severe cyclonic storms crossing Andhra Pradesh coast exhibits QBO and that crossing West Bengal coast shows QBO as well as 4-5 years cycle of oscillation. There is no periodicity in the frequency of disturbances landfalling over other coastal states of India. The results and analysis for other member countries of WMO/ESCAP Panel, as per the above mentioned procedure, has been presented and discussed in detail in this study.

Keywords: Cyclone variability, WMO/ESCAP Panel

INTRODUCTION

Understanding the patterns of the frequency of cyclonic disturbances over the tropical Oceans assumed importance in the scenario of global climate change. In association with an increasing trend in the global temperature, it is of interest to examine the frequency of cyclones. For the Indian region surrounded by north Indian Ocean, cyclonic storms generally form during pre-monsoon & post monsoon seasons and cause devastation due to heavy rainfall causing flood, strong wind damaging structures and storm surge inundating the low line coastal areas. In recent years, a few severe cyclone storms like Gonu, Sidr and Nargis have developed over this Ocean basin cause huge loss of life and property. The trends and variability of cyclonic disturbances developing over the north Indian Ocean have been analysed by various authors (Bhaskar Rao et al., 2001). However, a few attempts have been made to analyse the trends and variability of landfalling disturbances over the north Indian Ocean. In this background, a study has been undertaken on the trends and variability in the frequency of cyclonic disturbances developing over the north Indian Ocean and landfalling over World Meteorological Organisation (WMO)/ Economic and Social Cooperation for Asia and the Pacific (ESCAP) Panel member countries (Figure 1).

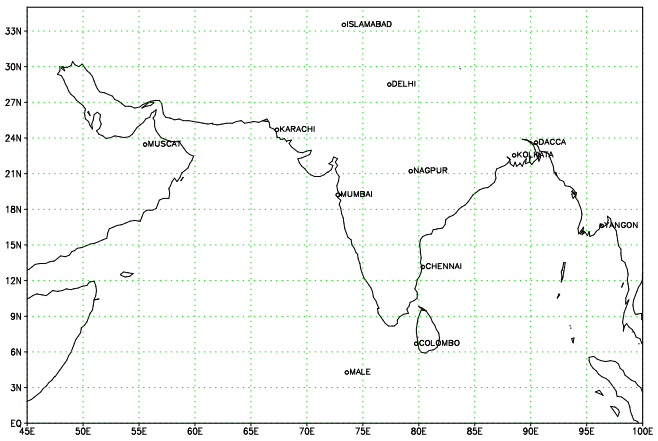

Figure 1 - Area of responsibility of RSMC- Tropical Cyclone, New Delhi.

1. DATA AND METHODOLOGY

The study aims at analyzing the characteristics of interannual variation like coefficient of variation (CV), trends and periodicities etc. in the annual frequencies of different categories of disturbances such as depressions, cyclonic storms, severe cyclonic storms, total cyclonic storms and total cyclonic disturbances landfalling over different coastal states of India and other member countries (Figure 1) of WMO / ESCAP Panel based on the data of 115 years (1891-2005). The detailed classification of the cyclonic disturbances into depression and different stages of cyclones as adopted by India Meteorological Department (IMD) is discussed in cyclone manual published by IMD (2003). The annual frequencies of cyclonic disturbances crossing different coastal belts have been collected from the Storm Atlas of India published by IMD (IMD, 1979, 1996, 2008). For the purpose of analysis, depression and deep depression have been considered as single category. Similarly severe cyclonic storm, very severe cyclonic storm and super cyclonic storm have been considered as single category. Hence, the frequencies of cyclonic disturbances have been analyzed in three categories, viz (1) depression/deep depression (D), (2) cyclonic storm (C) and (3) severe cyclonic storm and above (S). The significance of trend coefficient has been tested at 95% level of confidence. The sixth order polynomials have also been fitted to the frequency series of disturbances to find out the trend and variability.

2. RESULTS AND DISCUSSION

The characteristics of landfalling cyclonic disturbances over India are presented and discussed in sec. 2.1. The characteristics of landfalling disturbances over other member countries of WMO/ESCAP Panel are analysed and presented in sec. 2.2. The broad conclusion of the study is presented in sec. 4.

2.1 Landfalling cyclonic disturbances over India

Considering different coastal states of India, about 68% of the disturbances developing over the Bay of Bengal have landfall over east coast and about 30% of the disturbances developing over the Arabian Sea have landfall over west coast. The trends in the frequencies of cyclonic disturbances over east and west coasts of India are shown in Figure 2 .There is no significant change in the frequency of different categories of cyclonic disturbances crossing west coast of India. There is decreasing trend in the frequency of total cyclonic storms landfalling over the east coast of India. It may be due to the fact that the number of low intensity cyclonic storms and depressions has reduced significantly during the monsoon season (Mohapatra and Mohanty, 2007). However there is no significant change in the frequency of severe cyclonic storms landfalling over the east coast of India.

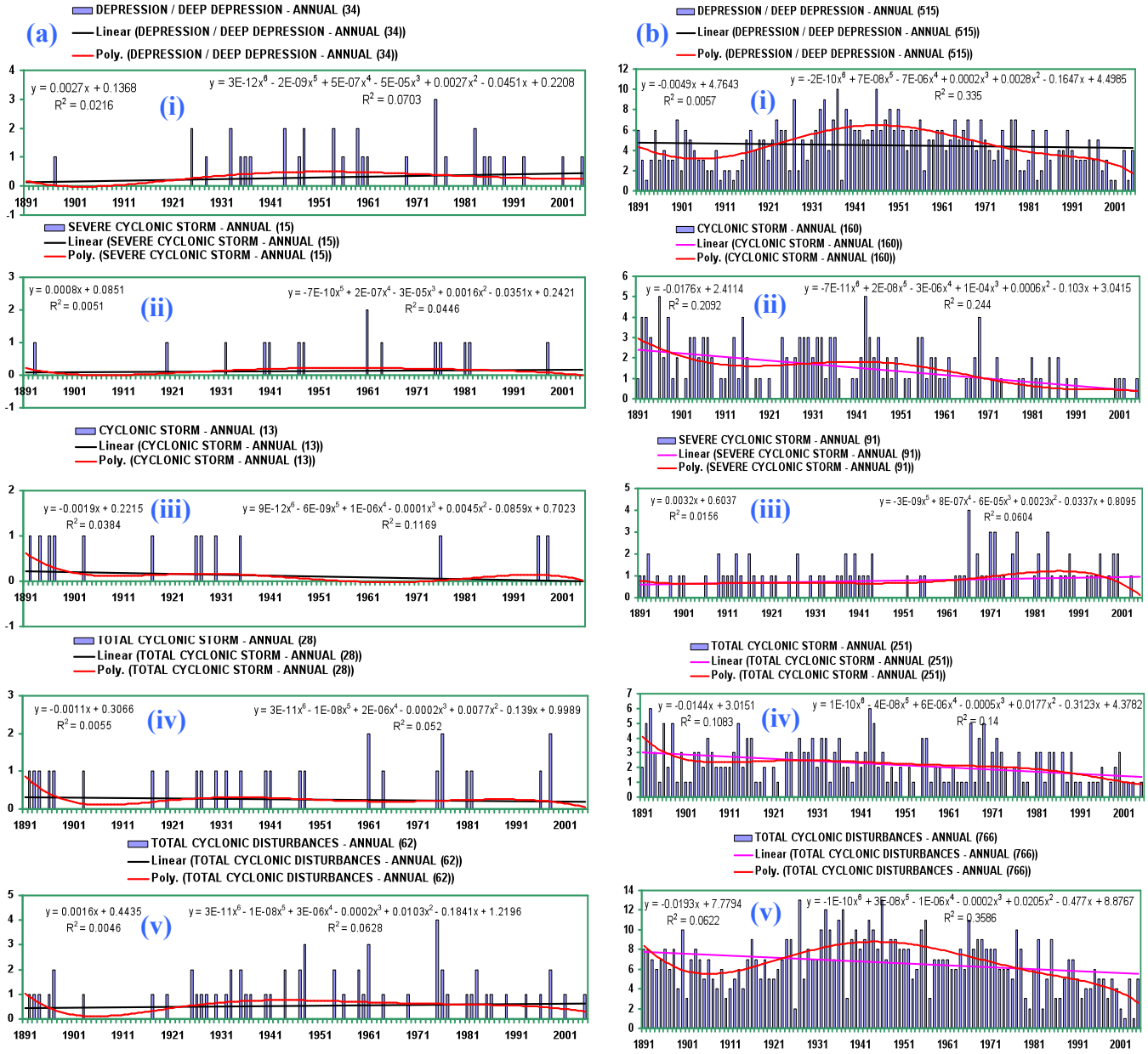

Figure 2 - Annual frequency of cyclonic disturbances landfalling over (a) west coast and (b) east coast of India during 1891-2005.

2.1.1 Landfalling cyclones over different coastal states of India

About 44% of total disturbances crossing east coast of India have landfall over Orissa coast. Similarly about 85% of total disturbances landfalling over west coast cross Gujarat coast. The trends in landfalling cyclonic disturbances over different coastal states of India are shown in Figures (3-5). While the frequency of severe cyclonic storms crossing Andhra Pradesh coast shows significant increasing trend, the frequencies of cyclonic storms crossing Orissa, West Bengal and Gujarat coasts show significant decreasing trends.

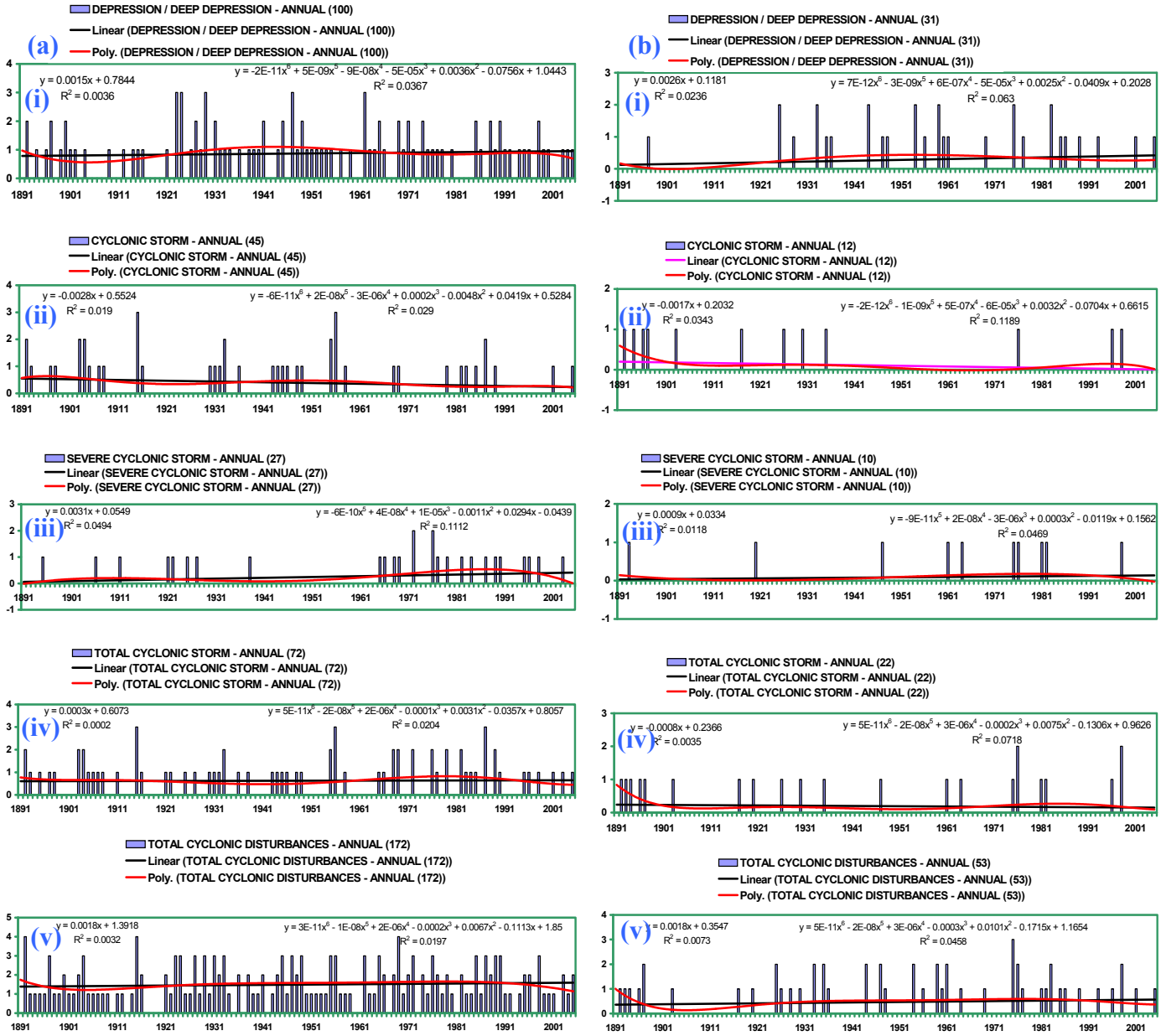

Figure 3 - Trends in frequency of cyclonic disturbances during 1891-2005 crossing (a) West Bengal coast and (b) Orissa coast.

The sixth order polynomial trends could be well fitted to the frequencies of different categories of disturbances crossing the coasts during this period. The quasi-biennial oscillation (QBO) is significantly observed in the frequency of cyclonic storms crossing Orissa coast (not shown). The cyclonic storms crossing Andhra Pradesh and Tamil Nadu coasts show significant cycles of 5-6 years. The severe cyclonic storms crossing Andhra Pradesh coast exhibits QBO and that crossing West Bengal coast shows QBO as well as 4-5 years cycle of oscillation. There is no periodicity in the frequency of disturbances landfalling over other coastal states of India.

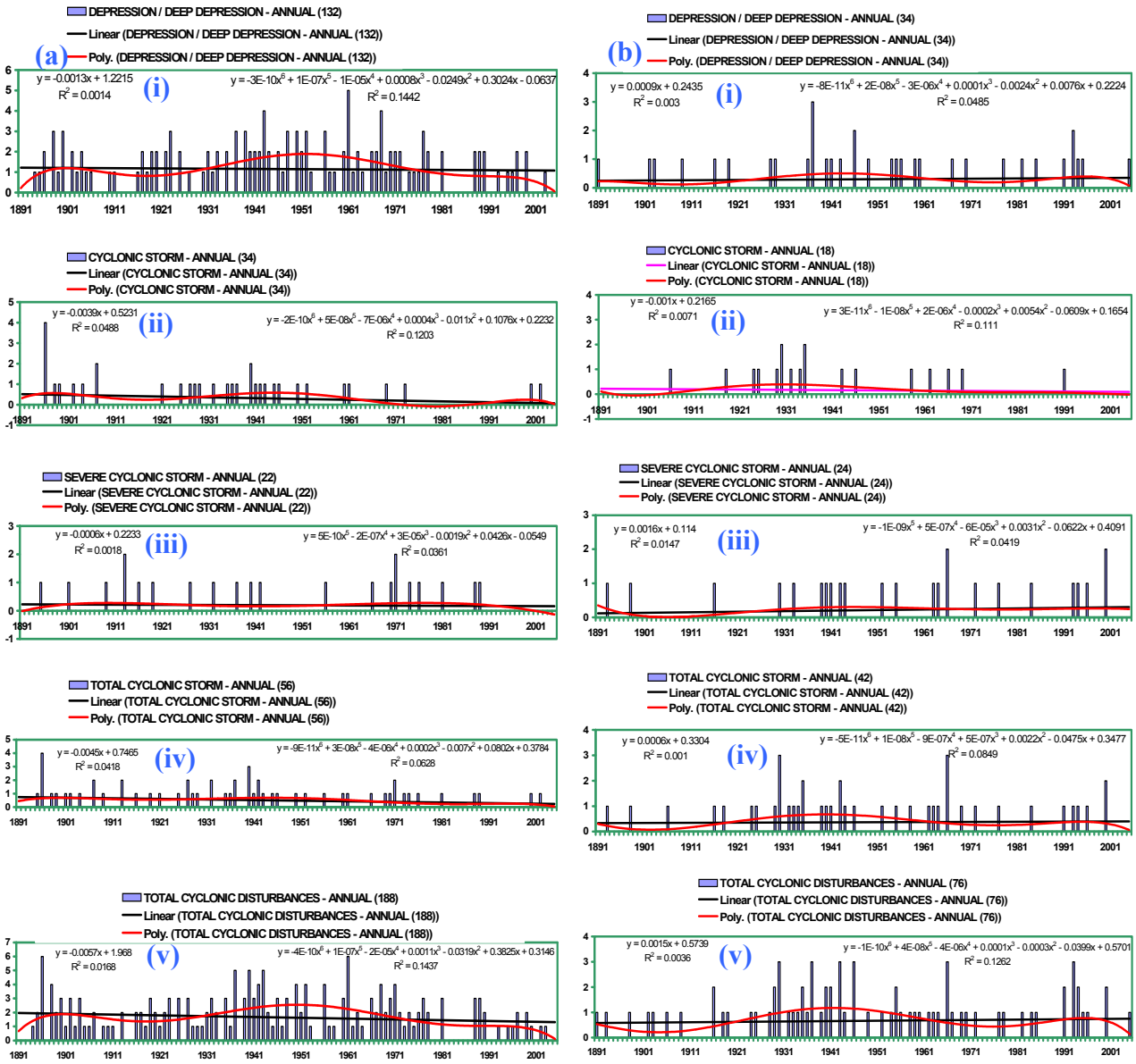

Figure 4 - Trends in frequency of cyclonic disturbances during 1891-2005 crossing (a) Andhra Pradesh coast and (b) Tamilnadu coast.

2.2 Landfalling cyclones over other member countries

The results and analysis for other member countries of WMO/ESCAP Panel, as per the above mentioned procedure, has been presented and discussed in detail in this study. The frequency is very rare for all the countries except Bangladesh and Myanmar. The trend analysis indicates that there is no significant trend in frequencies of cyclonic disturbances landfalling over different countries except Bangladesh and Myanmar. On the other hand, the decadal frequencies of total cyclonic disturbances show epochal nature with three epochs during 1891-1930, 1941-1980 and 1991-2007 for Oman coast. The frequency of disturbances has been significantly less over Arakan coast and Sri Lanka coast during last three decades. However, the frequency of cyclones does not show any such trend. The frequency of cyclones over Bangladesh was higher during 1891-1910 and 1961-2000 with at least one cyclone in two years. Similarly, the frequency of cyclone was higher over Arakan coast during 1911-20 and 1921-1930 with one cyclone in two years and one cyclone per year respectively. The trend analyses for landfalling disturbances over Bangladesh and Myanmar are shown in Figure 8 and Figure 9 respectively. It indicates that the frequency of cyclonic storms and hence total cyclones landfalling over Arakan coast show significant decreasing trend during the period under study. The frequency of total cyclonic

disturbances also shows significance decreasing trend for this coast. Considering landfalling cyclonic disturbances over Bangladesh coast, there is no significant trend in frequencies of any category of cyclonic disturbances.

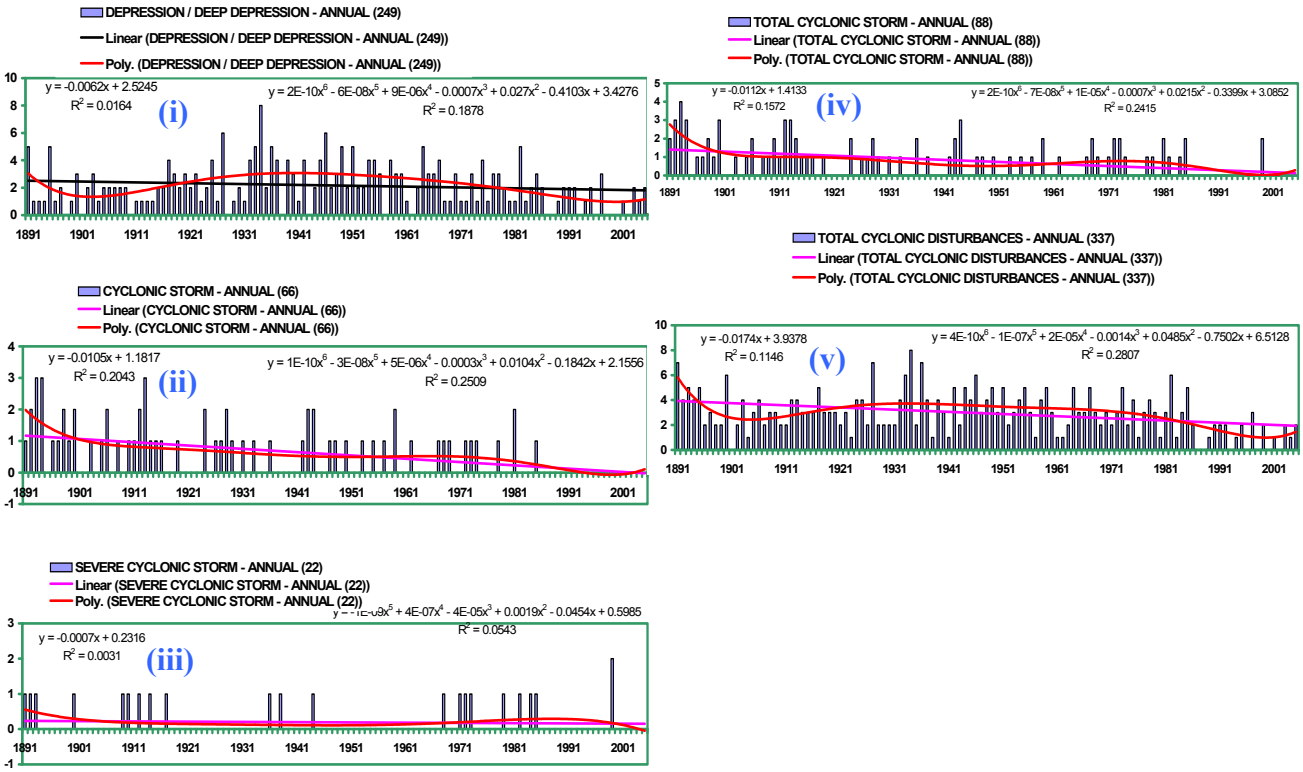

Figure 5 - Trends in frequency of cyclonic disturbances crossing Gujarat coast during 1891-2005.

Conclusions

Orissa and Gujarat are most prone for landfalling of cyclonic disturbances developing over the Bay of Bengal and Arabian Sea respectively. About 44% of Bay of Bengal disturbances crossing east coast of India cross Orissa coast and 85% of Arabian Sea disturbances crossing west coast of India cross Gujarat coast. There is no significant trend in frequencies of different categories of cyclonic disturbances crossing west coast of India, Pakistan, Oman and west coast of Sri Lanka. However, considering individual coastal states in west coast of India, there is significant decreasing trend in the frequencies of cyclonic storms landfalling over Gujarat coast. There is decreasing trend in the frequency of total cyclonic disturbances landfalling over the east coast of India, east coast of Sri Lanka and Arakan coast. There is no significant trend in frequency of different categories of disturbances crossing Bangladesh coast. Considering individual states in east coast of India, there is significant increasing trend in the frequency of severe cyclones landfalling over Andhra Pradesh. There is decreasing trend in the annual frequency of cyclonic storms crossing Orissa and West Bengal mainly due to decrease in frequency of cyclones during monsoon season.

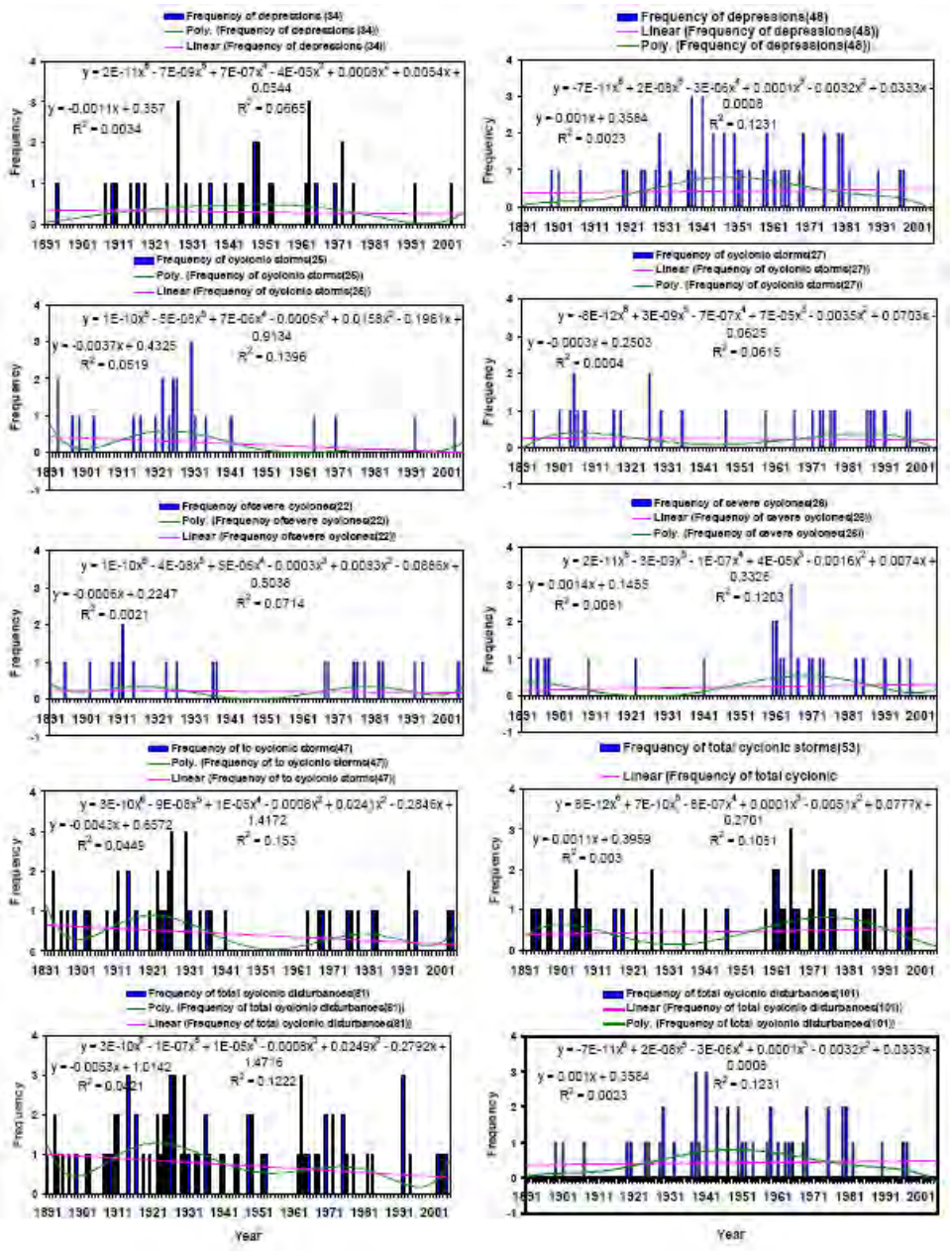

Figure 6 - Frequency of cyclonic disturbances landfalling over (a) Arakan and (b) Bangladesh coasts.

References

Bhasker Rao, D. V., Naidu, C. V., Srinivasa Rao B. R., 2001, Trends and fluctuations of cyclonic systems over north Indian Ocean , *MAUSAM,* 52, 37-46.

IMD, 1979, Tracks of storms and depressions over the Bay of Bengal and the Arabian Sea, *Storm Track Atlas published by IMD, New Delhi.*

IMD, 1996, Tracks of storms and depressions over the Bay of Bengal and the Arabian Sea - An addendum to the Storm Track Atlas (1891-1970)

IMD, 2003, Cyclone Manual, Published by IMD, New Delhi.

IMD, 2008, Track of storm and depressions over the Indian Seas during 1891-2007, *'Cyclone e-Atlas of IMD'*, *published by IMD, Chennai.*

Mohapatra, M. and Mohanty, U. C., 2007, Inter-annual variability of summer monsoon rainfall over Orissa (India) in relation to cyclonic disturbances, *Nat. Hazards*, 42, 301-315.

TOWARD IMPROVED PROJECTION OF THE FUTURE TROPICAL CYCLONE CHANGES

Masato Sugi
Research Institute for Global Change, JAMSTEC
3172-25 Showa-machi, Kanazawa-ku, Yokohama, Kanagawa 236-0001, Japan
and
Meteorological Research Institute, JMA
1-1 Nagamine Tsukuba, Ibaraki 305-0052, Japan

Abstract

We conducted an experiment using a 20 km resolution AGCM to make a detailed projection of future climate change. In the experiment, tropical cyclones have been simulated much more realistically than lower resolution models. By the experiment we could show that the global number of tropical cyclones will decrease due to global warming, but the number of intense tropical cyclones will increase. We have noted, however, there remains a considerable uncertainty in the projection of the future tropical cyclone change, particularly in the future regional changes. To reduce the statistical uncertainties, we need a large number of ensemble experiments with longer period using a lower resolution models. To further improve the simulation of tropical cyclones, we need to improve the model, particularly the cumulus parameterization scheme. We also need to improve our understanding of the mechanism of tropical cyclone genesis and development, and improve the interpretation of the GCM experiment results based on the understanding. We are now conducting a new series of experiments using the 20km mesh AGCM with the improved cumulus parameterization scheme, together with a large number of ensemble simulation with 60km mesh AGCM, aiming at submitting improved projections of the changes in tropical cyclone activity, regional climate and extreme events to IPCC AR5.

Keywords

Tropical cyclone, climate change, global warming

INTRODUCTION

Climate change projection experiment is usually conducted by using a climate model (atmosphere-ocean coupled model). As a climate projection calculation needs long time integration (several tens of years to hundreds of years), relatively low resolution models are used as compared with numerical weather predictions. On the other hand, a high resolution model is necessary to simulate a mature stage tropical cyclone with a large pressure gradient and strong winds near the cyclone centre. Therefore, climate change experiments of tropical cyclones (projections of the changes in frequency and intensity of tropical cyclones) using a climate model has been difficult. To overcome the difficulty, the climate change projection of tropical cyclones has been usually done by a two-tier method. In the first tier of the two-tier method, a relatively low resolution climate model (atmosphere-ocean coupled model) is used to project the future sea surface temperature (SST) changes. In the second tier, a climate change calculation is made with a relatively high resolution AGCM (atmosphere model) using the projected SST in the first tier. The second-tier time integration is performed usually for a limited time period (time slice method). For example, for a projection of the climate of 100 years ahead, the 20 year simulation with the projected SST of the last 20 years in the 100years is compared with the 20 year simulation with the present day SST.

The Meteorological Research Institute (MRI), Japan Meteorological Agency (JMA) and Advanced Earth Science and Technology Organization (AESTO) research team has been conducting a series of climate change projection experiments with a very high resolution AGCM using the Earth Simulator. They used a 20 km mesh AGCM for climate change projection experiments in the KYO-SEI project (FY2002-2006). The 20 km mesh AGCM is essentially the same as the current operational NWP model at JMA, although some physical processes are updated for the NWP model. The experiment is a time-slice type AGCM experiment with the SST projected by low resolution MRI CGCM. By the experiment we could show that the global number of tropical cyclones will decrease but the number of intense tropical cyclones will increase.

We have noted, however, there remains a considerable uncertainty in the projection of the future tropical cyclone change, particularly in the future regional changes. To reduce the statistical uncertainties, we need a large number of ensemble experiments with longer period using a lower resolution models. We have also noted some major deficiencies in the model. We have much less number of typhoons in the western Pacific in the model than reality. The average intensity of simulated tropical cyclones is considerably weaker than that of the observed tropical cyclones even with the 20km resolution model. To further improve the simulation of tropical cyclones, we need to improve the model, particularly the cumulus parameterization scheme. We also need to improve our understanding of the mechanism of tropical cyclone genesis, and improve the interpretation of the GCM experiment results based on the understanding.

In a new five-year project KAKUSHIN programme (FY2007-2011), the MRI/JMA/AESTO research team has been working to improve the model aiming at improving the climate change projection, particularly reducing the uncertainty in the projections of regional climate change and extreme events including tropical cyclones. The preliminary results of the experiment using the new model are encouraging.

In section 2 of this paper, main results of the 20 km mesh AGCM experiment, with a discussion of the mechanism of future tropical cyclone frequency and intensity changes, are presented. In section 3, the main conclusion of the Inter governmental Panel on Climate Change fourth assessment Report (IPCC AR4) on the projection of tropical cyclone activity is reviewed and the remaining issues are discussed. Some preliminary results of the new project KAKUSHIN programme is presented in section 4, followed by a summary in section 5.

1. PROJECTION OF FUTURE TROPICAL CYCLONE ACTIVITY

In KYO-SEI project (FY2002-2006), MRI/JMA/AESTO research team conducted a series of climate change projection experiments with a 20 km mesh AGCM using the Earth Simulator. A main result of the 20 km mesh model experiment has been reported by Oouchi et al. (2006). In the experiment, the climatological SST (without interannual variation but with seasonal variation) is used for present day climate simulation. For the future climate simulation, SST change at the end of the 21st century computed by a MRI coupled GCM using the IPCC A1B scenario is added to the SST used for the present day simulation. Atmospheric concentration of greenhouse gas and aerosols are taken from the values of the integration period in the A1B scenario.

One of the greatest advantages of the 20 km mesh AGCM is that the model is able to simulate tropical cyclones much more realistically than lower resolution models (Figure 1 and Figure 2). By comparing the present day climate simulation (Figure 2b) and the future climate simulation (Figure 2c), we can see a significant reduction in the number of typhoons in the future over the western North Pacific, while we see some increase in the number of hurricanes in the future over the North Atlantic. It has been shown from the experiment that the global number of tropical cyclones will decrease by about 30% in the future.

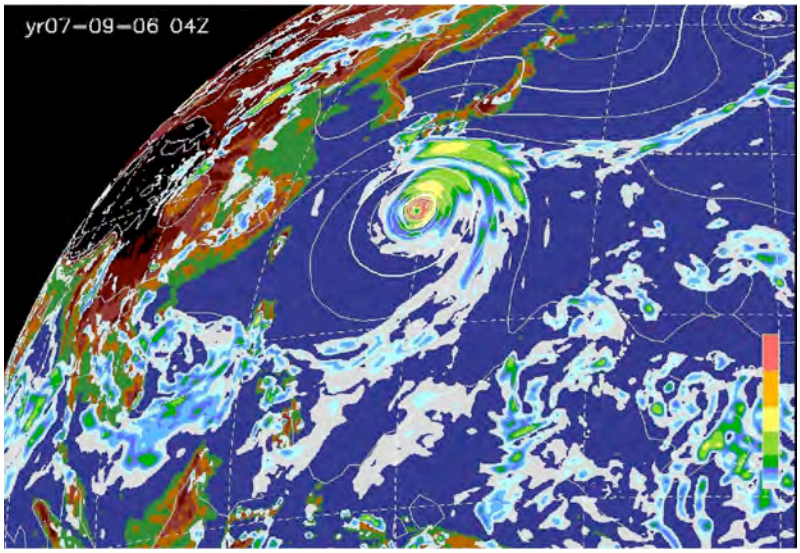

Figure 1 - A typhoon simulated by 20km-mesh MRI/JMA AGCM. Eye, eyewall clouds and spiral rainbands are simulated. (from MRI/JMA/AESTO Research Team in Kyo-sei Project (FY2002-2007)).

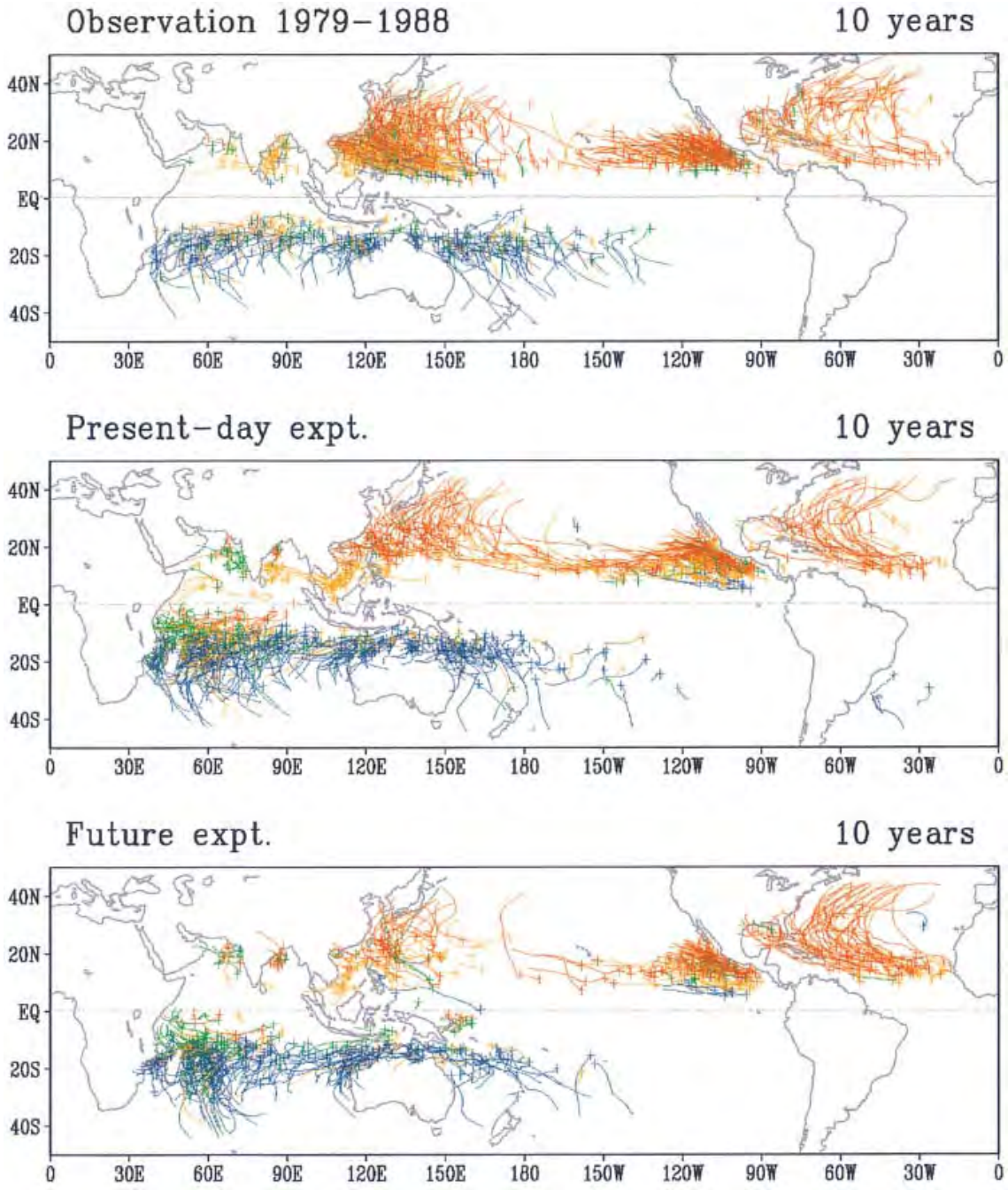

Figure 2 - Tropical cyclone tracks of the observational data (top), the present-day (middle), and the future climate experiments (bottom). The initial positions of tropical cyclones are marked with ‘‘plus’’ signs. The tracks detected at different seasons of each year is in different colors (blue for January, February, and March; green for April, May, and June; red for July, August, and September; orange for October, November, and December). (from Oouchi et al. 2006).

Figure 3 shows the annual frequency of tropical cyclones as a function of maximum wind speed of each tropical cyclone. This Figure shows that the global tropical cyclone frequency will decrease in the future due to global warming, while the frequency of intense tropical cyclones may increase. In other word, the global number of tropical cyclones would decrease, but the future tropical cyclones would intensify.

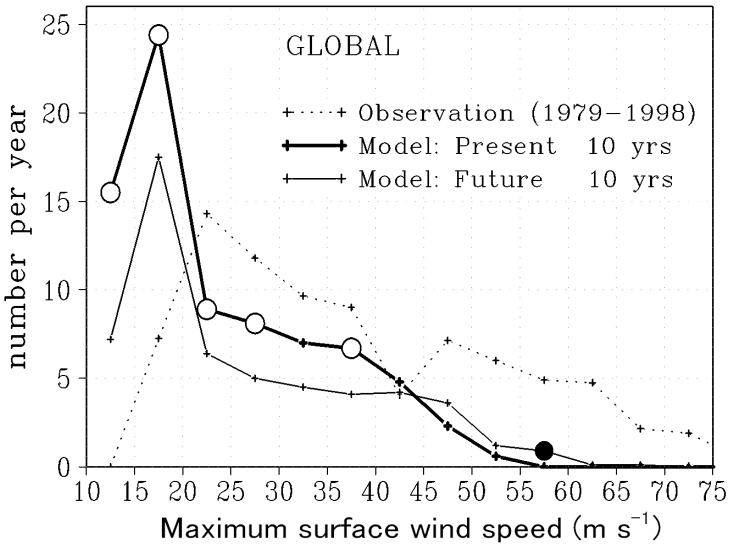

Figure 3 - Global frequency distribution of tropical cyclones as a function of life-time maximum wind speed of each tropical cyclone. (Oouchi et al, 2006).

The intensification of tropical cyclones in the future warmer and wetter climate is rather expected result. On the other hand, the decrease in the number of tropical cyclones is a little surprising and is not readily acceptable result without a good explanation. Sugi et al. (2002) argue that the reduction of the number of tropical cyclones is closely related to a weakening of the tropical circulation (upward mass flux) due to the increased stability in the future warmer climate (Figure 4). The important point is that, when the atmospheric moisture significantly increases due to warming, the stability significantly increases, while the precipitation (heating) increases not as much. This is because the precipitation (heating) is not controlled by availability of moisture, but by atmospheric radiative cooling (Allen and Ingram, 2002). Sugi and Yoshimura (2004) found that the radiative cooling does not increase so much as moisture, partly due to the overlap effect of water vapour and CO_2 long wave radiation absorption bands.

Figure 5 shows the precipitation and water vapour increase as a function of surface temperature increase when atmospheric CO_2 concentration is doubled. The Figure shows that the rate of precipitation increase is about 3% per 1°C of surface temperature increase, which is about a half of the rate of water vapour increase. Furthermore, the line of precipitation change does not pass through the origin of the graph. The line crosses the ordinate at the value of about -5%, indicating that precipitation decreases by about 5% due to the overlap effect if the surface temperature does not increase when CO_2 is doubled.

This would not happen in the real world, but we can conduct an experiment to see what will happen if the surface temperature does not increase when CO_2 is doubled. Yoshimura and Sugi (2005) conducted an experiment to examine the effect of CO_2 increase and SST increase separately on tropical cyclone frequency. It has been shown that, due to the overlap effect, number of tropical cyclones decreases if the CO_2 is increased without increasing SST, while number of tropical cyclone does not change much if the SST is increased without increasing CO_2 (Figure 6). This indicates that the overlap effect of water vapour and CO_2 long wave radiation absorption bands is playing a fundamental role in the reduction of tropical cyclone frequency due to global warming.

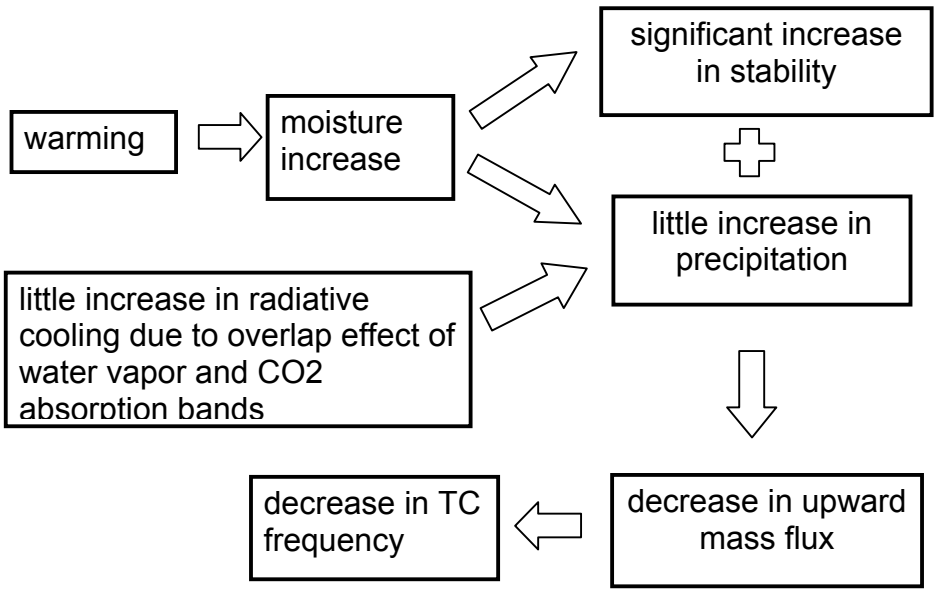

Figure 4 - Schematic diagram showing the mechanism of the reduction of global tropical cyclone frequency in the future warm climate.

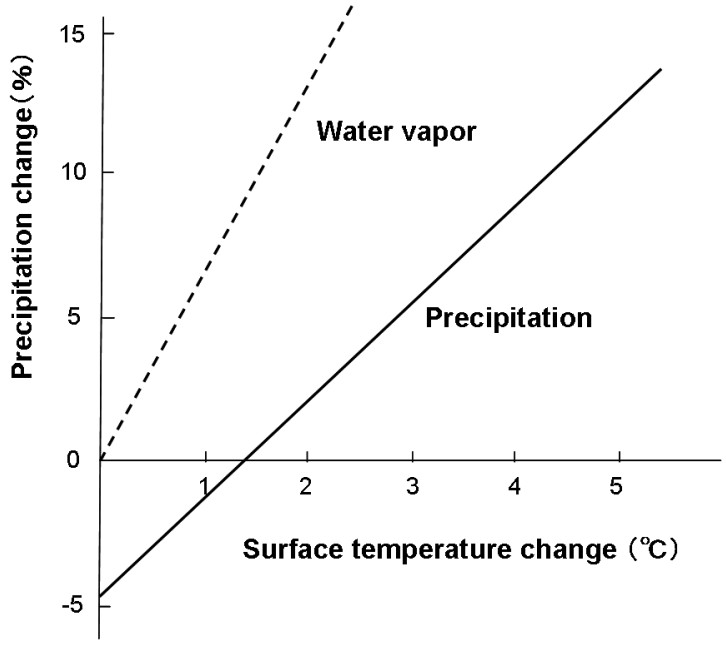

Figure 5 - Precipitation and water vapor change as a function of surface temperature increase when atmospheric CO2 concentration is doubled. (adapted from Allen and Ingram, 2002).

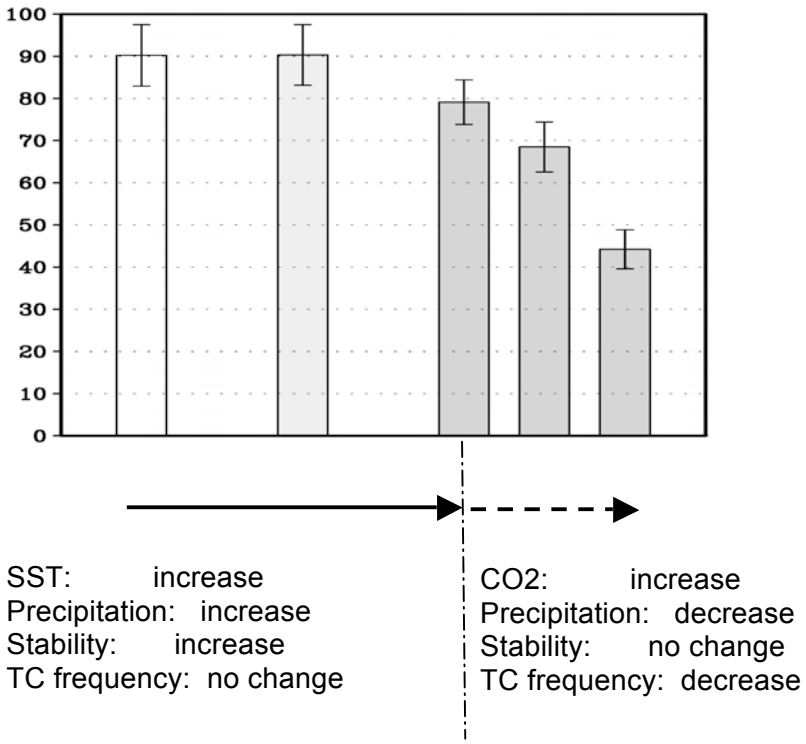

Figure 6 - Changes in tropical cyclone frequency when the SST is increased without changing CO2 (left three bars), and when the CO2 is increased without changing SST (right three bars). (Yoshimura and Sugi, 2005).

2. IPCC CONCLUSIONS AND REMAINING ISSUES

IPCC (2007) concluded regarding the future changes in tropical cyclone activities as "Based on a range of models, it is *likely* that future tropical cyclones (typhoons and hurricanes) will become more intense, with larger peak wind speeds and more heavy precipitation associated with ongoing increases of tropical sea surface temperatures. There is *less confidence* in projections of a global decrease in numbers of tropical cyclones." This conclusion is based on the discussion in Chapter 10 of the IPCC (2007). In the chapter, the discussion on the tropical cyclone intensity change is based on the experiments of a 20 km mesh global model (Oouchi et al., 2006) and two high resolution (9km mesh and 30 km mesh) regional models (Knutson and Tuleya, 2004, Walsh et al., 2004). These high resolution model results consistently indicate an intensification of future tropical cyclones. On the other hand, the discussion on the global tropical cyclone frequency change is based on the results of six global model experiments (Sugi et al., 2002; Yoshimura et al., 2006; McDonald et al., 2005; Bengtsson et al., 2006; Tsutsui, 2002; Oouchi et al., 2006). Among these six experiments, results of the medium resolution (grid size of about 100km) models (Sugi et al., 2002; Yoshimura et al., 2006; McDonald et al., 2005) and a result of high resolution (20km mesh) model (Oouchi et al., 2006) consistently indicate a significant decrease in global numbers of tropical cyclones, while results of lower resolution (grid size of 180km or larger) models (Bengtsson et al. 2006, Tsutsui 2002) show insignificant increase or decrease. In the discussion of IPCC (2007), the medium resolution models are regarded to fall into first category models, which are not able to simulate tropical cyclones reasonably and are not reliable.

Generally speaking, higher resolution models are able to simulate tropical cyclones more realistically, particularly the intense mature stage tropical cyclones, and the results of higher resolution models are considered to be more reliable. Regarding projections of the change in maximum intensity of tropical cyclones, the results from the medium resolution (grid size of about 100km) models are different from those of high resolution (grid size of about 50km or less) global and regional models, indicating that the medium resolution is not sufficient to reasonably simulate intense tropical cyclones. On the other hand, regarding the projection of the change in global

frequency in tropical cyclones, the results of the medium resolution models are consistent with those of higher resolution models, indicating that the medium resolution is sufficient to represent this aspect of tropical cyclones.

We should note that the IPCC conclusions about the projections of future changes in tropical cyclone activities are only qualitative statements and there are large quantitative uncertainties in these conclusions. Furthermore, there are even qualitative uncertainty in the projections of regional changes of tropical cyclone frequency and intensity. Although the medium and high resolution models consistently show a reduction of global tropical cyclone frequency, the projection of regional tropical cyclone frequency changes varies a lot among the models. For example, Sugi et al. (2002) and Oouchi et al. (2006) show an increase in tropical cyclone frequency over the North Atlantic, while Bengtsson et al. (1996) and McDonald et al. (2005) show a reduction of tropical cyclone frequency there.

Remaining major issue is, therefore, how we can improve the models and reduce the uncertainties. Although the 20-km mesh AGCM is able to simulate tropical cyclones much more realistically than lower resolution models, the intensity is still considerably weaker than reality (Figure 3). Is this because the resolution is still not sufficient? Can we simulate more intense tropical cyclones by improving cumulus parameterization scheme? We have noted that there is a considerable disagreement among the models regarding the regional changes in the future tropical cyclone frequency. Is this because simulation of tropical cyclone genesis process is very sensitive to the cumulus parameterization schemes in the models? Are the models not able to simulate tropical cyclone genesis process properly?

3. TOWARD IMPROVED PROJECTION OF TROPICAL CYCLONE CHANGES

In order to reduce the uncertainty in the projection of future tropical cyclone intensity and frequency changes, we need to improve models. Basic questions regarding the model

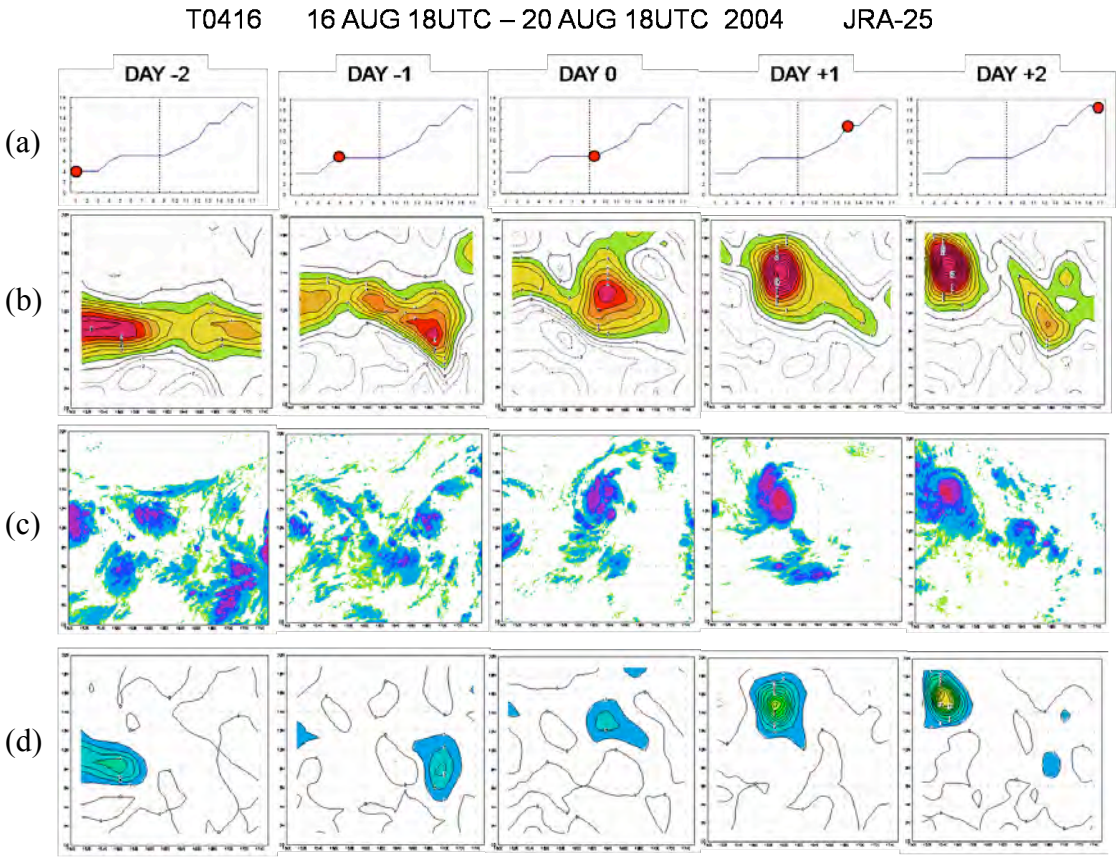

Figure 7 - Geneis process of typhoon T0416 (CHABA) during 18UTC 16 August - 18UTC 18 August 2004. (a) Voticity at 925 hPa vortex centre. (b) Vorticity at 925hPa. (c) GMS IR image (TBB). (d) Convergence of absolute vorticity at 925 hPa (- (□ + *f*) D).

improvement are 1) what resolution is required for a physically reasonable simulation of tropical cyclones, and 2) whether we can simulate genesis and development processes of tropical cyclones reasonably well by using a model with cumulus parameterization or we need a cloud resolving model. To answer these questions, we first need to understand the basic mechanism of tropical cyclone genesis and development processes.

In the KAKUSHIN programme so far, we examined the role of convection in the tropical cyclone genesis process. There is no doubt that the genesis and development of tropical cyclones are cooperative process between the cumulus convection and tropical cyclone scale vortex. Examination of high-resolution reanalysis data JRA-25 and geostationary satellite GMS IR data indicate that a large-scale low level convergence of absolute vorticity is the most essential process in tropical cyclone genesis (Figure 7). It should be noted that the large-scale low-level convergence is caused by an ensemble of convective clouds scattering around the pre-storm vortex. This suggests that tropical cyclone genesis can be simulated by a GCM if the effects of an ensemble of convective clouds are properly parameterized, even though the individual clouds are not simulated.

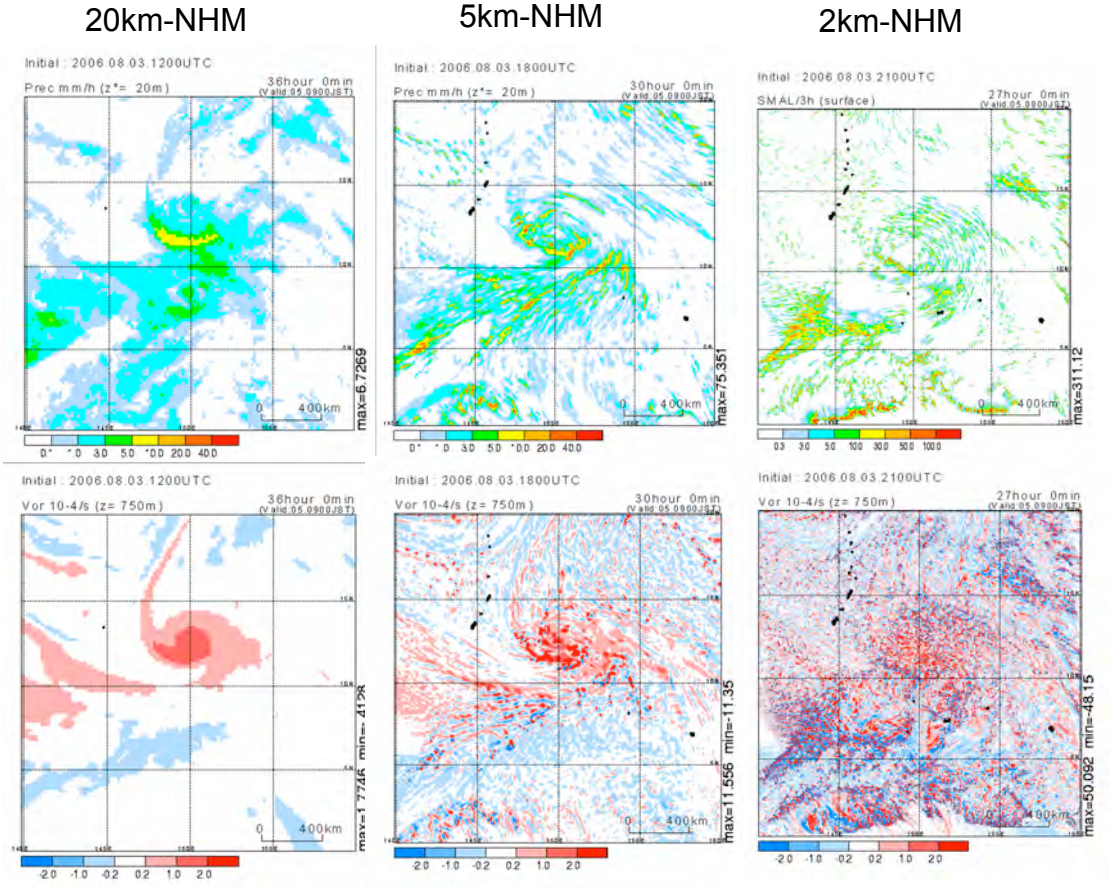

Figure 8 - Simulation of genesis process of typhoon T0608 (SAOMAI) at 00UTC 5 August 2006 with 20km-NHM, 5km-NHM and 2km-NHM (from left to right). Top panels show three-hour precipitation. Bottom panels show vorticity at 750m altitude.

We further examined the role of convection-scale vortices in tropical cyclone genesis process. Figure 8 shows the simulations of tropical cyclone genesis with 20km-, 5km- and 2km-mesh nonhydrostatic model JMA/MRI NHM. In 20km-NHM and 5km-NHM, Kain-Fritch scheme is used for cumulus convection parameterization, while in the 2km-NHM cumulus convection is computed explicitly. We can see many convection-scale vortices in the 5km-NHM and 2-km NHM. There are many anti-cyclonic vortices as well as cyclonic vortices associated with convective clouds. And if we take area average over an active convection area of 100km scale, the averaged positive vorticity is not so large and the smoothed vorticity field is very similar to that of 20km-NHM.

This suggests that these convection-scale vortices do not play essential role in the development of positive vorticity associated with the tropical cyclone scale rotation. This again supports the idea that tropical cyclone genesis can be simulated by a GCM, even though the individual clouds are not simulated.

After the IPCC (2007), some studies using higher resolution models appeared (Bengtsson et al., 2007; Gualdi et al., 2008; Sugi et al. 2009). The high resolution (60km and 40km mesh) AGCM experiments by Begtsson et al. (2007) showed that the global (Northern Hemispheric) tropical cyclone frequency will decrease due to global warming, while number of intense tropical cyclones will increase, as in the Oouchi et al. (2002). Gualdi et al. (2008) showed a significant reduction of global tropical cyclone frequency due to CO_2 increase by using a 120km mesh CGCM (atmosphere-ocean coupled model). From a series of high resolution (60km and 20km mesh) AGCM experiments, Sugi et al. (2009) found that the reduction of global tropical cyclone frequency is a robust feature, while the change in regional tropical cyclone frequency varies a lot among the experiments with different SST change distribution (Table 1). It has been shown that the regional while tropical cyclone frequency change is sensitive to relative SST change distribution, and therefore, for a reliable projection of the regional change, a reliable projection of relative SST distribution is vitally important. Recently, Vecchi and Soden (2007) showed that regional change in the tropical cyclone maximum potential intensity is also sensitive to a relative SST distribution change.

Table 1 -The changes in tropical cyclone frequency as projected by 20km-mesh and 60km-mesh global atmospheric model experiments. The changes are shown in terms of the ratio of future frequency to present frequency. Statistically significant increase (decrease) at 95%confidence level by two-sided t-test is indicated by red (blue) color. Experiment "O" indicates the experiment by Oouchi et al. (2006)

Experi-ments	Resolution	ΔSST	Integra-tion	Ratio(%) of TC frequency Future/Present								
				Global	NH	SH	N Indian	NW Pacific	NE Pacific	N Atlanti	S Indian	S Pacific
O	TL959, 20km	MRI CGCM2.3	10yr	70	72	68	48	62	66	134	72	57
A0	TL959, 20km	MRI CGCM2.3	20yr	71	69	73	61	64	61	122	72	78
A1	TL959, 20km	MRI CGCM2.3	20yr	75	75	75	71	71	70	123	75	73
A2	TL959, 20km	MIROC-H	10yr	73	85	58	132	128	50	82	76	10
A3	TL959, 20km	CMIP3	25yr	80	79	81	85	74	75	105	95	58
B1	TL319, 60km	MRI CGCM2.3	25yr	80	79	83	88	66	69	158	78	92
B2	TL319, 60km	MIROC-H	25yr	94	100	84	179	164	58	106	110	31
B3	TL319, 60km	CMIP3	25yr	79	81	75	133	86	67	104	82	64
B4	TL319, 60km	CSIRO	25yr	78	71	89	93	113	51	63	78	110

As mentioned before, the intensity of the tropical cyclones simulated in the 20km mesh model is still considerably weaker than the observation (Figure 3). We have examined the impact of cumulus parameterization scheme on the intensity of simulated tropical cyclones. Figure 9 shows the simulations of a typhoon development using 20km mesh models with three different cumulus parameterization schemes: prognostic Arakawa Schubert (AS) scheme, Kain-Fritch (KF) scheme and Tiedke type (YS) scheme. It has been shown that the intensity of simulated tropical cyclones can significantly vary depending on the cumulus parameterization schemes. This indicates that there is a possibility to significantly improve the intensity of simulated tropical cyclone by improving the cumulus parameterization scheme in the GCM. Indeed, a preliminary result of an experiment using the model with Tiedtke type cumulus parameterization scheme is encouraging, i.e. the intensity distribution curve is much closer to the observation.

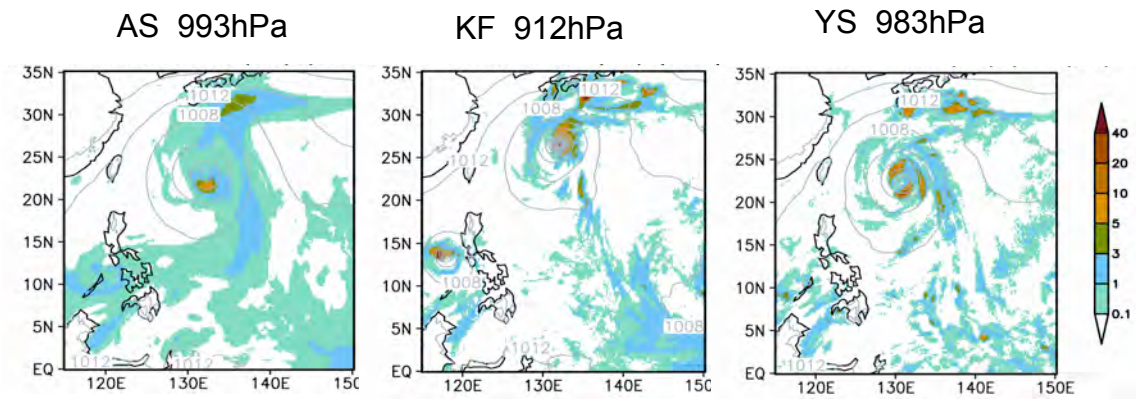

Figure 9 - Sea level pressure and precipitation of typhoon T0422 (MA-ON) at 00UTC 8 October 2004 simulated by 20km-AGCM with Arakawa-Schubert (AS) convection scheme, Kain-Fritch (KF) convection scheme and Tiedtke type (YS) convection scheme. Simulated central pressure is shown on the top of each panel. Observed central pressure was 920hPa.

4. SUMMARY

It seems that the recent studies have reached a qualitative consensus regarding the future projections of tropical cyclone frequency and intensity changes due to global warming: tropical cyclones are likely to intensify, but the global frequency may decrease. However, there remain large quantitative uncertainties in these projections. Furthermore, probably more importantly, there are even qualitative uncertainties in the projections of regional changes. To reduce these uncertainties is vitally important for the projection information to be used effectively by various impact assessment studies. Probably, the most important thing to do to reduce the uncertainty in the projections of tropical cyclone frequency and intensity changes in the future is to develop a better cumulus parameterization scheme for the GCM. Our recent study suggests that tropical cyclone genesis and development can be simulated by a GCM, if the effects of an ensemble of convective clouds are properly parameterized, even though the GCM are not able to simulate individual clouds.

In the new five-year project KAKUSHIN programme (FY2007-2011), we are aiming at improving the climate change projection, particularly reducing the uncertainty in the projections of regional climate change and extreme events. We have noted that an improvement of the cumulus convection in the model is vitally important for an improved GCM projection of future tropical cyclone activity. Improving cumulus convection parameterization is also a key to the improvement of GCM projection of regional scale climate changes. So far, we have developed a new convection scheme, and the result of the preliminary experiment is encouraging. By conduction a series of climate projection experiments using the 20km mesh AGCM with the improved cumulus parameterization scheme, together with a large number of ensemble experiments with 60 km mesh AGCM, we are aiming at submitting improved projections of the changes in tropical cyclone activity, regional climate and extreme events to IPCC AR5.

Acknowledgment

The Earth Simulator has been used for the climate change projection experiments with high resolution AGCM in the KYO-SEI Project and KAKUSHIN Programme. Both of these projects are supported by MEXT (Ministry of Education, Culture, Sports, Science and Technology, Japan).

References

Allen, M. R., and W. J. Ingram, 2002, Constraints on future changes in the hydrological cycle. Nature, 419, 224–228.

Bengtsson, L., M. Botzet and M. Esch, 1996, Will greenhouse gas-induced warming over the next 50 years lead to higher frequency and greater intensity of hurricanes? *Tellus*, 48A, 57-73.

Bengtsson, L., K. Hodges, and E. Roeckner, 2006, Storm tracks and climate change. *J. Climate,* 19, 3518-3543.

Bengtsson, L., K. I. Hodges, M. Esch, N. Keenlyside, L. Kornblueh, J.-J. Luo and T. Yamagata, 2007, How may tropical cyclones change in a warmer climate? *Tellus A*, *59*, 539-561, doi: 10.1111/j.1600-0870.2007.00251.x.

Gualdi, S., E. Scoccimarro, and A. Navarra, 2008, Changes in tropical cyclone activity due to global warming: results from a high-resolution coupled general circulation model. *J. Climate*, 21, 5204-5228..

IPCC, 2007, The Physical Science Basis of Climate Change: A report of Working Group I. Fourth Assessment Report of Intergovernmental Panel on Climate Change. Cambridge University Press.

Knutson, T. R., and R. E. Tuleya, 2004, Impact of CO2-induced warming on simulated hurricane intensity and precipitation: sensitivity to the choice of climate model and convective parameterization. *J. Climate,* 17, 3477-3495.

McDonald, R. E., D. G. Bleaken, D. R. Cresswell, V. D. Pope, and C. A. Senior, 2005, Tropical storms: representation and diagnosis in climate models and the impacts of climate change. *Clim. Dyn.,* 25: 19-36, DOI: 10.1007/s00382-004-0491-0.

Oouchi, K., J. Yoshimura, H. Yoshimura, R. Mizuta, S. Kusunoki, and A. Noda, 2006, Tropical cyclone climatology in a global-warming climate as simulated in a 20km-mesh global atmospheric model: frequency and wind intensity analysis. *J. Meteorol. Soc. Japan*, 84, 259-276.

Sugi, M., A. Noda, and N. Sato, 2002, Influence of global warming on tropical cyclone climatology: an experiment with the JMA global model. *J. Meteorol. Soc. Japan* 80: 249-272, DOI:10.2151/jmsj.80.249.

Sugi, M., and J. Yoshimura, 2004, A mechanism of tropical precipitation change due to CO_2 increase. *J. Climate,* 17, 238-243.

Sugi, M., H. Murakami and J. Yoshimura, 2009, A Reduction in Global Tropical Cyclone Frequency due to Global Warming, *SOLA*, 5, 164-167, doi:10.2151/sola.2009-42.

Tsutsui, J., 2002, Implications of anthropogenic climate change for tropical cyclone activity: A case study with the NCAR CCM2. *J. Meteorol. Soc. Japan*, 80, 45-65, doi:10.2151/jmsj.80.45.

Vecchi, G. A., and B. J. Soden, 2007, Effect of remote sea surface temperature change on tropical cyclone potential intensity. *Nature*, 450, 1066-1070.

Walsh, K. J. E., K.-C. Nguyen, and J. L. McGregor, 2004, Fine-resolution regional climate model simulations of the impact of climate change on tropical cyclones near Australia. *Clim. Dyn.,* 22, 47-56, DOI: 10.1007/s00382-003-0362-0.

Yoshimura, J. and M. Sugi, 2005, Tropical cyclone climatology in a high-resolution AGCM - impacts of SST warming and CO2 increase. *SOLA*, 1, 133-136, doi: 10.2151/sola.2005-035.

Yoshimura, J., M. Sugi and A. Noda, 2006, Influence of greenhouse warming on tropical cyclone frequency. *J. Meteor. Soc. Japan*, 84, 405-42.

AN ASSESSMENT OF CLIMATE CHANGE IMPACT ON CYCLONE FREQUENCY AND DESIGN WAVE HEIGHT IN THE OMAN SEA

Mohammad Dibajnia[1], Mohsen Soltanpour[2], and Doug Scott[3]

[1]PhD, Associate, Baird & Associates, Canada
[2]PhD, Assistant Prof., Civil Eng. Dept., K.N. Toosi University of Technology, Iran
[3]PhD, Principal, Baird & Associates, Canada

Abstract

The Oman Sea (Gulf of Oman) is subject to tropical cyclone influence on an infrequent basis; however, these cyclones can generate relatively large sea states that are the dominant coastal design wave conditions. Recently, in early June 2007, Cyclone Gonu entered the Oman Sea and large waves were experienced along the Iranian and Omani coastlines. In this study, historic tropical cyclones in the Arabian and Oman seas were reviewed in an attempt to assess the design wave height and identify possible climate change impacts on cyclone frequency and intensity in the Oman Sea. Due to the limited availability of historical data, a Monte Carlo methodology was used to derive estimates of extreme wave conditions along the Oman Sea coast of Iran. It was also concluded that it is still difficult to determine if there has been any significant change in cyclone frequency and patterns due to climate change.

Key Words

Gonu, Tropical cyclone, Oman Sea, Field measurements, Cyclone frequency, Climate change

INTRODUCTION

The Oman Sea and its neighbouring countries' (Iran and Oman) coastlines are subject to tropical cyclone influence on an infrequent basis; however, these cyclones can generate extremely large sea states. In general, cyclones generated in the Arabian Sea tend to travel either due west towards Oman or re-curve north to strike Pakistan or India. They rarely enter the Oman Sea. Recently, in early June 2007, cyclone Gonu entered the Oman Sea and large waves were experienced along the Iranian and Omani coastlines. This cyclone had an unusual path, travelling much further west and north than the typical cyclone. Significant wave heights in excess of 4 meters were measured at Chabahar located on the south coast of Iran bordering the Oman Sea.

A detailed investigation of the wave climate on the Oman Sea coastline of Iran has been recently carried out in support of a comprehensive study of coastal zone processes (project MONITOR SB&B by Ports and Maritime Organization of Iran) in Chabahar Bay area. The project involved an extensive one-year field measurement campaign, a 25-year wave hindcast for the Oman Sea and various 2DH and 3D numerical modelling of hydrodynamics and sediment transport in Chabahar Bay. The field measurement campaign involved measurements of waves and currents at 6 locations, water levels at 3 locations and winds at 1 location. Figure 1 shows locations of the instruments at the time of cyclone Gonu. The present paper provides a summary of cyclone wave climate investigation conducted in the above study for the Oman Sea.

1. Historical Tropical Cyclones

An assessment of historical tropical cyclones was undertaken using the following tropical cyclone datasets:

- The U.S. Navy Joint Typhoon Warning Centre (JTWC) "Best Track" digital dataset. The current version of this dataset covers the period from 1945 to 2003.

- Historical Tropical Storm and Depression tracks available from the India Meteorological Department in printed format. These data were used to evaluate cyclones occurring prior to 1945.

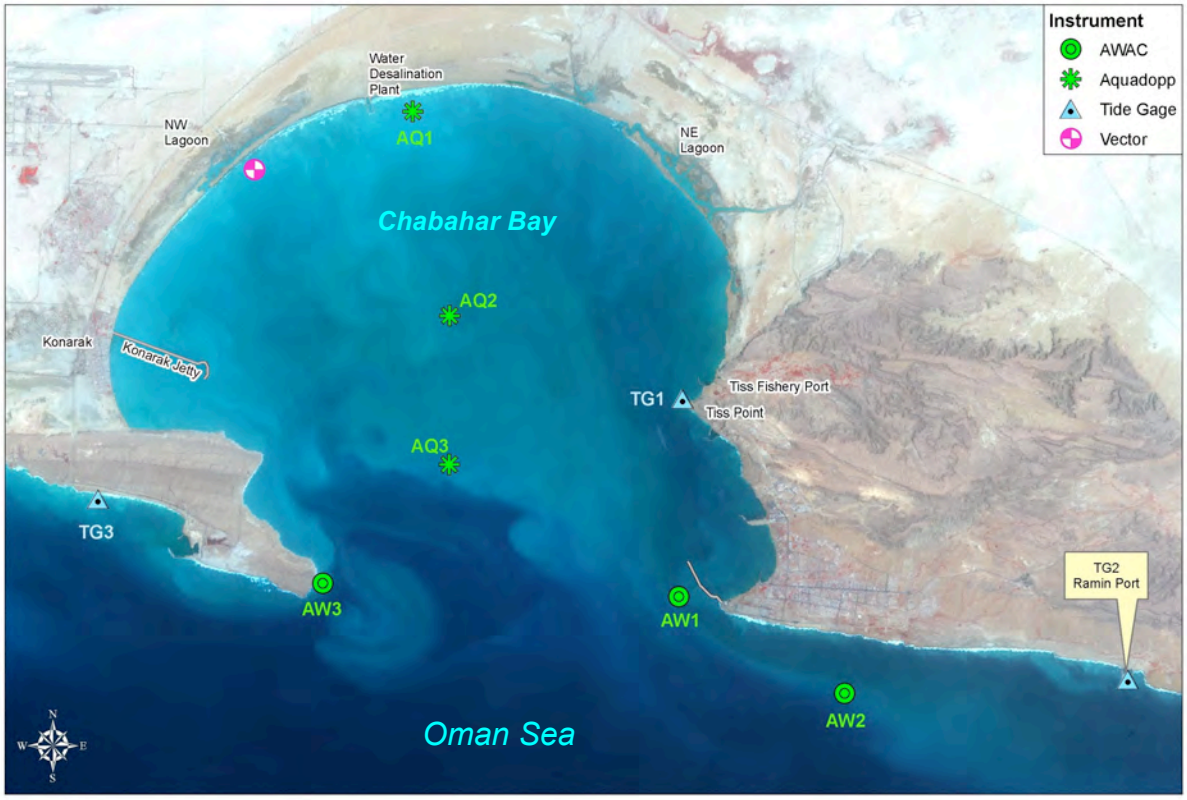

Figure 1 - Instrument locations during cyclone Gonu event (June, 2007).

1.1 Assessment of Digital "Best Track" Data (1945-2003)

The JTWC "Best Track" data are based on a re-analysis of historical cyclone data to provide "best" estimates of each cyclone track and intensity on a six-hourly basis. As the re-analysis of the data is undertaken on an irregular basis, the data provided are not fully up to date (i.e. to 2008). The "Best Track" tropical cyclone database was searched for storms within radial distances ranging from 250 km to 1000 km from Chabahar Bay near the eastern end of the Iranian coastline on the Oman Sea, as shown in Figure 2. In the Figure, cyclones that have peak wind speed data available are shown in colour that varies with the wind speed. There were only 23 tropical cyclone tracks, starting in 1977, that contained wind speed data. It is also important to note that the wind speed estimates for the cyclones were likely derived by means of Dvorak analysis (using satellite imagery of cloud patterns), and are not the result of aircraft reconnaissance or dropsonde data.

Figure 2 shows that the majority of the cyclones have occurred south and east, and at a significant distance from the Iranian coastline. This is important in that the height associated with cyclone-generated wave conditions reduces significantly with distance. The closest cyclone event to Iran in the "Best Track" dataset occurred in 1948 and was, at closest approach, approximately 250 km from Chabahar. We note that cyclone Gonu which is not in the Best Track dataset, approached in closer proximity to Iranian and Omani coastlines in the Oman Sea.

In general the cyclones tend to travel either due west towards Oman or re-curve north to strike Pakistan or India. Cyclones in close proximity to Iran (< 300km) are relatively infrequent. The dataset indicates that there are two distinct tropical cyclone periods: May to July; and September to November. As the southwest monsoon becomes more prominent during the summer months, the potential for tropical cyclones to develop is reduced. Figure 3 shows paths of recent most strong cyclones (excluding Gonu) from Best Track data.

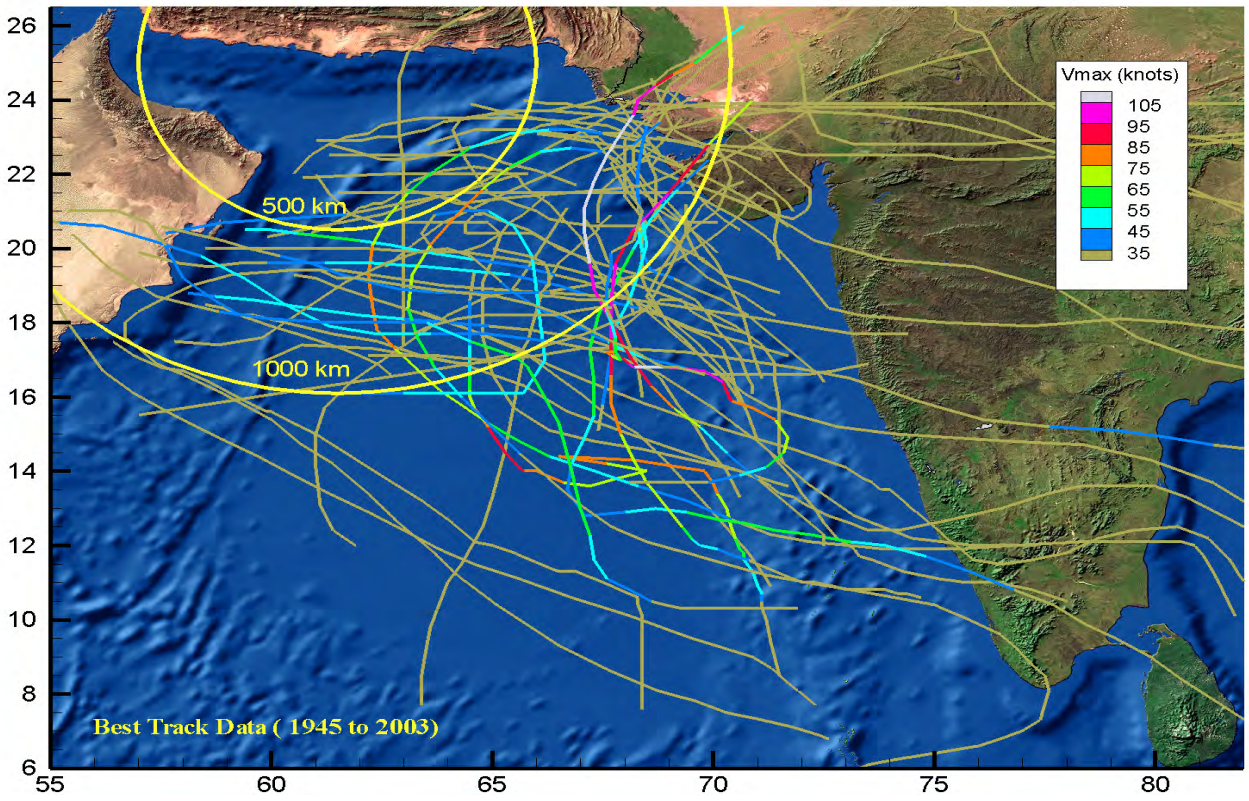

Figure 2 - Tropical storm tracks within 1000 km of Chabahar on the Oman Sea Coastline.

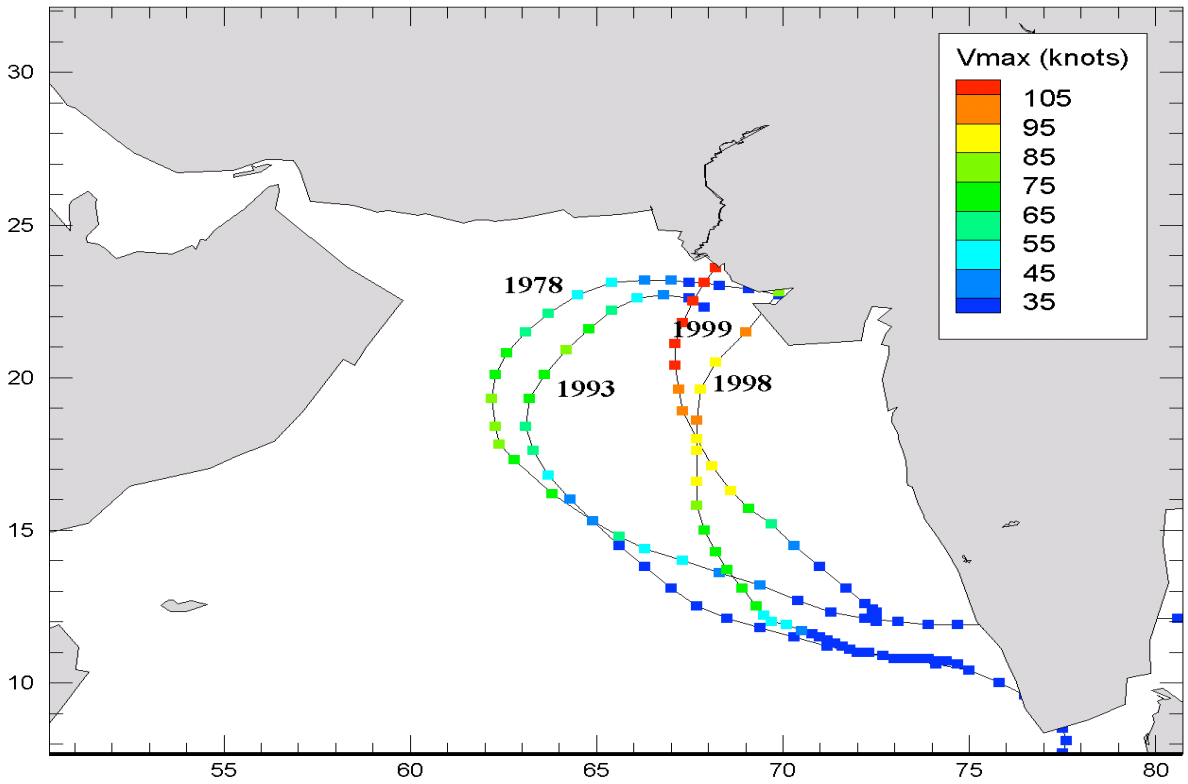

Figure 3 - Recent powerful cyclones in the Arabian Sea (Best Track data).

1.2 Assessment of India Meteorological Department Cyclone Data

The India Meteorological Department compiled an extensive summary of cyclonic storm tracks for the period from 1877 to 1970. Review of the historical cyclone tracks showed that a number of Severe Tropical Storms entered the Oman Sea that would potentially generate large waves that would impact the Iranian and Omani shorelines. These events included storms from the following time periods: June 1889, June 1890, May 1898 and April 1901. The associated cyclone tracks are shown in Figure 4.

It is worth noting that the "Best Track" data does not show the presence of storms with Severe Tropical Storm strength in as close proximity to the Iranian and Omani shorelines on the Oman Sea as the data from late 1800's and early 1900's. This may potentially indicate that there has been a temporal shift in the tropical cyclone climatology of this region, reducing cyclone frequency in the Oman Sea. On the other hand, recent occurrence of cyclone Gonu (see the next section) suggests that Severe Tropical Storm events in the Oman Sea may have a long-term cycle with a period of about 100 years. Therefore, it is still difficult to determine if there has been any significant change in cyclone frequency and patterns due to climate change. Monitoring cyclone activity in upcoming years would help answering this question.

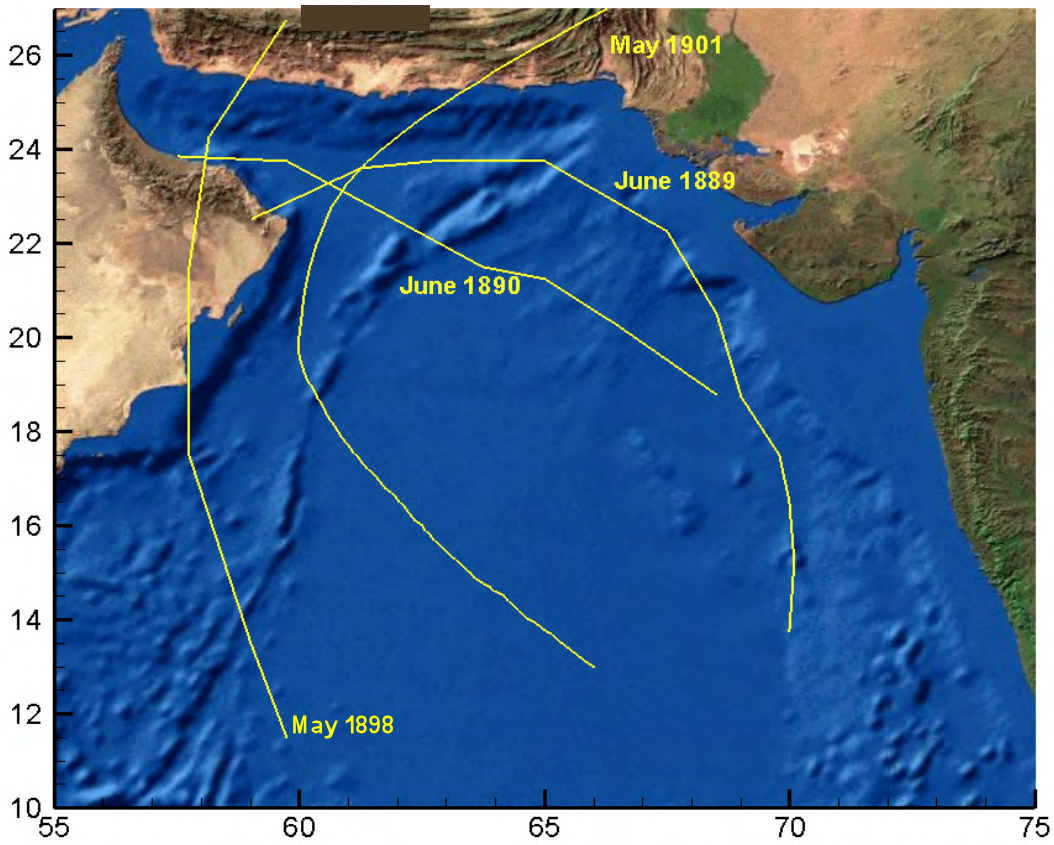

Figure 4 - Historical cyclones selected from India Meteorological Dataset.

1.3 Cyclone Gonu 2007

Cyclone Gonu, which existed from June 1 to 7, 2007, was the most intense tropical cyclone on record in the Arabian Sea. It developed from an area of persistent convection in the eastern Arabian Sea, and intensified to a Category 5 cyclone with maximum wind speeds of 250 kph (140 knots) by June 4. The cyclone moved in a northwest direction, making landfall at the easternmost tip of the Arabian Peninsula in Oman, and then proceeded into the Oman Sea. The storm decreased in intensity as it moved northward from Oman.

AW2 sensor (Figure 1) located in 30 m depth at Chabahar measured wave for this time period. Figure 5 provides a time series plot showing significant wave height and peak wave period measured during Gonu. The waves achieved a maximum significant wave height of approximately 4.2 m with an associated period of 10 seconds. A maximum wind speed of 16 m/s from SE direction was measured in the evening on June 6.

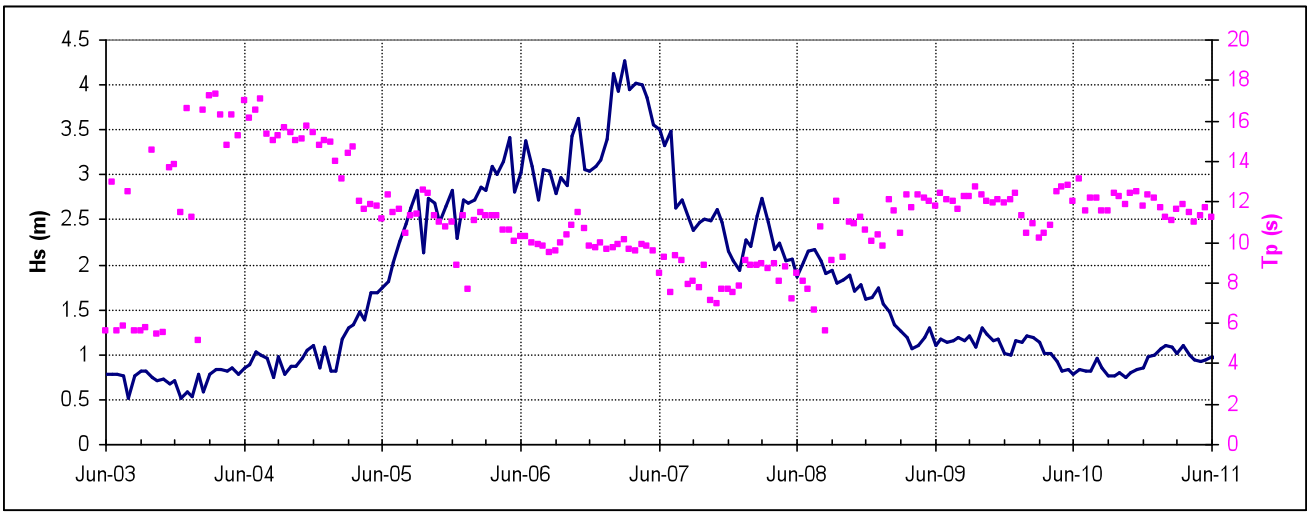

Figure 5 - Time series of waves at Chabahar (30 m depth) during Gonu.

2. SIMULATION OF CYCLONES

Numerical modelling of tropical cyclone wave generation was used in this study to both simulate historical storm events and to investigate potential design wave conditions. The WAVAD model, as summarized in Resio (1981) and Resio and Perrie (1989), was used for the tropical cyclone wave simulations. This model was utilized for both purposes of computational efficiency and its accuracy in simulation of rapidly changing wind fields that occur in a tropical cyclone. Over 200 model simulations were carried out.

WAVAD is a second generation (2G) spectral wave model that maintains an equilibrium between the wind source and non-linear wave energy flux with an assumed f-4 shape for the wave spectrum. Inputs to the WAVAD model consist of a regular grid defining the shoreline and bathymetry in the region of interest as well as a spatially and temporally varying wind field defined at the grid points. Output from the model include the spectral wave energy densities at all grid locations, from which standard parameters such as significant wave height (*Hs*), peak wave period (*Tp*), peak wave direction and wave directional spreading are derived. The model grid had 191 longitudinal grid points and 171 latitude grid points at an equal resolution of 0.1°. A time step of 15 minutes was used in all of the simulations. A total of 23 frequencies were employed, ranging from 0.039 to 0.317 Hz, in conjunction with a directional resolution of 15° (24 directional bins). There are no calibration parameters within the WAVAD model.

The cyclone wind field model that was used to drive the WAVAD wave model was based on the parametric representation of Holland (1980). Input data to the wind field generation model included the cyclone path, and the peak wind speed, cyclone central pressure, distance to the maximum wind speeds (Rmax) and an empirical shape factor ("B"), all defined on a 6-hourly basis. Estimates of Rmax and B were derived from recent work by Willoughby et al. (2004) for Atlantic Ocean hurricanes. The output wind fields are defined on an hourly basis.

The results of numerical simulation of cyclone Gonu and the 1889 cyclone are presented here. Input parameters for cyclone Gonu were based on currently available track data from JTWC for this cyclone. It is important to note that these data are not complete and should be considered preliminary in nature; these data may vary in the future when more detailed re-analyses are carried

out. Figure 6 shows the maximum significant wave height estimated at each grid point throughout the passage of Gonu. Peak wave heights adjacent to the cyclone were in the order of 10 meters when the cyclone entered the Oman Sea but reduced as the intensity of the cyclone decreased with time. Figure 7 shows a time series comparison to the measured wave height, wave period and wave direction at Chabahar. Excellent agreement was achieved between the measured and hindcast waves. Note that background wave conditions in the Indian Ocean were not included in the simulation, which would have little effect on the peak of the storm event but could affect the magnitude of lesser wave conditions before and after the cyclone passage.

Contour plot of the maximum significant wave height calculated at each grid point during the 1889 cyclone simulation is presented here for comparison. The India Meteorological Department reference (1979) does not identify the specific maximum wind speeds associated with these events. It is only noted if the wind speed is greater than 50 knots. Therefore, cyclone simulations were carried out with different peak constant wind speeds. Figure 8 shows the results with a peak speed of 90 knots. It may be noted that this cyclone event may have potentially created very large wave conditions along both Iranian and Omani coastlines in the Oman Sea. Although, there is a fundamental concern as to the accuracy of this early data, the recent occurrence of cyclone Gonu does indicate the possibility that such events might readily occur.

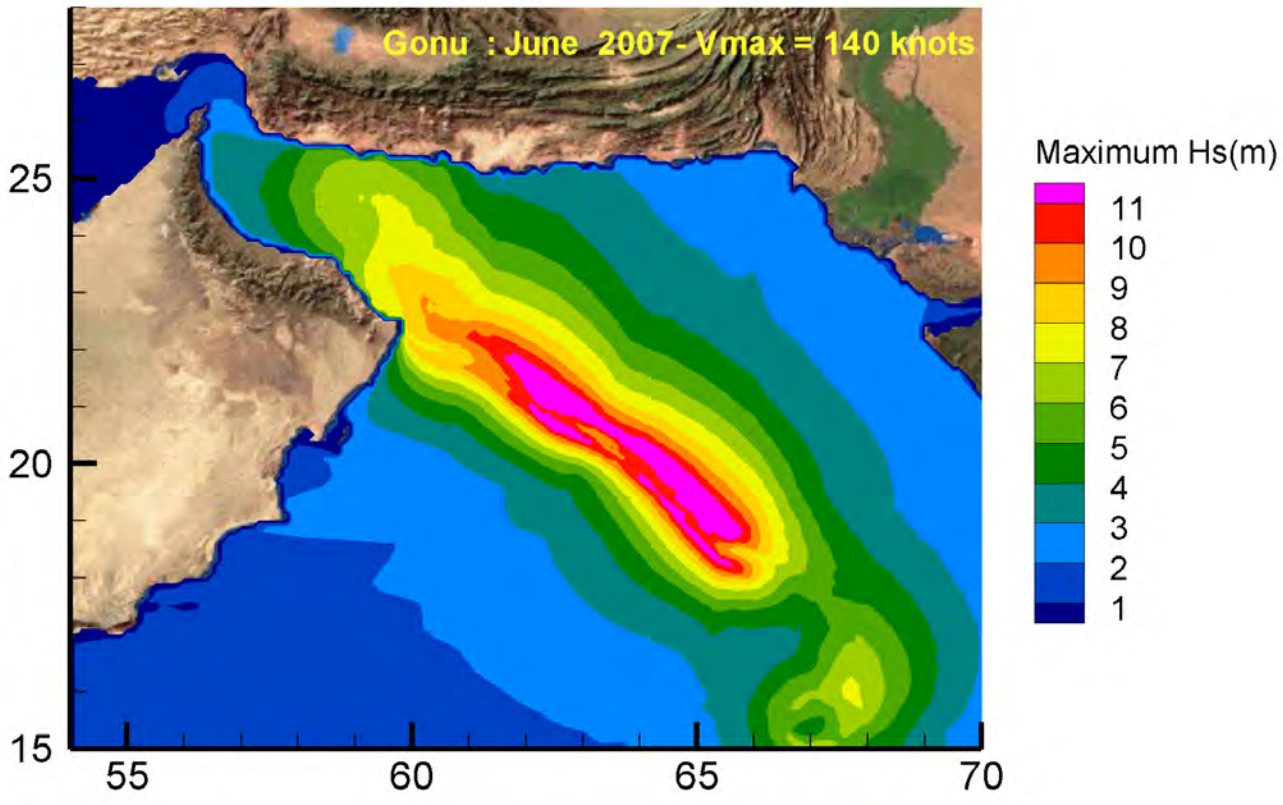

Figure 6 - Predicted maximum significant wave height in Arabian and Oman seas during Gonu.

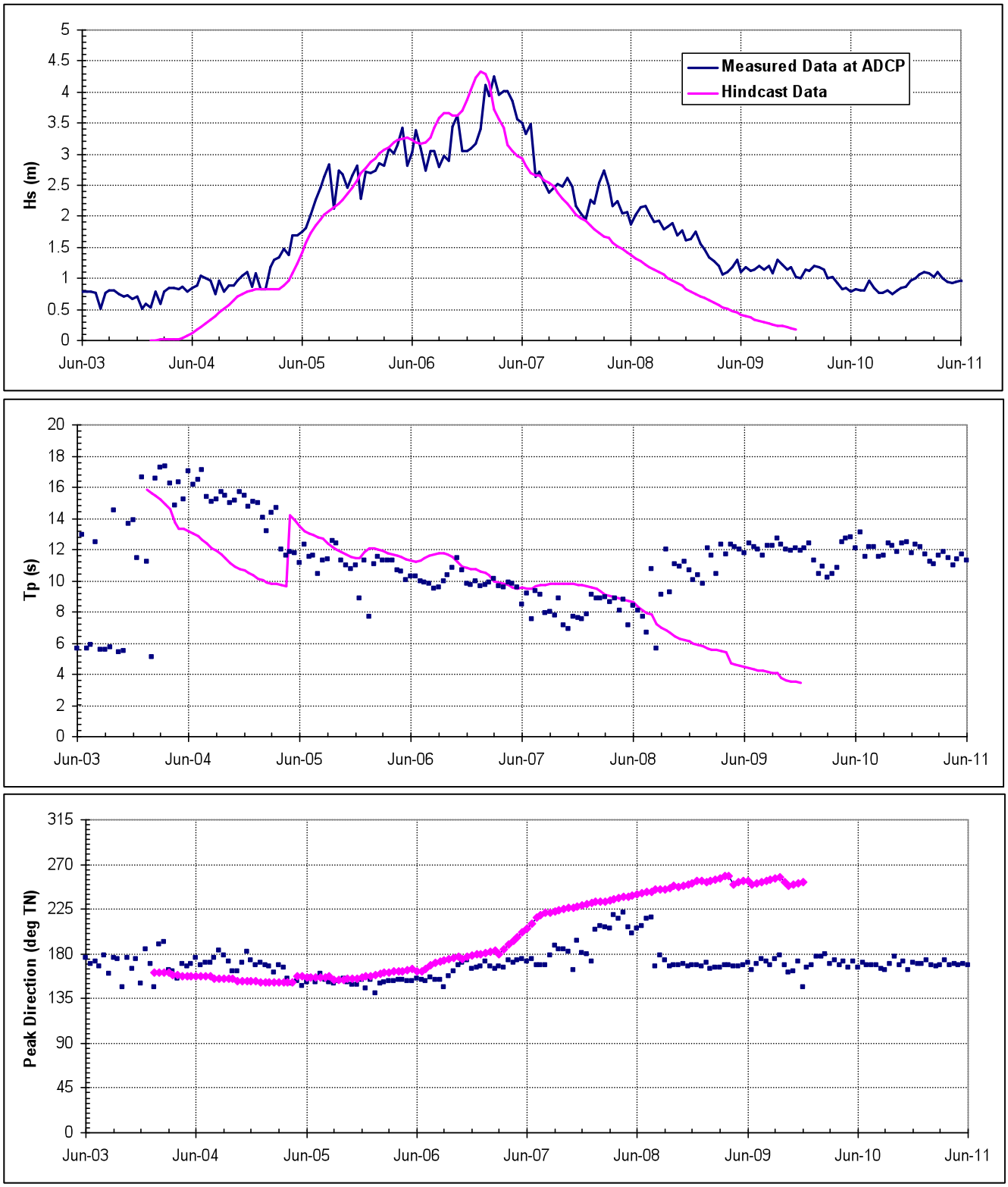

Figure 7 - Time series comparison of wave height, period and direction at Chabahar (30 m depth).

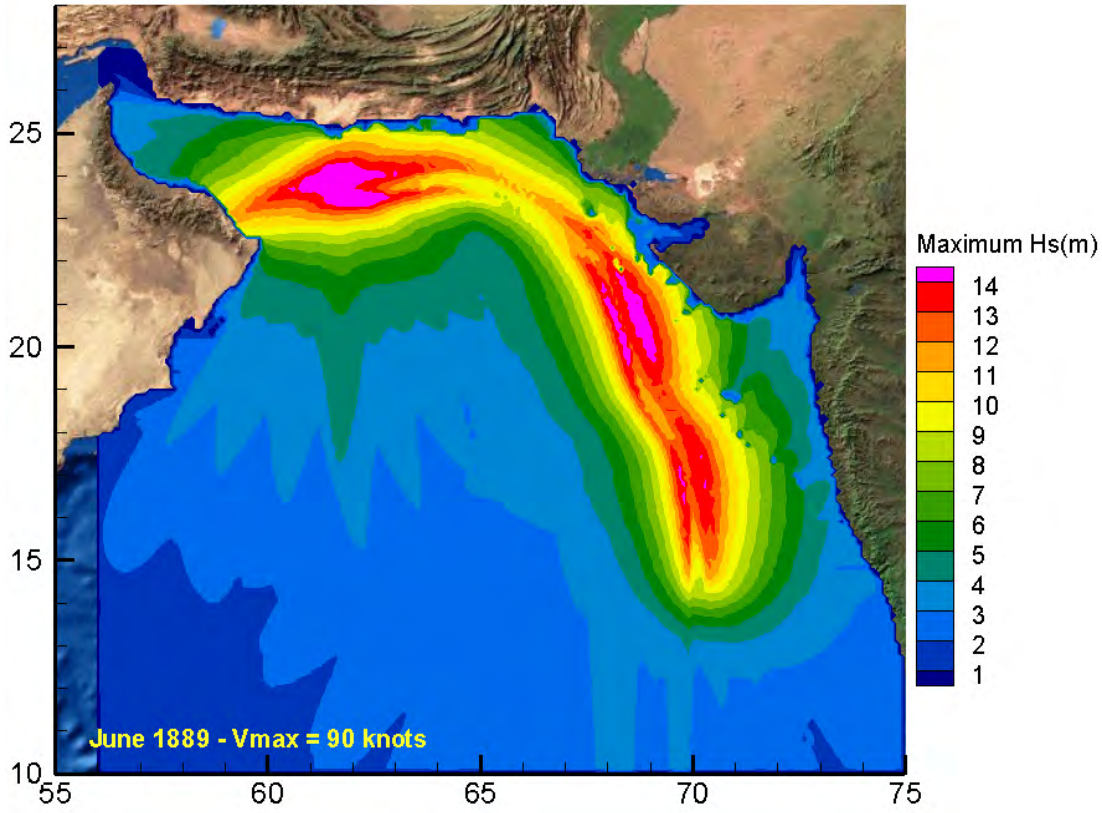

Figure 8 - Predicted maximum significant wave height in the Arabian and Oman seas during the 1889 cyclone.

3. IMPACT ON DESIGN WAVE HEIGHT

One of the challenges in evaluating tropical cyclone wave generation in the Arabian and Oman seas is the limited availability of historical data. Although, the paths of historical cyclone events have been established through various data sources, the severity of the cyclones is not well known except for storms occurring over the past 30 years. As well, the relative infrequency and significant spatial variability of tropical cyclones in this region (particularly the Oman Sea) implies that a simple assessment of historical storm events is not sufficient for statistical evaluation of design wave conditions.

Derivation of design wave conditions directly from numerical simulation of the historical tropical cyclones alone could lead to potential under- or over-estimation of the design waves due to the limited number of historical events with reliable wind speed information. In this study, to overcome some of the limitations with the historical data, a Monte Carlo methodology has been used to derive estimates of extreme wave conditions along the Oman Sea coast of Iran. This method involves the development of a synthetic tropical cyclone database using the properties of the existing historical tropical cyclone population. In total more than 200 synthetic storm events were created through random perturbation of actual historical events since 1977. Figure 9 shows the tracks of more than 200 synthetic cyclones that were generated in the Monte Carlo process. Note that the overall annual probability for a tropical event affecting Iranian coastlines on the Oman Sea is 1.20. Thus, 200 storm events represent an approximate temporal coverage of 170 years.

The maximum wave height calculated for each cyclone simulation was extracted from the model results at locations of interest along the Iranian coastline. Statistical extreme value analysis was then performed on the data to define design wave conditions. Simulations were completed with and without inclusion of cyclone Gonu's track. The results of simulations without inclusion of Gonu track indicated a range in the 100-year deep water design wave height from 1.4 m at the western end of the Iranian coastline on the Oman sea to 5.6 m at the eastern end (when the

simultaneous presence of swell waves is considered). In comparison, when cyclone Gonu track was included, the results indicated a range in the 100-year deep water design wave height from 2.4 m at the western end of the coastline to 8.8 m at the eastern end (when background swell waves are considered). The change from 5.6 m to 8.8 m design wave height has a significant impact on the design and corresponding costs associated with coastal infrastructure.

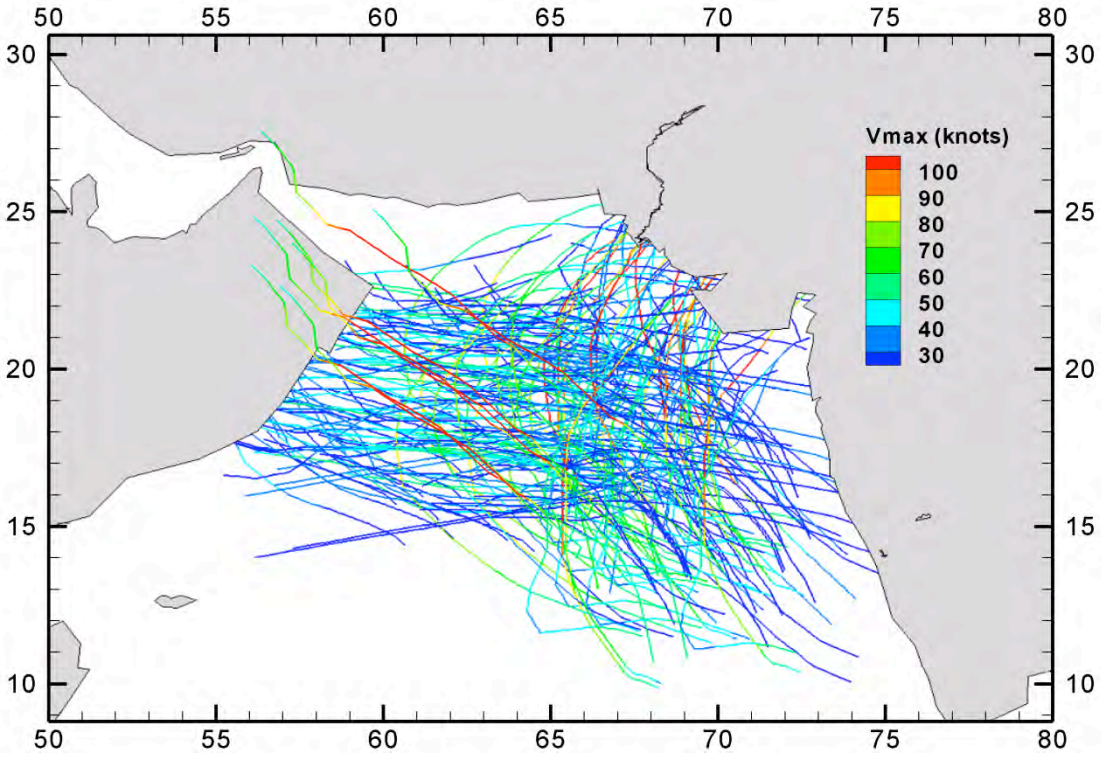

Figure 9 - Monte Carlo simulation of cyclone tracks when Gonu is included.

Conclusions

Cyclone Gonu, which occurred from June 1 to June 7, 2007, was the most intense tropical cyclone on record in the Arabian Sea. This cyclone entered the Oman Sea with high wind conditions, generating waves in excess of 9 meters. Older historical tropical cyclone data (prior to 1945) indicates the occurrence of several cyclones within the Oman Sea, particularly in the late 1800's and early 1900's. Tropical cyclone data from the past 30 years, including Gonu, indicate maximum offshore design significant wave heights of up to 8.8 meters along Iranian coastline. If the cyclone track data from the late 1800's and early 1900's is considered reliable, the potential for even larger cyclone design wave heights is feasible. In general, the selection of design wave heights along the Oman Sea shores depends largely on the risk to be assumed and on the reliance that is placed in older records of tropical cyclone events. As this potential variability in design wave height has a significant impact on the costs associated with coastal infrastructure, a more detailed investigation of these historical events should be carried out. Such an investigation would require research into historical records with a view to establishing the track and intensity of these events.

The data employed in this study has shown that there may be considerable temporal variability in the frequency of occurrence of tropical cyclones in the Arabian and Oman seas, raising the possibility of climate change effects. We note that the technical community remains divided as to the potential effects of climate change on the frequency and intensity of tropical cyclones. A recent Statement on Climate Change effects by the World Meteorological Organization (2006), and one of the most thorough studies conducted by a number of cyclone experts, Henderson-Sellers et al. (1998), have indicated that there is insufficient historical

information to determine if tropical cyclones are being affected by global warming. The present study confirms this conclusion. The recent occurrence of cyclone Gonu does indicate the possibility that Severe Tropical Storm events might readily occur and suggests that such events in the Oman Sea may have a long-term cycle with a period of about 100 years. Therefore, it is still difficult to determine if there has been any significant change in cyclone frequency and patterns due to climate change. Monitoring cyclone activity in upcoming years would help clarifying this question.

References

Henderson-Sellers (1998). "Tropical Cyclones and Global Climate Change: A Post-IPCC Assessment". Bulletin of the American Meteorological Society. 79. pp. 19-38.

Holland, G. (1980). "An Analytic Model of the Wind and Pressure Profiles in Hurricanes". *Monthly Weather Review*. Volume 108. 1212-1218.

India Meteorological Department. (1979). Tracks of Storms and Depressions in the Bay of Bengal and the Arabian Sea 1877-1970.

Resio, D. and Perrie, W. (1989). "Implications of an f^{-4} Equilibrium Range for Wind-Generated Waves". *Journal of Physical Oceanography*. Volume 19, pp. 193-204.

Resio, D. (1981). "The Estimation of Wind-Wave Generation in a Discrete Spectral Model". *Journal of Physical Oceanography*. Vol. 11, No. 4.

Statement on Tropical Cyclones and Climate Change (2006). The World Meteorological Organization.

Willoughby, H.E. and Rahn, M.E. (2004). Parametric representation of the primary hurricane vortex. Part I: Observations and evaluation of the Holland (1980) model. *Monthly Weather Review* Vol. 132, pp. 3033-3048.

The U.S. Navy Joint Typhoon Warning Centre (JTWC) "Best Track" digital dataset.
http://metocph.nmci.navy.mil/jtwc.php

LONG-RANGE PREDICTION OF TROPICAL CYCLONES FOR BANGLADESH

Saleh A. Wasimi
CQ University, Rockhampton, Queensland 4702, Australia

Abstract

This paper deals with long-range prediction of topical cyclones (TCs) that make landfall in Bangladesh. Recent scientific and technological advances have made it possible for the people to be forewarned about an impending TC, but the lead time is only a few days. Such a short lead time, though undoubtedly is saving many lives and properties, is inadequate in Bangladesh context in view of the country's infrastructure and socio-economic conditions. Short-term forecasts have been made reliable through numerical modelling, analysis of satellite images, and synoptic methods but these forecasts cannot be extended to longer lead times because TCs grow from a state of non-existence to full strength within a few days. In such circumstances, as in many branches of science, statistical methods remain as the only viable option for long-range forecasts. This paper develops the framework upon which a statistical formulation of the prediction problem can be based.

In statistical prediction problem, it is necessary to identify the dependent and independent variables which can come from physical considerations. A literature survey has been made to identify the hydro-meteorological variables which can be possible candidates for independent variables. The cyclones that hit Bangladesh are almost all formed in the Bay of Bengal in the main development region (MDR) of 85^0E-95^0E and 5^0N-15^0N. After a cyclone is formed, two aspects that are important in Bangladesh context are its intensity and the track. These are the dependent variables. The intensity is captured through the energy of the cyclone and the prediction of tracks is limited to the prediction of possible recurvature. Bangladesh coast would directly be in the path of a TC formed in the Bay of Bengal only if recurvature occurs to its track. The prediction model is first formulated as a linear regression model gradually built by stepwise regression up to the number of independent variables equal to the significant number of principal components. The usefulness of the series of models in prediction is then tested by the techniques of artificial intelligence, specifically by artificial neural networks and support vector machines. In model testing, data are split into 70% for training and 30% for testing which is the standard industrial practice. Finally, the model variables which have most predictive capability in the context of Bay of Bengal cyclones are identified.

Keywords
Tropical cyclones, Bay of Bengal, Bangladesh, Statistical prediction

INTRODUCTION

Bangladesh is one of the most densely populated countries in the world where majority of the population live in a flat deltaic plain. The low topography combined with houses not designed to withstand cyclones make people very vulnerable to the destructive forces of tropical cyclones (TCs). TCs in the region have claimed by far more lives than anywhere else in the world – 49 percent of world's total fatalities by cyclone occurred in Bangladesh alone and 22 percent in India (Ali, 1996). The tropical cyclones that hit Bangladesh are mostly formed in the Bay of Bengal and their destructive force is primarily due to the accompanying storm surge whose development is influenced by unique features such as shallow bathymetry and near funnel shape of the Bay (Mandal et al., 2007). As cyclones at different oceans form at different times, it is now well established that regional climate and weather patterns play an important role in cyclogenesis (JTWC annual reports; Vecchi and Soden, 2007). The climate of the region around Bangladesh besides its latitudinal and longitudinal location is influenced by the presence of the highest mountains to its north and northeast. In summer (May-October), a low pressure system is created in northwest India by heating of landmass that marks the position of the monsoon trough, which causes wind to blow northeast from the Bay of Bengal over the shallow ocean waters to Bangladesh and then get deflected by the mountains to northwest. In winter (November-March) the monsoon trough is over the Bay of Bengal and cold airmass over land in north India moves outward through Bangladesh into the Bay of Bengal in southwest direction. The transition period

(May or November) is when the wind is slowest offering ideal conditions for tropical cyclones to form over warm waters.

The factors that affect the formation of tropical cyclones are a topic of research and we still have a long way to go to understand the causes fully (Lee et al., 2008). Why some irregular atmospheric disturbances transform into cyclones and others do not is a perplexing question for the scientists. Once formed, cyclones derive their energy from the latent heat of condensation of water vapour, and rapid intensification of cyclones generally occur when their translation speed is between 3m/s and 8m/s (Zeng et al., 2007) – at lower speeds negative feedback from cold waters from upwelling deprives them of the energy, and at higher speeds, the shape gets asymmetric resulting in non-uniform angular acceleration. Many studies point to the fact that warm sea surface temperature (SST) above 26^0C, conditional instability and high relative humidity in the middle troposphere, and low vertical wind shear are prerequisites for the genesis of cyclones (Webster et al., 2005). Kotal et al. (2009) developed a genesis parameter for the Bay of Bengal as the product of four variables, namely vorticity at 850 hPa, middle tropospheric relative humidity, middle tropospheric instability, and the inverse of vertical wind shear. DeMaria et al. (2001) defined a genesis parameter for the North Atlantic basin based on SST, mid-level moisture, vertical shear, and vertical instability. ENSO has a significant role to play in the frequency and intensity of cyclones which has been established (Camargo et al., 2007; Emanuel, 2008). Ralph and Gough (2009) have shown that even in the same ocean, such as Eastern North Pacific, TCs can have different characteristics based on the main development region (MDR) of its formation.

Historical data on cyclones of the Bay of Bengal is available since 1877 (Singh et al., 2001; Islam and Peterson, 2009) but its accuracy in early years is doubtful because dates, positions, and intensities are deduced through estimates and compromise among various reports using synoptic and climatological judgment (FNMOC, 1998). However, reliable data (though primarily from satellite imagery) on the formation of major tropical cyclones in the Bay of Bengal, their tracks and their wind speeds at six hour intervals are available since 1971 from the Joint Typhoon Warning Centre (JTWC) in Hawaii – detailed information on each TC is available in graphical and tabular forms. Frank and Young (2007) question the reliability of JTWC data but corrections of their data were made later to improve the quality of data. JTWC uses a number of numerical models and an expert system TAPT to predict the tracks and characteristics of the TCs but frequently those turn up to be very different from the reality. Nicholls (2001) notes in this context that statistical analysis and numerical analysis are complementary, and together are more reliable than numerical analysis alone. Aberson (2009) identifies some pitfalls of statistical analysis and emphasizes the need to be cautious with statistical inferences. Nevertheless, Kotal et al. (2008) demonstrates that statistical analysis of the TCs in the Bay of Bengal yields useful results.

This study attempts to perform some statistical analysis with a view to developing a model that is capable of predicting the cyclonic activity over Bangladesh. There is considerable literature available on forecasting of cyclones. A brief summary of the forecasting techniques in use is presented in the next section. These forecasting techniques have been very useful to save lives and properties. However, the forecasting techniques are considered reliable for up to 72 hours. In Bangladesh context, where majority of the population in the coastal areas are rural poor living on subsistence farming in deltaic flats, a forecast lead time of several weeks or months can be of enormous benefit. Where physics-based models do not seem to offer any plausible solution to the problem of long-range forecasting, a black box model such as a regression model or Box-and-Jenkins type of models have been applied in many areas of science to derive useful knowledge in long-term outlooks. This is the primary research path that underpins this paper. There can be many steps in statistical analysis beginning from pre-whitening or detrending of data to residual analysis. To accomplish all the tasks comfortably a statistical software product such as SPSS or SAS is indispensable. This paper primarily uses the software packages SPSS and WEKA, which have found extensive use in published literature. In section 3 the trend characteristic of cyclonic activity in Bangladesh is analysed. Section 4 is on data selection process and source. Section 5 is on some statistical characteristics of the TCs in the Bay of Bengal and section 6 is on statistical modelling. The paper ends with some concluding remarks.

1. TROPICAL CYCLONE PREDICTION

The destructive power of a TC lies in its maximum sustained wind speed and the atmospheric pressure drop that it creates, which is responsible for violent seas that result in storm surges. Prediction or forecasting in this context may mean several things or their combinations. Forecasting can be of the maximum sustained surface wind speed, height of the storm surge or track of the TC. Forecasting of the maximum sustained surface wind speed has not received much attention in published literature because normally a cyclone would attain its maximum potential intensity unless an adverse factor such as strong steering current or high vertical wind shear prevails. Commonly, Dvorak's (1984) method of analysing satellite data is used to estimate a cyclone's intensity. Most of the focus of published literature however is on the track of a TC. The forecasting techniques for cyclone tracking can be loosely grouped into the categories of persistence-based, climatology-based, synoptic technique-based, satellite-based, dynamics-based, and statistics-dynamics-based.

Persistence-based techniques use some sort of polynomial fit to extend the path already traced out into the future. In advanced methods a form of regressive filter such as Kalman filter is used. In climatology-based technique searching is done in the historical record to find similar cyclones within a preset spatial, seasonal and translational velocity range of the cyclone to be forecast. The forecast track is derived as the mean of all these cyclones. A significant number of meteorologists believe that cyclones are carried by the steering current along its way. According to them therefore a cyclone's track can be determined by the direction of the environmental flow. Synoptic technique-based methods use historical observations of a cyclone's translation in the context of its relative location with features such as subtropical ridge, upper-level troughs and quasi-stationary features such as Tibetan High. Satellite-based techniques involve interpreting satellite imagery of cloud patterns. The pioneering work in this regard was done by Dvorak. Cloud bands in outer circulation can indicate the direction of translation. Dynamics-based techniques are essentially numerical models solving analytical equations which can range from simple conceptual models to complex distributed models integrated over many days on a global domain. Statistics-dynamics-based techniques use output from a numerical model to be filtered by statistical parameters which are obtained from statistical screening of past storms.

Intuitively, statistics-dynamics-based techniques are the most reliable because it uses both physics and statistics. This is supported by evidences at many cyclone forecasting centres. For example, CSUM used by JTWC, NHC90 used by NHC (National Hurricane Centre), and SD75 used by China showed consistent improved performance over other techniques. The usefulness of the dynamical component begins to fade as we extend the forecasting lead time beyond 72 hours. Therefore, when we are seeking a forecasting lead time of several weeks or months, the only tool available to us is apparently statistical techniques.

2. IS THERE A TREND IN CYCLONIC ACTIVITY OVER BANGLADESH?

Development of a statistical model often requires that the data satisfy the condition of wide sense stationarity. If the data is not stationary, usually data transformation is implemented to render stationarity in the data. One basic such transformation is detrending. Whether detrending is required would depend on if there is any trend in the data. To seek an answer to this question, historical cyclone activity in Bangladesh is analysed.

EM-DAT (The OFCA/CRED International Disaster Database, Brussels, Belgium) has time series data of the number of destructive tropical storms that lashed Bangladesh over the years. This information is captured in Figure 1. Khan et al. (2000) after analysing data of the Bay of Bengal for the period 1877-1998 obtained from the IMD (India Meteorological Department) claim that there is a positive trend in cyclonic activity with a gradient of 0.0027 per year in May and 0.0067 in November which is correlated with rising SST with a significance level of above 90 percent. In this study an independent investigation is done using the concept of NTA proposed by Kwon et al. (2007). The focus is only on TC but not on tropical depressions. A TC is assumed to be formed when the maximum sustained surface winds (MSSW) is 34 knots or above. A tropical depression has a wind speed of 33 knots or less. This is in accordance with the Global Tropical

Cyclone Climatic Atlas (GTCCA) and also with WMO classification (Islam and Peterson, 2009). According to Kwon et al. Normalized Typhoon Activity (NTA) is given by the relation

$NTA = \sum \frac{1}{4}\left(\frac{V_{\max}}{V_{TY}}\right)^2$, where the summation is over the total cyclone duration, $V_{\max}$ is maximum wind speed at 6-hour intervals, V_{TY} is typhoon wind speed which is 64 knots, and division by 4 is because cyclone information is issued four times a day by JTWC. JTWC data is used in this analysis.

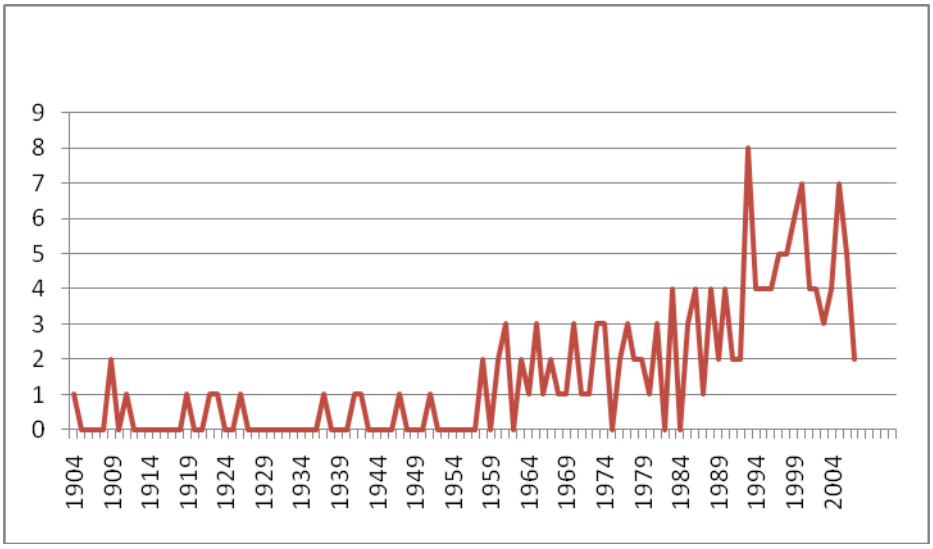

Figure 1 - Number of destructive tropical storms in Bangladesh occurring annually.

To look into the significance in trend of annual NTA of the Bay of Bengal, rather than seeking a significant numeric value for the slope which can be doubtful unless confidence intervals are properly captured, a nonparametric approach was adopted that can yield a simple 'yes' or 'no' answer to the question if the cyclone activity is really increasing. In this approach, first, a jack-knife analysis was done where the data were divided roughly into two equal parts – one part consisting of data for the period 1971-1989 and the other part consisting of the period 1990-2008. Next, Wilcoxon signed-rank test (Miller and Miller, 1999) was performed with the alternative hypothesis that the mean for the 1990-2008 period is greater than the mean for the entire period which is 1971-2008. The annual mean NTA for the entire period is 8.10. T^+ for the hypothesis test is found to be 102, T^- is found to be 69, and T = 69. The critical T value at 1 percent level of significance is 33 and at 5 percent level of significance is 47. The critical values are lower than the T value, and therefore, we cannot reject the null hypothesis. To seek further corroboration of this statistical inference more tests were performed. In published literature, there are three methods which have been recommended by WMO and other agencies to test for the existence of significant trends in time series data – Mann-Kendall (M-K) test, Spearman rank correlation (SRC) test, and the least squares linear regression (LR) test. LR test outcome has been presented earlier as perfomed by Khan et al. M-K test is a non-parametric test (for details see Xu et al., 2005) which requires the data be prewhitened if there is autocorrelation in the data. A plot of autocorrelation function (ACF) showed no significant autocorrelation and therefore no prewhitening was necessary. After doing the computations, it has been found that S = 100, Var (S) = 5846 and Z = 1.31. Since Z is less than the critical value of 1.96 for 95% confidence level, the null hypothesis could not be rejected. For the SRC test (for details see Khaliq et al., 2009) Σd_i^2 is found to be 7374, r_{SRC} = 0.1259, and t_{SRC} = 0.75. The critical t value for 5% level of significance is 2.02 and therefore the null hypothesis could not be rejected for this situation as well. Thus, both parametric and non-parametric analyses lead consistently to one conclusion that there is not sufficient evidence to infer that cyclonic activities are increasing in the Bay of Bengal though it contradicts with the inferences made earlier by Khan et al. (2000) and Webster et al. (2005). One criticism that can be made of the analysis just

presented is the shortness in the length of the data. This criticism would not affect the modelling efforts made in this paper because the intended projection into the future is of much shorter length compared to the past period analysed.

In fact further analysis by the author of other variables which could be related to the cyclonic activity over Bangladesh revealed that it cannot be conclusively established if there is any trend in any of the variables. Nor could it be established if there is any temporal change in the standard deviation of the data. These analyses were routinely done mostly visually using the software package SPSS. It is therefore perhaps logical to state that simple statistical relationship can be developed from the data without the need to perform any kind of transformation of the data.

3. DATA SELECTION AND SOURCE

Two aspects of tropical cyclones which are important in Bangladesh context are rapid intensification and recurvature. Rapid intensification causes the cyclone to attain devastating levels of maximum sustained surface winds (MSSW). There exists a relationship between MSSW and MSLP (minimum sea-level pressure), which in turn determines the height of the storm surge. For a tropical cyclone situation the relationship between MSSW and MSLP can be dynamically captured by a cyclostrophic wind equation of the form $V_m = a(b - p)^c$, where V_m is MSSW in knots, p is MSLP in millibars, and a, b, and c are constants determined by least squares. There are other methods as well which are used to capture the wind-pressure relationships such as by Atkinson and Holliday (1977) and Dvorak (1975). In this study the analysis of the cyclone data of the Bay of Bengal for the period 1971-2008 yields the following cyclostrophic equation.

$$V_m = 6.0(1011 - p)^{0.67} \qquad (1)$$

Equation (1) has a coefficient of determination (R-square) value of 0.9558 and is different from the relationships given by Brown et al. (2009) for other oceans. This R-square value is also higher than that reported by Brown et al. for other oceans. This means that if we know MSSW, we can reliably estimate MSLP which in turn can be used to estimate the height of the storm surge that would hit Bangladesh coast using a two-dimensional hydrodynamic model. Hydrodynamic modelling is not within the scope of this study, and therefore, the focus has been confined within the hydro-meteorological variables that contribute to MSSW.

However, the other aspect of a cyclone that is important for this analysis is the track. Cyclones do not usually form within a band of 5^0 latitude around the equator because of the low Coriolis effect. In the Bay of Bengal it forms mainly in the region 5^0N-15^0N and 85^0E-95^0E. Once formed a cyclone tends to move poleward and westward. If this is the case, Bangladesh would not be in the path of a cyclone. When a cyclone changes its course and turns eastward, the process is called recurvature. With recurvature Bangladesh coast is likely to fall into the path of a cyclone formed in the Bay of Bengal. Thus for TC predictive purposes recurvature as a response variable should be considered along with MSSW.

The hydro-climatic factors which have been identified to influence rapid intensification and recurvature in TCs of the Bay of Bengal from literature survey and correlation analysis within MDR are sea surface temperature (SST), ocean temperature up to a depth of 60m, sea-level pressure (SLP), vertical wind shear, latent heat flux (proxy for atmospheric moisture), wind speed, and curl of wind; and outside MDR are atmospheric temperature over land in Delhi and ENSO. Data on MSSW of cyclones, their tracks, and wind speed were obtained from JTWC in Hawaii (1971-2008). SST and other ocean-atmosphere interface data were obtained from NOAA-NCDC-ERSST. Vertical water temperature profile data was obtained from Carton-Giese SODA data. Climatic indices and other data were obtained from KNMI. The temperature data of Delhi was obtained from IMD.

Since the focus of this study is long-range forecasting, only monthly values were used in the statistical analysis. The dependent variables were the NTA, which follows from the concept of kinetic energy of a cyclone, and recurvature which has been considered as a binary variable with 0 indicating no recurvature and 1 indicating at least one recurvature. Each independent variable had

at most twelve values, six values at lags 1 to 6 and six values of standard deviation within MDR also for lags 1 to 6. The truncation at lag 6 is based on the assumption that the system memory for the genesis of a cyclone does not extend beyond six months. Also, lag 0 data were not considered since we are interested in prediction of one or more months in advance. Obviously, such a selection of independent variables would have significant cross-correlations. To avoid problems associated with high cross-correlations such as multicollinearity problem it is necessary to restrict use of multiple highly correlated variables as inputs in the formulation of a forecasting model. This has been accomplished by the application of principal component analysis.

4. SOME STATISTICAL CHARACTERISTICS OF THE TCS OF THE BAY OF BENGAL

Some statistical characteristics of the tropical cyclones of the Bay of Bengal have been analysed in the framework of the following characteristics. The characteristics are described briefly in the following paragraphs and their properties are captured in Table 1. These statistical characteristics are presented to provide some insight on the behaviour of the cyclones in the Bay of Bengal.

Annual number of TCs – This is the total number of cyclones that occur in one calendar year.

Annual sum of NTA – NTA has been defined earlier which is a measure of the strength of a cyclone. Annual sum of NTA measures the total energy that exists in all TCs that occur in a year. It only measures the energy of TC as displayed in wind speed and excludes that of tropical depression or other atmospheric disturbances.

Landfall Recurrence (*LR*) – This is the relative frequency of cyclones making landfall in the proximity (within 100 nautical miles) of another cyclone's path within a 12-month period (or 14-month period to include two consecutive cyclone seasons). In other words, it is the ratio of the number of TCs which land within 100nm of another cyclone's path to the total number of TCs formed in the Bay of Bengal in two consecutive post-monsoon (Oct-Nov) periods. This has implications in that people especially the farmers can get into great hardship if they are hit again before they have time to recover from the previous onslaught.

Intensification Rate (*IR*) – This is the fastest recorded rate of increase in surface wind speed of a cyclone near its centre. This index would capture the rapid intensification character of a cyclone.

Number of Curvature Reversals (*NCR*) – It is the number of reversals (or points of inflection) in the curvature of a cyclone's track. This index is supposed to capture the degree of uncertainty of a cyclone's path. In fact, this index and the next index is a simple attempt to capture some aspects of the fractal dimensions (for details see Peitgen et al. 1993) of a cyclone's track.

Curvature Ratio (*CR*) – It is the ratio of the total distance traversed by a cyclone to the straight line distance at the transition points with tropical depression stage and dissipating stage. A TC is assumed to be formed when the maximum sustained surface winds (MSSW) is 34 knots or above. This is expected to be an independent characteristic of a cyclone because the cyclones are relatively sparse in the Bay of Bengal, and therefore, there is no or very little interaction between cyclones such as the Fujiwhara effect.

Tropical Cyclone Duration (*TCD*) – It is the lifetime of a cyclone beginning at the transition from tropical depression and ending at the transition into dissipating stage.

Median Translation Speed (*MTS*) – the median velocity of the steering current that moves the eye of the cyclone.

Maximum Sustained Surface Winds (*MSSW*) – It is the maximum surface wind speed near the centre of the organized wind circulation averaged over a ten-minute period.

Table 1 - Some statistical properties of cyclones in the Bay of Bengal.

Variable name	Mean	Standard deviation	Annual trend
Annual number of TCs	3.16	1.46	0.024
Annual sum of NTA	8.10	4.77	0.083
Biennial LR	0.53	0.28	0.000
Annual average IR	1.72 knots/hr	0.63	0.026
Annual average NCR	1.91	1.37	0.028
Annual average CR	1.19	0.18	0.001
Annual average TCD	76.32 hours	23.64	0.221
Annual average MTS	7.98 knots	1.91	–0.016
Annual average MSSW	66.08 knots	15.26	0.103
Annual maximum MSSW	91.08 knots	30.89	0.699

Pearson correlation coefficients between some of these statistical characteristics are presented in Table 2.

Table 2 - The Pearson correlation matrix of some of statistical characteristics.

Indices	NTA	TCD	IR	MTS	NCR
TCD	0.762 (Significant at 0.01 level)				
IR	0.544 (Significant at 0.01 level)	0.325 (Significant at 0.01 level)			
MTS	– 0.128	– 0.344 (Significant at 0.01 level)	0.076		
NCR	0.543 (Significant at 0.01 level)	0.622 (Significant at 0.01 level)	0.285 (significant at 0.01 level)	– 0.213 (significant at 0.05 level)	
CR	0.218 (significant at 0.05 level)	0.445 (significant at 0.01 level)	0.105	– 0.307 (significant at 0.01 level)	0.279 (significant at 0.01 level)

5. STATISTICAL MODELLING

Statistical modelling in this study has been done using the software packages SPSS and WEKA. SPSS is a commercial product which can be purchased from www.spss.com. WEKA is an open source data mining tool developed at The University of Waikato, New Zealand. The software is downloadable for free from the website http://www.cs.waikato.ac.nz/ml/weka/. WEKA is written in java and therefore can be used with any platform. WEKA has graphical user interface (GUI) and therefore there is no need to write the code to run any programme. To learn how to use WEKA in real world application, the reader is referred to Ali and Wasimi (2007).

The first step that was undertaken in the development of the statistical model using SPSS was to perform a principal component analysis of the input variables. This yielded nine significant principal components. It was therefore decided for simplicity that each model – one on NTA and the other on recurvature – will be allowed to have a maximum of nine independent variables and no two of them can have a cross-correlation which has been identified as significant in the correlation analysis procedure. For the NTA model a stepwise linear regression model was adopted. In the first iteration the two independent variables which were selected by the procedure are SLP_{t-2}, and $D57T_{t-2}$, where $D57T_{t-2}$ is the subsurface water temperature at a depth of 57 meters two months earlier. The first procedure yielded an R-square value of 0.62. Next these two variables were removed from the database and stepwise regression was done again. In the second iteration SST_{t-2} was selected. For the third iteration SST_{t-2} was removed from the database before rerunning the stepwise regression procedure, which resulted in $Wind_{t-2}$ to be selected as the next variable. The procedure kept on being repeated till nine independent variables were selected which

ultimately yielded an R-square value of 0.84. For the recurvature model a similar procedure was followed. In the first iteration SST_SD_{t-2} was selected, in the second iteration $CWind\_SD_{t-2}$ was selected, and so on; where SST_SD_{t-2} is the standard deviation of SST within MDR and $CWind\_SD_{t-2}$ is the standard deviation of the curl of the wind within MDR.

The regression models applied here are limited by the fact that they assume linearity in the relationships which is hardly ever true in the real world. To assess the nonlinearity of the problems two techniques on artificial intelligence using WEKA were applied to the data; one is artificial neural networks (ANN) and the other is the support vector machines (SMO). For the NTA model ANN yielded an R-square value of 0.94 and SMO yielded an R-square value of 0.81 compared to 0.84 by linear regression for nine independent variables. So far, the analyses have been essentially curve fitting exercises and their suitability as a predictive tool can only be judged if part of the data is used for model development and the rest of the data are used for model testing. The industry practice is to use 70% of the data for training and 30% of the data for testing. With testing for predictability, the ANN approach turned out to be the best in selecting the number of the independent variables that is most suitable for prediction. The ANN approach for the best NTA model suggested that six independent variables be used, which are SLP_{t-2}, $D57T_{t-2}$, SST_{t-2}, $Wind_{t-2}$, LHF_SD_{t-2}, and VW_Sheart_{t-1}; where LHF stands for latent heat flux and VW_Shear is vertical wind shear. The ANN approach further suggested that the best recurvature model comprise of the four variables SST_SD_{t-2}, $CWind\_SD_{t-2}$, SLP_{t-2}, and $D57T_{t-2}$. The probability of correct prediction for NTA with these variables is around 0.70 and that for recurvature is around 0.61.

Conclusions

The main cyclone seasons in the Bay of Bengal are October-November and May, when devastating cyclones make landfall. Advance warning of the category of a cyclone is now available a few days ahead. Due to poor infrastructure in the region and agriculture being the primary economic activity, a forecast of few weeks or months in advance would be of immense benefit to the population. With that in view a forecasting model comprised of hydro-climatic variables with a forecast lead time of several months was attempted. It has been found that development of such a model is possible which would be able to predict if a powerful cyclone is likely or unlikely in the coming season with about a months lead time. Few of the interesting discoveries made during this modelling exercise are that ENSO has no influence on the predictability nor does the land temperature. The factors that control the formation of future cyclones entirely lie within the main development region. Whereas the absolute values of the hydro-meteorological parameters tend to influence the NTA or cyclones' energy, it is the variation of these parameters within MDR that tend to influence the recurvature. It should however be pointed out here that the analysis has been done with limited data. The conclusions could be different if longer periods of data are analysed or a different ocean used.

The statistical analysis in this study was mostly confined within the framework of regression analysis, and the final result was the selection of the hydro-meteorological variables that can serve as explanatory variables. No final regression model has been presented in order to leave the option to an analyst of selecting any linear or nonlinear models. The cyclones that hit the coast of Bangladesh are fairly predictable in terms of time of the year when they can be expected but unpredictable as to their ferocity and track. The modelling approach suggested in this paper is capable of predicting the likelihood of these two characteristics about a month in advance. For a more useful picture on prediction, coupling a hydrodynamic model depicting the storm surge with the statistical model is warranted because destructions are not caused so much by the wind as by the storm surge.

References

Aberson, S.D., 2009, Regimes or cycles in tropical cyclone activity in the North Atlantic. *Bull. Amer. Meteor. Soc.* January. 39-43. Doi: 10.1175/2008BAMS2549.1.

Ali, A., 1996, Vulnerability of Bangladesh to climate change and sea level rise through tropical cyclones and storm surges. *Water Air and Soil Pollution*, 92, 171-179.

Ali, S. and Wasimi, S.A., 2007, *Data Mining: Methods and Techniques*. Thomson, Australia. pp. 299.

Atkinson, G.D. and Holliday, C.R., 1977, Tropical cyclone minimum sea level pressure/maximum sustained wind relationship for the western North Pacific. *Monthly Weather Review*, 105, 421-427.

Brown, D.P., Franklin, J.L., and Landsea, C., 2009, A fresh look at tropical cyclone pressure-wind relationships using recent reconnaissance-based "best track" data (1998-2005). NOAA/NWS/NCEP/Tropical Prediction Centre, Miami, Florida. URL: http://ams.confex.com/ams/pdfpapers/107190.pdf. Accessed on 17 April 2009.

Camargo, S.J., Emanuel, K.A., and Sobel, A.H., 2007, Use of a genesis potential index to diagnose ENSO effects on tropical cyclone genesis. *Journal of Climate*, 20, 4819-4834.

DeMaria, M., Knaff, J.A., and Connell, B.A., 2001, A tropical cyclone genesis parameter for the North Atlantic. *Weather and Forecasting*, 16, 219-233.

Dvorak, V.F., 1984, *Tropical cyclone intensity analysis using satellite data*. National Oceanic and Atmospheric Administration, Washington, DC, NOAA-TR-NESDIS-11.

Dvorak, V.F., 1975, Tropical cyclone intensity analysis and forecasting from satellite imagery. *Monthly Weather Review*, 103, 420-462.

Emanuel, K., 2008, The hurricane-climate connection. *Bull. Amer. Meteor. Soc.* May. ES10-ES20. Doi: 10.1175/BAMS-89-5-Emanuel.

FNMOC, 1998, Data base description for global tropical cyclone tracks (GTCT). Public release for distribution by Fleet Numerical Meteorology and Oceanography Centre, Asheville.

Frank, W.M. and Young, G.S., 2007, The interannual variability of tropical cyclones. *Monthly Weather Review*, 135(10), 3587-3598.

Islam, T. and Peterson, R.E., 2009, Climatology of landfalling tropical cyclones in Bangladesh 1877-2003. *Natural Hazards*, 48, 115-135.

JTWC, Annual Tropical Cyclone Reports, Joint Typhoon Warning Centre, Pearl Harbor, Hawaii.

Khaliq, M.N., Ouarda, T.B.M.J., Gachon, P., Sushama, L., and St-Hilaire, A., 2009, Identification of hydrological trends in the presence of serial and cross correlations: A review of selected methods and their application to annual flow regimes of Canadian rivers. *Journal of Hydrology,* 368, 117-130.

Khan, T.M.A., Singh, O.P., and Rahman, M.S., 2000, Recent sea level and sea surface temperature trends along the Bangladesh coast in relation to the frequency of intense cyclones. *Marine Geodesy*, 23, 103-116.

Kotal, S.D., Kundu, P.K., and Bhowmik, S.K.R., 2009, Analysis of cyclogenesis parameter for developing and nondeveloping low-pressure systems over the India Sea. *Natural Hazards*, Doi 10.1007/s11069-009-9348-5.

Kotal, S.D., Bhowmik, S.K.R., Kundu, P.K., and Das, A.K., 2008, A statistical cyclone intensity prediction (SCIP) model for the Bay of Bengal. *J. Earth Syst. Sci.,* 117(2), 157-168.

Kwon, H.J., Lee, W.-J., Won, S.-H., and Cha, E.-J., 2007, Statistical ensemble prediction of the tropical cyclone activity over the western North Pacific. *Geophysical Research Letters*, Vol. 34, L24805. Doi: 10.1029/2007GL032308.

Lee, C.-S., Cheung, K.K.W., Hui, J.S.N., and Elseberry, R.L., 2008, Mesoscale features associated with tropical cyclone formations in the western North Pacific. *Monthly Weather Review*, 136(6), 2006-2023.

Mandal, M., Mohanty, U.C., Sinha, P., and Ali, M.M., 2007, Impact of sea surface temperature in modulating movement and intensity of tropical cyclones. *Natural Hazards*, 41, 413-427.

Miller, I. and Miller, M., 1999, *John E. Freund's Mathematical Statistics*. (6th ed). Prentice Hall, Englewood Cliffs, New Jersey, USA.

Nicholls, N., 2001, Atmospheric and climatic hazards: Improved monitoring and prediction for disaster mitigation. *Natural Hazards*, 23, 137-155.

Peitgen, H.-O., Jurgens, H., and Saupe, D., 1993, *Chaos and Fractals: New Frontiers of Science*. Springer, New York. pp. 984.

Ralph, T.U. and Gough, W.A., 2009, The influence of sea-surface temperatures on Eastern North Pacific tropical cyclone activity. *Theoretical and Applied Climatology*, 95(3-4), 257-264.

Singh, O.P., Khan, T.M.A., and Rahman, M.S., 2001, Has the frequency of intense tropical cyclones increased in the north Indian Ocean? *Current Science*, 80(4), 575-580.

Vecchi, G.A. and Soden, B.J., 2007, Effect of remote sea surface temperature change on tropical cyclone potential intensity. *Nature*, Vol. 450. Doi: 10.1038/nature06423.

Webster, P.J., Holland, G.J., Curry, J.A., and Chang, H.-R., 2005, Changes in tropical cyclone number, duration, and intensity in a warming environment. *Science*, 309, 1844-1846.

Xu, Z.X., Takeuchi, K., Ishidaira, H., and Li, J.Y., 2005, Long-term trend analysis for precipitation in Asian Pacific FRIEND river basins. *Hydrological Processes*. 19. 3517-3532.

Zeng, Z., Wang, Y., and Wu, C.-C., 2007, Environmental dynamical control of tropical cyclone intensity – An observational study. *Monthly Weather Review*, 135(1), 38-60.

ON DEVELOPING A TROPICAL CYCLONE ARCHIVE AND CLIMATOLOGY FOR THE SOUTH INDIAN AND SOUTH PACIFIC OCEANS

Y. Kuleshov[1], L. Qi[1], R. Fawcett[1], D. Jones[1], F. Chane-Ming[2], J. McBride[3] and H. Ramsay[3]

[1]National Climate Centre, Australian Bureau of Meteorology, GPO Box 1289, Melbourne, Victoria 3001, Australia

[2]Laboratoire de l'Atmosphère et des Cyclones, UMR CNRS-Météo-France-Université de la Réunion, La Réunion, France

[3]Centre for Australian Weather and Climate Research, Bureau of Meteorology, GPO Box 1289, Melbourne, Victoria 3001, Australia

Abstract

Tropical cyclones (TCs) are the most dangerous and damaging weather phenomena to regularly affect countries in the South Indian Ocean (SIO) and the South Pacific Ocean (SPO). The year-to-year impact varies, and historical records demonstrate significant interannual variability in TC frequency and spatial distribution. Additionally, the climate is changing on a global scale and it is important to understand how a warmer climate may affect TC activity. To confidently assess whether significant change in TC activity has occurred, and in which direction, a reliable and homogeneous TC database is essential. To address this important scientific question, the TC archive for the Southern Hemisphere (SH) has been developed at the National Climate Centre, Australian Bureau of Meteorology and it is now consists of the TC best track data for the 1969/70 – 2006/07 TC seasons. Based on the data from the SH TC archive, influence of the El Niño-Southern Oscillation (ENSO) phenomenon on TC activity has been examined and a comprehensive TC climatology for the SIO and SPO has been developed. Data from the SH TC archive have been stratified between El Niño and La Niña years, and significant changes in TC occurrences and cyclogenesis in terms of geographical distribution and intensity of maxima have been found. TC characteristics such as cyclone hours, system density, system flux, system intensity and intensity tendency have been computed. Sea surface temperature, vertical wind shear, lower tropospheric vorticity and mid-tropospheric relative humidity have been investigated as primary large-scale environmental parameters to examine their contribution to variations in TC characteristics related to the warm and cold ENSO phases. From the results of the composite analysis, it has been found that each individual field studied here can explain some of the TC variations. The major mechanisms through which ENSO affects TC activity across the SIO and the SPO are discussed.

Changes in TC occurrences in the SH, the SIO and the SPO have also been analysed over the 26-year period 1981/82 to 2006/07, as complete TC intensity records in the SH TC archive start in 1981/82. Over this period, there are no significant trends in the annual numbers of TCs (SPO, SIO, SH) attaining a life-time mean central pressure of 995 hPa or lower, and the numbers of severe TCs (mean central pressure of 970 hPa or lower) in these three regions. Positive trends in 945 hPa and 950 hPa TCs in the SIO (and consequently the SH) are statistically significant, but appear to be influenced to some extent by changes in data quality. As TC observation and analysis techniques in the regions of the SH evolved, the trends in TC numbers appear to be affected, at least to some extent, by step changes which may reflect data homogeneity issues. However, given the theoretical expectation that the response to the warming oceans will be in the number of most intense cyclones, it is also possible that the trends are indicative of this physical effect. Given concerns over the data quality, re-analysis of the historical TC data is required to obtain globally homogeneous records and to address the important question of how TC activity is changing and it possible relationship to global climate change.

Key Words

Tropical cyclones, El Niño-Southern Oscillation, South Indian Ocean, South Pacific Ocean, trends

INTRODUCTION

In *Climate Change 2007*, the Fourth Assessment Report of the United Nations Intergovernmental Panel on Climate Change (IPCC), it is stated that warming of the climate system is unequivocal and most of the observed increase in globally averaged temperatures since the mid-20th century is very likely due to the observed increase in anthropogenic greenhouse gas concentrations [IPCC 2007]. Climate change and associated climatic hazards affect different regions in different ways, even within one continent or over the same ocean basin. Therefore, studies on regional impact of climate change are of high importance. Tropical cyclones (TCs) are the most dangerous and damaging weather phenomena to regularly affect countries in the tropics. Historical records demonstrate significant interannual variability in TC frequency and spatial distribution of TC tracks and as a result the year-to-year TC impact varies. Additionally, rising concentrations of populations and infrastructure in coastal regions cause a significant increase in societal impact from TCs. For example, insured market losses from TCs in the North Atlantic (US, Caribbean, Mexico) in 2004 and 2005 were approximately US$115 bn and overall losses from the TC Katrina (August 2005) were estimated as US$120 bn [Munich Re, 2006]. As the climate is rapidly changing, it is important to understand how a warmer climate may affect global and regional TC activity. Consequently, trends in TC occurrences and intensity, and possible physical mechanisms for change, have been widely discussed.

One of the important large-scale environmental contributors governing TC genesis and development is ocean thermal energy. Tropical ocean sea surface temperatures (SSTs) increased by approximately 0.5°C between 1970 and 2004 [Agudelo and Curry 2004] and it is very likely that this warming of world's oceans is human-induced [Barnett *et al.* 2005]. Physical mechanisms of cyclone formation and development suggest strong relationship between TC activity and SSTs [Gray, 1968]. As the thermodynamic aspects have become more favourable for TC genesis and development it has lead to the hypothesis that TC intensity will increase with increasing global mean temperatures [Emanuel 1987, Holland 1997, Knutson and Tuleya 2004]. To verify this hypothesis, changes in TC occurrences and intensities over various ocean basins have been analysed based on observational data. Among the recent global observational analyses are those of Webster *et al.* (2005) who analysed TC changes over the period 1970 to 2004. This study found no global trend in the total number of TCs, but a shift towards stronger systems. Elsner *et al*. (2008), using data derived from a reanalysis of satellite records for 1981 to 2006 [Kossin *et al.* 2007] also found a widespread increase in the life-time maximum wind speeds of the strongest storms. Recently, Kuleshov *et al.* (2008) examined TC trends in the Southern Hemisphere (SH; specifically the area south of the equator, 30°E to 120°W). It was found that across the 1981/82 to 2005/06 TC seasons, there were no apparent trends in the total numbers of TCs, nor in the numbers of TCs with minimum central pressure of 970 hPa or lower, but a significant positive trend in the occurrence of severe TCs with minimum central pressure of 945 hPa or lower has been reported.

However, both thermodynamic and dynamic aspects are required to be favourable for TC genesis and development. Therefore factors of the tropical environment other than SSTs (*e.g.* vertical wind shear) are also critically important for TC intensification [Gray 1979, McBride 1995, Michaels *et al.* 2006], but significance of these thermodynamic and dynamic factors for TC formation and development vary over the different ocean basins. For example, examining the relationship between the seasonally averaged maximum potential intensity over the different ocean basins and the seasonal frequency of occurrence of intense TCs, Chan (2009) found that only in the Atlantic thermodynamic factors are responsible, but still only to a certain extent, for the climate variations of intense TCs; in other ocean basins, it appears that the dynamic factors are much more dominant. Chan (2008) also demonstrated that the frequency of intense TC occurrence in the western North Pacific undergoes a strong multi-decadal (16–32 years) variation due to similar variations in the planetary scale oceanographic and atmospheric conditions that govern the formation, intensification and movement of TCs; these latter variations are largely contributed by the El Niño and the Pacific Decadal Oscillation on similar time scales. Once again, it highlights importance of *regional* TC studies in order to better understand dominant large-scale environmental factors responsible for variations in TC activity.

Numerous studies on TC activity in various regions of the Northern and Southern Hemispheres have been completed with the aim to develop TC climatologies and to establish driving forces behind TC temporal and spatial variability. Many studies have focussed on relating TC activity to the El Niño-Southern Oscillation (ENSO) phenomenon. In the Northern Hemisphere, a significant reduction (*increase*) of TC activity is observed over the Atlantic basin during El Niño (*La Niña*) events [*e.g*. Gray 1984]. Significant spatial and temporal variations of TC activity over the western North Pacific associated with the ENSO phases have been reported [*e.g*. Chan 2000]. ENSO also affects TC frequency in the North Indian Ocean, with a reduction in TC activity over the Bay of Bengal during El Niño events [Singh *et al.* 2000]. In the SH, attempts to develop a TC climatology for the Australian region have been made by Holland (1984), who analysed data for the period 1958-1979, and Nicholls (1985) who examined records of Australian TC numbers from 1909/10 to 1982/83. A nonlinear rising trend, with fewer TCs observed at the beginning of the century, was attributed to improvements in observing systems and networks. However, variations in TC activity occur around this trend and Nicholls (1985) found a strong and stable relationship between TC numbers/TC days in the Australian region and Darwin pressure.

El Niño events cause TC activity in the South Pacific Ocean (SPO) to occur further eastward than normal and also to bring about a general suppression of TC activity in the Coral Sea and north Australian region [Gray 1988, Ramsay *et al*. 2008]. Basher and Zheng (1995), analysing spatial patterns and relationships of TCs in the western SPO to the Southern Oscillation Index (SOI) and SSTs, found that the geographical distribution of TC incidence shifts eastward and northward during negative SOI phases and vice versa. The western South Indian Ocean (SIO) is also a region of high TC activity in the SH – it accounts for 14% of global TC occurrences. Climatological associations and characteristics of TCs in the western SIO (5-25°S, 50-75°E) during 1972-1991 were studied by Jury (1993), however no statistically significant correlation between the SOI and TC numbers was found. The earlier studies on TC activity in different regions of the SH were mainly focussed on examining variations in TC occurrences [*e.g.* Holland 1984, Nicholls 1985, Basher and Zheng 1995, Kuleshov *et al.* 2009a]. However, a comprehensive TC climatology for the whole SH that includes other TC characteristics (*e.g*. intensity, density, flux, *etc*.) had not yet been developed. The present work applies a uniform statistical approach to analysis of TC activity in the SIO and the SPO with respect to changes in oceanic and atmospheric conditions related to the ENSO phenomenon. Changes in TC occurrences in the SH, the SIO and the SPO are also analysed and possible causes for trends are discussed.

1. TROPICAL CYCLONE ARCHIVE FOR THE SOUTHERN HEMISPHERE

To accurately assess whether a significant change in TC activity has occurred in the historical records, a reliable and homogeneous TC database is essential. In the report of the IPCC's Working Group I it is stated that "There is observational evidence for an increase in intense tropical cyclone activity in the North Atlantic since about 1970, correlated with increases of tropical sea surface temperatures. There are also suggestions of increased intense tropical cyclone activity in some other regions where concerns over data quality are greater. Multi-decadal variability and the quality of the tropical cyclone records prior to routine satellite observations in about 1970 complicate the detection of long-term trends in tropical cyclone activity. There is no clear trend in the annual numbers of tropical cyclones" [IPCC 2007]. As a result of many years of international collaborative efforts, a comprehensive SH data set based on the official best tracks of the World Meteorological Organization Regional Specialised Meteorological Centres and Tropical Cyclone Warning Centres in the Southern Hemisphere has been assembled. The first attempt to prepare a consolidated archive of TCs for the SH was by Kuleshov and de Hoedt (2003). More recently, the TC archive for the SH (the SHTC) has been further developed at the National Climate Centre (NCC), Australian Bureau of Meteorology [Kuleshov *et al.* 2008] and it is now consists of the TC best track data for the 1969/70 – 2006/07 TC seasons.

Based on the data from the SHTC archive, the present study is aimed at summarising the extensive existing knowledge by applying a uniform approach to analysis of TC activity in the SIO (defined here as the area west of 135°E) and the SPO (defined here as the area east of 135°E). The division of the SH into the SIO and SPO in the current study is derived from the local minimum in the average annual number of TCs at around 130°E to 135°E [Kuleshov *et al.* 2009b]. Our

analysis only considers TCs from the 1981/1982 SH TC season onwards, as complete TC intensity records in the SHTC archive start from that season.

2. CLIMATOLOGY

To analyse characteristics of the TC climatology, we have employed the NCC's vortex tracking computer package. The package is a set of FORTRAN programmes that generate a wide range of statistics based on the data from the SHTC archive. The package was originally developed at the University of Melbourne, and subsequently further developed and updated at the Australian Bureau of Meteorology [Murray and Simmonds 1991, Jones 1994]. The package statistics are derived from the individual TC positions using a dual process of interpolation. The first step involves interpolation in the time domain, using bicubic splines to compute the intermediate data along the tracks based on the raw system positions. This is to ensure consistency of statistics along system tracks. The second interpolation involves the distribution of data from the raw and interpolated systems using a Cressman weighting scheme applied to the specified output grid. In this study, TC characteristics such as cyclone hours, system density, system flux, system intensity and intensity tendency have been computed using the methodology described in detail in Jones (1994). In the SPO, a noticeable eastward displacement of TC genesis position during El Niño seasons compared to La Niña seasons (see Kuleshov *et al*. (2008) for a list of these ENSO seasons) is observed, in agreement with the earlier studies.

Analysis of TC hours stratified by ENSO warm and cold phases reveals an area with increased TC hours over the eastern part of the SIO during La Niña seasons. The opposite relationship occurs over the northern regions of the SPO – that is, increased TC hours are noted during El Niño seasons with two major maxima located in the Coral Sea and around Vanuatu (Figure 1).

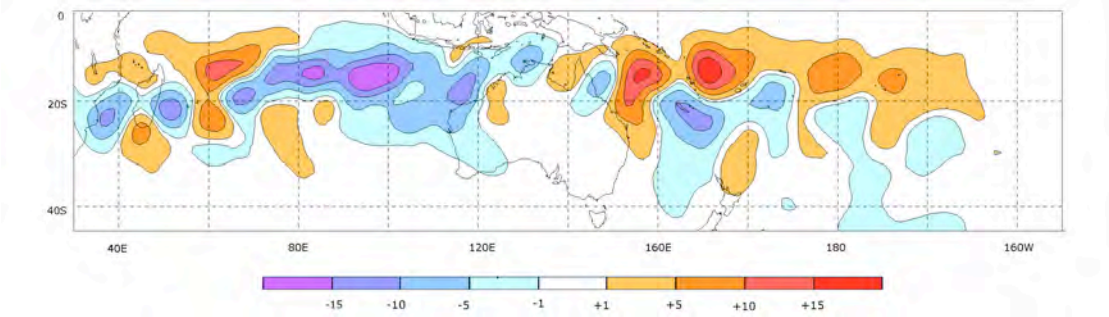

Figure 1 - The TC hour difference between El Niño seasons and La Niña seasons.

ENSO has a significant impact on the annual average TC transport, as shown by the differences between El Niño and La Niña seasons in Figure 2. In La Niña seasons the peak fluxes over the SIO are higher than those in El Niño seasons, while in the SPO, the fluxes in La Niña seasons are somewhat weaker than those in El Niño seasons (Figures not shown). The major flux centre in the SH is located at about 65°E in the SIO (Figure 2).

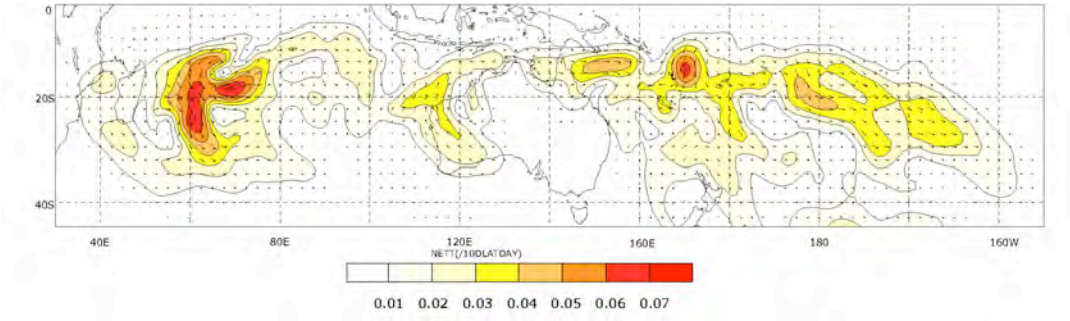

Figure 2 - Difference in average annual TC transport between El Niño seasons and La Niña seasons.

The climatological location of average annual TC intensity reveals that generally TCs intensify while moving in the areas between the equator and around 20°S, and then weaken in the higher latitudes, presumably as they encounter colder SSTs and stronger vertical wind-shear associated with mid-latitude systems. In El Niño seasons, there are four major maxima of TC intensity located along about 20°S and positioned around 90°E, 115°E, 165°E and 155°W, respectively (Figure 3).

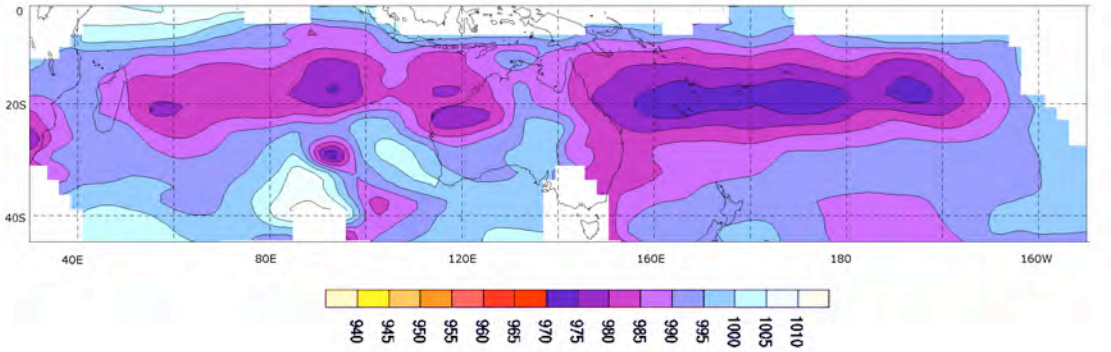

Figure 3 - Average annual TC intensities for El Niño seasons.

Over the SPO during La Niña seasons (Figure 4), the area with TC mean central pressure 980 to 970 hPa is significantly weaker than in El Niño seasons. The region of maximum intensity (970-980 hPa) around 90°E in the SIO during El Niño seasons (Figure 3) is not evident during La Niña seasons (Figure 4), while another TC intensity centre in the area around 20°S, 115°E intensifies in La Niña seasons – representing the area of the most intense TC activity in the Australian region (Figure 4). The results from the TC intensity tendency analysis demonstrate that, over the SIO and the SPO, cyclone systems mostly develop in the areas north of about 20°S, and start to weaken south to it.

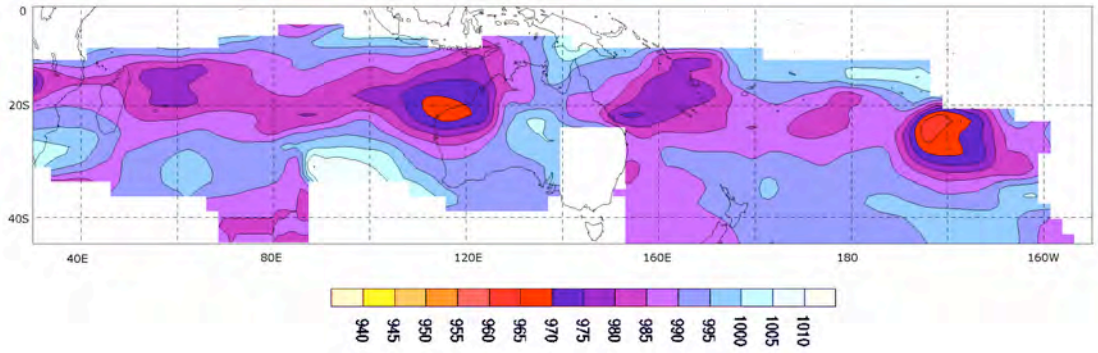

Figure 4 - Average annual TC intensities for La Niña seasons.

SST, vertical wind-shear, lower tropospheric vorticity and mid-tropospheric relative humidity are investigated in this study as primary large-scale environmental parameters to examine their contribution to variations in TC characteristics related to the ENSO phenomenon. From the results of the composite analysis, it is found that each individual field studied here can explain some of the TC variations. Composites have been carried out for El Niño and La Niña seasons of the large scale parameters known to have an influence on tropical cyclogenesis on a climatological basis, following Gray (1968), McBride (1995) and others. Care should be taken in interpreting these results as all interannual variations of all six of the components of the Gray genesis parameter are themselves highly correlated to indices of ENSO; so the parameters are not independent. In the Northern Hemisphere, particularly the North Atlantic, it is well established that ENSO affects interannual variability of TC activity primarily through vertical wind-shear variations [*e.g.*, Gray 1984]. In the Southern Hemisphere it is less obvious that this should be the case. This is because the SH cyclogenesis regions are characterised by quite large values of vertical wind-shear, with a

north-south gradient of strong westerly shear pole-ward of 20°S and a tendency towards weak or even easterly shear near the equator. This is supported by our findings in which the El Niño *versus* La Niña shear differences are not easily interpreted (not shown). Similarly the SST difference composites (also not shown) simply reproduce the large scale structure of the SST patterns of ENSO and show little or no *in-situ* relationship to TC activity.

Physically, one would expect modification of SH cyclone behaviour by ENSO to be through the vertical motion fields, associated with the well-documented variations in the upward and downward branches of the Walker Cell with ENSO, and through low-level vorticity. The reason for the latter is that ENSO affects the strength of the easterly and westerly winds close to the equator. Given a much smaller influence on the trade winds pole-ward of 20°S, this variation in low-latitude zonal flow will bring about large differences in the vorticity of the monsoon trough. For example, in an El Niño event the low-latitude westerlies extend far into the central Pacific, bringing about a monsoon trough and low-level cyclonic vorticity far into the central Pacific.The Gray genesis parameter does not contain large scale vertical motion. This field is represented through the proxy of mid-level relative humidity which has a positive anomaly when the vertical motion is upward and a negative anomaly when there is subsidence. The composites of low-level vorticity and relative humidity are shown in the upper and lower panels of Figure 5.

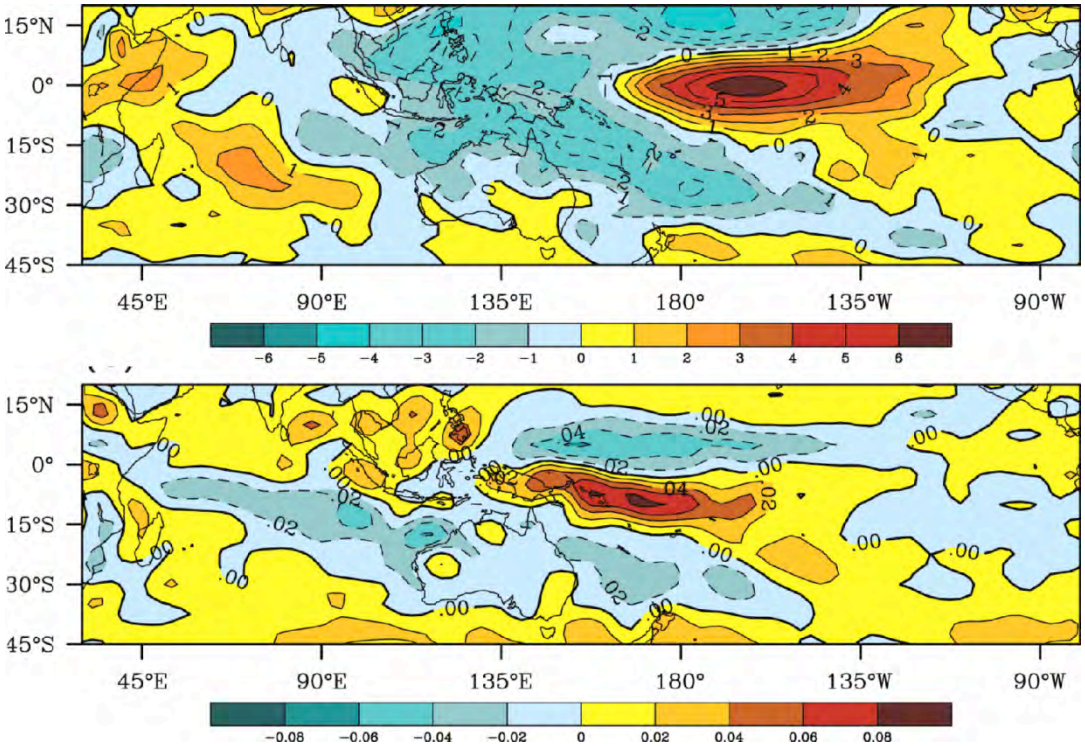

Figure 5 - Differences between El Niño seasons and La Niña seasons. Upper panel: Relative humidity difference: the actual field is a composite of relative humidity anomaly in El Niño seasons; Lower panel: Low level relative vorticity difference: the plot is a relative vorticity anomaly composite in La Niña seasons.

As can be seen from casual inspection of Figure 5, the major mechanism through which ENSO affects TC activity across the SPO is through large-scale vertical motion, which provides convection and so feeder or precursor convective systems, and through the relative vorticity in the monsoon trough, mainly through the changes in the low-latitude westerlies equator-ward of the trough. Some of these conclusions were previously obtained by Ramsay *et al.* (2008).

3. TRENDS

Trends in TC occurrences and intensity, and possible physical mechanisms for change, have much been discussed widely in recent years [Webster *et al.* 2005, Emanuel 2005, Kuleshov *et al.* 2008]. A major uncertainty with all analyses of TC intensity, in particular, is that of data homogeneity and quality. Analysing interannual variability of TCs near Australia with implications for the response to global warming [McBride, 2008], we further inspected the SHTC archive and learned that the increased occurrences of the strongest TCs around Australia may be partially attributed to in homogeneities in the data. Similar conclusions have been made for the Northern Hemisphere [Landsea *et al.* 2006]. In this study, the statistical significance of the linear trends in the various TC time series was assessed in three ways. The first is the standard linear regression approach, based on the assumption of identically independently normally distributed residuals. Because the TC data, being (non-negative) integer-valued, depart considerably from this assumption, we have also calculated the statistical significances by Monte Carlo simulation (5,000 iterations) involving resampling the time series with and without replacement. It is important to note that any linear trends (whether real or only apparent) in the TC data cannot be extrapolated indefinitely into the past or future, because such a trend would (necessarily) eventually predict a negative annual TC count (on the one hand), or in the case of the intense TC counts (possibly) contradict an opposing trend in total TC numbers (on the other hand). It is likewise very difficult to distinguish between a linear trend and oscillatory behaviour with periodicity more than twice the length of the data from an inspection of the data alone. Therefore, we have also subjected the TC time series to two single break-point testing procedures, a parametric one based on the null hypothesis that the data are normally distributed, and an analogous non-parametric one based on the Mann-Whitney statistic [Pettitt 1979], the non-parametric one being of greater relevance given the characteristics of the data. A minimum of four seasons either side of the break was imposed in the assessment. One motivation for the use of break-point analysis is that it can identify artificial changes in the data which might not be evident in trends or raw time-series. The two most critical issues impacting on the homogeneity of TC records, and the associated confidence in climate change analyses, is changes in analysis practice and changes in the quality of satellite data. If step changes in the TC data coincide with known changes in data or practices then a case might be made for the change to be artificial.

Lastly, because both these approaches (linear regression and breakpoint analysis) merely lead to the rejection of the null hypothesis of no change, without establishing the departure from no change as being specifically linear or step-change (for example), we have compared three competing models (constant, linear, step-change) under leave-one-season-out cross-validation, to determine which of the three models generates the least root-mean-square-error (RMSE). Analysing TC occurrences, the following intensity thresholds (in terms of mean central pressure) were used: 995 hPa or lower (*970 hPa or lower*) for a system to be counted as a TC (*a severe TC*). Examining changes in severe TCs, six thresholds were explored – 945, 950, 955, 960, 965 and 970 hPa, to explore the consistency of the results for severe TCs. Changes in TC occurrences in the SH, the SIO and the SPO were analysed over the 26-year period 1981/82 to 2006/07. Over this period, there are no significant trends in the annual numbers of TCs (SPO, SIO, SH) attaining a life-time mean central pressure of 995 hPa or lower, and the numbers of severe TCs (mean central pressure of 970 hPa or lower) in these three regions. Positive trends in 945 hPa and 950 hPa TCs in the SIO (and consequently the SH) are statistically significant, but appear to be influenced to some extent by changes in data quality and therefore should not be taken at face value. As TC observation and analysis techniques in the regions of the SH evolved, the trends in TC numbers appear to be affected, at least to some extent, by step changes which may reflect data homogeneity issues. On the other hand, theory and modelling suggest that an increase in TC intensity is a possible response to the increase of global temperatures. Investigation of physical mechanisms responsible for TC variability will be a topic of further research.

Concluding remarks

A comprehensive Southern Hemisphere Tropical Cyclone archive based on the official best tracks of the World Meteorological Organization Regional Specialised Meteorological Centres and Tropical Cyclone Warning Centres has been developed. Data from the SHTC archive have been stratified between El Niño and La Niña years, climatology of TCs over the SIO and SPO has been

analysed and significant changes in TC occurrences and cyclogenesis in terms of geographical distribution and intensity of maxima have been found. Trends in occurrences of TCs in the SH, the SIO and the SPO have been examined in detail. For the 1981/82 to 2006/07 period, there are no apparent trends in the total numbers of TCs reaching 995 hPa, and the numbers of severe TCs (mean central pressure of 970 hPa or lower) in these three regions. Positive trends in 945 hPa and 950 hPa TCs in the SIO (and consequently the SH) are statistically significant, but appear to be influenced to some extent by changes in data quality. However, given the theoretical expectation that the response to the warming oceans will be in the number of most intense cyclones, it is also possible that the trends are indicative of this physical effect.

Attempts have been made to prepare consolidated TC datasets [*e.g*. Kossin *et al.* 2007, Kuleshov *et al.* 2008] and there are further plans to continue these efforts [*e.g.* Knapp *et al*. 2009]. However, consolidation of historical data from various regions is currently limited by the inhomogeneity of TC observation and analysis practice. It is essential to initiate an international project on re-analysis of the historical TC data under the World Meteorological Organization's umbrella in order to obtain globally homogeneous records which are required to address the important question of how TC activity is changing and it possible relationship to global climate change.

References

Agudelo, P. A., and J. A. Curry, 2004: Analysis of spatial distribution in tropospheric temperature trends, *Geophys. Res. Lett.* **31**, L22207, doi:10.1029/2004GL020818

Barnett, T. P., D. W. Pierce, K. M. AchutaRao, P. J. Gleckler, B. D. Santer, J. M. Gregory, W. M. Washington, 2005: Penetration of Human-Induced Warming into the World's Oceans, *Science*, 8 July 2005, Vol. 309. no. 5732, 284 – 287, DOI: 10.1126/science.1112418

Basher, R.E. and Zheng, X., 1995: Tropical cyclones in the Southwest Pacific: spatial patterns and relationships to Southern Oscillation and sea surface temperature. *J. Climate*, **8**, 1249-1260.

Chan, J.C.L., 2000: Tropical cyclone activity over the western North Pacific associated with El Niño and La Niña events. *J. Climate*, **13**, 2960-2972.

Chan, J. C. L., 2008, Decadal variations of intense typhoon occurrence in the western North Pacific, Proc. R. Soc. A, **464**, no. 2089, 249-272, doi: 10.1098/rspa.2007.0183.

Chan, J. C. L., 2009, Thermodynamic control on the climate of intense tropical cyclones, *Proc R Soc A,* **465,** no 2110, 3011-3021, doi:10.1098/rspa.2009.0114.

Elsner, J. B, J. P. Kossin and T. H. Jagger, 2008, The increasing intensity of the strongest tropical cyclones, *Nature, 455*, 92-95 doi:10.1038/nature07234.

Emanuel, K. A., 1987, The dependence of hurricane intensity on climate. *Nature, 326*, 483–485

Gray, W.M., 1968: Global view of the origin of tropical disturbances and storms. *Mon Wea. Rev.*, **96**, 669-700.

Gray, W.M., 1979: Hurricanes: Their formation, structure and likely role in the tropical circulation. *Meteorology over the Tropical Oceans*, D.B. Shaw, Ed., Royal Meteorological Society, 155-218.

Gray, W.M., 1984: Atlantic seasonal hurricane frequency. Part I: El Niño and 30 mb quasi-biennial oscillation influences. *Mon. Wea. Rev*., **112**, 1649-1668.

Gray, W.M., 1988: Environmental influences on tropical cyclones. *Aust. Meteor. Mag*., **36**, 127-139.

Holland, G.J., 1984: On the climatology and structure of tropical cyclones in the Australian / southwest Pacific region: I. Data and tropical storms. *Aust. Meteor. Mag*., **32**, 1-15.

Holland, G. J., 1997, The maximum potential intensity of tropical cyclones. *J. Atmos. Sci. 54*, 2519-2541.

IPCC, 2007: IPCC WG1 AR4 Report: ipcc-wg1.ucar.edu/wg1/wg1-report.html

Jones, D.A., 1994: A numerical vortex finding, tracking, and statistics package. *BMRC Research Report*, No. **41**, 35pp.

Jury, M.R., 1993: A preliminary study of climatological associations and characteristics of tropical cyclones in the SW Indian Ocean. *Meteorol. Atmos. Phys*. **51**, 101-115.

Kossin, J.P., K.R. Knapp, D.J. Vimont, R.J. Murnane, and B.A. Harper, 2007: A globally consistent reanalysis of hurricane variability and trends. *Geophys. Res. Lett.,* **34**, L04815, doi:10.1029/2006GL028836.

Knapp, K. R., M. C. Kruk, D. H. Levinson, and E. J. Gibney, 2009: Archive compiles new resource for global tropical cyclone research, *Eos, Transactions, AGU*, **90**, 46, doi:10.1029/2009EO060002

Knutson, T. R. and R. E. Tuleya, 2004, Impact of CO_2-induced warming on simulated hurricane intensity and precipitation: Sensitivity to the choice of climate model and convective parameterization. *J. Clim. 17*, 3477–3495.

Kuleshov, Y., and G. de Hoedt, 2003: Tropical cyclone activity in the Southern Hemisphere. *Bull. Austral. Met. Ocean. Soc*., **16**, 135-137.

Kuleshov, Y., L. Qi, R. Fawcett and D. Jones, 2008: On the El Niño-Southern Oscillation and tropical cyclone activity and trends in the Southern Hemisphere, *Geophys. Res. Lett.,* **35**, L14S08, doi:10.1029/2007GL032983.

Kuleshov, Y., F. Chane-Ming, L. Qi, I. Chouaibou, C. Hoareau, and F. Roux, 2009a: Tropical cyclone genesis in the Southern Hemisphere and its relationship with the ENSO, *Ann. Geophys*., *27*, 2523-2538.

Kuleshov, Y., L. Qi, R. Fawcett, and D. Jones, 2009b: Improving preparedness to natural hazards: Tropical cyclone prediction for the Southern Hemisphere, in *Adv. Geosci.*, *12 Ocean Science* (ed. Gan, J.), World Scientific Publishing, Singapore, 127–143.

Landsea, C.W., B.A Harper, K. Hoarau, and J.A. Knaff, 2006: Can we detect trends in extreme tropical cyclones? *Science*, **313**, 452-454.

McBride, J.L: 1995: Tropical cyclone formation. Chapter 3 of Global Perspectives on Tropical Cyclones, edited by Russell Elsberry, World Meteorological Organization.

McBride, J.L., 2008: Interannual Variability of Tropical Cyclones Near Australia: Implications for the Response to Global Warming. *Eos Trans*. *AGU* **89**, West. Pac. Geophys. Meet. Suppl. Abstracts U34A-08.

Michaels, P. J., P. C. Knappenberger, and R. E. Davis, 2006, Sea-surface temperatures and tropical cyclones in the Atlantic basin. *Geophys. Res. Lett*., *33*, L09708, doi:10.1029/2006GL025757.

Munich Re, 2006: Hurricanes – More Intense, More Frequent, More Expensive: Insurance in a Time of Changing Risks. Available at

http://www.munichre.com/en/publications/default.aspx?id=790. Retrieved on 1 October 2009.

Murray, R.J. and I. Simmonds, 1991: A numerical scheme for tracking cyclone centres from digital data. Part I: development and operation of the scheme. *Aust. Meteor. Mag*., **39**, 155-166.

Nicholls, N., 1985: Predictability of interannual variations of Australian seasonal tropical cyclone activity. *Mon. Wea. Rev*., **113**, 1144-1149.

Ramsay, H.A., L.M. Leslie, P.J. Lamb, M.B. Richman, and M. Leplastrier, 2008: Interannual Variability of Tropical Cyclones in the Australian Region: Role of Large-Scale Environment. *J. Climate*, **21**, 1083–1103.

Pettitt A.N., 1979. A non-parametric approach to the change-point problem, *Appl. Statist.*, **28**, 126-135.

Singh, O.P., T.M.A. Khan, and M.S. Rahman, 2000: Changes in the frequency of tropical cyclones over the North Indian Ocean. *Meteorol. Atmos. Phys.*, **75**, 11-20.

Webster, P. J., G. J. Holland, J. A. Curry and H.-R. Chang, 2005, Changes in tropical cyclone number, duration, and intensity in a warming environment. *Science*, *309*, 1844-1846.

INTERNATIONAL BEST TRACK ARCHIVE FOR CLIMATE STEWARDSHIP (IBTrACS): SYNTHESIZING GLOBAL TROPICAL CYCLONE BEST TRACK DATA

David H. Levinson, NOAA NCDC, 151 Patton Ave., Asheville, NC
Paula A. Hennon, STG, Inc. 151 Patton Ave., Asheville, NC
Michael C. Kruk, STG, Inc. 151 Patton Ave., Asheville, NC
Kenneth R. Knapp, NOAA NCDC, 151 Patton Ave., Asheville, NC
Howard J. Diamond, NOAA NCDC, 151 Patton Ave., Asheville, NC

Abstract

This paper provides an overview of the best track dataset merging process used to develop a new global tropical cyclone dataset - the International Best Track Archive for Climate Stewardship (IBTrACS). The best track data provided in this archive are the positions and intensities (via minimum central pressure and maximum sustained wind) of each storm available from all resources and was derived using detailed quality assessments. In the process of merging the data from each of the forecast centres, statistics were calculated to provide information on the variations in position and intensities. Also, prior to merging the best track data, quality assessments of the position and intensity were made using objectively derived criteria. While some gross position errors were found and corrected, all intensity values were retained in the final data along with the quality assessment results. The IBTrACS positions and intensities are, therefore, the average position and intensity tracked by official forecast centres.

It has been demonstrated that in creating a new global tropical cyclone best track dataset, it is imperative that best track data be included from all forecast centres that tracked each storm operationally. This is especially critical when analyzing global tropical cyclones since using data from any one centre will likely result in missed tropical cyclones. One major advantage the IBTrACS dataset has over other best track data currently available is that it provides the full range of reported values for pressure, intensity, and position, for each 6-hr time step. This information was previously unavailable for assessing data quality and variance, and allows users to compare this information for assessing data reliability during the life-cycle of each TC when tracked by multiple centres.

Keywords

Tropical cyclones, hurricanes, typhoons, best track data, historical, archive, global

INTRODUCTION

Global tropical cyclone (TC) data have a wide variety of applications, including performing climate change research, determining appropriate building codes for coastal zones, assessing risk for emergency managers, and analyzing potential losses for insurance and business interests (Landsea et al. 2004). TC tracks are used in constructing automated analyses of tropical cyclones, such as performed by Kossin et al. (2007), which used the Hurricane Satellite (HURSAT) dataset (Knapp and Kossin 2007). Furthermore, tracks have been used to investigate changes in extreme rainfall from tropical cyclones (Lau et al. 2008). Thus, it is important to accurately understand the global distribution, frequency and intensity of tropical cyclones.

While numerous studies have investigated the global climatology of tropical cyclones, prior research generally has used a small subset of available best track data. For example, recently Emanuel (2005) and Klotzbach (2006) referenced data from two centres: the Joint Typhoon Warning Centre (JTWC, Chu et al. 2002), and the Hurricane Database[1] (HURDAT, Jarvinen et al. 1984) of the National Oceanic and Atmospheric Administration (NOAA). Although gathering and combining data from these two centres may provide data for all basins globally, numerous other agencies also compile best track data. Therefore, despite the importance and impact that TCs have worldwide, until recently there has been no publicly-available non-proprietary dataset that incorporates documented TC best track (BT) data for all TC-prone basins and from all available agencies. Optimally, best track data are the result of post-season reanalysis of a storm's position

[1] HURDAT is available at the following URL: http://www.nhc.noaa.gov/pastall.shtml#hurdat.

and intensity from all available data - for example, ship, surface and satellite observations - although the level of reanalysis will vary by agency and basin due to data availability. However, despite advances in observing system technologies, operational procedures and scientific knowledge, the historical record of best tracks remains inhomogeneous by construction (see Landsea et al. 2004).

To address this need NOAA's National Climatic Data Centre (NCDC), in concert with the World Data Centre for Meteorology – Asheville, has developed a comprehensive dataset of global tropical cyclone best track data. The goal of this effort is to inventory reported tropical cyclones worldwide along with their characteristics and to provide the data as one comprehensive global dataset: the International Best Track Archive for Climate Stewardship (IBTrACS, Knapp et al., 2009). In addition, the IBTrACS team adopted five governing principles to help define and guide the effort: global, open, provenance, ongoing, and accessibility (see Figure 1 for more details).

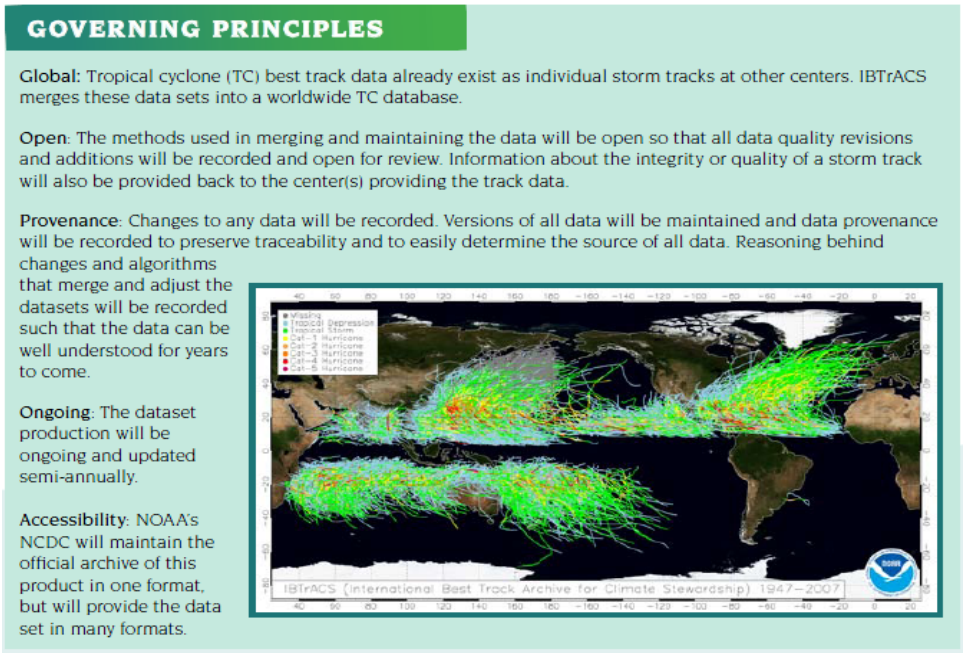

Figure 1- The five governing principles adopted as part of the IBTrACS dataset development.

It should be noted that the primary intent of IBTrACS is to support scientific research efforts. The IBTrACS data usage policy follows that of the WDC for Meteorology which employs a policy of full and open access to the data. Therefore, agreement has been reached with each of the Regional Specialized Meteorological Centres (RSMCs) that provided their best tracks to make the IBTrACS data open for distribution as a contribution to global tropical cyclone research. Coupled with the WDC policy for data access, the IBTrACS data access policy also adheres to the World Meteorological Organization's (WMO) Resolution 40 regarding such data exchange[2], and serves as the guide vis-a-vis any questions concerning the commercial use of the data.

Although IBTrACS is a logical extension of previous work carried out at NOAA's NCDC (Crutcher and Quayle, 1974; Neumann, 1999), no reference has been made to original land and ship reports, newspaper accounts, satellite pictures, aircraft reconnaissance reports, etc. such as is being conducted for the Atlantic basin (Fernandez-Partagas and Diaz, 1996; Landsea et al., 2004). Thus, IBTrACS is not a reanalysis; rather, it provides a collation of currently available best track data from agencies worldwide. In combining these disparate datasets, IBTrACS uses objective techniques that necessarily account for the inherent differences between international agencies (Knapp and Kruk 2009). Unlike any other global tropical cyclone best track dataset,

[2] http://www.wmo.int/pages/about/Resolution40.html

IBTrACS provides a measure of the inter-agency variability, which helps to identify uncertainty in the TC best track record.

DATA SOURCES

Tropical cyclone best track data are required by the World Meteorological Organization (WMO) to be reported by each of the Regional Specialized Meteorological Centres (RSMC) and Tropical Cyclone Warning Centres (TCWC) that are part of the WMO Tropical Cyclone Programme. In addition, several other agencies track TCs in ocean basins where their country has an interest. The agencies that provided historical BT data are shown in Table 1.

Table 1 - Summary of best track data acquired from each source (see Appendix A for list of acronyms).

Center	Period of Record[1]	# of Storms[2]	# of storms 1980-2005	Storms unique to each center
NHC (N. Atlantic)	1851-2007	1386	305	1381
NHC (E. Pacific)	1949-2007	825	435	95
JTWC (E. Pacific)	1949-2000	759	381	72
CPHC	1966-2003	166	121	21
JTWC (C. Pacific)	1950-2002	47	28	1
JTWC (W. Pacific)	1945-2007	1830	803	161
JMA	1951-2007	1515	686	6
STI	1949-2007	2048	812	304
HKO	1961-2007	1439	770	11
JTWC (Indian Ocean)	1945-2007	635	129	552
IMD	1990-2007	140	125[3]	59
JTWC (S. Hemisphere)	1945-2007	1795	733	196
Neumann	1960-2007	1375	765	9
BoM	1907-2007	864	293	183
FMS	1992-2008	101	86[3]	0
MSNZ	1968-2008	362	254	19
MFLR	1848-2008	1252	273	662

[1] The first year a storm is observed regardless of the completeness of the archive that particular year
[2] Total number of storms provided in the best track files. This does not limit storm occurrence to some intensity threshold (e.g., hurricane strength).
[3] Period of record is a subset of the time period in this summary (1980-2005)

As shown in Figure 2 these agencies are designed to cover each major ocean basin where tropical cyclones occur: the North Atlantic (NA), Eastern Pacific (EP), western North Pacific (WP), North Indian Ocean (NI), South Indian Ocean (SI), and South Pacific (SP) .Best track data are generally produced for each tropical cyclone with an intensity of at least 25 kt (WP), 30 kt (NA, EP), and 35 kt (NI, SI, SP), based on the cyclone's maximum sustained winds (MSW). Tropical cyclogenesis and cyclolosis dates, as well as reporting times, and intensities also often vary by agency. Ideally, a global BT dataset should integrate information from all available resources to ensure completeness.

There are, however, differences (both documented and undocumented) in how each agency determines the best position of the centre of circulation and intensity (minimum central pressure, MCP and maximum sustained wind, MSW) for each tropical cyclone which will lead to differences in the combined result. Given a lack of quantifiable error assessments of each agency, the treatment of each source dataset in IBTrACS is weighted equally when combined with data from other agencies. This combination constitutes the most complete set of tropical cyclone data available.

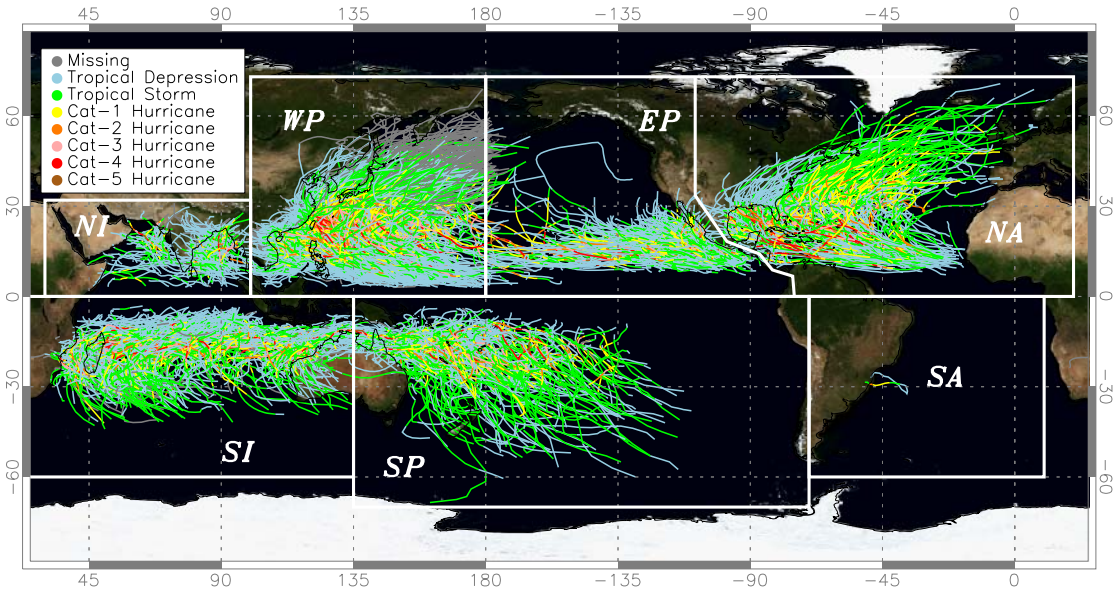

Figure 2 - All IBTrACS storm tracks (1979-2007) colored by their SSHS category (where missing indicates MSW was not reported).

COMBINING BEST TRACK DATA

The main processing steps and data flow that was developed for creating and maintaining the IBTrACS dataset is shown in Figure 3. The first step in combining best track data is to identify each storm uniquely, that is, which storms reported from one agency are also reported by another agency. This is done through comparisons of each storm's position in space and time using an algorithm that also accounts for possible errors in longitude (i.e., wrong sign when a storm crossed the dateline) or time (such as when a storm is reported by two agencies with a one-day offset between their respective times).

Identifying unique storms is important even when using data from only one forecast centre, as failing to account for unique storms may result in erroneous statistics. While six major basins are provided in the data, the identification of unique storms in IBTrACS advocates that any individual or research group can compute regionally specific statistics based on their own basin-boundary definitions. Figure 4 shows the tracks of those storms that were added to the IBTrACS dataset when other BT sources besides JTWC and HURDAT were incorporated (more than 200 storms with MSW > 30 kt, and more than 25 storms with MSW > 56 kt).

The second step toward a global dataset was identifying large errors in track positions. These often tended to be keying errors when digitizing the track data (e.g., transposing numbers or repeating a position). Next, storm tracks were queried to determine which storms were identified by one or more forecast centres. Finally, the storm positions were averaged to derive a single track.

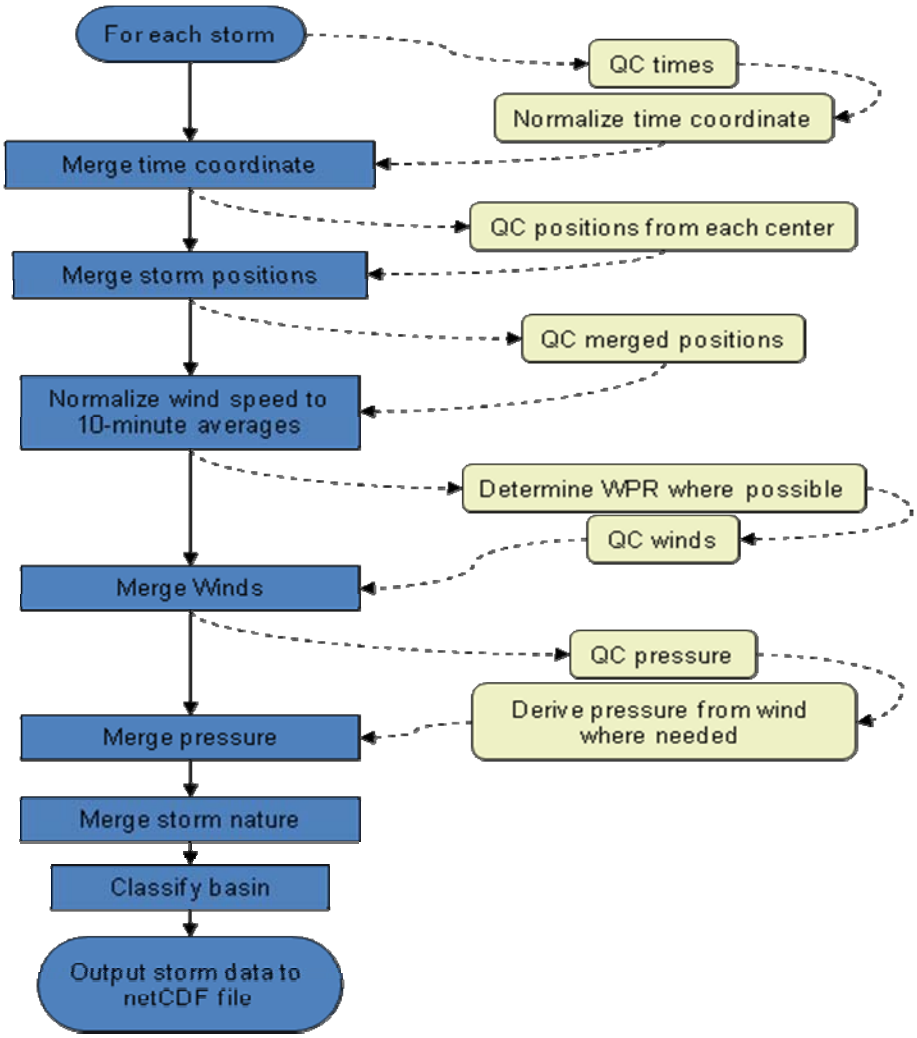

Figure 3 – IBTrACS processing flow diagram showing the primary steps used to combine best track positions and intensities.

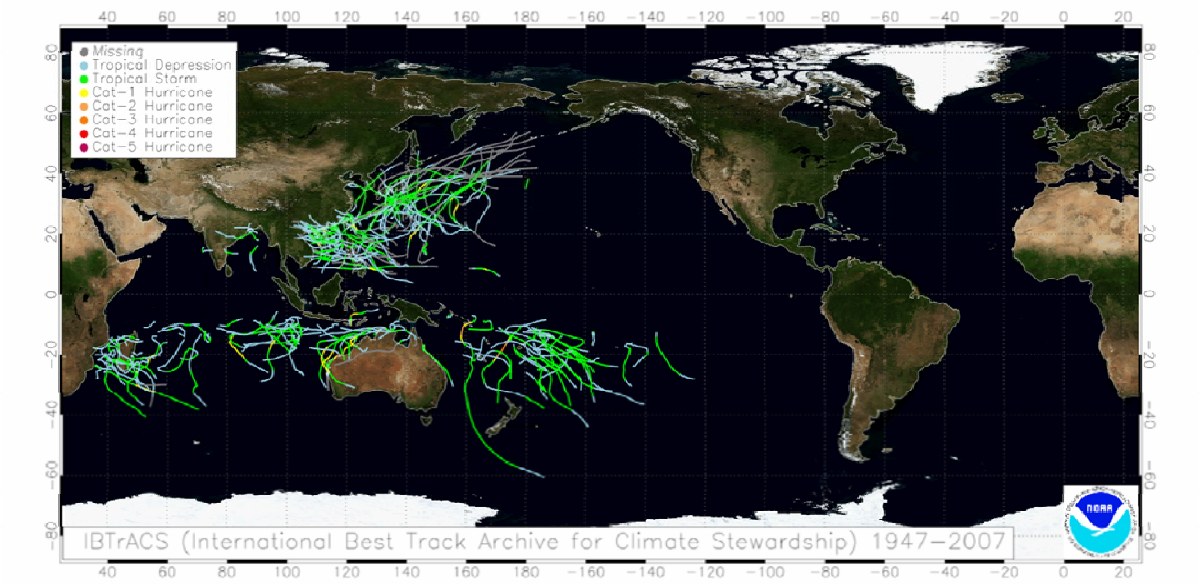

Figure 4 – Map of tropical cyclone tracks of those storms that were added to the IBTrACS dataset when other BT sources besides JTWC and HURDAT were incorporated.

QUALITY CONTROL OF TROPICAL CYCLONE POSITIONS

The goal of the position quality assessment was to identify large errors in storm position at each 6-hr best track point for each storm in the data set. The term "large" refers to gross errors that are approximately 111 km (1° latitude) or more between locations tracked by different forecast centres. Potential errors in a storm track were assessed based on how well a track followed a "smooth" path. First, track positions were converted from latitude, longitude and distance from the Earth's centre to three-dimensional Cartesian coordinates (x, y, z) to avoid discontinuities at either the Dateline or Prime Meridian. The smoothness of any point along a TC track in Cartesian coordinates was assessed using cubic-spline interpolation. That is, for the i^{th} point in the j dimension, there is a point A^j_i where A is one of the Cartesian coordinates (x, y, or z). Then five TC track subsets, S_k which contain A^j_i are:

$$S_k = [A^j_{i-4+k}: A^j_{i+k}], \text{ for } k=0,1,2,3,4 \qquad (1)$$

For each S_k, the point A^j_i is removed while the remaining points are interpolated using cubic-splines to create a new estimate at point i, $E^j_{i,k}$. This produces five estimates of A^j_i, one from each of the five time series. The mean and standard deviation of $E^j_{i,k}$, $\overline{E_i^j}$ and $s_{E_i^j}$ (respectively) are used in calculating a z-score of A^j_i, Z^j_i, which is a measure of the anomaly of $A^j_i$from the mean interpolated position via:

$$Z_i^j = \frac{A_i^j - \overline{E_i^j}}{s_{E_{i,k}^j}} \qquad (2)$$

When Z^j_i is large the distance between the reported position (A) and the mean estimated position (E) is much larger than the variance of the estimated positions, thus it is likely that the track position is in error. Z-scores from all the Cartesian dimensions were combined such that the total deviation of any point in the time series was a combination of the absolute value of z-scores from each dimension:

$$Z_i = \sum_j \left| Z_i^j \right| \qquad (3)$$

Larger values of Z_i deviate more from a smooth, cubic-spline track, thus are more likely erroneous. Also, rather than choosing a fixed threshold for Z_i above which points are assumed errant, a point is flagged if Z_i is more than three standard deviations above the mean of all Z_i for an individual storm track. This method allows each track to have its own threshold, thereby enhancing the robustness of the position quality assessment. In general, A^j_i was replaced by E^j_i if it met the following conditions:

- The adjacent points in the five time series appeared smooth, thus not corrupting the estimates, $\overline{E_i^j}$.
- The new location was a large distance from the reported position (thus, limiting the replacements to large corrections).
- The new location resulted in a set of positions which significantly decreased the total Z-score of the storm track.

Finally, the latitude and longitude of each replacement position was determined from the Cartesian coordinates.

However, there are often large variations in reported positions for weak storms whose centres of circulation are difficult to diagnose. In some cases, the differences in positions are so great (e.g., more than 100 km) that portions of the storm track are denoted in IBTrACS as alternate tracks. Furthermore, issues arise when two storms merge into one circulation, albeit a rare event. In these instances, the IBTrACS path of a single storm ends at the merge point while the other track continues until the storm dissipates.

Figure 5 shows the IBTrACS storm tracks for a) Typhoon Clara (1961) with multi-agency track discrepancies, b) Typhoon Pat merging with Typhoon Ruth (1994), and c) Typhoon Kathy (1954) a storm that split with a main track and a spur.

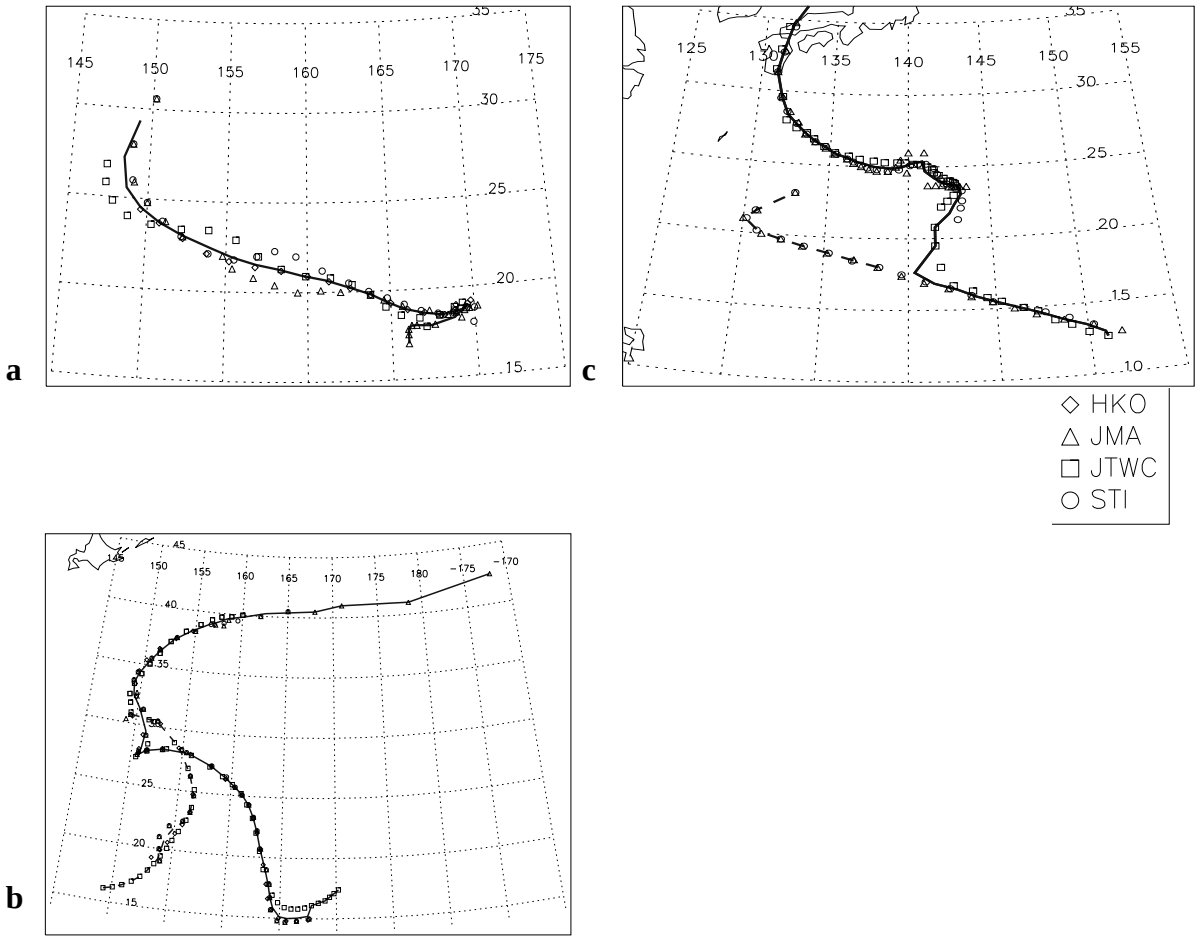

Figure 5 - Result of the IBTrACS algorithm to combine tracks for: a) 1961 Typhoon Clara tracked by four centres, b) 1994 Typhoon Pat and 1994 Typhoon Ruth, which merged together and c) 1954 Typhoon Kathy which split. Black lines are the main IBTrACS storms and dashed lines are the associated storms.

The time of each reported position is also assessed. In some cases, reports from different forecast centres had similar positions for a storm with some offset in time. An algorithm compares the distances between reported positions from different centres. When the algorithm finds shorter mean distances between reported positions by shifting (either forward or backward) the time for a centre in an increment of 6 hr, then the correction is kept in IBTrACS. The time-check algorithm, however, cannot objectively determine which centre was reporting the correct time.

QUALITY CONTROL OF TROPICAL CYCLONE INTENSITIES

Assessing the quality of TC intensities, and combining different intensity estimates from multiple sources is the next step in the process. There is a common definition of mean sea level pressure (MSLP) amongst all forecast agencies, which makes combining it straightforward. However, there is an inherent difference in the definition of MSW between various agencies, which complicates a direct comparison of this intensity parameter. According to the WMO (1983), the maximum sustained wind is a 10-min average wind speed at 10 m height above level ground. In spite of a WMO standard, various agencies use different averaging period that include 1-, 2-, 3- and 10-min averages. Conversion to a common averaging period is necessary before the MSW

can be compared between agencies. Figure 6 shows the global distribution of maximum and mean MSW for the IBTrACS period of record.

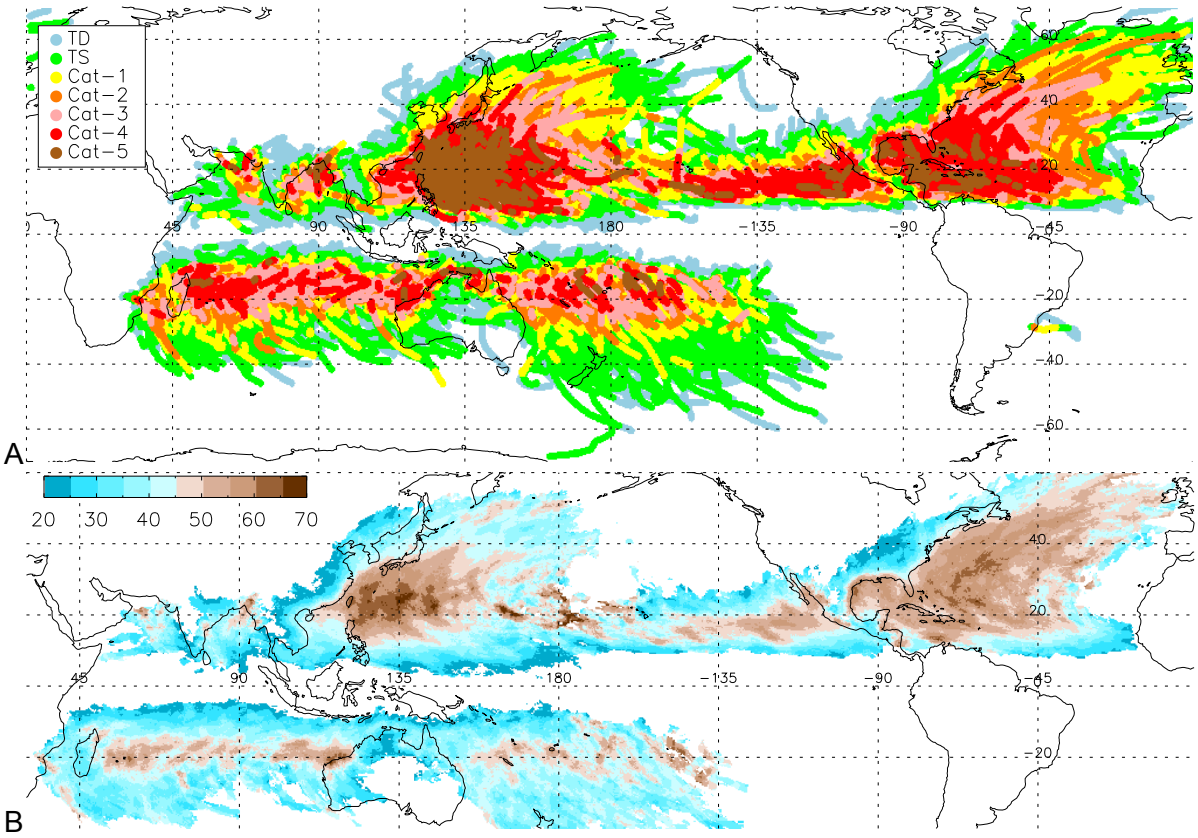

Figure 6 – Global map of IBTrACS A) maximum MSW by Saffir-Simpson category, and B) mean MSW for storms within 55km of any point during the IBTrACS period of record (1848-2007).

For IBTrACS, MSWs are converted to 10-minute period (V_{10}). While various theoretical conversion factors exist (Harper et al., 2008a), the principal need for a global dataset reduces to converting between 10-min and 1-min estimates. The WMO standard for MSW is a 10-min average (WMO 1983), which is used at most of the forecast centres. Variations from the WMO standard include a 1-min average in use by the U.S. (JTWC, NHC and CPHC), a 2-min average used at STI and a 3-min average used at IMD. Converting between these wind speed periods has historically been done at agencies and must be accounted for prior to any comparison, although the appropriateness of this practice has been questioned (Harper et al. 2008a). Since a primary goal of the IBTrACS project was to produce a homogeneous best track dataset, all non-10-min winds (V) were normalized to the 10-min average (V_{10}) via:

$$V_{10} = 0.88 \cdot V \qquad (4)$$

The factor 0.88 was chosen[3] since it is the median of the values used by Neumann (1993, 0.87), and that which has been used operationally at JTWC (0.88; Sampson 1995), La Reunion (0.88) and HKO (0.9). This assumption is itself a source of some uncertainty given that, notwithstanding

[3] Some agencies that report a 10-minute wind speed (MSW_{10}) use 0.88 as their conversion factor, such as BoM (Harper et al., 2008; Trewin, 2008), MSNZ (Steve Ready, personal communication, 2009), FMS (Gary Padgett, personal communication, 2009) and MFLR (Philippe Caroff, personal communication 2009). Wu et al. (2006) report that 0.9 is used at HKO to convert their 1-min Dvorak intensity estimates to MSW_{10}. However, while Yu et al (2007) do not explicitly state the procedures at CMA to convert to a 2-min MSW, they do use 0.871 when comparing to JTWC wind speeds. At JMA, instead of a scaling factor, they use a separate mapping of CI to MSW_{10} based on Koba et al. (1991).

historical practice, recent recommendations to WMO suggest a ratio of 0.93 for the storm MSW in open sea conditions (Harper et al., 2008a). The conversion of all basins' MSW to a 10-min average is also consistent with Neumann (1993) and allows for a globally-consistent approach to tropical cyclone statistics. In the IBTrACS data, the reported wind is a 10-min maximum sustained wind which is the mean of all available wind reports, although a statistical median, range, and standard deviation of wind speeds is also provided.

The intent of the wind speed conversion is to make the MSW parameter as consistent as possible in the dataset. However, IBTrACS provides MSW in numerous ways given the complications of combining this information. First, IBTrACS provides the original MSW and MSLP values as reported by each forecast centre. This allows users to choose their own method of combining MSW or MSLP, or to preferentially select one forecast centre, as well as facilitates interagency comparisons. In addition, the mean, maximum, minimum and standard deviation of MSLP and MSW from all agencies are also provided purely as summary parameters. Providing an average value allows the data to be served in formats already in use by the tropical cyclone community, many of which restrict TC intensity to one value of MSLP and MSW.

It is important to note that the mean MSW as provided in IBTrACS should not be used as the final value, or the "best" of the best track estimates. First, it is against the consensus of the agencies themselves, who recommended that the mean MSW not be used but stopped short of providing an alternative to the mean (Levinson et al., 2009). Second, it combines estimates of MSW based largely on different operational procedures that are yet to be documented (that is, a better correction may be possible once best tracking procedures are documented). Thus, until a complete reanalysis is made of global tropical cyclones or operating procedures are more completely documented, the IBTrACS project will continue to provide a mean MSW as a summary statistic. In the meantime, the IBTrACS project strongly urges users to examine the raw data from each agency. Version 3 of the data set will incorporate the WMO adopted conversions developed by Harper et al. (2008a).

THE COMBINED BEST TRACK DATASET

The latest version of the IBTrACS dataset is provided in seven different user-friendly formats: netCDF, Automated Tropical Cyclone Forecast (ATCF) format, HURDAT, cyclone extended markup language (cXML), WMO revised standard format, and comma separated values (CSV). IBTrACS is also provided via Web Feature Service and is able to be exported to keyhole markup language for use in such software as Google Earth (Knapp et al. 2009). However, not all storm attributes are available in each format due to the restrictive nature of some formats. For example, the 80-column HURDAT format limits 6-hr storm attributes to only one position, MCP and MSW. Therefore, it is recommended that the user selects one of the two formats of IBTrACS that retains all attributes unique to the dataset (netCDF or CSV), that include the original MSW and MCP reports from each agency.

QUANTIFYING INTERAGENCY VARIABILITY

Although IBTrACS is not a reanalysis, as a result of the multiple data sources IBTrACS provides a measure of the inter-agency variability related to best track uncertainty (Knapp and Kruk, 2009) when a TC is tracked by multiple centres. For basins with sufficient agency overlap, a summary of the intra-agency differences for position, MSW and MCP are shown in Figure 7 by decade and storm intensity. The values shown are the mean intra-agency deviation for each decade, so they do not represent uncertainty ranges. The degrees of freedom in most cases are too small to construct confidence limits. These plots only show the tendencies of interagency differences in time and space and do not assess the overall quality of the best track data.

In light of such caveats, Figure 7 does provide some insight into interagency differences. First, whether due to increased data availability or inter-agency communication, the various centres appear to be providing more congruent estimates of cyclone position. Since intense storms generally have an easily identified centre of circulation (e.g., an eye), the variance of their position is less than that for weaker storms. The variance does have a lower limit however, since BT data are reported only to tenths of degrees East or North, which results in a precision limited to ~10 km.

Interestingly, all hurricane strength storms (V_{10}> 56 kt) approach this lower limit in the most recent decade. Second, the variation in MSW is slowly decreasing. In general, differences are larger for cyclones with stronger winds. It should again be noted that the values, such as the convergence towards 5 kt in the South Pacific, does not represent the error of the data, but rather illustrates that the MSW data are becoming more consistent between the agencies. Lastly, and surprisingly, the MCP values are not generally converging. Instead, the values are diverging, especially in the Western North Pacific. Such a divergence over the last several decades could be linked to the cessation of aircraft reconnaissance in the 1980s. Unlike wind speed that showed decreasing interagency disparities, the pressure values in Figure 7 show little to no agreement between the agencies.

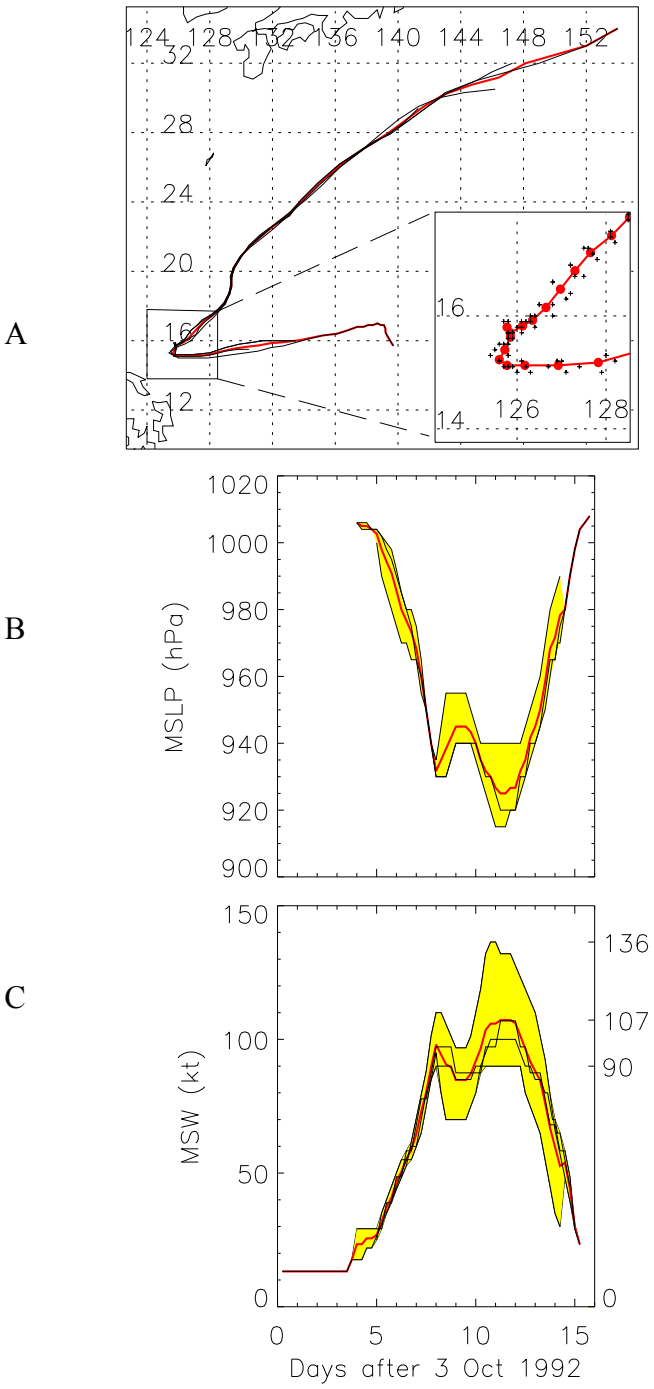

Figure 7 - Tracks of 1992 Typhoon Yvette (a) from various agencies (black) and IBTrACS (red). Time series of MSLP (b) and MSW (c) for Yvette from various agencies are shown in black with the mean value in red. Shading represents the span of the values from the agencies.

SETTING THE STAGE FOR REANALYSIS

The extensive work in the Atlantic basin reanalyzing TC tracks as far back as 1851 (e.g., Fernandez-Partagas and Diaz 1996; Landsea et al. 2004) have led to new techniques that would aid in a global reanalysis effort that is needed to homogenize historical TC intensities in the best track record. A complete reanalysis of each basin at least back to the beginning of the geostationary satellite era has previously been identified as critical and timely (Levinson et al. 2009), especially given the ability to reanalyze intensities using subjective and objective Dvorak techniques. In addition, an important aspect of any reanalysis effort is the need to determine "missed" storms—known TCs that aren't included in historical best track datasets. These are especially important for accurately determining trends in storm counts and cyclogenesis points.

Conducting any reanalysis effort basin-by-basin, rather than globally for any given year, would allow for complete coverage of a particular basin but would require extensive coordination between agencies with forecast responsibilities within that basin given the inter-agency variability that is present in the historical record. Inter-agency variability can be considered a proxy for MSW uncertainty that can be used to prioritize cyclones in need of reanalysis. Measures of uncertainty include:

- *Storm category differences*: Since their peak MSW often categorizes storms, examining the range of agency reported MSW for each storm (MSW_{max} – MSW_{min}) defines ΔMSW. For example, 1992 Typhoon Yvette ΔMSW is 46 kt as the range of reported MSW values was 136 – 90 kt.
- *Changes in Accumulated Cyclone Energy (ACE)*: Storm summaries are often made by summing the square of the 6-hr MSW over a storm's lifetime to obtain the ACE (ACE, Bell & Chellia 2006). Calculating ACE using MSW_{max} and MSW_{min} defines ΔACE, which integrates the intensity differences over the lifetime of a storm (instead of an instantaneous report, such as ΔMSW). This metric tends to give more weight to longer-lived storms.
- *Relative changes in ACE*: Lastly, ΔACE is normalized by the ACE calculated from the mean MSW to obtain ΔACE_N for each storm. This provides an estimate of the uncertainty in the intensity record for a particular storm.

To illustrate how these metrics, derived from IBTrACs data, can be used to rank storms from most uncertain to most certain. The above three metrics are combined using their mean ranking to show the five least certain storms from 1945-2007 for the WP (Table 2.) The most uncertain storms in the WP occurred during the pre-satellite era when storm observations were few. Notably, the 1951 Typhoon Marge has the largest ΔMSW (which is also the largest in all IBTrACS). While this treatment may be a worst-case scenario, it represents the storms for which the greatest amount of inter-agency disagreement exists. Only a global reanalysis of all tropical cyclones can resolve such differences.

Table 2 - Five storms with most inter-agency variability for a) Western Pacific Ocean, b) South Indian Ocean, and c) South Pacific Ocean. The range of MSW used to calculate ΔMSW are shown parenthetically in knots.

a) West North Pacific Ocean:

Year	Name	ΔMSW (kt)	ΔACE (10^4 kt^2)	ΔACE_N(%)
1951	Marge	87 (175-88)	40	90
1952	Bess	58 (146-88)	19	105
1969	Ida	56 (156-100)	20	86
1959	Tilda	55 (165-110)	23	76
1954	June	51 (165-114)	24	69

b) Southern Indian Ocean:

Year	Name	ΔMSW (kt)	ΔACE (10^4 kt^2)	ΔACE_N(%)
1971	Sally	48 (88-40)	7	170
1985	Isobel	40 (84-44)	9	122
1971	Shelia/Sophia	48 (110-62)	7	126
1992	Irna/Jane	51 (126-75)	17	83
1987	Elsie	44 (97-53)	7	111

c) Southern Pacific Ocean:

Year	Name	ΔMSW (kt)	ΔACE (10^4 kt^2)	ΔACE_N(%)
1972	Carlotta	40 (97-57)	26	130
1972	Wendy	36 (106-70)	17	152
1972	Gail	37 (92-55)	11	125
2004	Fay	27 (106-79)	18	100
1972	Emily	35 (92-57)	7	112

Inter-agency intensity differences based on IBTrACS also affect annual and decadal tropical cyclone ACE calculations. In Figure 8 the time series of annual ACE derived from IBTrACS are shown by basin. The ACE values calculated from MSW_{min} and MSW_{max} are shown via whisker points. For the WP, large differences exist in any given year. The normalized difference (ΔACE_N) shows no temporal trend, suggesting the intensity estimates from various agencies in the WP are just as different today as in the 1970s. The SI has a shorter period of record with multiple agencies reporting. None of the linear regression trends for WP and SI are statistically significant at the 95% confidence interval. For the SP, the trend in ACE is not significant but the ΔACE_N is significant. The trend remains significant even after removing the high values from 1970-1972.

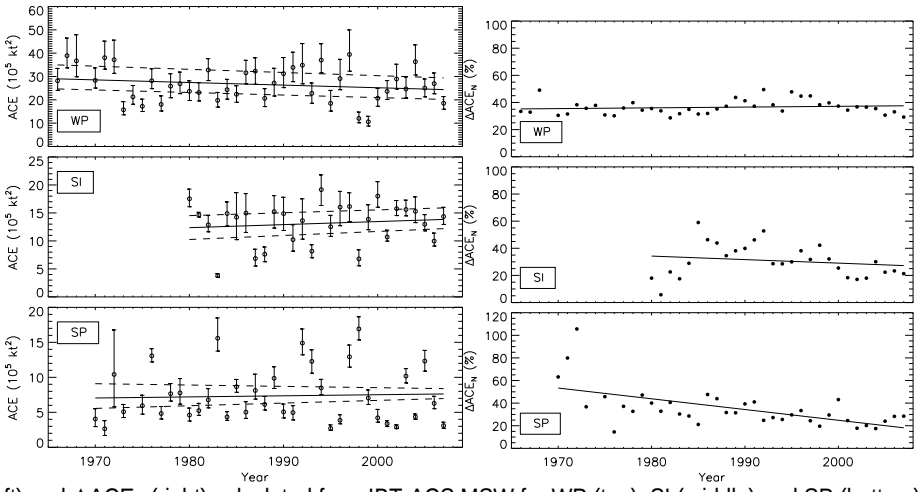

Figure 8 - ACE (left) and ΔACE_N (right) calculated from IBTrACS MSW for WP (top), SI (middle) and SP (bottom) basins. Range in ACE shows extent of ACE from maximum and minimum MSW. Solid lines show linear regression while dashed lines show linear regression of minimum and maximum ACE.

Finally, the annual ACE was summed to determine the impact of the inter-agency variability on decadal statistics. ACE values computed from IBTrACS are provided in Table 3 for two decades (1986-1995 and 1996-2005) following Klotzbach (2006). Between these decades, the ACE decreases, increases and hardly changes for the WP, SI and SP respectively. However, since the range of ACE_{min} and ACE_{max} overlap for each decade, the significance of the inter-decadal changes in the WP and SI are questionable. Furthermore, since winds are squared in calculating ACE, the difference between MSW_{min} and MSW_{max} are disproportionately emphasized.

Thus, great care is needed when gleaning trends or changes (or lack thereof) from annual or decadal data.

Table 3 – ACE calculated from mean MSW, MSW_{min} (ACE_{min}) and MSW_{max} (ACE_{max}) for the period 1986-1995 and 1996-2005. ACE (10^4 kt^2) is calculated only when storms were not identified as extra-tropical and the mean MSW > 30 kt.

	1986-1995				1996-2005			
Basin	ACE	ACE_{min}	ACE_{max}	ΔACE_N (%)	ACE	ACE_{min}	ACE_{max}	ΔACE_N (%)
WP	3335	2592	4152	47	2899	2334	3645	45
SI	1384	1065	1734	48	1536	1304	1839	35
SP	914	770	1124	39	908	792	1067	30

Summary

The IBTrACS dataset is the result of a globally coordinated and collaborative project. IBTrACS provides the first publicly available centralized repository of global tropical cyclone best track data from the RSMCs and other agencies. The World Data Centre for Meteorology – Asheville maintains the permanent archive of IBTrACS, offering semi-annual updates. Versions of all data are maintained and data provenances are recorded to preserve traceability and to easily determine the source of all data. The reasoning behind changes and algorithms that merge and adjust the datasets such as data quality revisions and additions are open for review. Information about the integrity or quality of a storm track is also provided back to the agencies providing the track data.

While IBTrACS is not a reanalysis (e.g., Fernandez-Partagas and Diaz, 1996; Harper et al., 2008b; Landsea et al., 2004), the derived uncertainty metrics can serve as a stepping stone in identifying those tropical cyclones which are in most need of reanalysis. As IBTrACS data stand, numerous inhomogeneities exist in the intensity record due to inter-agency differences in available technologies, observations and procedures over time. For example, inhomogeneities were introduced when various satellite data became available at an agency or when forecasters were trained in different analysis techniques. As discussed in Levinson et al. (2009), efforts are underway at NCDC to document the operating procedures at the various RSMC and forecast offices, with an emphasis on changes in processes or capabilities that affect dataset homogeneity. Finally, IBTrACS is expandable to allow for inclusion of other best track datasets that may become available. This allows input from individuals and/or agencies that have yet to make best track data available. IBTrACS could become even more useful by including other information on global tropical cyclones. For example, non-developing storm tracks could be included for the tropical cyclone forecasting community in a future version. Such data are necessary to compile statistical tropical cyclone intensity prediction models (e.g., DeMaria and Kaplan, 1999). Furthermore, some agencies provide non 6-hr analyses and other storm parameters (such as radius of maximum winds, storm size, eye diameter, and radius of the outermost closed isobar), which could be incorporated into IBTrACS making it more useful to surge and wave modellers, emergency managers and reinsurance groups.

To download the freely available dataset, visit the IBTrACS website:
http://www.ncdc.noaa.gov/oa/ibtracs/.

Acknowledgments

Numerous people and agencies have contributed data and provided critical information to the IBTrACS project since its inception. We would like to especially thank Charlie Neumann for providing his historical best track data and Ethan Gibney at IMSG, Inc. for his GIS support to the IBTrACS project. We would also like to acknowledge the support of the forecast centres and

meteorological agencies that provided their best track data to the IBTrACS project, including the WMO Regional Specialized Meteorological Centres (Miami, Honolulu, La Reunion, Nadi, New Delhi, Tokyo, and Wellington), the Australian Bureau of Meteorology's Tropical Cyclone Warning Centres (Brisbane, Darwin and Perth), the China Meteorological Agency's Shanghai Typhoon Institute, the Hong Kong Observatory, and the U.S. Department of Defense' Joint Typhoon Warning Centre (JTWC). Additional funding for improvements to the IBTrACS dataset was provided by the NOAA Climate Programme Office' Climate Change Data and Detection (CCDD) Programme.

References

Bell, G and M. Chelliah, 2006, Leading Tropical Modes Associated with Interannual and Multidecadal Fluctuations in North Atlantic Hurricane Activity, *Journal of Climate*, (19) 4, 590-612.

Chu, J-H., C. R. Sampson, A. S. Levine and E. Fukada, 2002, The Joint Typhoon Warning Centre tropical cyclone best-tracks, 1945-2000, *NRL/MR/7540-02-16*, Naval Research Laboratory, Washington, D.C.

Crutcher, H. L. and R. G. Quale, 1974, Mariners worldwide guide to tropical storms at sea, *NAVAIR 50-1C-61*, NOAA/EDS/National Climatic Centre, Asheville, NC.

DeMaria, M. and J. Kaplan, 1999, An Updated Statistical Hurricane Intensity Prediction Scheme (SHIPS) for the Atlantic and Eastern North Pacific Basins, *Weather and Forecasting*, (14) 3, 326-337.

Emanuel, K., 2005, Increasing destructiveness of tropical cyclones over the past 30 years, *Nature*, (436), 686-688.

Fernandez-Partagas, J. and H. F. Diaz, 1996, Atlantic Hurricanes in the Second Half of the Nineteenth Century, *Bulletin of the American Meteorological Society*, (77) 12, 2899-2906.

Harper, B. A., J. D. Kepert, and J. D. Ginger, 2008a, Guidelines for converting between various wind averaging periods in tropical cyclone conditions, *World Meteorological Organization*, Geneva.

Harper, B. A., S. A. Stroud, M. McCormack, and S. West, 2008b, A review of historical tropical cyclone intensity in north-western Australia and implications for climate change trend analysis, *Australian Meteorological Magazine*, (57) 2, 121-141.

Jarvinen, B. R., C. J. Neumann, and M. A. S. Davis, 1984, A tropical cyclone data tape for the North Atlantic Basin, 1886–1983: Contents, limitations and uses, *NOAA Tech. Memo. NWS NHC-22*, Washington, D.C.

Klotzbach, P. J., 2006, Trends in global tropical cyclone activity over the past twenty years (1986-2005), *Geophysical Research Letters*, (33) 10, 4.

Knapp, K. R. and M. C. Kruk, 2009, Quantifying inter-agency differences in tropical cyclone best track wind speed estimates, *Monthly Weather Review*, In Press. (doi:10.1175/2009MWR3123.1).

Knapp, K. R., M. C. Kruk, D. H. Levinson, H. J. Diamond, and C. J. Neumann, 2010: The International Best Track Archive for Climate Stewardship (IBTrACS): Unifying tropical cyclone best track data.*Bulletin of the American Meteor. Society*, In press (doi:10.1175/2009BAMS2755.1).

Knapp, K. R. and J. P. Kossin, 2007, New global tropical cyclone data from ISCCP B1 geostationary satellite observations, *Journal of Applied Remote Sensing*, (1), 013505.

Knapp, K. R., M. C. Kruk, D. H. Levinson, and E. J. Gibney, 2009, Archive Compiles A New Resource for Global Tropical Cyclone Research, *Eos, Transactions, American Geophysical Union*, (90), 46.

Koba, H., T. Hagiwara, S. Osano, and S. Akashi, 1991: Relationships between CI number and minimum sea level pressure/maximum wind speed of tropical cyclones. *Geophysical Magazine*, **44,** 15-25.

Kossin, J. P., K. R. Knapp, D. J. Vimont, R. J. Murnane, and B. A. Harper, 2007, A globally consistent reanalysis of hurricane variability and trends, *Geophysical Research Letters*, (34) L04815.

Kruk, M. C., K. R. Knapp, and D. Levinson, 2009, A technique for combining global tropical cyclone best track data, *Journal of Atmospheric and Oceanic Technology*, In Press (doi:10.1175/2009JTECHA1267.1).

Landsea, C. W., C. Anderson, N. Charles, G. Clark, J. Dunion, J. Fernandez-Partagas, P. Hungerford, C. Neumann, and M. Zimmer, 2004, The Atlantic hurricane database re-analysis project: Documentation for the 1851-1910 alterations and additions to the HURDAT database, *Hurricanes and Typhoons: Past, Present and Future*, R. J. Murnane and K.-B. Liu, eds, Columbia University Press, New York, NY., 177-221.

Lau, K. M., Y. P. Zhou, and H. T. Wu, 2008, Have tropical cyclones been feeding more extreme rainfall?, *J. Geophys. Res.*, (113), D23113.

Levinson, D. H., H. J. Diamond, K. R. Knapp, M. C. Kruk, and E. J. Gibney, 2009, Toward a homogenous global tropical cyclone best track dataset, *Bulletin of the American Meteorological Society*, In Press.

Neumann, C. J., B. R. Jarvinen, C. J. McAdie, and G. R. Hammer, 1999, Tropical Cyclones of the North Atlantic Ocean, 1871-1998, *NOAA - Historical Climate Series*, Silver Springs, MD.

Sampson, C. R., R. A. Jeffries, C. J. Neumann, and J. -H. Chu, 1995: Tropical Cyclone Forecasters Reference Guide, US Naval Research Laboratory, Chap. 6. NRL Report NRL/PU/7541-95-0012.

Trewin, B., 2008: An enhanced tropical cyclone data set for the Australian region. *20th Conference on Climate Variability and Change*, New Orleans, LA, American Meteorological Society, 12 pp.

WMO, 1983, Measurement of surface wind, *Guide to Meteorological Instruments and Methods of Observation*, WMO No. 8, 5th Ed., Geneva.

Wu, M. C., K. H. Yeung, and W. L. Chang, 2006: Trends in western North Pacific tropical cyclone intensity. *Eos*, **87,** 537-539.

Yu, H., C. Hu, and L. Jiang, 2007: Comparison of three tropical cyclone intensity datasets. *Acta Meteorologica Sinica*, **21,** 121-128.

APPENDIX A

List of Acronyms

ACE: Accumulated Cyclone Energy
ATCF: Automated Tropical Cyclone Forecast
BT: tropical cyclone best track data
BoM: Australian Bureau of Meteorology (as TCWC Brisbane, Darwin, and Perth)
CPHC: Central Pacific Hurricane Centre (as RSMC Honolulu)
CSV: comma separated values
cXML: cyclone extended markup language
EP: Eastern Pacific
FMS: Fiji Meteorological Service (as RSMC Nadi)
HKO: Hong Kong Observatory
HURSAT: Hurricane Satellite dataset
IBTrACS: International Best Track Archive for Climate Stewardship
IMD: India Meteorological Department (as RSMC New Delhi)
JMA: Japan Meteorological Agency (as RSMC Tokyo)
JTWC: U.S. Defense Joint Typhoon Warning Centre
MCP: minimum central pressure
MSW: maximum sustained wind
MFLR: MeteoFrance (as RSMC La Reunion)
MSNZ: Meteorological Service of New Zealand (as RSMC/TCWC Wellington)
NA: North Atlantic
NCDC: NOAA's National Climatic Data Centre
netCDF: network Common Data Form
NHC: NOAA's National Hurricane Centre (as RSMC Miami)
NI: North Indian Ocean
NOAA: National Oceanic and Atmospheric Administration
RSMC: Regional Specialized Meteorological Centre
SI: South Indian Ocean
SP: South Pacific
STI: Chinese Meteorological Administration's Shanghai Typhoon Institute
TC: tropical cyclone
TCWC: Tropical Cyclone Warning Centre
WDC: World Data Centre
WMO: World Meteorological Organization's
WP: Western North Pacific

SIMULATION OF TRACK AND INTENSITY OF GONU AND SIDR WITH WRF-NMM MODELLING SYSTEM

Sujata Pattanayak and U. C. Mohanty
Centre for Atmospheric Sciences, IIT Delhi, Hauz Khas, New Delhi-110016, India

Abstract

In recent years meso-scale models are extensively used for simulation of genesis, intensification and movement of tropical cyclones. In this study, the state-of-the-art non-hydrostatic meso-scale model (NMM) core of Weather Research and Forecasting (WRF), (WRF-NMM) model, developed at National Centre for Environmental Prediction (NCEP) is used to simulate the pre-monsoon cyclone Gonu and the post-monsoon cyclone Sidr of 2007, generated over Arabian Sea and Bay of Bengal respectively. In the first experiment i.e. in control simulation, the above stated meso-scale model is integrated up to 72hrs in a single domain with the horizontal resolution of 27 km and 51 vertical levels by taking the initial and lateral boundary conditions from Global Forecast System (GFS) analysis and forecast fields of the NCEP for both the cyclones. The result indicates a large initial positional error at the centre of the storm. Hence, in order to improve the initial analysis fields for the model integration, an attempt is made to initialize WRFNMM model with the WRF-VAR system developed at National Centre for Atmospheric Research (NCAR). In the second experiment, the impact of the data assimilation (DA) system is investigated by incorporating the available conventional and non-conventional data sets over Indian region. A number of meteorological fields' viz. central pressure / pressure drop, winds, precipitation etc. are verified against observations / verification analysis. The vector displacement errors in track forecast are also calculated and compared with observed track provided by the India Meteorological Department (IMD). The day-1 and day-2 forecast clearly demonstrates the improvement of 27.2% and 49.2% respectively in track prediction with the DA experiments compared to the control simulations.

Key Words

Mesoscale model, data assimilation, tropical cyclone, track, intensity

1. INTRODUCTION

The climate system is a complex, interactive system consisting of the atmosphere, hydrosphere, biosphere, cryosphere, lithosphere and outer space. The fourth assessment report (AS4) of Intergovernmental Panel for Climate Change (IPCC) has clearly indicated the change of the temperature both over land and ocean. As a result, the impact of disasters such as tropical cyclones, drought, flood and extreme temperature events etc. have an increasing trend with time. The extreme weather event like tropical cyclones varies abruptly from year to year in terms of frequency and intensity over all the basins. Tropical cyclones are organized convective activities, developed over warm tropical oceans. The Indian region is unique in nature than any other regions of the world, as far as the genesis and death toll due to tropical cyclone is concerned. The tropical cyclones affect this region in two seasons: Pre-monsoon (April-May) and Post-monsoon (October-December). The peak frequency is found to be in the months of May (secondary) and November (primary). The Bay of Bengal contributes about 5% of the global annual tropical storms. Though considered to be much weaker in intensity and smaller in size as compared to the cyclones of other regions, the Bay of Bengal storms are exceptionally devastating, especially when they cross the land. This is mainly due to shallow bathymetry, nearly funnel shape of the coastline and the long stretch of the low-lying delta region entrenched with large number of river systems leading to high storm surges and coastal inundations. So the Bay of Bengal tropical cyclone disaster is the costliest and deadliest natural hazard in the Indian sub-continent. It has a significant socio-economic impact on the countries bordering Bay of Bengal, especially India, Bangladesh and Myanmar. At the same time, Arabian Sea contributes 1-2% of the global annual tropical storms. Therefore, reasonably accurate prediction of these storms has great importance to reduce the loss of valuable lives.

There have been considerable improvements in the field of weather prediction by numerical models. In recent years mesoscale models are extensively used for the prediction of different weather events world wide. Also, a series of high-resolution, non-hydrostatic, primitive equation mesoscale models such as PSU/NCAR MM5, WRF (ARW & NMM), ARPS, ETA and HWRF are used for the simulation / prediction of tropical cyclones. The PSU/NCAR mesoscale model MM5 has been used in a number of case studies for the simulation of hurricanes over Atlantic (Liu et al., 1997, 1999; Braun and Tao 2000; Bao et al., 2000; Zhang & Wang 2003). These simulations have demonstrated the ability of the high-resolution models to re-produce the fine structures in the inner core and outer rain bands region of tropical cyclones. Krishnamurti et al. (2007) examined the influence of the physical initialization for the hurricane forecast by using the WRF model and suggested that, there is a positive impact on hurricane intensity prediction.

A number of case studies are there for the tropical cyclones over the Bay of Bengal with mesoscale models. Mohanty and Gupta (1997) described in detail the deterministic methods used for tropical cyclone track prediction. Mohanty et al. (2004) used MM5 model to simulate the Orissa super cyclone (1999). Mandal et al. (2004) used MM5 model to study the impact of parameterization of physical processes on prediction of tropical cyclones over the Bay of Bengal and suggested that convection has noticeable impact on the simulation of tropical cyclones. Pattanayak and Mohanty (2008) made a comprehensive study on the performance of both MM5 and WRF models in the simulation of tropical cyclones over Indian seas and suggested superiority of the WRF model over MM5.

Some of the observational studies also reveal that, the sea surface temperature (SST) over different basins (Webster et al 2005) is increasing. Observations also reveal that the mean analyzed surface temperature over continent wise has an increasing trend (Knutson et al 2006b). Thus, the mean surface temperature has an increasing trend globally as well as regionally, over both land surface and ocean. In India the analysis of observed data of temperature indicates that the temperature is increasing since late 1800's and the increasing trend is sharp after 1970. Webster et al (2005) studied the changes in tropical cyclone number and their intensity along with the sustainability in a warming environment over the period of 35 years. The study suggested that, there is a large increase in the number and proportion of hurricanes reaching categories 4 and 5. Mohanty et al (2009) demonstrated the changes in frequency and intensity of tropical cyclones over Indian seas in warming environment. The study clearly indicated the increasing trend of severe cyclonic storm with the warming environment. Hence, in the present paper, the studies of some of the very severe cyclonic storms over Indian seas are investigated.

In this study, the state-of-the-art mesoscale model WRF-NMM is used to simulate the pre-monsoon cyclone Gonu and the post-monsoon cyclone Sidr generated over Arabian Sea and Bay of Bengal respectively. The performance of the model has been evaluated and compared with observations and verifying analysis. Again, the advancement of data assimilation techniques indeed improves the forecast skill of the meso-scale models in wide ranges. A brief description of the mesoscale model used for the present study is given in section 2. The synoptic situation for the above mentioned cyclones are described in section 3. The numerical experiments and the data used are presented in section 4. The results are presented in section 5 and the conclusions are in section 6.

2. MODEL DESCRIPTION

The Non-hydrostatic Meso-scale Model (NMM) dynamic core of the Weather Research and Forecasting (WRF) system was developed by the National Centre for Environmental Prediction (NCEP) / National Oceanic and Atmospheric Administration (NOAA). The WRF-NMM is designed to be a flexible, state-of-the-art atmospheric simulation system that is efficient on available parallel computing platforms. The WRFNMM model is a fully compressible, non-hydrostatic model with a hydrostatic option (Janjic et al 2001; Janjic 2003a, Janjic 2003b). The horizontal Arakawa E-grid staggering is used for computational efficiency. The model uses a terrain following hybrid sigma-pressure vertical co-ordinate. The dynamics conserve a number of first and second order quantities including energy and enstrophy (Janjic 1984). Forward-backward time integration schemes are used for the horizontally propagating fast-waves and implicit scheme is used for the

vertically propagating sound waves. Adams-Bashforth scheme and crank-Nicholson scheme are used for horizontally and vertically propagating waves. The Geophysical Fluid Dynamic Laboratory (GFDL) long wave and short wave radiation schemes are incorporated in the model. The new generation of the MRF PBL scheme is introduced here as Yonsei University (YSU) PBL, has an explicit representation of entrainment at the PBL top which is derived from large eddy modelling. This scheme also adds non-local momentum mixing to provide a better wind profile in the PBL. It has the capability to remove the influence of convective velocity on the surface stress, which will alleviate a day-time low-wind speed bias. Simplified Arakawa-Schubert cumulus convection scheme is introduced in this dynamic core of WRF. It is based on Arakawa and Schubert (1974) and simplified by Grell (1993), which can simulate the penetrative convection. Hence, the model is widely used for simulation / prediction of severe weather events such as tropical cyclones, heavy rainfall, thunderstorms etc. The details of the model specifications are presented in Table 1.

Table 1- A brief description of the WRF-NMM model specifications.

Model	NCEP mesoscale model WRF-NMM V3.0.1
Dynamics	Non-hydrostatic with terrain following hybrid pressure sigma vertical co-ordinate.
Map projection	Rotated lat-lon
Resolution	27 km
No. of vertical levels	51
Horizontal grid scheme	Arakawa E-grid
Time integration scheme	Horizontally propagating fast-waves: Forward-backward scheme Vertically propagating sound waves : Implicit scheme Horizontal : Adams-Bashforth scheme Vertical : Crank-Nicholson scheme TKE, water species: Explicit, iterative, flux-corrected
Advection for T, U, V	Horizontal : 2nd order, energy & enstrophy conserving, quadratic conservative Vertical : 2nd order, quadratic conservative TKE, water species: Upstream, flux-corrected, positive definite, conservative
Lateral boundary condition	NCEP / NCAR GFS forecast
Radiation scheme	Long wave : GFDL Short wave : GFDL
Planetary boundary layer parameterization schemes	Yonsei University (YSU)
Cumulus parameterization schemes	Simplified Arakawa Schubert
Land surface physics	NMM
Microphysics	Ferrier

3. SYSTEMS DESCRIPTIONS

The descriptions of synoptic weather conditions for the above mentioned two very severe cyclonic storms are as follows.

3.1 Descriptions of the Arabian Sea Cyclone Gonu

Tropical cyclone Gonu was the strongest system on the recorded history in the Arabian Sea. The tropical storm Gonu was developed from a persistent area of convection as a depression over the east central Arabian Sea with centre near lat 15.0. N, long 68.0. E at 18 UTC 01 June 2007. It moved westwards and with a favourable upper-level environment and warm sea surface temperatures, it rapidly intensified into a cyclonic storm at 09 UTC 02 June 2007 near lat 15.0. N, long 67.0. E. It remained in that stage for 15 hours i.e. up to 00 UTC 03 June 2007. By 00 UTC 03 June 2007, it intensified into a severe cyclonic storm with the central pressure of 988 hPa and centred at lat 15.5. N, long 66.5. E and the storm remained in that stage for next 18 hours i.e. up to 18 UTC 03 June 2007. Continuing its northwestward movement, it further intensified into a very

severe cyclonic storm by 18 UTC 03 June 2007 and lay centred at lat 18.0. N, long 66.0. E with the central pressure of 980 hPa. It sustained in that stage for next 21 hours i.e. up to 15 UTC 04 June 2007. By 15 UTC 04 June 2007, the system moved west north westwards and further intensified as a super cyclonic storm and lay centred at lat 20.0. N, long 64.0. E with the minimum central pressure of 920 hpa. It remained in the super cyclonic storm stage for the next 6 hours i.e. up to 21 UTC 04 June 2007. Then the storm further moved in northwestward direction and weakened into a very severe cyclonic storm by 21UTC 04 June 2007 and lay centred over northwest Arabian Sea at lat 20.5. N, long 63.5. E with the minimum central pressure of 935 hPa. The storm remained in that stage for the next 48 hours i.e. up to 21 UTC 06 June 2007. Then the storm gradually weakened, moved northwestward and crossed the Makran coast near lat 25.0. N, long 58.0. E between 03 and 04 UTC 07 June 2007 as a cyclonic storm.

Intense cyclones like Gonu have been extremely rare over the Arabian Sea, as most of the storms in this area tend to be small and dissipate quickly. The cyclone caused about $4 billion in damage (2007 USD) and nearly 50 deaths in Oman, where the cyclone was considered the nation's worst natural disaster. Gonu brought heavy rainfall near the eastern coastline, reaching up to 610 mm (24 inches), which caused flooding and heavy damage. In Iran, the cyclone caused 23 deaths and $215 million in damage (2007 USD).

3.2 Descriptions of the Bay of Bengal Cyclone Sidr

On November 9, an area of disturbed weather developed southeast of the Andaman Islands, with a weak low-level circulation near the Nicobar Islands. Initially moderate upper-level wind shear inhibited organization, while strong influence aloft aided in developing convection. Vertical shear decreased significantly as the circulation became better defined, and the cyclone Sidr developed over southeast Bay near lat 10.5. N, long 91.5. E as a depression at 00 UTC 12 November 2007. As the storm picked up speed, the sea became turbulent with the gale force winds. On 13 November, Cyclone Sidr moved over south-east Bay and adjoining areas and moved north-westwards, concentrating into a severe cyclonic storm with the minimum central pressure of 968 hPa with a core of hurricane wind. It further intensified and reached the minimum central pressure of 944 hPa on 15 November with a core of strong winds in east central Bay. This position was an estimated 655 kilometres south-southwest of Chittagong port, 580 kilometres south-southwest of Cox's Bazar port and 595 kilometres south of Mongla port (near lat 17.0° N & long 89.2° E). Then it further moved in a northerly direction and crossed Khulna-Barisal coast of Bangladesh in the evening of 15 November 2007.

The damage due to cyclone Sidr came close to $450 million. The damage in Bangladesh was extensive, including tin shacks flattened, houses and schools blown away and enormous tree damaged. The coastal districts of Bangladesh faced heavy rainfall as an early impact of the cyclone. Dhaka and other parts of Bangladesh experienced drizzle and gusty winds.

The INSAT (Kalpana-1) infrared satellite imageries for both the cyclones are provided in Figure 1 (all Figures not shown). Figure 1 (a) shows the satellite imagery for the Arabian Sea cyclone Gonu valid at 12 UTC 04 June 2007, which clearly shown the eye of the cyclone. Figure 1 (b) shows the satellite imagery for the Bay of Bengal cyclone Sidr valid at 16 UTC 15 November 2007.

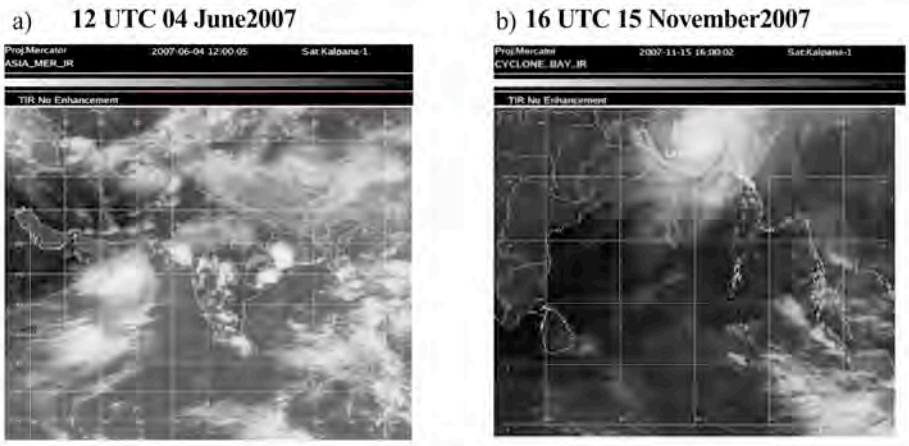

Figure 1 Satellite imageries as obtained from INSAT (Kalpana -1). a) valid at 12 UTC 04 June 2007and b) valid at 16 UTC 15 November 2007.

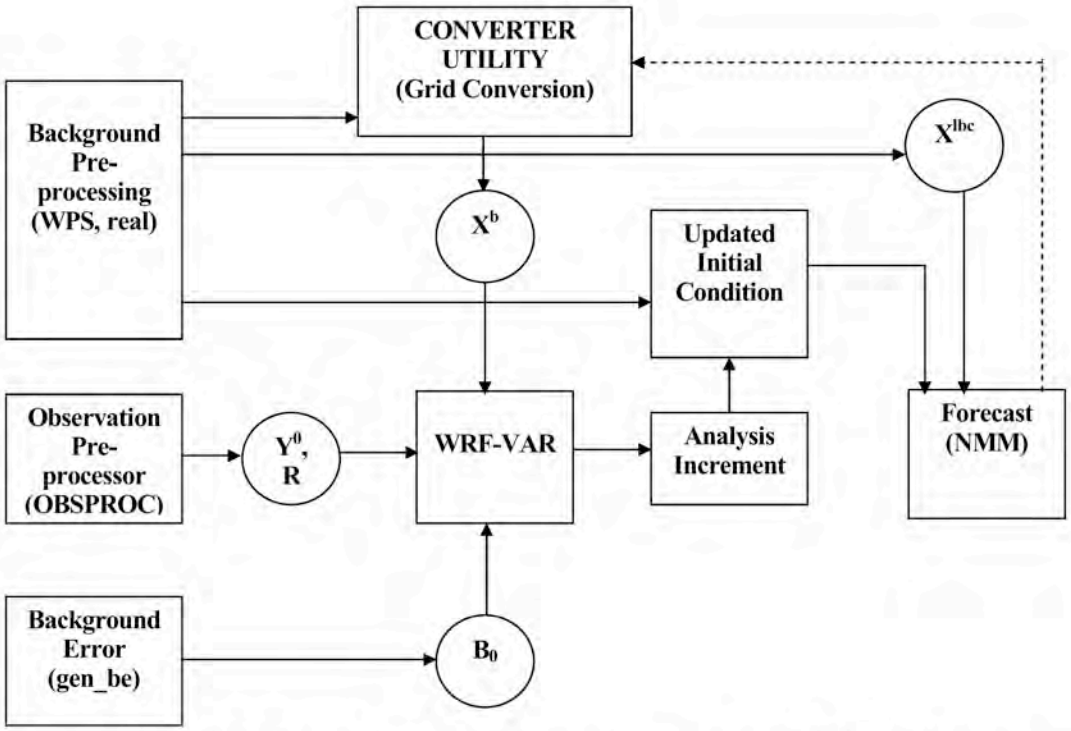

Figure 2 Flow chat for the development strategy of initialization of WRF-NMM with 3-DVAR

4. NUMERICAL EXPERIMENTS & DATA USED

Two sets of numerical experiments are carried out with the WRF-NMM model for each cyclone. In the first set of experiments, i.e. in the control simulation (CNTL), the model has been integrated up to 72 hours in a single domain with the horizontal resolution of 27 km along with 51 levels up to a height of 30 km in the vertical. The performance of any model can not give any concrete conclusion from a single run or from a single case. Keeping this view in mind, the model is integrated for two cyclones (Gonu and Sidr) with five different initial conditions for each cyclone and thus a total of ten cases are used to conclude some tangible results on the performance of the model in the simulation of track and intensity of tropical cyclones. For the Arabian Sea cyclone Gonu, starting from 00 UTC 02 June 2007 and at every 12 hour interval, the model is integrated for 72 hours for each simulation. Thus, five simulations are carried out from the initial conditions of 00 UTC 02 June 2007, 12 UTC 02 June 2007, 00 UTC 03 June 2007, 12 UTC 03 June 2007 and 00 UTC 04 June 2007. Similarly, for the Bay of the Bengal cyclone Sidr, starting from 00 UTC 13

November 2007 and at every 12 hour interval, the model is integrated for 72 hours for each simulation. Thus, five simulations are carried out from the initial conditions of 00 UTC 13 November 2007, 12 UTC 13 November 2007, 00 UTC 14 November 2007, 12 UTC 14 November 2007 and 00 UTC 15 November 2007. The initial and lateral boundary conditions for a limited area model are usually provided from the large scale global analysis and forecast systems. In these control experiments, the NCEP Global Forecast System (GFS) analyses and forecast products (1. X 1. horizontal resolution) are used to provide the initial and lateral boundary conditions respectively.

4.1 Upgradation of WRF-ARW 3DVAR assimilation system for WRF-NMM

The Mesoscale Microscale Meteorology (MMM) Division of National Centre for Atmospheric Research (NCAR) developed a unified (global/regional, multi-model, 3/4DVAR) model-space variational data assimilation system for the research community use which is mainly designed for WRF-ARW modelling system. The code is designed to be a community data assimilation system flexible enough to allow a variety of research studies (e.g. impact of new observation types, globally re-locatable etc) and also its implementation in operational mode. The WRF-3DVAR (thereafter 3DV) performs analysis on non-staggered Arakawa-A grid, where all the variables are available at every grid points. Main input from WRF-ARW model to 3DV are, the wind (U & V) components, perturbated potential temperature, surface pressure, height, mixing ratio on staggered Arakawa-C grid at sigma levels. The perturbation variables here are defined as deviations from a time invariant hydrostatically balanced reference state in the usual sense of WRF-ARW. So, a strategy has been build up to initialize WRF-NMM with 3DV. The system WRF-NMM is designed with Arakawa E-grid staggering with rotated lat/long projection and sigma-pressure hybrid vertical co-ordinate system (Detailed model description section provided in section 2). Hence, in order to accept the Arakawa-E grid data through 3DV, a detailed examination of the variable type and grid system is carried out. For this purpose, a utility known as “grid conversion” is developed, which plays an important role in the assimilation procedure. Figure 2 represents the modified flow chat developed to initialize WRF-NMM output (first guess) with 3DV with the use of newly developed converter utility. Also, keeping the main 3DV code as a unified system, a number of subroutines are developed for IO and analyzing the analysis increment fields while injecting the observational data sets through data assimilation. In this way, the final increments on the analysis fields are evaluated and the initial conditions to the model integration are updated suitably. In the second set of experiments, i.e. with the above stated data assimilation using 3DVAR system (DA), the impact of the observational data sets has been investigated by incorporating the available conventional and non-conventional data sets over Indian region. The analysis is carried out at 27 km horizontal resolution. Hence, for tropical cyclones of Indian seas (Gonu & Sidr), the model is integrated with different initial time each, as mentioned above with the improved initial conditions using WRF-3DVAR system.

5. RESULTS AND DISCUSSION

The results for the above mentioned two cyclones (total 10 cases with 72 hrs forecast each) are presented in this section. The results with the updated initial conditions using the 3DV analysis system are presented. Due to space limitation, for brevity, elaborated results are illustrated and discussed here from the initial condition of 00 UTC 03 June 2007 for Gonu and the results from the initial condition of 00 UTC 13 November 2007 for the Sidr. However, results from all the ten different initial conditions as ten different cases are used for computation of mean vector displacement errors and the percentages of improvements in track prediction with improved initial values in DA experiments are evaluated.

5.1 Mean sea level pressure and Wind at 850 hPa

5.1.1 Arabian Sea Cyclone Gonu

Figure 3 shows the day-1 and day-3 forecast of the MSLP and maximum sustained wind (MSW) as simulated by the model. Figure 3 (a) and (b) are the day-1 forecast of the MSLP with CNTL and DA simulations respectively valid at 00 UTC 04 June 2007. At the day-1 forecast, CNTL simulation shows that, the storm moved northwestward, but there is a formation of two centres with the minimum central pressure of 997 hPa. The DA simulation shows that the storm moved northwestward with the minimum central pressure of 994 hPa. The observed central pressure at

this time was 988 hPa. Figure 3 (c) and (d) are the day-3 forecast of the MSLP from CNTL and DA simulations respectively valid at 00UTC 06 June 2007. At the day-3 forecast, CNTL simulation shows that, the storm moved northwestward with the minimum central pressure of 980 hPa. The DA model simulation shows that the storm moved northwestward with the minimum central pressure of 960 hPa. The observed central pressure at that time was 970 hPa.

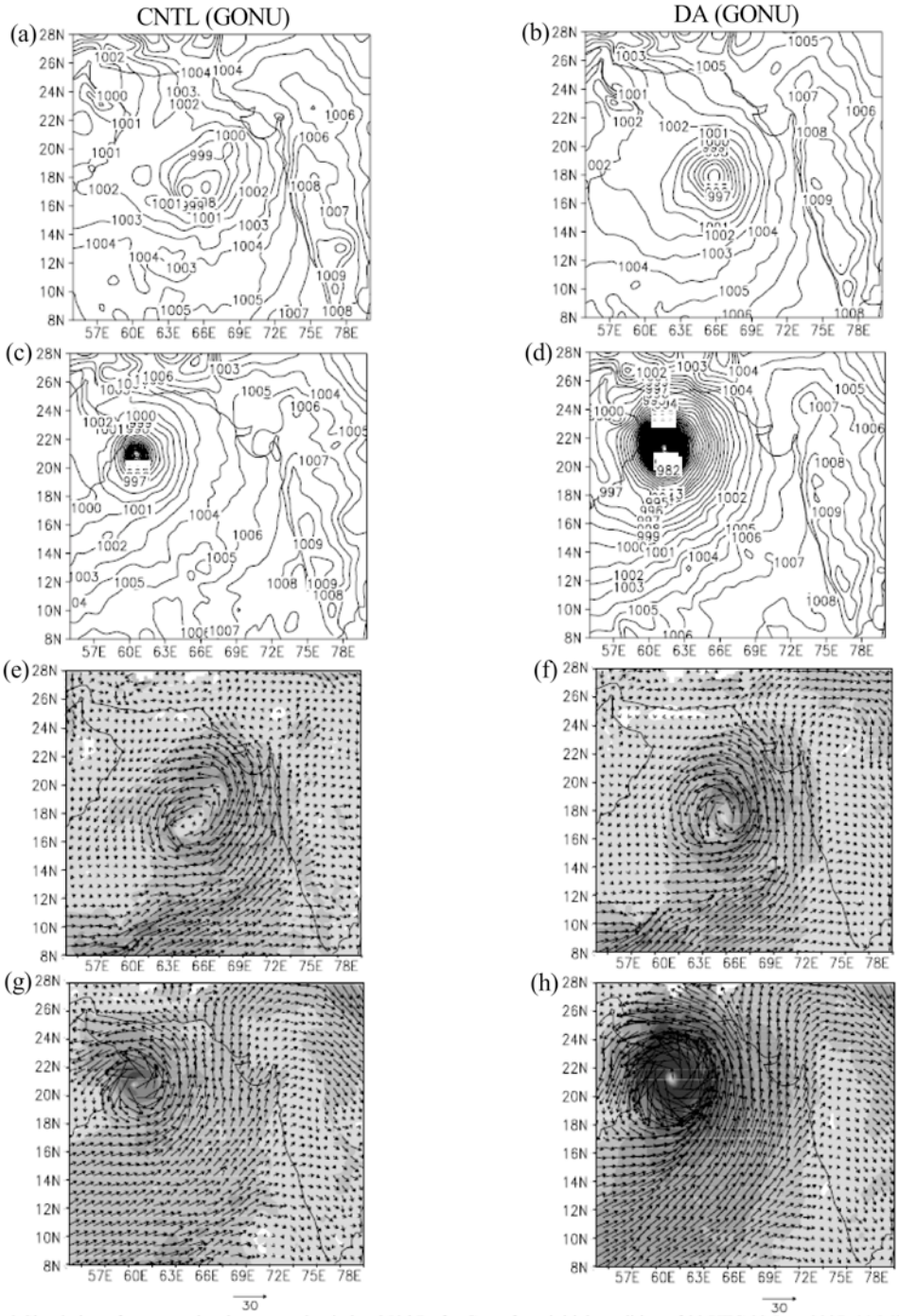

Figure 3 Simulation of mean sea level pressure & wind at 850 hPa for Gonu from initial condition of 00 UTC 03 June 2007. (a) MSLP for Day – 1 with CNTL, (b) MSLP for Day – 1 with DA, (c) MSLP for Day – 3 with CNTL (d) MSLP for Day – 3 with DA, (e) wind for Day – 1 with CNTL, (f) wind for Day – 1 with DA, (g) wind for Day – 3 with CNTL and (h) wind for Day – 3 with DA.

Figure 3 (e) and (f) represents the day-1 forecast of the wind at 850 hPa as obtained from CNTL and DA model simulations respectively valid at 00 UTC 04 June 2007. The day-1 CNTL forecast of wind at 850 hPa shows that the system is being elongated in northeast and southwest direction but the DA simulation shows more concentric wind pattern. Figure 3 (g) and (h) represents the wind at 850 hPa from CNTL and DA simulation valid at 00 UTC 06 June 2007. DA simulation shows much stronger wind than that of CNTL simulation. Again, simulated maximum surface wind is compared with the observed maximum surface wind. The observed maximum surface wind was 77kts valid at 00 UTC 06 June 2007, whereas the CNTL and DA experiments could simulate the maximum surface wind as of 45kts and 65kts respectively at that time.

5.1.2 Bay of Bengal Cyclone Sidr

Figure 4 shows the day-1 and day-3 forecast of the MSLP and maximum sustained wind as obtained from model simulations. Figure 4 (a) and (b) are the day-1 forecast of the MSLP from CNTL and DA experiments respectively valid at 00 UTC 14 November 2007. At the day-1 forecast CNTL simulation shows that the storm moved northward with the minimum central pressure of 998hPa. The DA experiment shows that the system moved northward with the minimum central pressure of 982hPa. The observed minimum central pressure at that time was 964 hPa. Figure 4 (c) and (d) are the day-3 forecast of the CNTL and DA experiments respectively valid at 00 UTC 16 November 2007. At the day-3 forecast, both the simulation clearly shows the landfall of the system with reasonably accuracy.

Figure 4 (e) and (f) represents the day-1 forecast of the wind at 850 hPa as obtained from both the experiments respectively. The day-1 CNTL forecast shows much stronger wind than that of DA simulation. Figure 4 (g) and (h) are the day-3 forecast from CNTL and DA simulations respectively valid at 00 UTC 16 November 2007. In both the experiments, the system is already over land. The observed maximum sustained surface wind was 115kts, whereas CNTL and DA experiments could simulate the maximum surface wind as 60kts and 78kts respectively.

5.2 Precipitation

Figure 5 represents the 24 hours accumulated precipitation as a merged analysis of TRMM, TMI and rain gauges observation carried out by NASA and model simulations for both the cyclones. Figure 5 (a), (b) and (c) shows the precipitations as obtained from TRMM, day-1 forecast of CNTL and day-1 forecast of DA experiments respectively valid at 03 UTC 04 June 2007. The observed precipitation is about 22 cm whereas CNTL and DA experiments could simulate the precipitation of 15 cm and 26 cm respectively. Figure 5 (d), (e) and (f) represents the precipitations as obtained from TRMM, day-3 forecast of CNTL and day-3 forecast of DA experiments respectively valid at 03 UTC 06 June 2007. The observed precipitation was about 16 cm whereas CNTL and DA experiments could simulate the precipitation of 12 cm and 20 cm respectively. Figure 5 (g), (h) and (i) shows the precipitations as obtained from TRMM, day-1 forecast of CNTL and day-1 forecast of DA experiments respectively valid at 03 UTC 14 November 2007. The observed precipitation was 27 cm, whereas CNTL and DA experiments could simulate the precipitation of 15 cm and 22 cm respectively. Figure 5 (j), (k) and (l) shows the precipitations as obtained from TRMM, day-3 forecast of CNTL and day-3 forecast of DA experiments respectively valid at 03 UTC 16 November 2007 from CNTL and DA simulations respectively. The observed precipitation was about 22 cm, whereas CNTL and DA could simulate the precipitation of 12 cm and 20 cm respectively.

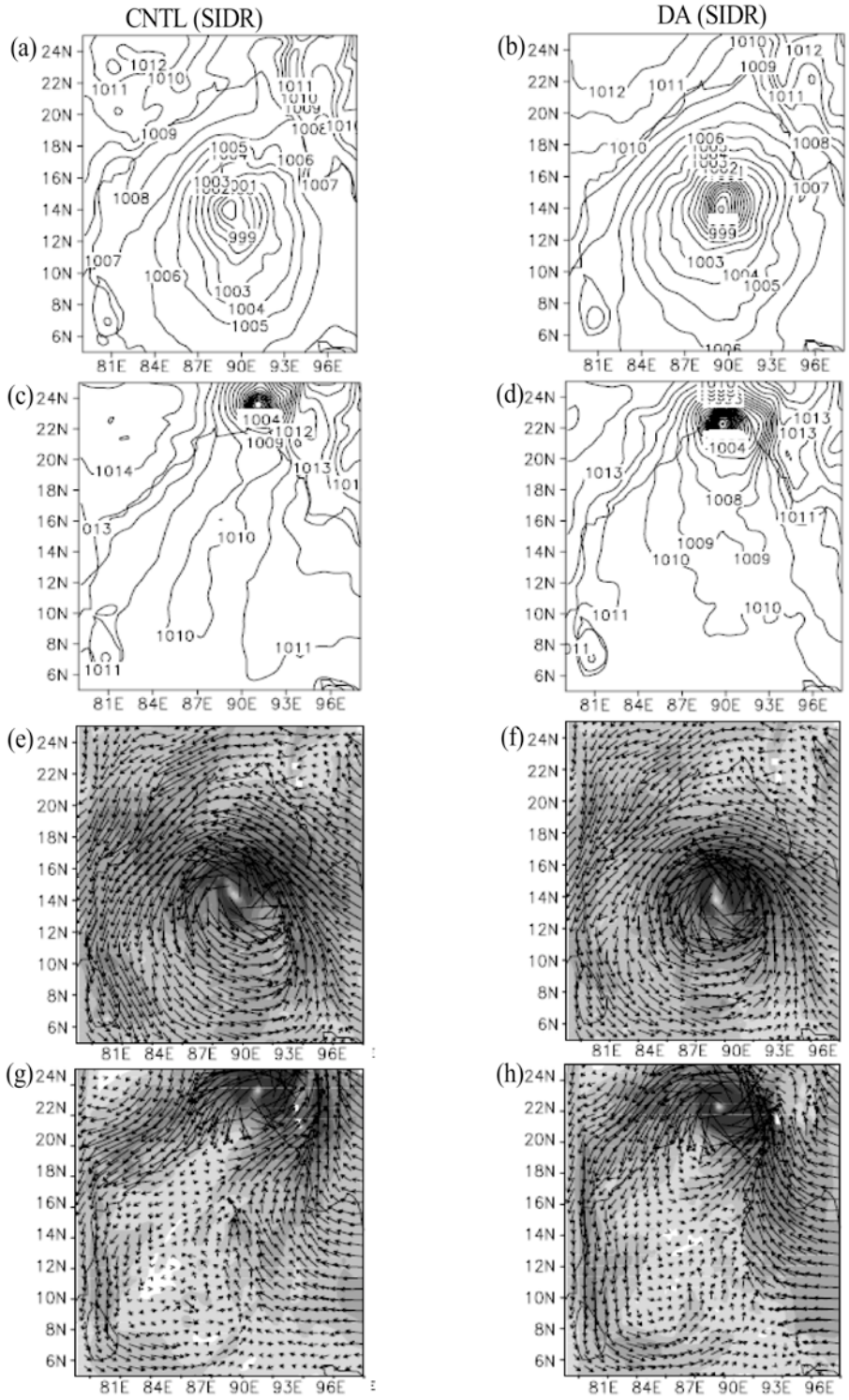

Figure 4 Simulation of mean sea level pressure & wind at 850 hPa for Sidr from initial condition of 00 UTC 13 November 2007. (a) MSLP for Day – 1 with CNTL, (b) MSLP for Day – 1 with DA, (c) MSLP for Day – 3 with CNTL (d) MSLP for Day – 3 with DA, (e) wind for Day – 1 with CNTL, (f) wind for Day – 1 with DA, (g) wind for Day – 3 with CNTL and (h) wind for Day – 3 with DA.

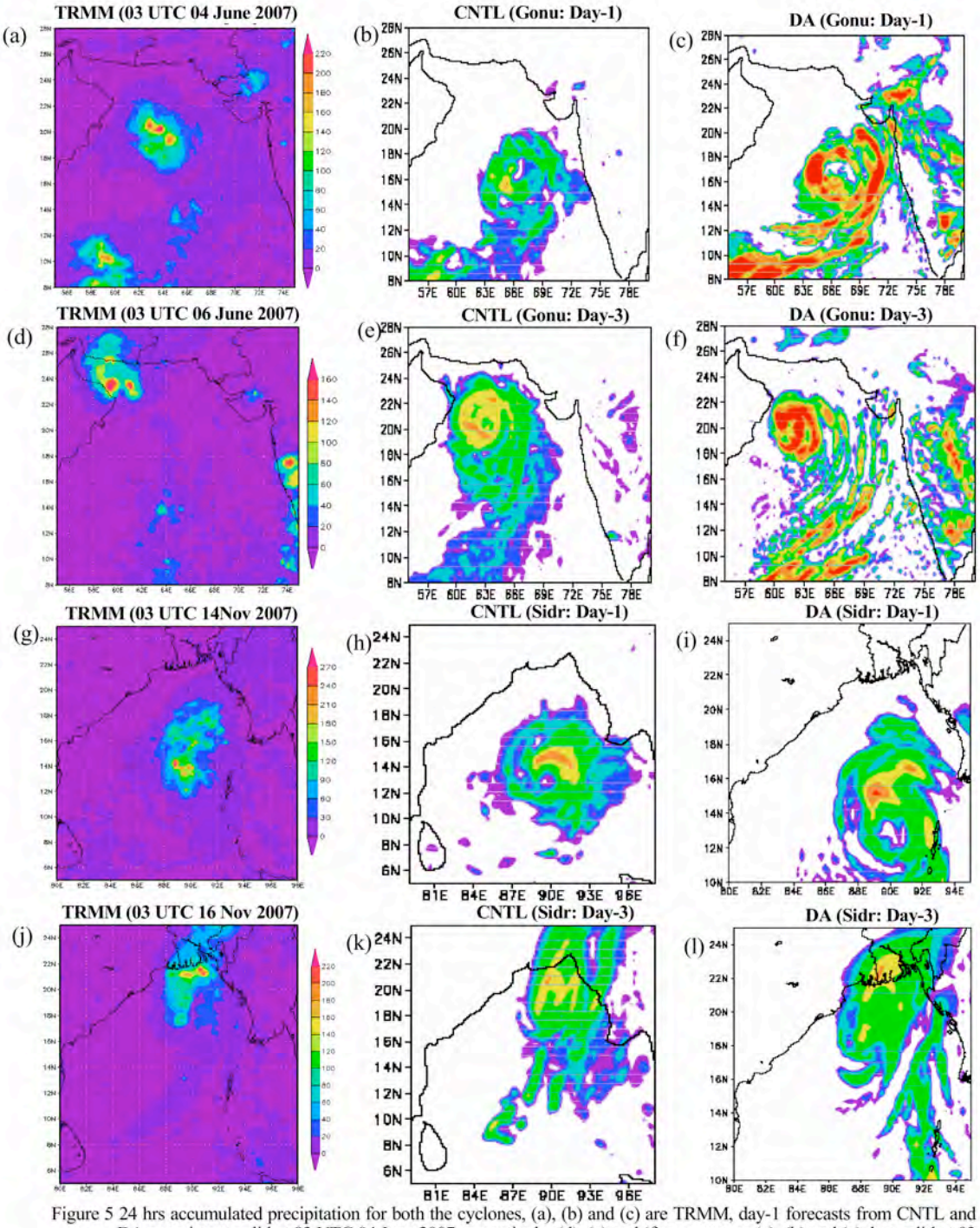

Figure 5 24 hrs accumulated precipitation for both the cyclones, (a), (b) and (c) are TRMM, day-1 forecasts from CNTL and DA experiment valid at 03 UTC 04 June 2007 respectively. (d), (e) and (f) are same as (a), (b) and (c), but valid at 03 UTC 06 June 2007. (g), (h) and (i) & (j), (K) and (l) are same as (a), (b) and (c) & (d), (e) and (f) but for Sidr cyclone and valid at 03 UTC 14 Nov 2007 and 03 UTC 16 Nov 2007 respectively.

5.3 Track

The track of the cyclone as obtained with both the model simulations from different initial conditions are evaluated and compared with the best-fit track obtained from IMD. Figure 6 represents the tracks of the cyclones (Gonu and Sidr) from both control and data assimilation experiments. Figure 6 (a) and (b) are the tracks of the cyclone Gonu from CNTL and DA simulations respectively. Figure 2(c) and (d) are the tracks of the cyclone Sidr from CNTL and DA simulations respectively. The spread of the tracks are comparatively less in the DA experiments than the CNTL experiments. Vector displacement error (VDE) is also calculated by taking the track position from different initial conditions which is presented in Table 2. At the initial time, the mean VDE of 61 km and 54 km are calculated from CNTL and DA experiments respectively, which shows the improvement of 13.8% with DA experiments. The day-1 forecast clearly demonstrate the

VDE of 149 km and 117 km from CNTL and DA experiments respectively, which shows the improvement of 27% with the DA experiments. Similarly, the day-2 forecast demonstrate the improvement of 49% with the DA experiments than CNTL simulations.

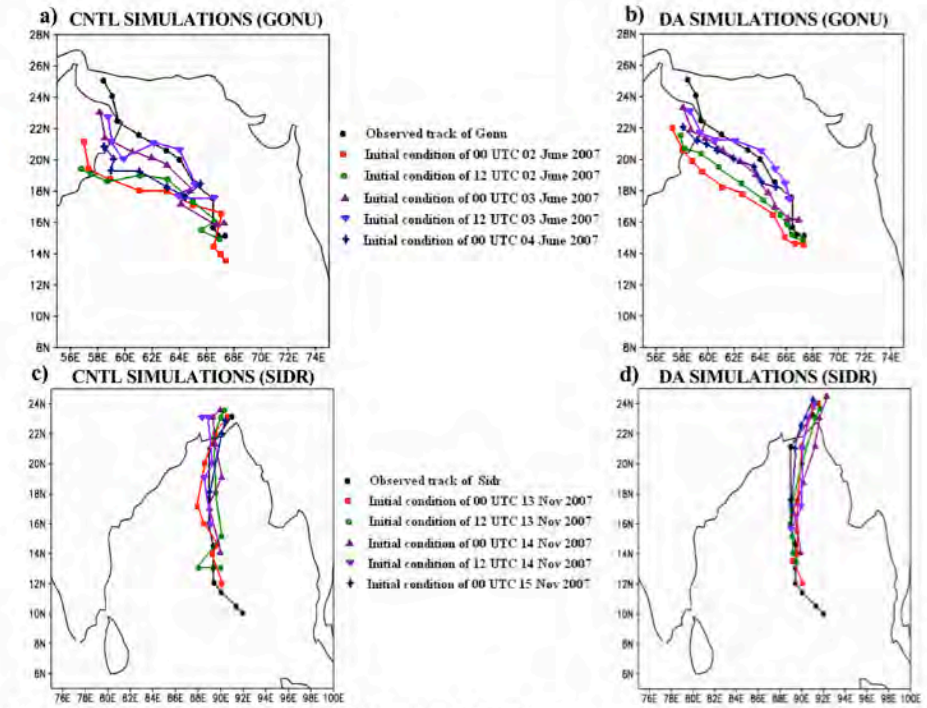

Figure 6 Tracks of the cyclones from different initial conditions: a) tracks of the cyclone Gonu from CNTL experiments, b) tracks of the cyclone Gonu from DA experiments, c) tracks of the cyclone Sidr from CNTL experiments and d) tracks of the cyclone Sidr from DA experiments.

Table 2 - Vector Displacement Errors (in km) for both the cyclones (Gonu & Sidr).

Initial time of model integration	00 hr		12 hrs		24 hrs		36hrs		48hrs	
	CNTL	DA	CNTL	DA	CNTL	DA	CNTL	DA	CNTL	DA
Gonu-1(0200)	100.0	65.0	95.0	55.0	88.5	64.3	128.1	72.2	142.0	77.5
Gonu-2(0212)	60.8	55.0	70.0	50.5	88.3	66.0	124.2	127.5	272.3	144.0
Gonu-3(0300)	32.0	25.0	65.4	54.0	140.7	95.0	188.0	135.2	225.0	175.4
Gonu-4(0312)	59.1	55.0	102.3	72.0	168.0	95.8	202.4	124.8	325.4	196.8
Gonu-5(0400)	50.1	24.4	84.1	61.1	125.1	79.5	223.6	102.5	371.0	155.0
Sidr-1(1200)	118.0	89.4	98.3	105.0	78.5	144.3	148.1	222.2	202.1	277.5
Sidr-2(1212)	80.8	55.5	71.1	59.7	172.3	166.5	248.2	277.5	372.3	44.0
Sidr-3(1300)	22.2	55.5	74.5	44.4	180.7	165.0	228.9	175.5	295.6	305.8
Sidr-4(1312)	35.1	70.1	115.9	78.4	248.2	175.5	323.6	246.2	546.6	496.5
Sidr-5(1400)	55.5	44.4	124.1	101.1	200.1	119.5	323.6	262.9	571.4	355.3
Mean Error	61.36	53.93	90.07	68.12	149.04	117.14	213.87	174.65	332.37	222.78
% of Improvement	**13.8**		**32.2**		**27.2**		**22.5**		**49.2**	

6. CONCLUSIONS

From the present study, following broad conclusions have been drawn. The WRF-VAR system is successfully upgraded for WRF-NMM which is clearly demonstrated through the flow chat mentioned above. The WRF-NMM model could simulate most of the features of the cyclones Gonu and Sidr with reasonable accuracy. From the results, it may be inferred that simulation with CNTL experiments gives the storm movement much faster. However, DA simulation results show reasonable accuracy with the observation. However, it may be noticed that, sometimes CNTL experiments could simulate the maximum sustained wind better than DA simulation results.

It may be noted that, both the experiments could simulated the precipitation well. However, the DA experiments are overestimating in some experiments. The tracks of both the cyclones are reasonably well simulated in both the experiments. Significant improvement of 27% and 49% are noticed from the day-1 and day-2 forecast respectively with the DA experiments than that of the CNTL simulations.

Acknowledgements

We sincerely thank to Mesoscale Microscale Meteorology (MMM) Division of NCAR for providing WRF-ARW modelling system and their valuable scientific help on the development aspect. We thank to NCEP for providing the WRF-NMM system and the real time large scale analyses as well as forecasts of Global Forecast System (GFS). The authors also gratefully acknowledge the IMD for providing observational data sets and best-fit track of the cyclones Gonu & Sidr.

References

Arakawa, A., and W. H. Schubert, 1974, Interaction of a cumulus cloud ensemble with the large scale environment. Part I. J. Atmos. Sci., 31, 674-701.

Bao, J. –W., Wilczak, J. M., Chio, J. –K and Kantha, L. H., 2000, Numerical simulation of air-seas interaction under high wind conditions using a coupled model: a study of hurricane development, Monthly Weather Review, 128, 2190-2210.

Barker, D. M., Huang, W., Guo, Y. –R., Bourgeois, A. J. and Xiao, Q. N., 2004, A Three-dimensional Variational Data Assimilation System for MM5: Implementation and Initial Results, Monthly Weather Review, 132, 897-914.

Braun, S.A. and W.–K. Tao, 2000, Sensitivity of high-resolution simulations of hurricane Bob (1991) to planetary boundary layer parameterizations, Monthly Weather Review, 128, 3941-3961.

Grell, G. A., 1993, Prognostic evaluation of assumptions used by cumulus parameterizations. Monthly Weather Review, 121, 764-787.

Janjic, Z. I., 1984, Non-linear advection schemes and energy cascade on semi-staggered grids. Monthly Weather Review, 112, 1234-1245.

Janjic, Z. I., 2003a, A Nonhydrostatic Model Based on a New Approach. Meteorology and Atmospheric Physics, 82, 271-285.

Janjic, Z. I., 2003b, The NCEP WRF Core and Further Development of Its Physical Package. 5th International SRNWP Workshop on Non-Hydrostatic Modeling, Bad Orb, Germany, 27-29 October.

Janjic, Z. I., J. P. Gerrity, Jr. and S. Nickovic, 2001, An Alternative Approach to Modeling. Monthly Weather Review, 129, 1164-1178.

Knutson, T.R., T.L. Delworth, K.W. Dixon, I.M. Held, J. Lu, V. Ramaswamy, D. Schwarzkopf, G. stenchikov and R.J. Stouffer, 2006b: Assessment of twentieth century regional surface temperature trends using the GFDL CM2 coupled models, Journal of Climate, 19 (9), 1624-1651.

Krishnamurti, T.N., Pattnaik, S. and Bhaskar Rao, D. V., 2007, Mesoscale moisture initialization for monsoon and hurricane forecasts, Monthly Weather Review, 135, 2716-2736.

Liu, Y., Zhang, D.–L. and M.K. Yau, 1997, A multi-scale numerical simulation of hurricane Andrew (1992). Part-I: Explicit simulation and verification, Monthly Weather Review, 125, 3073-3093.

Liu, Y., Zhang, D.–L. and M.K. Yau, 1999, A multi-scale numerical simulation of hurricane Andrew (1992). Part-II: Kinematics and inner core structure, Monthly Weather Review, 127, 2597-2616.

Mandal, M., Mohanty, U.C. and Das, A.K., 2006, Impact of satellite derived wind in mesoscale simulation of Orissa super cyclone, Indian Journal of Marine Sciences, 35(2), 161-173.

Mandal, M., Mohanty, U.C., S. Raman, 2004, A study of the impact of parameterization of physical processes in prediction of tropical cyclones over the Bay of Bengal with NCAR/PSU mesoscale model, Journal of the International Society for the Prevention and Mitigation of Natural Hazards, (31)2, 391 414.

Mohanty, U. C., Pattanayak, S. and Osuri, K. K., 2009, Changes in frequency and intensity of tropical cyclones over Indian seas in a warming environment, Disaster and Development (accepted).

Mohanty, U.C. and Gupta, A., 1997, Deterministic methods for prediction of tropical cyclone tracks, Mausam, (48)2, 257-272.

Mohanty, U.C., Mandal, M., S. Raman, 2004, Simulation of Orissa Super Cyclone (1999) using PSU/NCAR mesoscale model, Journal of the International Society for the Prevention and Mitigation of Natural Hazards, (31)2, 373-390.

Pattanayak, S. and Mohanty U. C., 2008, A comparative study on performance of MM5 and WRF models in simulation of tropical cyclones over Indian seas, Current Science, (95) 7, 923-936.

Webster, P. J., Holland, G. J., Curry, J. A. and Chang, H. –R., 2005, Changes in tropical cyclone number, duration and intensity in a warm environment, Science, 309, 1844-1846.

Zhang, D. –L. and Wang, X., 2003, Dependence of hurricane intensity and structure on vertical resolution and time-size, Advance Atmospheric Sciences, 20, 711-725.

NWP MODEL ASSESSMENT DURING THE TROPICAL CYCLONE GONU

Sultan Salim Al-yahyai
Directorate General of Meteorology and Air Navigation
P.O.Box 1, P.Code 111, Oman

Abstract

Directorate General of Meteorology and Air Navigation (DGMAN) is running the limited area model of Deutsher Wetterdinest (DWD), High Resolution Model (HRM) since November 1999. HRM is used operationally to forecast different weather parameters. HRM is running at two resolutions, 28km resolution that covers the Arabia peninsula and part of the Indian continent. Due to the lack of computational power, the 7km resolution covers Oman and small part of Arabia peninsula only. Oman forecasting centre have depended on the HRM_28km as well as other Global and regional NWP models before and during the tropical cyclone Gonu (2007) to issue the forecast and warnings. Recently, with kind co-operation with the Deutsher Wetterdinest (DWD), DGMAN was able to install Consortium for Small-scale Modeling (COSMO) model for scientific research and evaluation since April 2008 at 7 km resolution covering on the same domain as of HRM_07.

Even though, both models are not specialized cyclone tracking. The objective of this study is to evaluate the performance of DGMAN's NWP models during the tropical cyclone Gonu period. Both models were re-run to simulate the tropical cyclone Gonu during the period of 3-6 June 2007. The study covers evaluation of cyclone track, intensity and associated rainfall amount. This inter-comparison will also answer the question "Would the forecast be better if COSMO was there during the tropical cyclone Gonu?.

Key Words
HRM, COSMO, Gonu, assessment, Oman

Introduction

Historical Events: Tropical Storms and cyclones are almost entirely confined to two cyclone seasons namely the pre-monsoonal period (May-June) and post-monsoonal period (October-November) (Membery 1985). Most storms originate over the south-eastern Arabian Sea in the vicinity of the Laccadive Islands, but some late season storms start over the southeastern Bay of Bengal and move westwards across southern India re-generating as they cross over the warm waters of the Arabian Sea. Table 1 shows the frequency of tropical storms and cyclones (wind speeds of Beaufort force 10 or more) affecting the Arabian Sea, 1801-2000 (as given by Membery 2001). Two additional cyclones have been added to the table. One affected Salalah coast on 10 May 2002 (Al-Maskati 2006) and the second affected Muscat cost 6 June 2007. Tracks of the historical events on the Arabian Sea and the Pay of the Bengalis show in the Figure bellow.

Table 1 - Frequency of Tropical Storms and Cyclones

Jan.	Feb.	Mar.	Apr.	May	June	July	Aug.	Sep.	Oct.	Nov.	Dec.
1	0	1	9	27	30	1	2	4	19	31	4

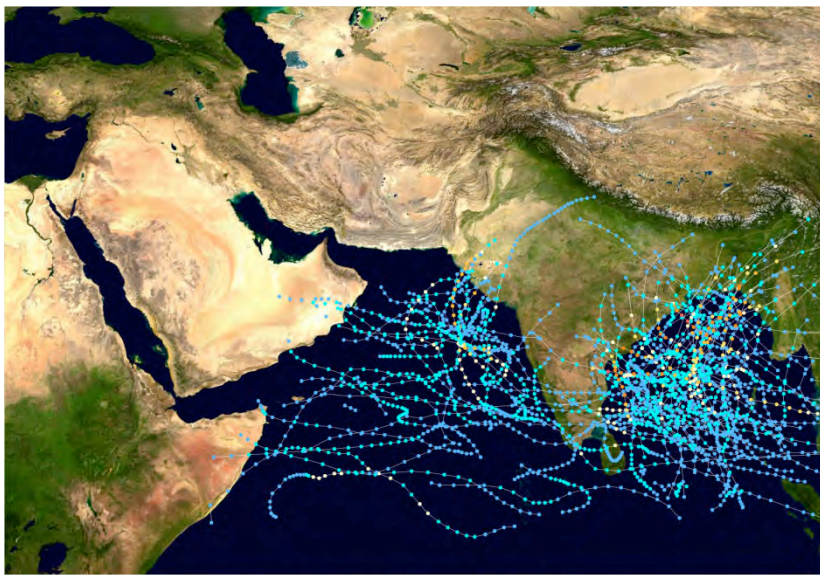

Figure 1 - Of the Historical Events on the Arabian Sea and the Pay of the Bengalis, 1985-2005 (Nilfanion 2005).

1. TROPICAL CYCLONE GONU (02A)

Gonu started as a low pressure system over the Indian Ocean on June 1st (15 N, 68.5 E) then it intensified to deep depression on June 2nd (700km south west of Mombai). On June 3rd, Gonu was a tropical storm and it was then called Gonu by the regional centre for tropical cyclone monitoring on the Indian Ocean (New Delhi). It was centred on the eastern part of the Indian Ocean (15.5N, 66.5E). on June 3rd, Gonu was about 1150km from Maserah Island and moving to the west with about 8-10km/h with maximum wind around the centre of about 90-100km/h. Gonu was classified as tropical cyclone on June 4th (Figure 2) where it was centred around 18.5N, 65E and it was about 700km from Maserah Island. Gonu was moving North to North West. During this day Gonu intensified and moved from Class2 to Class4 with maximum wind around the centre of about 213-232km/h .On June 5th, Gonu (Figure 2) started affecting the southern costs of Oman from Wusta region to Ras Al-Had associated with heavy rains, strong wind (Gusting 180km/h at Qalhat Station), and high waves.

Gonu started affecting Muscat on June 6th (Figure 2) at after mid night, where Mina Qaboos weather station recorded wind speed of 93km/h and then stopped as shown on Table 2. Associated clouds extended vertically about 17.5km between 2500 and 60000 feet above the ground with air temperature of about (-80) degrees on the upper levels of the atmosphere. During the day, Gonu continued to move north to north west toward Gulf of Oman with continuous heavy rain over Muscat, Dakheleya, and Batenah regions as shown on Figure 2. During this movement and due to the lake of moisture feeding, Gonu was weakening until it was downgraded to tropical storm on June 7th on its way to Iran as shown on Figure 2.

Table 2 - wind speed (km/h) recorded on different Oman weather station during June 5th and 6th.

Station Name	June 5th Wind speed (km/h)	June 6th Wind speed (km/h)
Qalhat	105	180
Sur	95	---
Seeb	32	86
Mina Qaboos	44	93
Maserah	65	72
Sohar	29	63
Ibra	59	72
Adam	59	49
Bahla	68	84
Buraimi	49	51
Nizwa	59	67
Sqiq	123	---
Rustaq	36	74
Samail	70	95

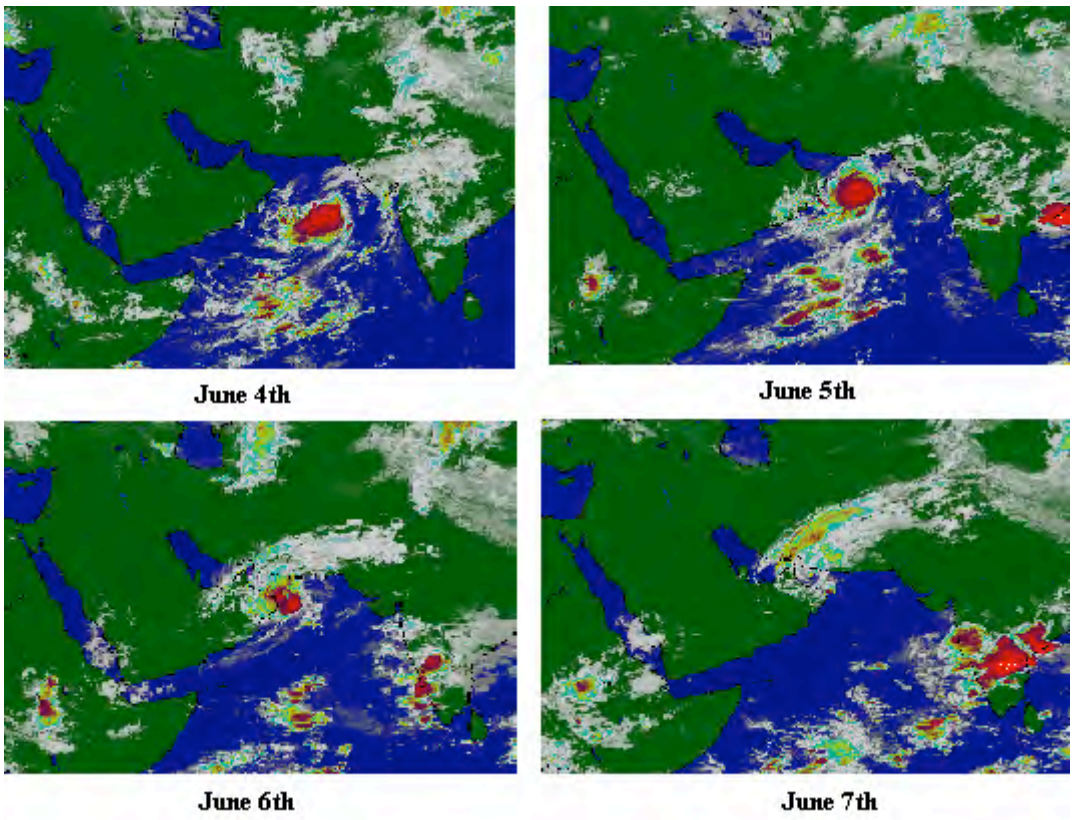

Figure 2 - Satellite images at 00UTC (4am LST). © Eumetsat.

Table 3 - Total accumulated rainfall for cyclone Gonu (5 & 6th June 2007).

Rainfall (mm)	Location
401	Qalhat
230	Sur
257	Seeb
60	Ibra
2.2	Masirah
78	Rustaq
83.2	Samail
4.8	Nizwa
253	Taiin Mountain
592	Abiadh Mountain
943	Asfar Mountain

2. NWP MODELLING

Oman Meteorological Department is equipped with two hydrostatic atmospheric numerical weather prediction models (HRM) which run operationally twice daily one at 28 km resolution and covers the Arabian Peninsula and Arabian Sea Figure 3A) and the other with a resolution of 7 km and covers Oman and the surrounding areas (Figure 3B). Hourly output from these two models is provided for seventy eight hours from the initial time. Ten meter winds from these models are used to drive wave model which also provides a forecast for seventy eight hours for the water bodies on the domain shown on (Figure 3A). With the kind scientific cooperation with German meteorological service, DGMAN was able to run COSMO model for scientific evaluation during summer rain activities. COSMO model run with 7km resolution.

HRM: **H**igh **R**esolution **M**odel HRM (Majewski 2009) is a hydrostatic mesoscale NWP model. It has been developed at The Deutscher Wetterdienst (DWD) and currently used in more than 30 universities and national weather services. It solves for surface pressure, temperature, water vapour, cloud water, cloud ice and horizontal wind components (u, v) explicitly, in addition with several surface/soil parameters. It uses regular or rotates latitude/longitude grid using Arakawa C-grid and Hybrid vertical coordinate based on (Simmons and Burridge, 1981). Different sub-grid scale processes are parameterized including radiation, convection and soil processes. HRM model is available free of charge for scientific, educational and operational use.

COSMO: **Co**nsortium for **S**mall-scale **Mo**deling **COSMO** (U. Schuattler 2008) was formed in October 1998. The consortium members include Germany, Switzerland, Italy, Greece, Poland and Romania. The COSMO is a nonhydrostatic limited-area atmospheric prediction model. It has been designed for both operational numerical weather prediction (NWP) and various scientific applications on the meso-β and meso-γ scale. The COSMO-Model is based on the primitive thermo-hydrodynamical equations describing compressible flow in a moist atmosphere. The model equations are formulated in rotated geographical coordinates and a generalized terrain following height coordinate. A variety of physical processes are taken into account by parameterization schemes. COSMO-Model is available free of charge for scientific and educational purposes, especially for cooperational projects with COSMO members.

3. CASE STUDY CONFIGURATION

During this study, both models have been re-run during the period 3-6 June 2007 based on the German Global Model GME 00/12UTC analysis.

Figure 3 (A,B) shows the operational domain for 28km and 7km resolutions respectively. It is clear that the 7km domain does not cover the area of Gonu during the period of the study, therefore the 7km domain was shifted southeasterly to cover the area 14–29N and 48.5-63.5E as shown on Figure 3 (C).

This case study was run on the operational PC cluster on DGMAN. The cluster consists of 40 Opteron AMD processors, each with 2GB of RAM. This machine is also used for the operational run of the NWP models at DGMAN. DGMAN archives the initial and the boundary condition files received from the German global model for future use and research purposes. Figure 4 shows the data flow diagram of the model. Global model data are sent through the internet to the DGMAN firewall system then the data are archived into the archive server. The initial and lateral boundary data are then sent to the PC_cluster machine and HRM_28 km resolution and COSMO_07 km resolution are started. HRM_28 provide data as initial and later boundary data for HRM_07km resolution. The outputs of all models are then sent to the verification process. Observation data and satellite images also needed during the verification process.

Figure 3 - Operational and case study model domain, A: HRM_28, B: Operational HRM_07/Cosmo_07 and C: Case study HRM_07/Cosmo_07.

For the purpose of the study, comparison data was collected from different sources. Best Track and wind intensity information were collected from the Joint Typhoon Warning Centre JTWC website archive. On the other hand Pressure intensity reports were collected from the DGMAN archive. The pressure intensity reports are originated at the Cyclone Warning Centre of India CWCI. Moreover the rainfall information was collected from the department of hydrology, Oman. The rest of the paper will be organized as follow: initial data analysis, track evaluation, rainfall evaluation, conclusion and future work.

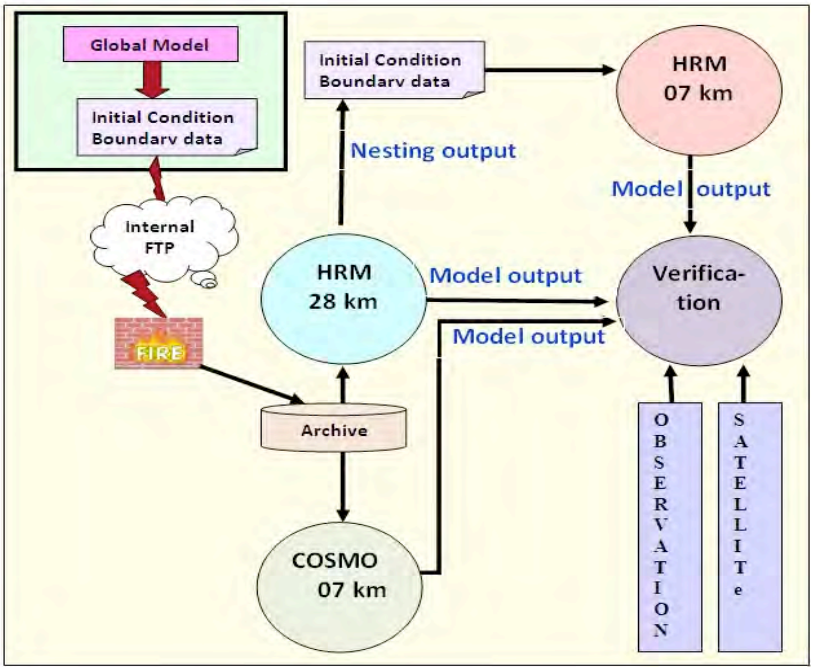

Figure 4 - Data flow of the case study.

4. INITIAL DATA ANALYSIS

German Global Model GME is the deriving global model for the operational runs at DGMAN. GME is currently running on 40km resolution and 40 vertical layers. Therefore GME is the deriving model for the study; on this section we will evaluate the GME analysis during the Gonu case.

Figure 5 shows comparison between Gonu Best Track and the track generated from the GME 00/12 UTC analysis. From the Figure we can notice the deviation on the cyclone centre according to GME analysis. This deviation reached more than one degree on June 5th 00 UTC analysis and on June 6th 00UTC analysis.

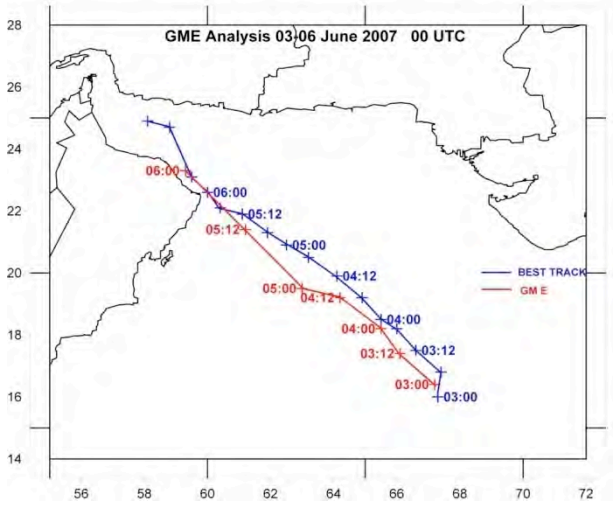

Figure 5 - Gonu Best Track and Track from GME 00/12 UTC analysis.

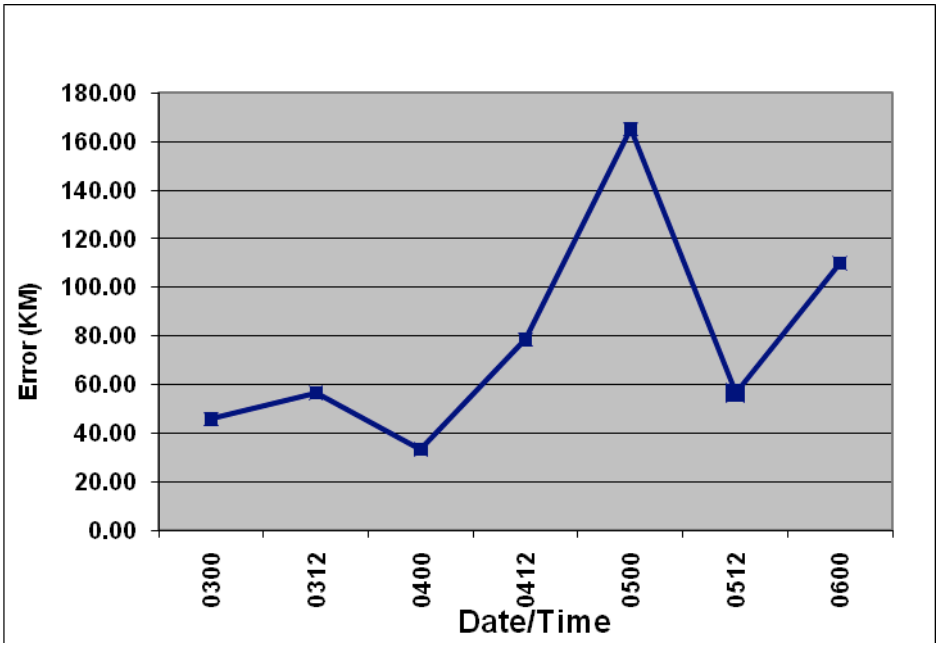

Figure 6 - Error (KM) of GME analysis with Respect to Gonu Best track.

With respect to the pressure intensity we can see from Figure 6 that the pressure drop on the GME analysis is much weaker than the estimated pressure drop of Gonu during the whole period of the study. The minimum pressure on the GME analysis was 990hpa on June 5th 12 UTC, while the minimum estimated pressure was 934hpa on June 4th 09 UTC.

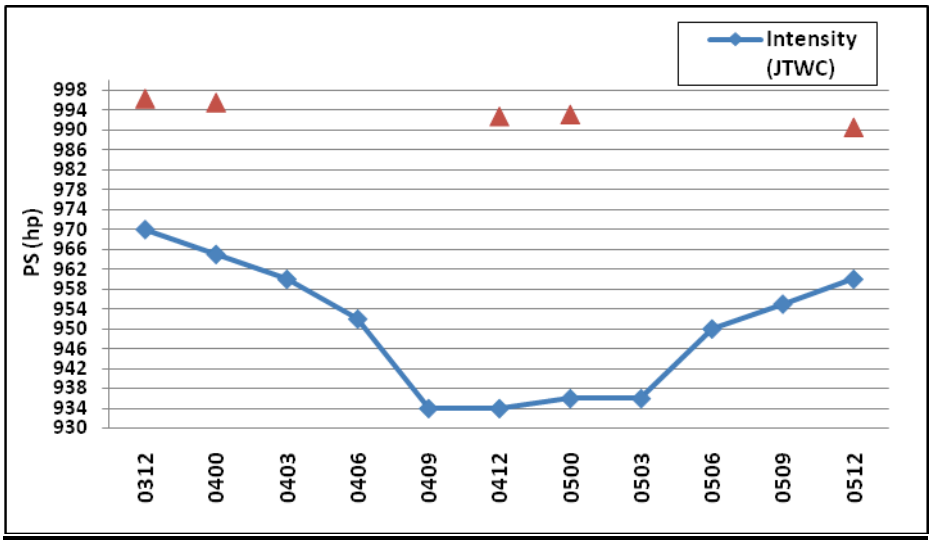

Figure 7 - Pressure intensity comparison between GME analysis and estimated pressure intensity from the JTWC.

Track Evaluation

On this section we compare forecasted tracks from both HRM/COSMO using different model runs against Gonu Bets Track. We also included the forecasted tracks from JTWC models to include at least one tropical cyclone specialized model (JTWC) against our models which are not tropical cyclone specialized models. The details of the forecasted tracks are shown on Figure 5. The Figure shows model run starting from June 3rd, 00 UTC to June 5th, 12 UTC.

Figure 8 shows the DGMAN NWP model track forecast are with agreement with the specialized JTWC model track forecast, and they all suggested that Gonu will make landfall on the area between Masera Island and Ras- Alhad during June 3rd for both 00/12 UTC. Starting from 4th June, JTWC made a significant change on the track forecast as the 12 UTC run forecasted Gonu to make landfall on Muscat. While both HRM and COSMO did not predict such a scenario, they only started predicting the landfall on Muscat during the 12 UTC run of June 5th with some variation from the JTWC model forecast.

Wind intensity evaluation

Figure 9 shows estimated wind intensity from JTWC and the wind forecasted from different model runs of COSMO and HRM models of both 28km and 7km resolution. HRM_28km and HRM_07 were not able to forecast wind speed of more than 45 knots during the whole period while the estimated wind from JTWC reached up to 140knots. On the other hand, COSMO model was able to forecast wind speed up to 60 knots which according to the Area Cyclone Warning Services (ACWC's) from India classification as a "Sever Cyclonic Storm" while Gonu was classified as "Super Cyclonic Storm" according to the Indian classification (wind > 120knots).

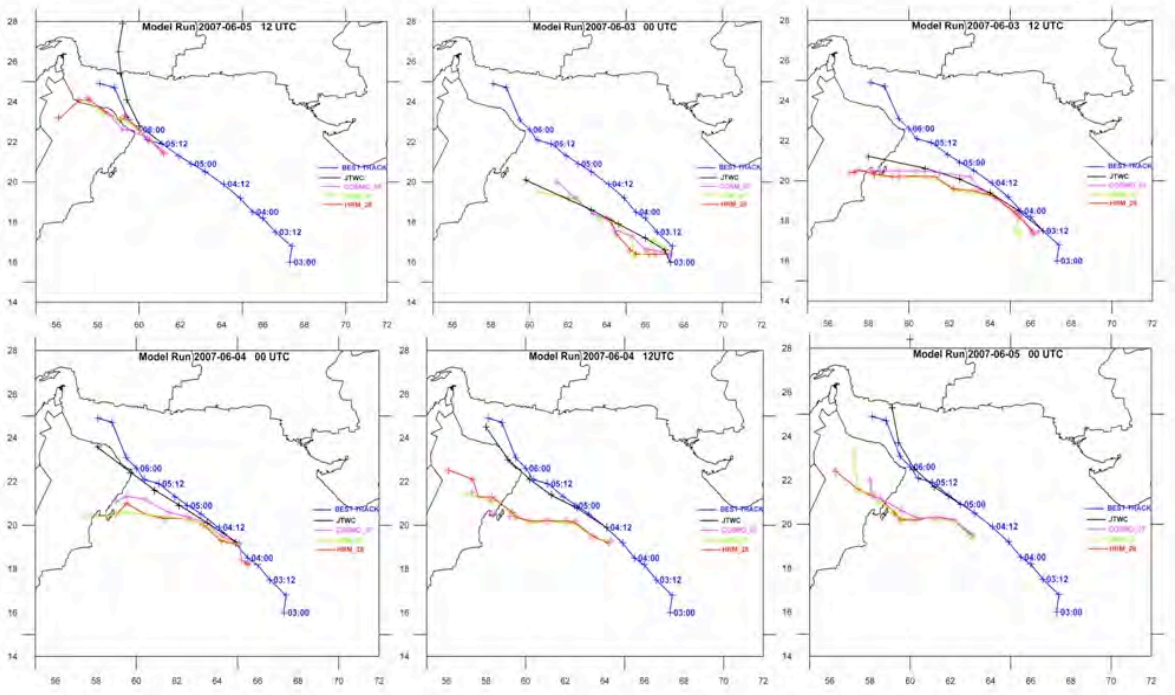

Figure 8 - Gonu Best Track and track forecast from different models and model runs. Best Track (blue), HRM_28(red), HRM_07 (green), COSMO (pink) JTWC (black).

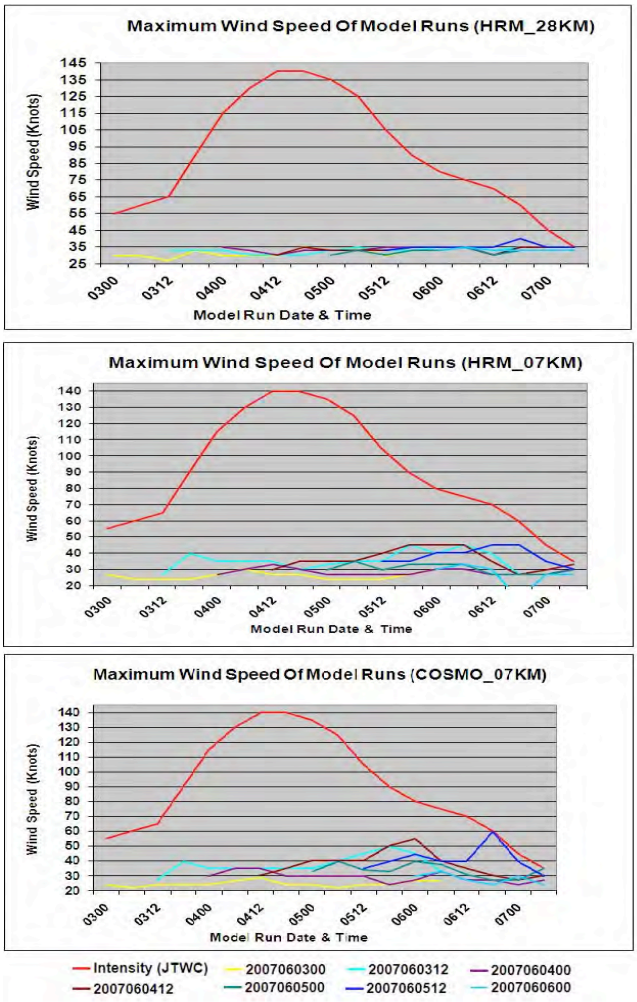

Figure 9 - Estimated wind speed intensity and wind forecast from HRM/COSMO.

Rainfall Evaluation

Figure 10 shows the 48h recorded rainfall (top left chart) between the period of June 5th – June 7th and forecasted rainfall amount from different model based on June 5th 00UTC run. HRM_28 was not able to forecast the maximum recorded rainfall of (900mm). It has forecasted up to 400mm. On the other hand, HRM_07 and COSMO models predicted rainfall of more than 1000mm. Location Weiss; all the models predicted two different maxima, the first maxima is far to the south from the recorded maximum. The Second maxima of both HRM_07 and COSMO model (787mm, 745mm respectively) is located closer with the recorded maximum.

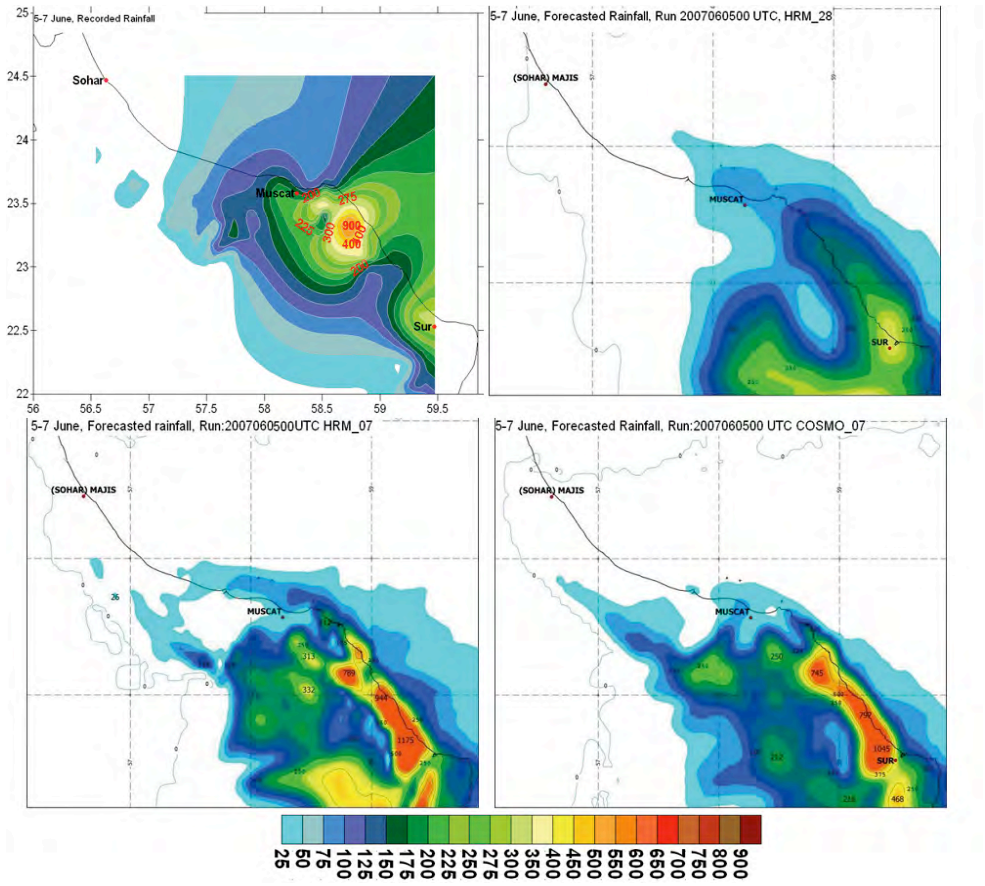

Figure 10 - 48h recorded (top left) rainfall amount and forecasted amount from different models based on June 5th 00UTC run. HRM_28 (top right), HRM_07 (bottom left), COSMO (bottom right).

Conclusion

On this paper we have presented an evaluation of DGMAN's NWP models during Gonu on the period of June 3rd to June 6th 2007. The study included rerun of HRM and COSMO models for the same period. Track forecast, cyclone intensity and associated rainfall were investigated. Moreover, we also evaluated the analysis of German Global model for the same period because it was the deriving global model for both regional models. From the evaluation study we can summarize the flowing:

- GME (driving model) miss located Gonu centre and underestimated the associated wind and pressure drop.
- § Clear dependency between GME forecast quality and HRM/COSMO forecast quality.
- § Even though HRM/COSMO are not TC specialized models, both have given the signal for Gonu.
- § COSMO_07 were able to forecast Gonu as Severe Cyclonic Storm starting from 12UTC run of 4th June 2007.

- § On average COSMO shows 5% improvement of track forecast and 3% on the wind intensity over HRM.
- § Both HRM_07 and COSMO_07 have signalled 48h rainfall of more than 900mm starting at June 5th with reasonable spatial and good amount agreement with the recorded rainfall.

Future work

DGMAN is planning to introduce a 3Dvar data assimilation system on the first half of 2010, and then the effect of the 3Dvar on the performance of both models will be investigated. Moreover a new version of HRM model is being developed to include tropical cyclone bogus scheme. The new scheme will be test for tropical cyclone track predictability using Gonu case on our domain. Finally, the effect of the initial state and lateral boundary condition of the deriving model GME was clear in the performance of both HRM and COSMO models. To avoid depending on one source for the deriving model, we plan to introduce a short range ensemble forecast SREF. The SREF system will also be tested for Gonu Case.

References

Al-katheri Ahmed, Radi AJJAJI, DHANHNI Abdullah, *Assimilation and simulation of Cyclone Gonu (2007) using the UAE WRFVAR system* [online]. Available: http://www.mmm.ucar.edu/wrf/users/workshops/WS2008/abstracts/P5-08.pdf [accessed 28 March 2009].

Global Tropical Cyclone Tracks by Nilfanion on WikiPedia (2005), http://en.wikipedia.org/wiki/File:Global_tropical_cyclone_tracks-edit2.jpg.

India Meteorological Department, Cyclone Warning Services (ACWC's) [online]. Available: http://www.imd.gov.in/main_new.htm [accessed 28 March 2009].

Juma Al-Maskari, Processes of convection and airflow over the Hajar Mountains, PhD thesis, University of Leeds, 2006.

Majewski Detlev, HRM user guide, Deutscher Wetterdienst , March 2009.

Membery, D., A unique August cyclonic storm crosses Arabia. Weather, 40, 108–115. 1985.

Membery D., Monsoon tropical cyclone: Part 1. Weather, 56, 431-438. 2001.

Regional and Mesoscale Meteorology Branch (RAMMB). Tropical Cyclone GONU [online]. Available: http://rammb.cira.colostate.edu/products/tc_realtime/storm.asp?storm_identifier=IO022007 [accessed 28 March 2009].

U. Schuattler, G. Doms, and C. Schraff, COSMO model user guide, Deutscher Wetterdienst, March 2008.

UNDERSTANDING THE TROPICAL CYCLONE GONU

*Khalid Ahmad Al Najar and*P.S. Salvekar*
Directorate General of Navigation and Meteorology, Salalah Airport, Oman
**Indian Institute of Tropical Meteorology, Pune-411008, India*

Abstract

May to mid of June is the most active period in which tropical storms and cyclones make landfall along Oman coasts. A total of 10 tropical cyclones as well as a total of 18 tropical storms or depressions affected Oman coasts in during the last 112 years. Recently in the first week of June 2007, one of the strongest cyclones, 'Gonu' reached Oman Coast.

The super cyclone Gonu is simulated using the non-hydrostatic MM5 model to study the track, the intensity and the evolution. Two nested domains were used with resolutions 45 and 15 km covering the Indian Ocean and the Arabian Sea. The MRF PBL and KF2 schemes were used for parametrizing the boundary layer and convection. This combination was able to predict the track of the cyclone. The period under study covered the three days from 4th June to 6th June. The maturity of the cyclone is indicated by a value of vorticity at lower levels about 25 x $10^{-5}s^{-1}$. The simulation produced pressure values at the centre of the cyclone as low as 990 hPa. Severe wind 20-26 m/s are noted at levels up to 400 hPa.

Key Words : Gonu, MM5, MRF PBL, KF2, tropical cyclone

INTRODUCTION

Tropical cyclones are non-frontal synoptic-scale warm-core low-pressure systems that originate over the tropical or subtropical oceans and contain organized deep convection and a well-defined cyclonic surface wind circulation. Tropical cyclones form over warm ocean waters which supply energy to the atmosphere in the form of latent and sensible heat. Under favourable atmospheric thermo-dynamical conditions associated with low level convergence a surface low develops into a cyclonic storm. The movement of the tropical cyclone is generally known by the knowledge of the upper atmospheric conditions and the prevailing circulations.

Based on intensity, tropical cyclones in the Atlantic, Eastern and Western Pacific are classified as a tropical depression for a weaker system with $V_{max} \leq 17$ m/s ($\approx$62 km /h), a tropical storm for a moderate system with 18 m/s $\leq V_{max} \leq$ 32 m/s, and a hurricane or typhoon for a strong system with $V_{max} \geq 33$ m/s. Hurricanes are called major hurricanes when $V_{max} \geq 50$ m/s and typhoons are classified as super typhoons when V max $\geq$ 67 m/s. The maximum wind speed of a strong tropical cyclone may exceed 100 m/s, which may produce storm surge by driving an ocean rise of several meters along the coast.

On the average about five tropical cyclones occur annually over the Bay of Bengal (Bhaskar Rao et al. 1999) in the north Indian Ocean which contributes 6 percent of the global annual frequency. Based on the maximum sustained winds associated with the system and geographical location of their occurrences, they are classified into a depression, a tropical storm, a severe cyclone or hurricane (Asnani, 1993). There are two cyclone seasons in the north Indian Ocean viz, pre-monsoon (especially May) and post-monsoon (October and November). A few cyclones can also form in the transitional monsoon months June and September (i.e. arrival and withdrawal phase of the Indian summer monsoon). It is shown by O.P.Singh et.al.,2001 that frequency of intense tropical cyclones is increased in the Indian ocean.

1. TROPICAL CYCLONES AT OMAN COAST

Oman suffers the danger of the tropical cyclones in the transitional seasons. The tracks of Tropical Cyclones affected Oman since 1948 are shown in the Figure 1. Recently in June 2007 the super cyclone Gonu reached Oman coast. The cyclone is considered as the strongest in the last hundred years. Observations contain phenomenal record such as 900 mm of rain during 5th June, very high wind about 130 km/h and sea level rising to 12 m during the passage of the cyclone.

About seven hours before passing near the northeastern Oman coastline, Cyclone Gonu began affecting the country with rough winds and heavy precipitation, with rainfall totals reaching 610 mm near the coast. Gonu produced strong waves along much of the coastline, leaving many coastal roads flooded. The cyclone caused extensive damage along the coastline, including in the city of Sur and the village of Ras al Hadd at the eastern most point of the Omani mainland. Around 20,000 people were affected, and damage in the country was estimated at around $4 billion USD, ranking it as the worst natural disaster on record in Oman. Due to this disastrous event, the understanding and prediction of Tropical cyclones along the Oman coast has got importance. Most of the tropical cyclones have very few observations in their vicinity. Therefore, impact of initial vortex to simulate tropical cyclone formed over the Arabian Sea during November 2003 is studied by Sandeep et.al., 2007 using MM5 model. In the literature numerical simulations of many other Indian Ocean cyclones are available using meso-scale models (e.g. Mandal et.al.2006, Trivedi et.al. 2006). Liu et.al (1997) carried out explicit simulation and verification of Hurrican Andrew using MM5 model. Here, the present study is attempted to simulate the Gonu cyclone track using meso-scale numerical model.

2. GONU CYCLONE CASE DESCRIPTION

On May 27, a widespread area of convection persisted over the southeastern Arabian Sea. By May 31, an organized tropical disturbance developed about 645 km south of Mumbai, India with cyclonic convection and a well-defined mid-level circulation. On June 1st the system it developed to the extent that the Indian meteorological department (IMD) classified it a depression. On June 2nd the joint Typhoon warning Centre (JTWC) classified it a tropical cyclone 02A while it was located about 685 km southwest of Mumbai, India. Gonu turned to the north and north east, though resumed a westward track. It rapidly intensified to attain a severe cyclonic status early on June 3rd. Gonu rapidly deepened and developed a well-defined eye. Late on June 3, the storm was classified as Very Severe Cyclonic Storm Gonu, upon which it became the most intense cyclone on record in the Arabian Sea. Gonu strengthened further to attain peak 1-min sustained winds of 260 km/h and gusts to 315 km/h while located about 285 km east-southeast of Masirah Island on the coast of Oman. The IMD upgraded it to Super Cyclonic Storm Gonu late on June 4, with 10-min sustained winds reaching 240 km/h and an estimated pressure of 920 mbar.

After maintaining peak winds for about 9 hours, the IMD downgraded Gonu to very severe cyclonic storm status early on June 5. Due to land interaction with Oman, the inner core of deep convection rapidly weakened, and over a period of 24 hours the intensity decreased by 95 km/h. That day evening Gonu reached Jabal Ras Al Had bringing torrential rains, high waves and very strong winds, Kalhat recorded 131 km/h at 2.50 A.M and rainfall was 235 mm. Also on the same day, during the passage of the cyclone Al Jabal Al Asfar station had an accumulated rainfall in 24 hours of 934 mm. As Gonu crossed the eastern-most tip the winds continued to gradually decrease due to interaction with land. After emerging into the Gulf of Oman, the cyclone intensified slightly, becoming the first recorded tropical cyclone in the Gulf of Oman.

On June 6, the cyclone turned to the north-northwest and downgraded to tropical storm status. The IMD downgraded Gonu to severe cyclonic storm status and later to cyclonic storm status early on June 7. Gonu crossed the Makran coast in Iran six hours later and the IMD stopped issuing advisories on the cyclone.

3. MODEL DESCRIPTION AND DATA

The present study utilizes the MM5 version 3.7. MM5 is a limited-area, nonhydrostatic, terrain-following sigma-coordinate system model designed to simulate or predict mesoscale atmospheric circulation. This model has been continuously improved over the years with incorporation of important processes such as radiation, convection and cloud micro-physics, terrain representation and nesting capability. Grell et. al.(1994) gives model description. The MM5 model was used by Liu et.al.(1999), to determine the inner core structure and intensification of Hurricane Andrew. It is well known that Florida State University provides experimental two times daily high resolution forecast for the Atlantic Basin using MM5 model. The sensitivity of high resolution simulations in hurricane case Bob is discussed by Braun and Tao (2000). It is interesting to note that the MM5 model has also been used by Someshwar Das (2005) to investigate the predictability

of rainfall over different part of Himalaya and Western Ghat mountains during passage of a western disturbance and an active monsoon spell.

Here the model is configured with 23 vertical layers and two nested domains as shown in the Figure 2 (outer domain: 45 km grid spacing with 150 x 110 grid cells in the east-west direction and north south directions; and inner domain: 15 km grid spacing with 193 x151 grid cells in the east-west and north-south direction). The options used are the Medium Range Forecast (MRF) PBL scheme, the Kain Fritsch 2 (KF2) for cumulus, a mixed-phase for explicit moisture, a cloud radiation scheme and multi-level soil model. The NCEP FNL reanalysis data available at 1^0 X 1^0 was used two develop the initial and lateral boundary conditions corresponding to 00 UTC of 4th June, 2007. In fact, the model was also run for different times using the same sources of data at 00 UTC June 3rd, 5th, 12 UTC June 3rd and 5th. The input data was not able to give a suitable position of the cyclone when they (MY) were used in the simulations. The combination of MARF PBL and KF2 for convection yielded the best results with regard to track of the cyclone and its evolution. In an another study by Trivedi et.al.(2006) it is reported that Kain Fritsch, MRF, and Simple Ice as the better combination of model physics compared with other physics combination for the study of Orrissa Super Cyclon. The data and position of the Gonu cyclone is taken from the IMD for comparison with model results. The station data are obtained from Omani Directorate General of Aviation and Meteorology (Figure 3).

The Kain-Fritsch scheme considers a Lagrangian parcel method along with vertical momentum dynamics to estimate properties of cumulus convection. It incorporates a trigger function, a mass flux formulation and closure assumption. The trigger function identifies the potential updraft source layers associated with convection, whereas the mass flux formulation calculates the updraft, downdraft and the environment mass flux associated with that. The closure assumption for the scheme is that the convective effects removes convective available potential energy (CAPE) in a grid element with an advective time period by rearranging mass in a column using updrafts, downdrafts, and environment mass flux until at least 90 % of the CAPE is removed. The CAPE is calculated based on the path of an entrained diluted parcel. The cloud radius which controls the maximum possible entrainment rate is specified as a function of sub-cloud layer convergence. A minimum cloud depth required for activation of deep convection is allowed to vary as a function cloud base temperature. The scheme assumes conservation of mass, thermal energy, total moisture and momentum, and since it represents different processes associated with convection, is used for this study.

4. RESULTS

The prediction of the track is of prime interest since any mistakes in the track can not be compensated by knowledge of any other quantities. The MRF and KF2 combination was able to detect the track of the cyclone with least error (Figure 4). For 72 hours of model integration and a time step of one hour the results were generally in agreement with the actual track except when the low retreats a little or meanders on its way.

The values of the pressure at the centre show the deepening of the cyclone to 993 mb when it hit the Omani coast. The size of the cyclone changes during its motion with the smallest size at the beginning of 5th June and growing in size as it enters Oman, and later gaining a smaller size as it enters the Gulf of Oman. The pressure values of the cyclones are in the range 996-990 which is underestimated in the model results. Some times the cyclone meanders in its way for few hours before following the track which approximates the actual track. At time 18 UTC the chart shows the cyclone inside the Arabian Peninsula; actually the greater part was but not all of it. The change in size is not accompanied with change in pressure at the centre of the cyclone before entering Oman. Model simulated wind speed and vorticity at different levels are shown in Figure 5. High cloud cover and the precipitable amount of water during the track of the cyclone are shown in Figure 6 and Figure 7 respectively. The wind speed at level 925 hPa is about 25 m/s. Winds are as high as could be seen at level 500 hPa and when we go up to level 200 hPa, very high winds 55 m/s are encountered in the region of the cyclone. The vorticity field at 925, 500 and 200 hPa shows positive cyclonic vorticity exceeding 25 x 10^{-5} s^{-1} and maintaining the same value in the region of the storm up to 500 hPa level. At 200 hPa, the cyclonic vorticity diminishes greatly to become

nearly 1 x 10^{-5} s^{-1} and then at level higher than 200 hPa, it is replaced by negative anticyclonic vorticity.

Conclusion

Oman suffered the danger of the tropical cyclone Gonu, which is considered as the strongest in a hundred years. Observations contain phenomenal record such as 900 mm of rain during 5th June, very high wind about 130 km/h and sea level rising to 12 m during the passage of the cyclone. The MM5 model was used to simulate the case of Gonu. A combination of MRT PBL and KF2 for convection was used and proved suitable in the prediction of the nearest track to the actual one. The model was run on two nested domains at resolutions of 45 and 15 km. The model rendered lowest MSL pressure of about 990 mb when it reached Oman coast and was able to describe the intensity of the wind speeds at three levels in the atmosphere 925, 500 and 200 hPa. Severe cyclonic winds were observed at lower levels up to 500 hPa and positive vorticity was as high as 25 x 10^{-5} s^{-1}. Beyond 200 hPa anti-cyclonic circulation is seen by an area of high pressure. The model was not able to simulate the location and quantity of rain fall exactly. Precipitable amount of water distribution was given and it followed the locations of the cyclone. The cloud cover is also found to follow the track of the cyclone.

Acknowledgements

Authors are grateful to the Directorate General of Navigation and Meteorology, Oman and Director of forecasting and observing at Muscat airport. Authors are thankful to Director of Salalah Airport, Oman and Director Indian Institute of Tropical Meteorology, Pune India for supporting the collaborative work and extending the necessary facilities.

References

Asnani, G. C. , 1993, Tropical Meteorology Vols. 1, 2 published by Prof. G. C. Asnani, c/o Indian Institute of Tropical Meteorology, Dr. Homi Bhabha Road, Pashan, Pune-411008, India.

Bhaskar Rao, D. V. and Ashok K., 1999, Simulations of tropical cyclone circulations over the Bay of Bengal. Part 1, description of the model, initial data and results of the control experiment, Pure Appl. Geophys. (156), 3, 525-542.

Braun, S. A. and Tao W. K., 2000, Sensitivity of high resolution simulations of hurricane Bob (1991) to planetary boundary layer parameterization, Mon. Wea. Rev,(128), 3941-3961.

Grell, G. A., Dudhia J. and Stauffer, D. R., 1994, A description of the fifth generations Penn State/ NCAR Mesoscale Model (MM5)/ NCAR Technical Note NCAR/ Tn 398 TSR, 117 pp.

Liu Y., D. L. Zhang and M. K .Yau, 1997, A multiscale numerical study of Hurricane Andrew (1992) Part I Explicit Simulation and Verification, Mon. Wea. Rev, (125), 3073-3093.

Liu Y., D. L .Zhang and M. K .Yau, 1999, A multiscale numerical study of Hurricane Andrew (1992) Part II Kinematics and Inner core Structure, Mon. Wea. Rev, (127) , 2597-2616.

Mandal M., U. C. Mohanty and A. K. Das, 2006, Impact of Satellite derived wind in mesoscale simulation of Orrissa Super Cyclone, Indian Jour. Of Marine Science, (35),161-173.

Sandeep S., A. Chandrasekar and S. Dash, 2007, Impact of modification of initial cyclonic structure on the prediction of a cyclone over the Arabian Sea, Natural Hazards (41), 487-499.

Singh O. P. et al, 2001, Has the frequency of the intense tropical cyclones increased in the Indian Ocean, Curr. Sci., (80), 4, 575-580.

Someshwar Das, 2005, Mountain Weather Forecasting using MM5 modelling system, Current Science, (88), 6.

Trivedi, P. Mukhopadhyay and Vaidya, S. S., 2006, Impact of physical parameterization scheme on numerical simulation of Orissa Super cyclone (1999), Mausam, (57), 1, 97-110.

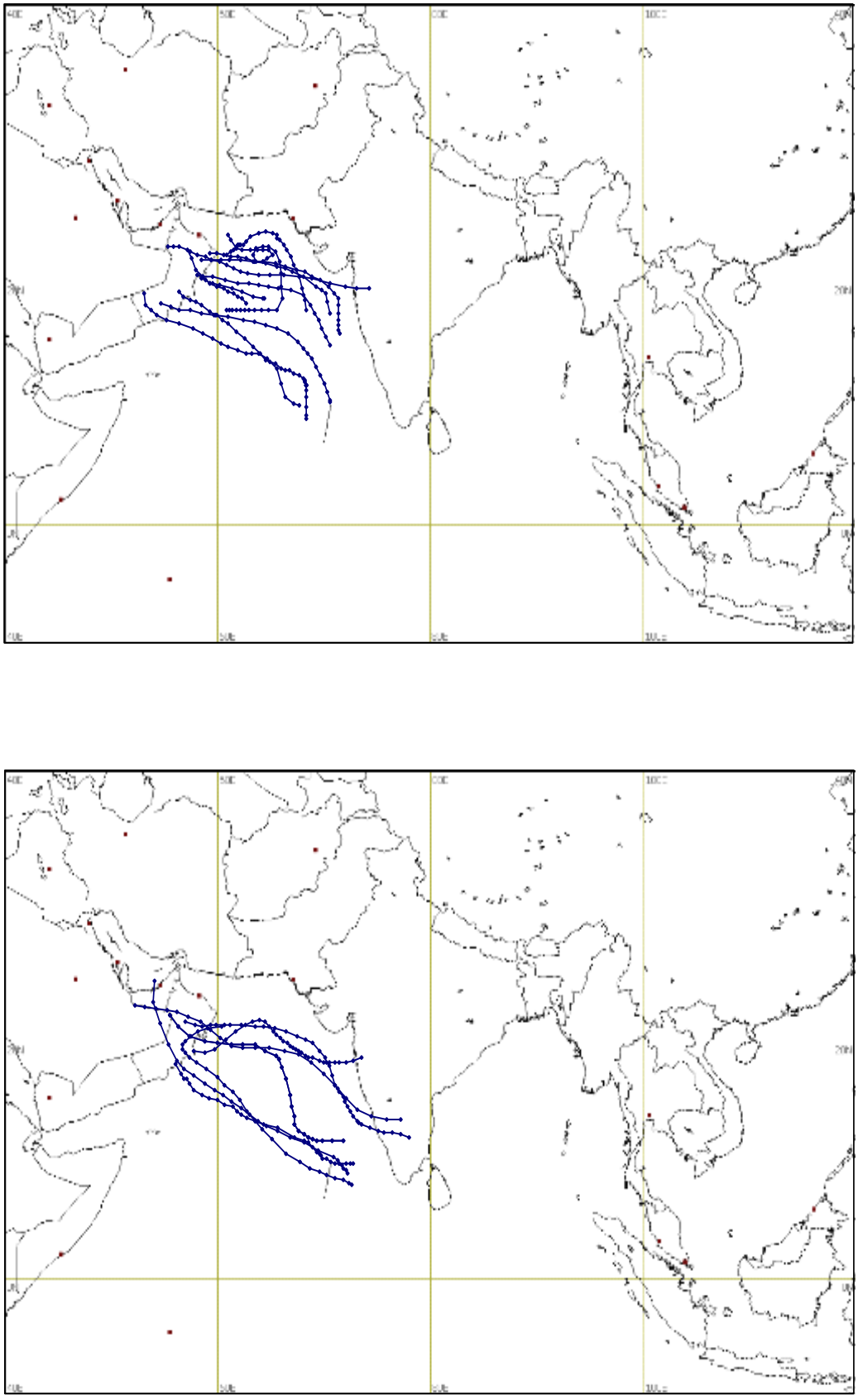

Figure 1 - Tracks of the tropical cyclones over the Arabian Sea and affected Oman in first transitional period (left) and second transitional period (right) since 1948 till now (the tracks are based on data taken from http://weather.unisys.com).

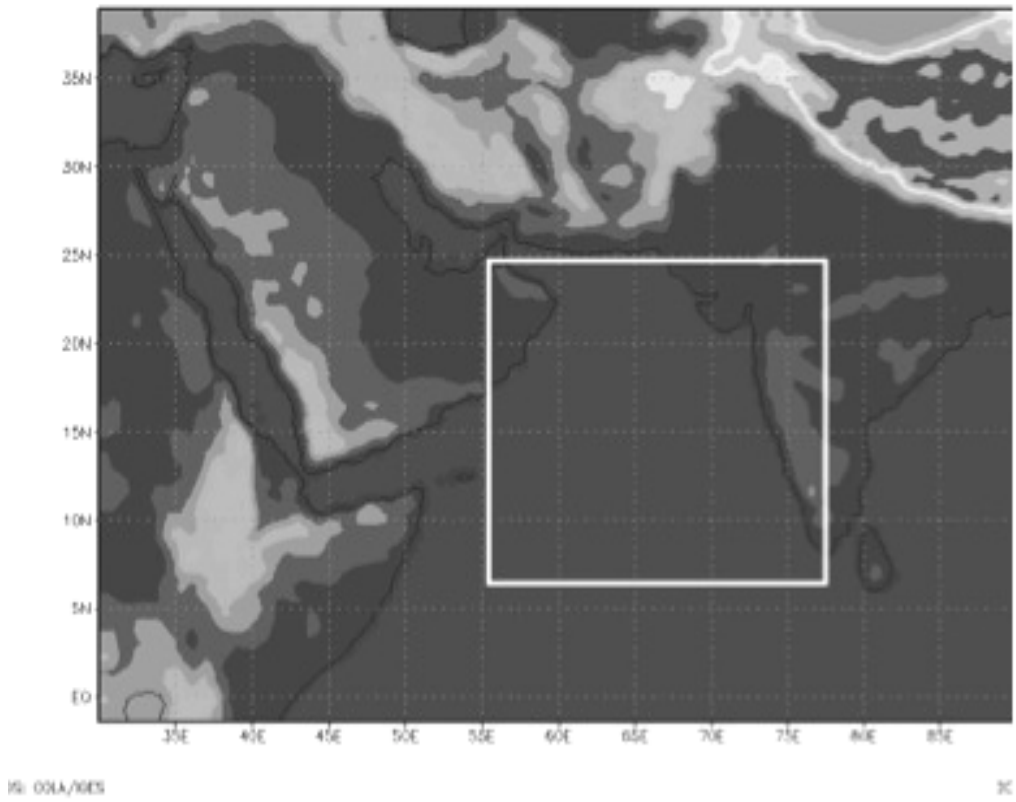

Figure 2 - The two domains used for simulation of the cyclone Gonu. The inner domain is indicated by a white rectangle.

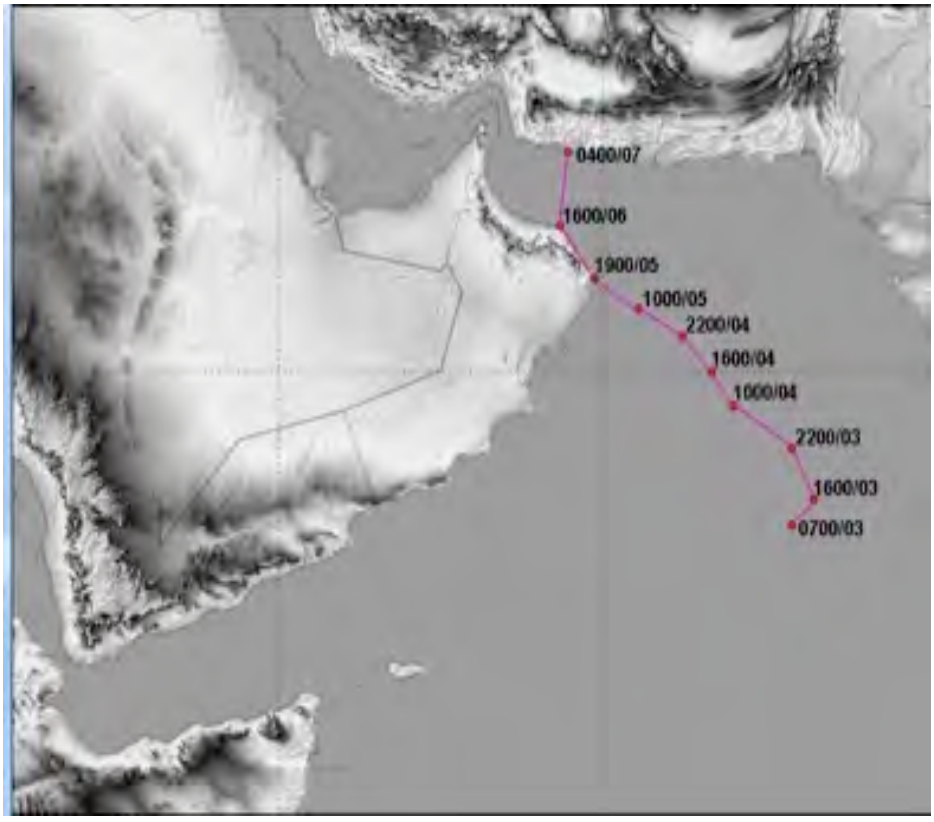

Figure 3 - The red curved line shows the actual track of Gonu starting 07 UTC 3rd June till 04 UTC 7th June 2007.

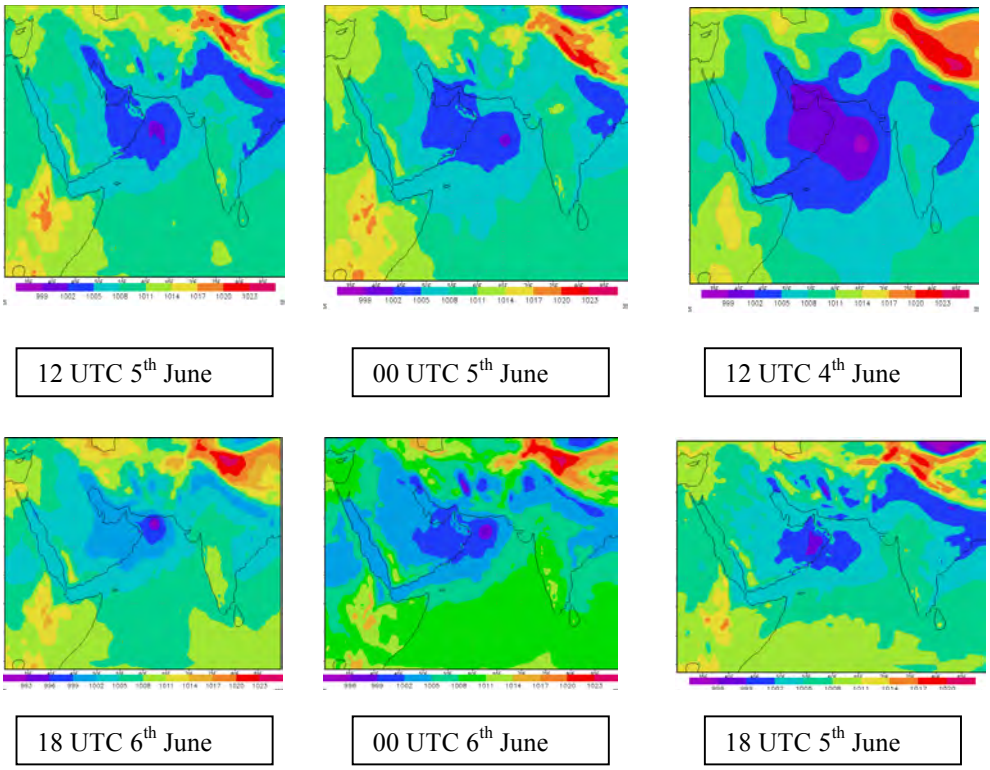

Figure 4 - MSLP charts showing the simulated positions of the track of the cyclone.

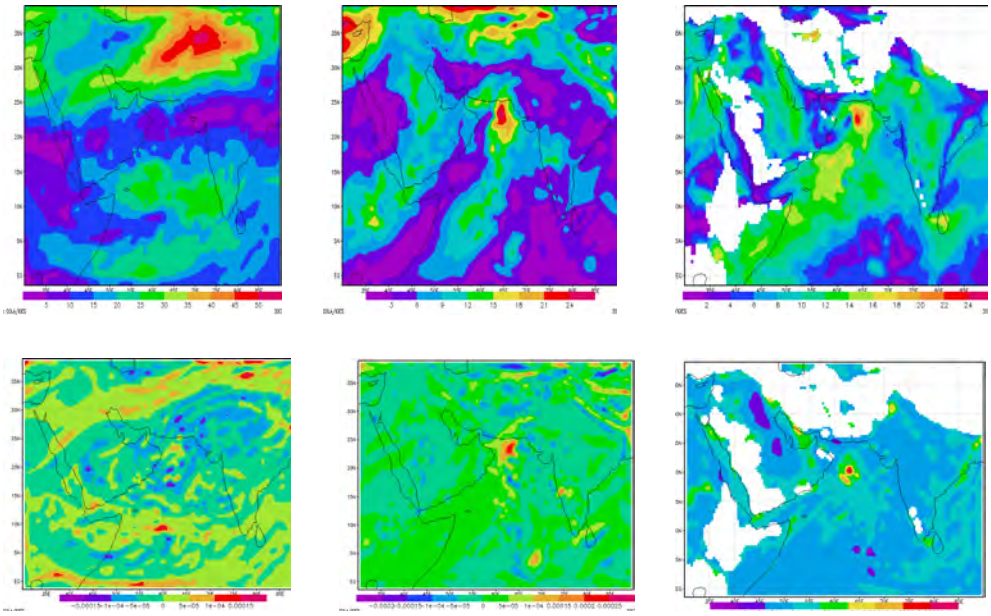

Figure 5 - The wind speed and vorticity at levels 925 and 500 and 200 hPa for 12 UTC 6 June (from right to left; the upper charts are the wind speed in m/s and the lower charts are the vorticity in units of s^{-1}.

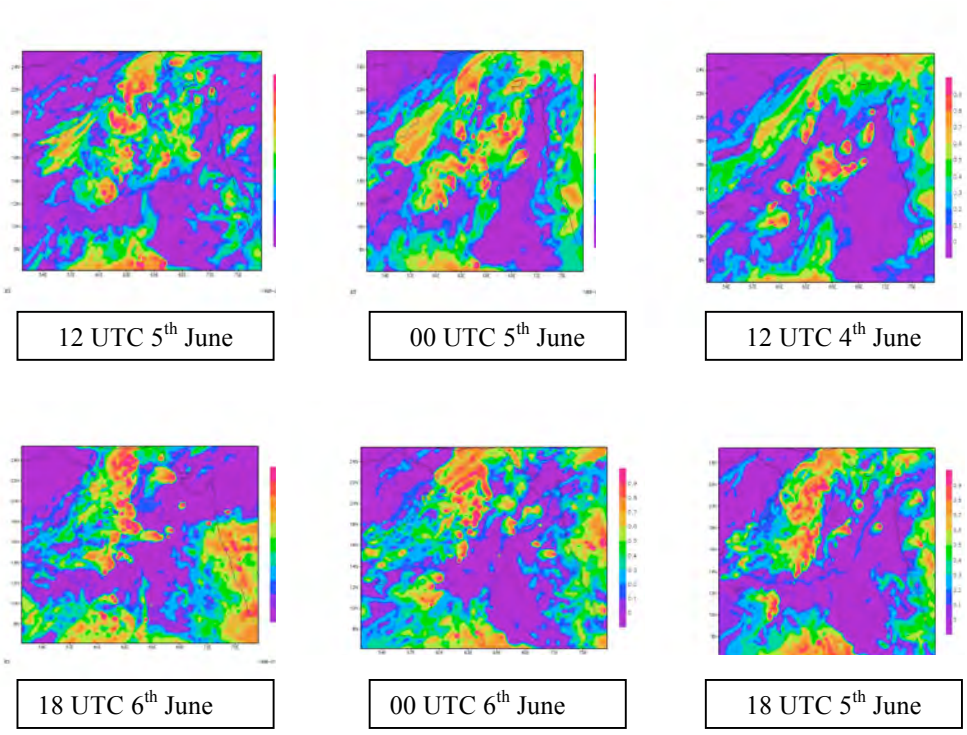

Figure 6 - High cloud cover during the track of the cyclone.

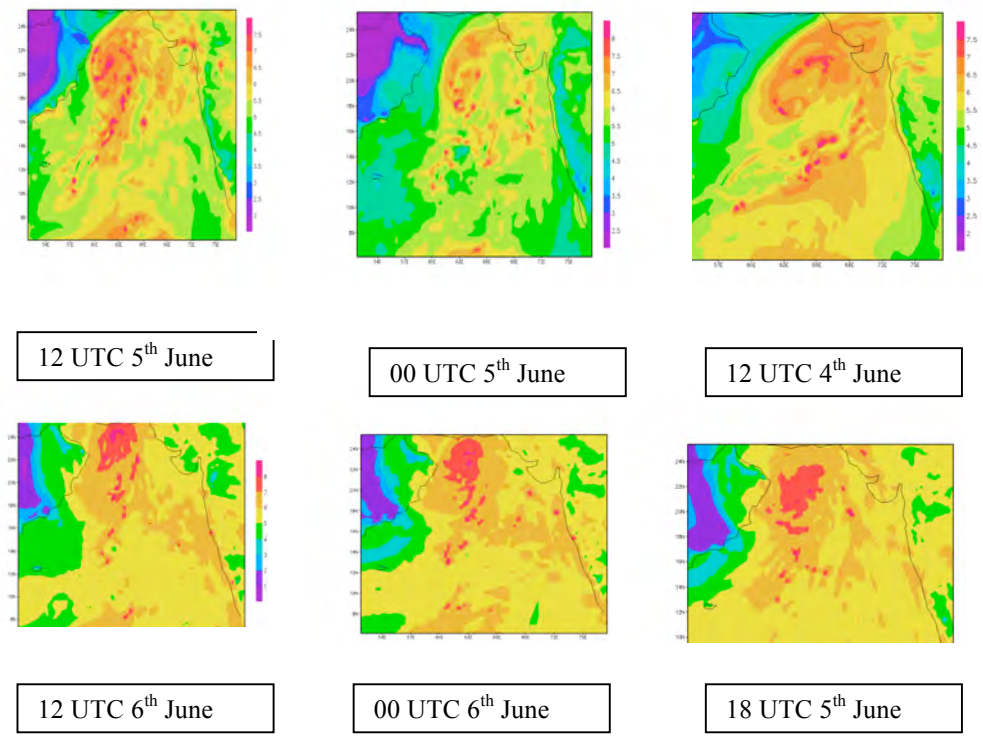

Figure 7 - Precipitable amount of water during the track of Gonu cyclone.

THE USE OF RS AND GIS TO EVALUATE THE EFFECTS OF TROPICAL CYCLONES: A CASE STUDY FROM A'SEEB, MUSCAT AFTER GONU CYCLONE

Dr Talal Al-Awadhi
Geography Department, Sultan Qaboos University

Abstract

From time to time, the World is faced with natural disasters such as earthquakes, volcanoes and cyclones which may lead to serious damage to lives, property and buildings. Due to the location of Sultanate of Oman is facing the Arabian Sea and Indian Ocean, adverse weather is very frequent and the occurrence of tropical cyclones is not a rarity. On June 5th, 2007 GONU cyclone hit the Southern coast of Oman and reached Muscat on June 6th. Weather Satellites such as Meteosat observed the cyclone for the first time on May 27 over the Indian Ocean. GONU reached to grade 5 based on Saffir-Simpson cyclone scale on June 4th but was downgraded to grade 1 on June 8th while crossing Iran lands. The cyclone resulted in enormous material losses in Oman which amounted to 4 billion USA Dollars, while human deaths were 49 in addition to 27 people who were lost according to government estimation. Therefore, it was considered the national worst natural disaster.

Such an event with this magnitude needs to be comprehensively assessed. Therefore, an attempt has been made to identify the size and nature of damage by applying Remote Sensing (RS) and Geographical Information System (GIS) techniques. Two high resolution images (IKONOS) have been used. The analysis results show that, more than 37% of the study area was affected by GONU cyclone either by flooding or by clay sediments. The results also show that clay and water were accumulated along the building boundary and road. The damage was so significantly sever to the extent that a clear detailed map of the study area can easily be drawn.

INTRODUCTION

The Sultanate of Oman is located in the Southeastern corner of the Arabian Peninsula between 16° 39' and 26° 30' north of the equator. It has a coastal line extended to more than 3000 km from the North at Strait of Hormuz to the borders of the Republic of Yemen. Oman is surrounded by two gulfs (Arabian Gulf and Oman Gulf) and one sea (Arabian Sea). From this location, Oman is closed to cyclone development area over Indian Ocean. In the last 50 years ago several cyclones were recorded in Oman but the most famous cyclones hit Oman are:

- Muscat Cyclone on June 5th, 1890 and more than 285 mm of rainfall were recorded.
- Masirah Cyclone on June 13th, 1977 and more than 431 mm of rainfall were recorded.
- Masirah Salalah on May 24th, 1959 and more than 117 mm of rainfall were recorded.

GOUN cyclone is the strongest cyclone ever known in the Arabian Sea. It is also classified as the second strongest cyclone hit the northern half of the Indian Ocean in 2007. The Akash cyclone was the strongest one which crossed Bengal Gulf from 13th to 15th May and hit the coast of Bangladesh and Myanmar on 15th May 2007. The name of GUNO has been selected based on the agreement between eight countries (Bangladesh, India, Maldives, Myanmar, Oman, Pakistan, Sri Lanka and Thailand). Each of the countries submitted eight nominations to be used to describe any cyclones which could be appeared on Indian Ocean for the period from 2004 to 2011. The name of JUNO was in fact proposed by the Maldives to depict the cyclone that that hit the eastern coast of Oman in June 2007.

Geographic Information Systems (GIS) and Remote Sensing (RS) could be integrated as one system to be used as spatial decision support systems (SDSS) for several subjects. They can offer decision-makers with a wealth of information for assessment, analysis and monitoring of natural disasters such as Hurricanes, Tornados and Cyclone damage from small to large regions around the World. High resolution imagery such as QuickBird or IKONOS can be used in case of cyclone: to identify where previous hazard events have occurred, to identify where they are likely to occur in the future, to identify the costs associated with events and to determine the extent of

landscape change and monitor the progress of recovery.

Geographical Information Systems (GIS) and Remote Sensing (RS) technologies were intensively used to monitor flooding and evaluate its damage during several years. Several studies of GIS & RS techniques in the field of cyclone could be identified. For example UAMKASEM B. (2008) tried to apply RS and GIS in flood risk management in Sukhothai, Province in Thailand. SMARA Y. & Others (2005) also used these two techniques to manage flooding disaster in Algeria. Pramanik M. (1994) tried to implement the idea of remote sensing and GIS to monitor the disaster in Bangladesh. However, this work is just an example to employ these technologies to assess identification of GONU Cyclone damage in Oman.

1. THE DAMAGES

During the period of the passage of GOUN cyclone near the coast of the Sultanate was exposed to large amounts of rainfall has not witnessed before. For example, in Dam Altaeeyan station recorded more than 900 mm rainfall (Directorate General of Civil Aviation and Meteorology (Meteorological Department)). Figure 1 shows the total rainfall in some stations around Muscat area on 6th June 2007, while Figure 2 describes the wadi water level in the same area between 6th June 2007 – 11th June 2007.

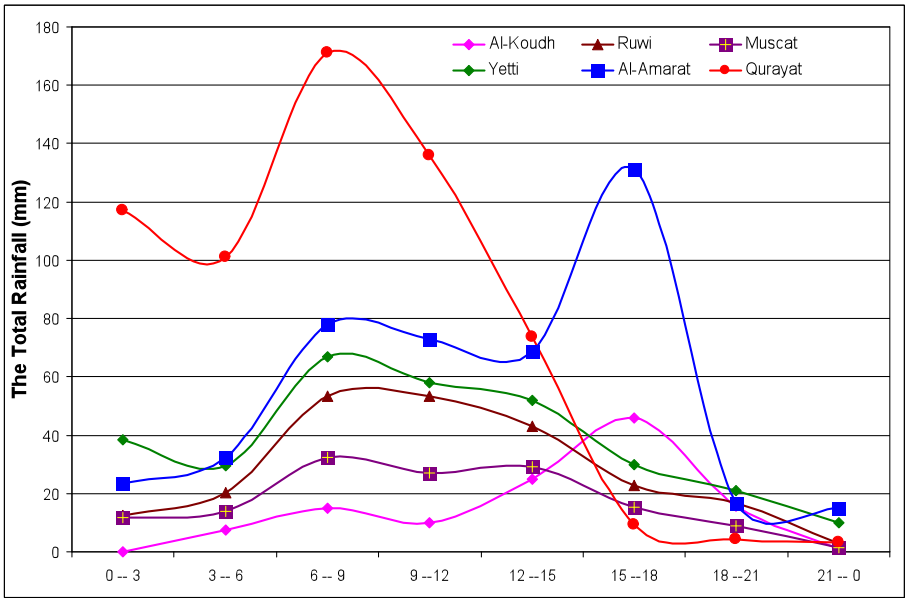

Figure 1 - The total rainfall in Muscat Governorate on 6th June 2007.

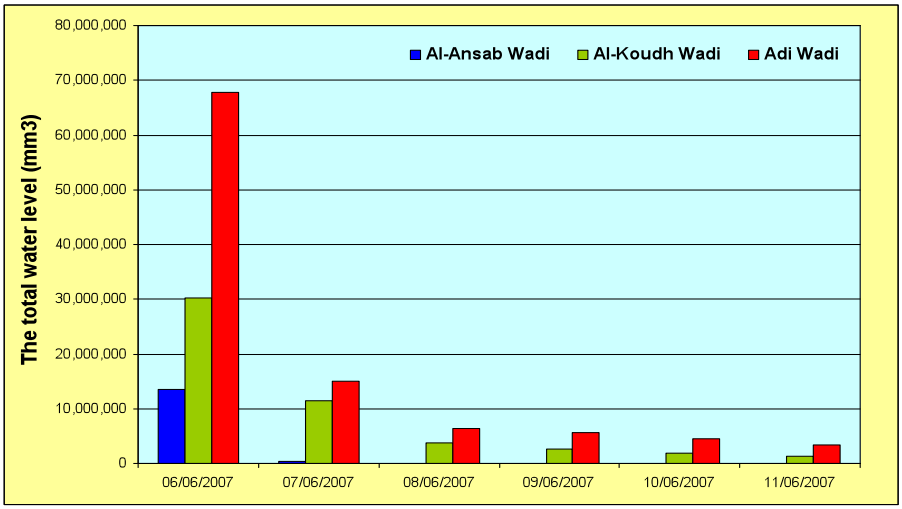

Figure 2 - The total water level (mm3) Muscat Governorate (6th June 2007 – 11th June 2007).

The cyclone resulted huge amount of rainfall which led to massive distractions never seen in Oman before. The total damages caused by cyclone GUNO in Oman cost around US$4 billion (See Figure 3 for some example of distractions), while human deaths were 49 in addition to 27 people who were lost according to official government estimation. Flooding caused by the Cyclone GUNO left many damaged, such as: the fall of the bridges, the uprooting of trees, collapse of houses, and broken roads …etc. Muscat Governorate was not only area affected by the cyclone but other areas also can be identified in Oman especial area along the coast from Sur to Quriyat. Oman Government immediately after GUNO cyclone survey the total damage over the Sultanate as it is described in Table 1. The surveyed shows that more than 60000 built units have been surveyed and 50% of surveying units were declared damaged. Muscat capital had almost 85% of surveying units and 77% declared damage. More than 13000 cars were declared damaged, more than 88% without any comprehensive insurance.

Figure 3 - An example of distraction of CUNO cyclone.

Table 2 - The details of Destruction Survey.

Willayat	House Surveyed	House Accounted	House Damaged	Furniture	House Equipments	Personal Belongs	Transportation Vehicles
Mutrah	4273	1135	888	718	730	542	428
Bosher	7179	3894	2776	2680	2721	2310	4065
A'Seeb	30498	12239	9035	7614	7888	6311	5676
Al-Amerat	5968	3468	3089	2013	2044	1419	397
Muscat	607	500	470	387	359	369	144
Qurayat	3512	3115	2891	2470	2478	2436	944
Barka	828	20	552	404	414	318	188
Dbai Al-Bayah	68	68	56	54	39	44	3
Bidbid	95	95	86	73	61	73	5
Sur	5984	4825	4294	3458	3132	2764	386
Al-Qabil	7	7	7	0	1	0	0
Dami	160	159	153	76	90	88	10
Al-Kamil	141	134	121	15	29	33	2
Galan Bani Bo Ali	1396	936	759	599	394	511	6
Galan Bani Bo Husain	213	135	117	78	17	56	1
Wadi bani Khalid	130	129	125	15	21	14	0
Total	61058	31459	25419	20654	20418	17287	12255

2. STUDY AREA

Muscat Governorate, situated in the north-east between 23° 30´ and 23° 45´ north latitude and 57° and 59° east longitude, is the capital of the Sultanate of Oman (Figure 4). It extends from A'Seeb in the north to the fishing port of Quariyat in the south along a coastline that runs around 200 km along the Gulf of Oman. It is divided into six Wilayats (Administrative units in Oman): Wilayat of Muscat, Mutrah, Busher, A'Seeb, Al'Amarat and Qurayyat. The total land area of the Muscat Governorate is 35000 km^2 (Oman Census, 2003) with a total population of 631031 inhabitants. Table 4 shows more details about the population of each Wilayat based on 2003 Census results.

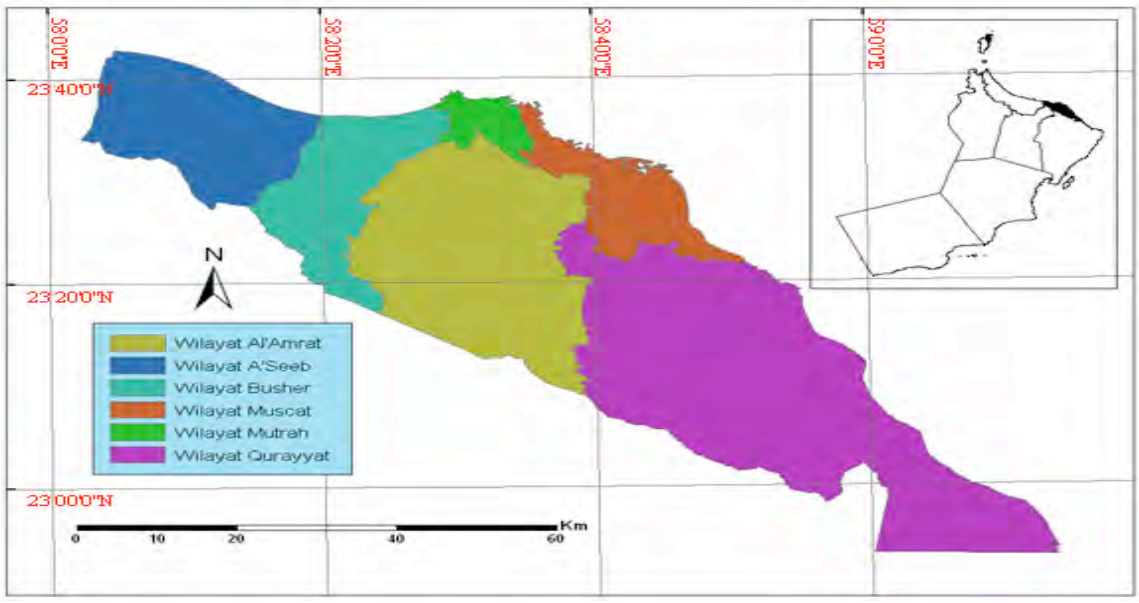

Figure 4 - The 6 Wilayats of Muscat Governorate.

Basically, Muscat Governorate was not fully covered by high resolution satellite images such as Ikonos for two different periods. Therefore, just part of Wilayat A'Seeb which is the biggest populated area in Oman (more than quarter Million inhabitants according to 2003 census) as shown in Figure 5. These part including Al-Mawalah, Al-Koudh and Al-Amarat. According also to the surveyed damage results, Wilayat A'Seeb had more than 50% of surveyed built units and 39% of these units declared damaged. More than 45% of cars declared damaged, and 91% with only 3rd party insurance were also registered in Wilayat A'Seeb (See Figure 6 for more details).

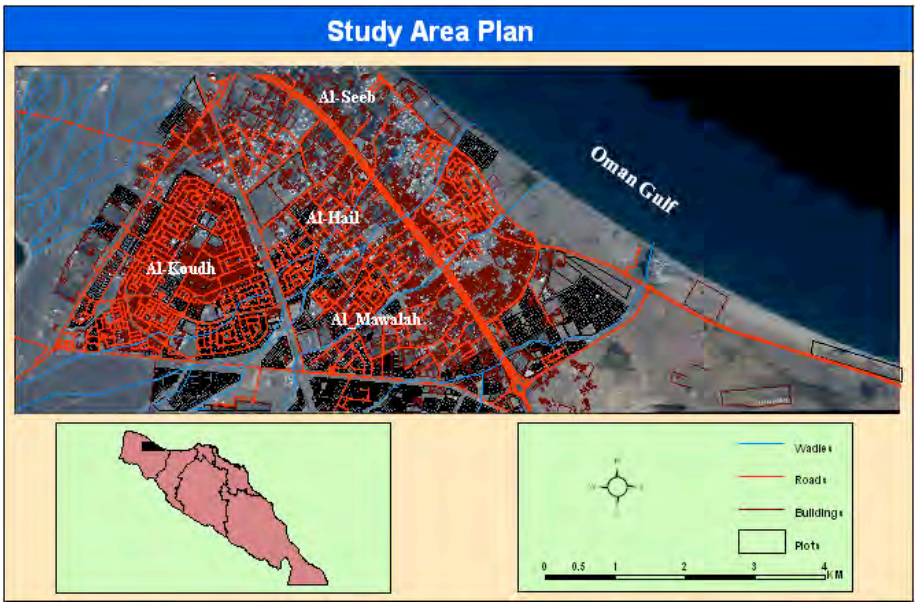

Figure 5: The plan for study area.

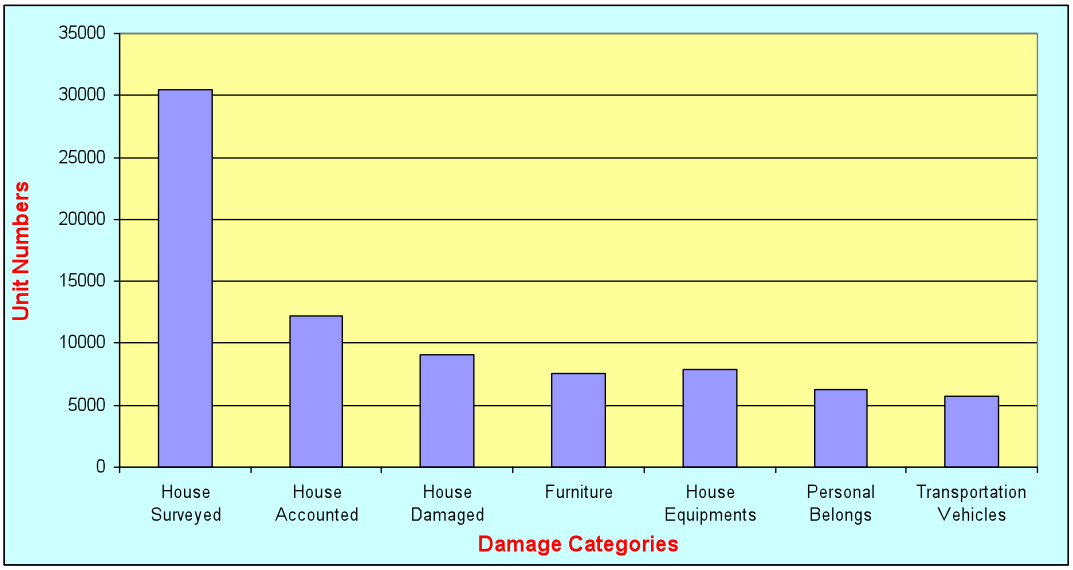

Figure 6 - The detailed results of survey damage in Willayat A'Seeb.

3. METHODOLOGY

The basic idea of the methodology is to clarify the overlap and integration between GIS and remote sensing in spatial decision support systems. These two technologies could offer compressive information about the direction of the cyclone and the area affected as well as to evaluate the damage and the affected areas. The general methodology for identifying the damage

are designed as flowchart as shown in Figure 7.

The main idea of this works is to identifying and evaluating the damage by using the scene of change detection technique. According to Singh (1989), change detection could be described as the operation of recognition differences in the state of an object or area by comparing two or more image at different times. Change detection is an active research topic in the last thirty years and it is also could be applied to cover several area such as environmental change, landscape change, land use change, urban growth, forest or vegetation change …. etc. Therefore, several methods have been applied worldwide to identify the change using change detection techniques such as Image Difference technique, Principal Component Analysis (PCA) technique, Image Regression technique, selective principal component analysis Post-classification technique, spectral mixture analysis, artificial neural networks (ANN), and the method of Manual On-screen Digitization of Change (for more details about change detection methods see Singh (1989) Lu D. et al (2003), and Kwarteng & Chavez (1998)). In this study, the Principal Component Analysis (PCA) technique was applied to determine the changes between two different images that have been mentioned before. The main advantage of PCA is to reduce data redundancy between image bands and to highlight different information in the derived component. One the other hand, PCA is scene dependent, it is difficult to interpret and label the change detection results that show between different dates. It also cannot provide a complete matrix of change class information. According to D. LU et al (2003), two approaches exist to apply PCA to perform change detection. The first one is to use two different image periods in one file, then use this file to extract and analysis change information. The second one is to complete the PCA individually, then subtract the second image from the first image. For this piece of work, the second approach was implemented to complete the work objective.

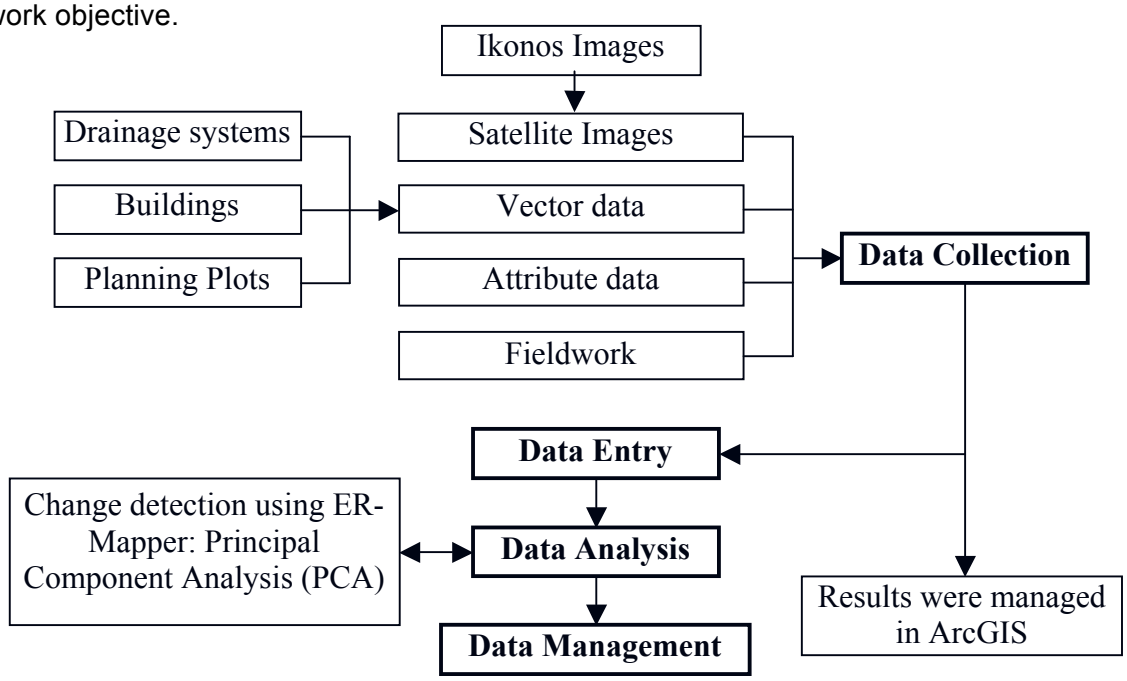

Figure 7 - The planning process to evaluate the GUNO Cyclone damages in the study area.

The methodology divided in two main parts: the first part is to use ER-Mapper for identifying the damage and the second part is to manage the results is ArcGIS (ArcMap) software. Tow Ikonos images (Figure 8) were used to study the implications of GUNO cyclone. The first images acquired 18 months before the event which was on 8th January 2006, and the other images was recorded after 4 days of the cyclone passed Oman lands on 12th June 2007. The first step was to prepare the two Ikonos images for the analysis. Image enhancement and geometry correction were done in ER Mapper software. UTM WGS84 Zone 40N was used. Road Network from Muscat Municipality was used to complete the first image registration. Then this image was used to update the second image registration, which represents the region immediately after the cyclone. The damages and changes have been carried out using the feature comparison mechanism to identify

the damages (Change Detection) using the ER Mapper software. Then the results were exported to suitable format for ArcMap to identify and quantify the damage. Spatial analyst extension and image analyst extension were used to regroup the number of pixels to suitable number. Four groups of land use were applied: clay accumulation, flooding, marsh and no change. The final output then converted to vector format manage it in ArcGIS (ArcMap) for better data management. Other data were also used such as road networks, plan plot and valley networks to facility better decision.

Figure 8 - Two raw images from Ikonos satellite (Sours: Supreme Committee for Town Planning, Sultanate of Oman, Muscat).

4. RESULTS & DISCUSSIONS

High resolution images within 1 m spatial resolution such as Ikonos help the user to identify the damage easily. For example visual evaluation is simple method to identify the damage between the two Ikonos images as shown in Figure 9. There are two type of results would be able to obtain it from applying the mentioned methodology. The first one concerned the total change in the study area. Other one concerned the evaluation and understanding the results in ArcGIS.

These results indeed are only presenting the change after almost five days of the event. Therefore, some changes may not appear during the application of the methodology. The results were group into four groups as summarized in Table 3 and Figure 10. The total area size of the study area is 39.59 km^2. 30% of this area is affected either by clay accumulation, flooding and marsh. The major change in land use after GUNO cyclone was to the marsh class. Thus, what led to these destructions? There are several reasons: (1) the strength of the cyclone as it mentioned before, and (2) planning processes.

Figure 9 - An example of simple evaluation by comparing two Ikonos image.

Table 3 - The result of total change in the study area.

Types	Area M^2	Area Km^2	%
Clay accumulation	3791872.3	3.79	9.6%
Flooding	3004714	3.00	7.6%
Marsh	4749437	4.75	12.0%
No Changes	28040547	28.04	70.8%
Total	39586570.3	39.59	100%

The second part of the methodology concerned the understanding and manipulation. The study area has two of the biggest wadis in Muscat (Wadi Al-Koudh and Wadi Al-Jifinian). Usually Oman has uncommon heavy rains which lead to flow these wadis. Therefore, area around these wadis were planned and built resulting blocking wadis flow towards the sea. During the cyclone event, Oman has never seen these amounts of rainfall. Therefore the flooding and clay accumulation were spread into the most of the study area. Using simple spatial analysis function such as map overlay or buffer zone, more than 2500 plots with 100 meter buffer from valley path could be affected by floods. This number could rise to more than 3700 if the buffer were 150 meter. The changes also were along roads and building edges. The changes in the land use were also significantly severe to the extent that a clear detailed map of the study area can easily be drawn as shown in Figure 10.

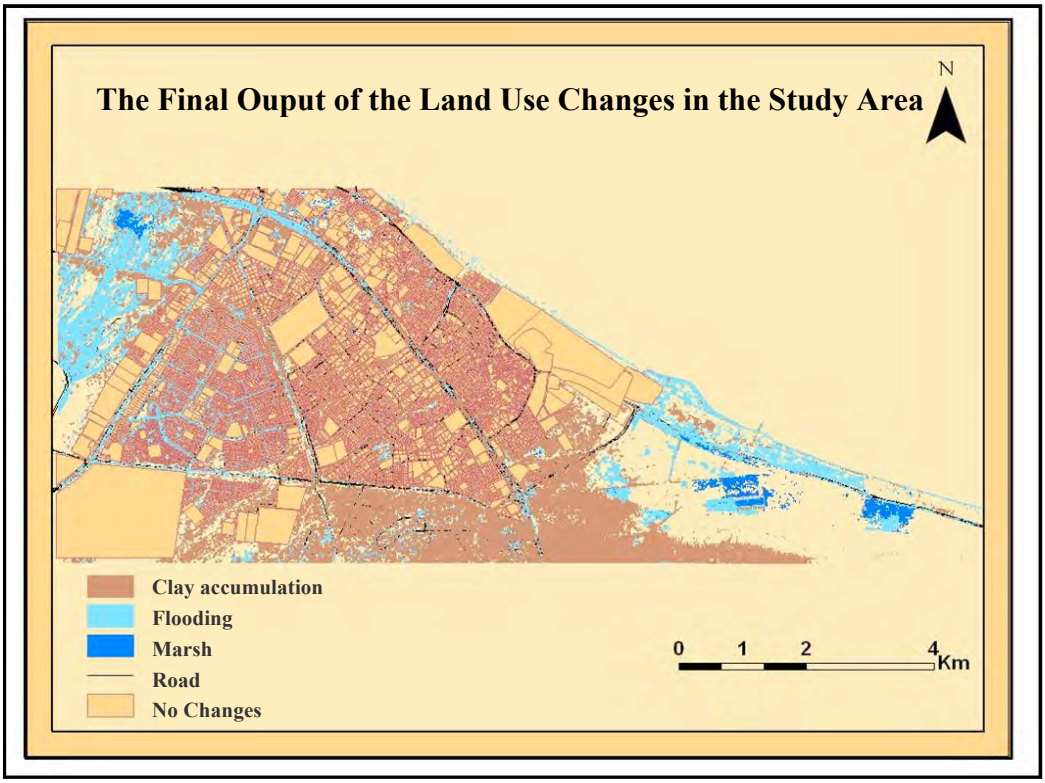

Figure 10 - The plan of the final out put of the applying the methodologies.

Conclusion

In Oman, CUNO cyclone left a devastating impact on western coast of Oman mainly in the Muscat Governorate. These effects can be felt for many years. Therefore, it was considered as the national worst natural disaster. The event in reality showed the strength of Omani people to support each other and not stopped them continuing building their country. Using GIS & RS techniques with high resolution images help several users particularly urban planner, engineer, manger to have better vision to support their decision especially in the crisis from having their planning away from wadi bath.

The results demonstrated that the impact was more around wadi bath .

References

Chavez, P.S. Jr. and Mackinnon D. (1994). "Automatic detection of vegetation changes in the southwestern United States using remotely sensed images", *Photogrammetric Engineering and Remote Sensing*, 60, 571-583.

Jensen, J. R., and Toll D. L. (1982). "Detecting residential land-use development at the urban fringe", *Photogrammetric Engineering and Remote Sensing*, 48, 629-643.

Lu D., Mausel P., Brondizio E. & Moran E. (2004), "Change detection techniques" *Int. J. of Remote Sensing,, Vol. 25, No. 12, 2365–2407.*

Kwarteng, A. & Chavez, P. (1998), "Change Detection Study of Kuwait City and Environs Using Multitemporal Landsat Thematic Mapper data". *Int. J. of Remote Sensing, Vol. 19, No. (9). 1651-1662.*

Pramanik M. (1994). "Remote Sensing Applications in Disasters Monitoring in Bangladesh", *ACRS Conference 1994*.

"http://www.gisdevelopment.net/aars/acrs/1994/ts3/ts3005.asp, last visit 18th May 2009"

Singh, A. (1989). "Review article: Digital change detection techniques using remotely-sensed data", *International Journal of Remote Sensing*, 10, 989-1003.

Smara Y. & others (2005). "Application of GIS and Remote Sensing Technologies in Disaster Management in Algeria", *FIG Working Week 2005 and 8th International Conference on the Global Spatial Data Infrastructure (GSDI-8), Cairo, Egypt 16 – 21 April 2005.*

Uamkasem B. (2008), "RS/GIS for Flood Risk Management in Sukhothai Province", *11th Annual International Conference and Exhibition on Geospatial Information, Technology and Application - Map India 2008, 5th – 8th February 2008, Great Noida, India*.

INFLUENCE OF CYCLONE GONU AND OTHER TROPICAL CYCLONES ON PHYTOPLANKTON BLOOMS

Sergey A. Piontkovski and Adnan R.Al-Azri
College of Agricultural and Marine Sciences, Sultan Qaboos University, PO34, Al-Khod 123, Sultanate of Oman

Abstract

Cyclone Gonu (which made landfall on the coast of Oman on June 5th, 2007) was documented as the strongest cyclone ever recorded in the North Indian Ocean over the past 60 years. Satellite derived (9-km spatial resolution MODIS Aqua) data for sea surface temperature, sea surface heights, and chlorophyll *a* were used to analyze responses of these fields to the passage of Gonu. The concentration of chlorophyll *a* along the track exceeded the background concentration in the adjacent regions. The enhanced concentration was observed over the final (western) part of the track, corresponding to a super cyclone phase. The persistence of the enhanced concentration induced by the passage of Gonu did not reach the concentration typical for the Omani coastal upwelling in summer, which is the season of the highest concentration of the chlorophyll *a* due to the south-west monsoon. Data analysis on 29 other tropical cyclones reported for the Atlantic, Pacific and Indian Oceans, has shown that the magnitude of chlorophyll *a* increase after cyclone passage depends (exponentially and negatively) on the translation speed of a cyclone. On the other hand, the magnitude of chlorophyll increase after cyclone passage depends (exponentially and positively) on the gradient of sea surface temperature (which is the difference of temperature before and after cyclone passage).

Key Words

Chlorophyll a, tropical cyclone, sea surface temperature, phytoplankton bloom, Arabian Sea.

INTRODUCTION

Tropical cyclones are important elements of the ocean-atmosphere interaction responsible for significant cooling and vertical mixing of the upper layers of the ocean (Sriver and Huber, 2007). Every year, about 80 tropical cyclones (with wind speeds above 17 m s^{-1}) form in the world's ocean (McBride 1995) and affect physical, chemical, and biological processes in the upper layer. The cyclones with maximal wind speed exceeding 33 m s^{-1} are known as typhoons in the Pacific Ocean and as hurricanes in the Atlantic Ocean (Badarinath et al., 2008; Kokhanovsky and Von Hoyningen-Huene, 2004Badarinath et al., 2008 K.V.S. Badarinath, S.K. Kharol, K.V. Prasad, D.G. Kaskaoutis and H.D. Kambezidis, Variation in aerosol properties over Hyderabad, India during intense cyclonic conditions, *International Journal of Remote Sensing* **29** (15) (2008), pp. 4575–4597. **Full Text** via CrossRef | View Record in Scopus | Cited By in Scopus (2)). Devastating consequences of the hurricanes and typhoons have reportedly reached billions of dollars in reparation of damages and tens of thousands in deaths. For instance, super cyclone Sidr (which formed in November 2007 in the Bay of Bengal and made a landfall on the Bangladesh coast) claimed the lives of about 10, 000 people (Joint Typhoon Warning Centre, 2007; Rahman, 2007). On a climatic scale, it is believed that global warming (affecting sea surface temperature and heat balance of the ocean) will result in increase of cyclone intensity (Pielke et al., 2005).

In terms of biological consequences, the cyclone wind field causes local mixing resulting in the injection of nutrients into the upper layer of the ocean and inducing phytoplankton bloom (Subrahmanyam et al. 2002). In some cases, the magnitude of the hurricane-induced bloom could reach gradual (30-fold) increase in surface chlorophyll *a* concentration, as well as an increase in primary production (Lin et al. 2003; Smitha et al. 2006). For example, an average of 14 cyclones pass over the South China Sea annually, which suggest the contribution of cyclones to annual new production to be as much as 20–30% (Lin et al. 2003).

About 7 to 13% of the world tropical cyclones were reported for the northern part of the Indian Ocean (Gray 1968, 1985). Hurricane Gonu (which made landfall on the coast of Oman on June 5th, 2007) was documented as the strongest cyclone ever recorded in the North Indian Ocean

over the past 60 years. Two days prior to landfall, Gonu had intensified to a super storm with maximum winds of about 260 km hr $^{-1}$ becoming the first documented category 4 cyclone in the Arabian Sea, as well as the first cyclone to traverse this basin.

Remote sensing is one of the approaches broadly used in monitoring and analysis of tropical cyclones, as well as the phytoplankton blooms, for which the chlorophyll *a* is widely used as an indicator. Through the analysis of remotely sensed data we were aimed at seeking the relationship between some basic characteristics of tropical cyclones and the response of chlorophyll *a* to the passage of these cyclones in the World Ocean, with a special reference to cyclone Gonu as the latest one in our region.

1. METHODS

Data on 29 cyclones reported for the tropical latitudes of the Atlantic, Pacific and Indian Oceans were assembled from the literature (Table 1). The selected data were based on and predetermined by availability of atmospheric, physical and biological measurements carried out simultaneously for a certain cyclone. In some cases (cyclone Gonu), 9-km spatial resolution SeaWIFS or MODIS Aqua weekly and monthly Level-3 sea surface temperature and chlorophyll *a* were used to fill in the gaps in the data missed in appropriate references found for a certain cyclone. The QuikSCAT scatterometer data (available on the PO-DAAC ftp site- ftp://podaac.jpl.nasa.gov/ocean_wind/quikscat/NRT/) were used to determine the scale, location, and wind field characteristics of a cyclone over time.

Maps for the sea surface height anomaly were produced from Jason, TOPEX/Poseidon and Geosat altimeter data processed in near real-time. An analysis product (developed by the Colorado Centre for Astrodynamic Research) was based on the latest 10 days of Jason and T/P, and 17 days of Geostat sampling. Mapping the chlorophyll field along the Gonu track, the three 2^{o} by 2^{o} quadrates have been used to analyze changes of chlorophyll *a* concentration in June 2007 compared to that throughout the annual cycle. From June 4th through June 6th, Gonu had passed through the following three quadrates:

1. (20-18^{o}N, 63-65^{o}E);
2. (22-20^{o}N, 61-63^{o}E), and
3. (22-24^{o}N, 60-62^{o}E), ending with landfall on the coast of Oman.

In order to compare the chlorophyll *a* concentration presumably induced by Gonu with the reported for the coastal upwelling of Oman, monthly averaged MODIS Aqua maps of the Arabian Sea for the years from 2002 through 2008 were used. This enabled us to compare the amplitudes of seasonal and interannual variability with a special reference to the Gonu- induced amplitude. Monthly time series used in this study were acquired using the GES-DISC Interactive Online Visualization and Analysis Infrastructure software as part of the NASA's Goddard Earth Sciences Data and Information Services Centre.

2. RESULTS

Chlorophyll a and hurricane Gonu

The first warning about a tropical cyclone 02A emerging 370 nautical miles southwest of Mumbai (India) and moving westward at a speed of 7 knots was issued by JTWC on June 2, although the beginning of track was attributed to June 01, near 14.2^{o}N/70.6^{o}E (https://metocph.nmci.navy.mil/jtwc.php). The end of track was reported on June 07, near southern coast of Iran (25.5^{o}N/58.1^{o}E).

During its peak intensity on June 4th , Gonu (moving at a speed of 19km h^{-1}) was located about 650km east-southeast of Masirah Island off the coast of Oman. The cyclone maintained its peak intensity for 12 hours and on June 6, the wind had dropped from 240 km h^{-1} in peak (Figure 1) to 157 km h^{-1}, with the centre of the cyclone located 185 km southeast of Muscat. In terms of size, the cyclone was slightly smaller at its peak than average tropical cyclone in which gale would extend outward from the centre for about 240 km (Padgett, 2008).

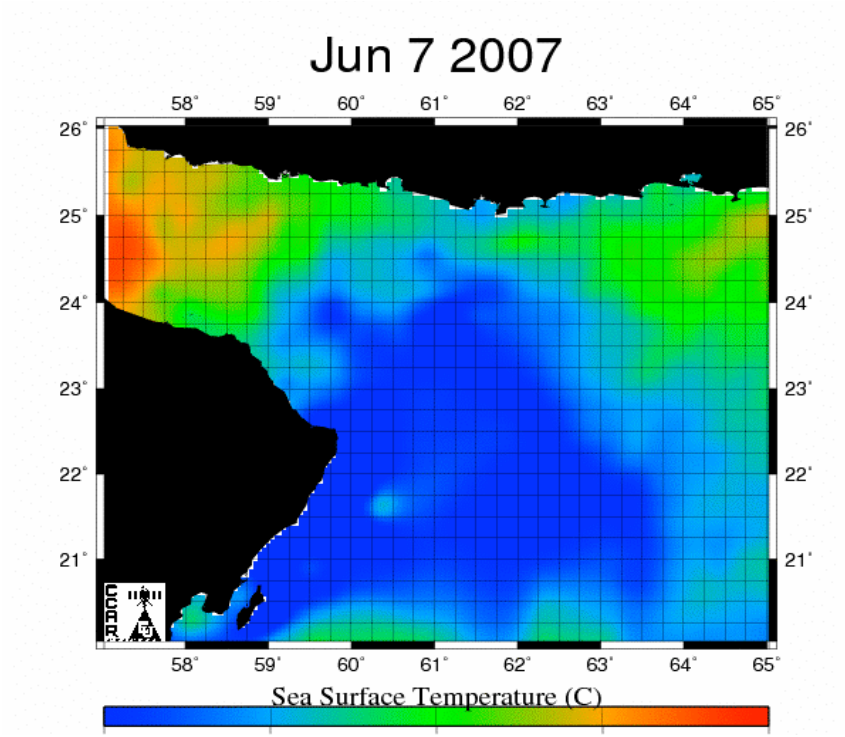

Figure 1 - Sea surface temperature after the passage of a cyclone Gonu (June 7; http://argo.colorado.edu).

The sea surface temperature 5 day composite (centred on June 7th) exhibited wide area of the north-western Arabian Sea occupied by waters with minimal temperature within the range observed (Figure 1). In comparison to the end of May (featuring the pre-cyclone mode), the area with a temperature of about 28^{o}C has expanded 10 fold, after the passage of a cyclone. In May, that level of minimal sea surface temperature has been observed in the coastal upwelling region only (Figure 2).

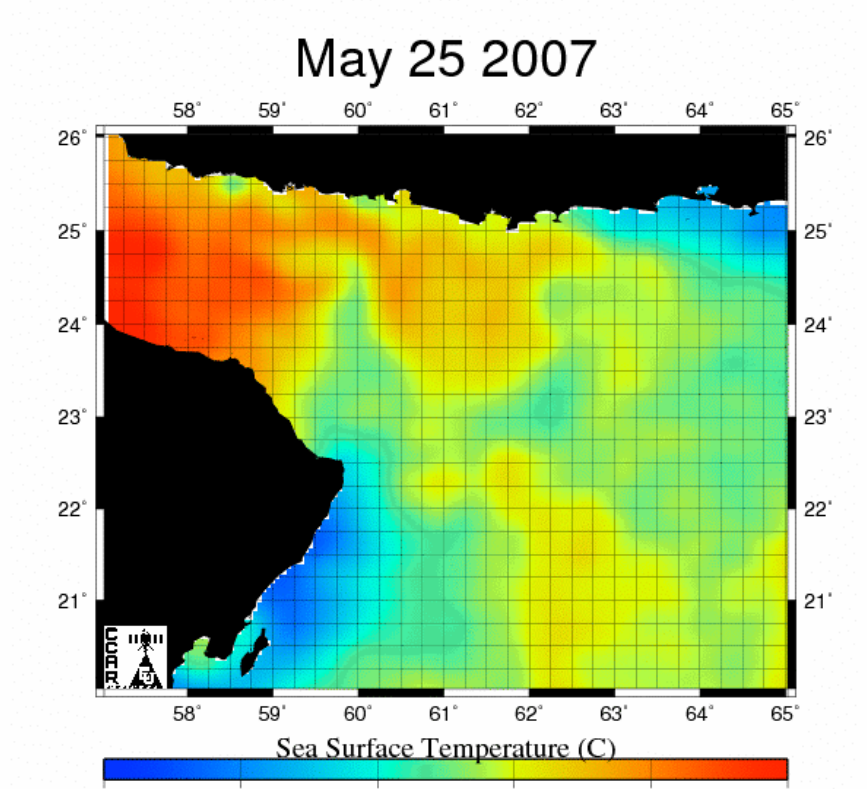

Figure 2 - Sea surface temperature before the passage of a cyclone Gonu (May 25; http://argo.colorado.edu).

The issue of significant cloud coverage has gradually complicated remote sensing of the chlorophyll concentration in the region. Few cloud windows in the images resembling the chlorophyll field on June 7th have enabled a sensor to detect the concentration range of about 8-10 mg m^{-3} for the region featuring the north-east periphery of the passed cyclone (23.4^{o}N/61.3^{o}E). Moreover, the reliability of these windows available for the analysis was low in general.

The 5 day composite of the chlorophyll *a* distribution (centred on June 4th) exhibited two major zones of enhanced concentration- the coastal one stretched along the Omani and Iranian coasts, and the oceanic one stretched longitudinally, between 61-62^{o}E (Figure 3).

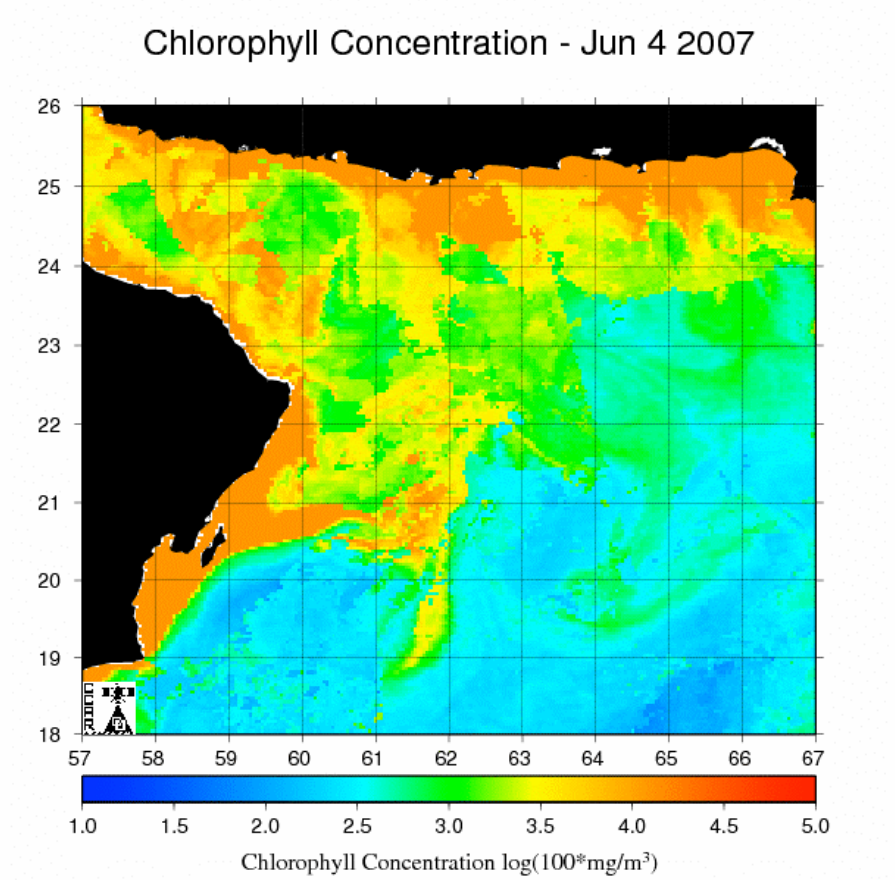

Figure 3 - Distribution of chlorophyll *a* on June 4, 2007 (5 day composite; http://argo.colorado.edu).

The mean chlorophyll concentration observed in the coastal zone 1.2 times exceeded that in the oceanic zone.

The MODIS database enables one to come up with monthly changes of chlorophyll over regions. In terms of our goal this means that the concentration observed in June (influenced by cyclone passage) could be compared to the range of concentration observed throughout the seasonal cycle. We retrieved monthly time series for the three 2 x 2^{o} quadrates covering the track of Gonu (Figure 4).

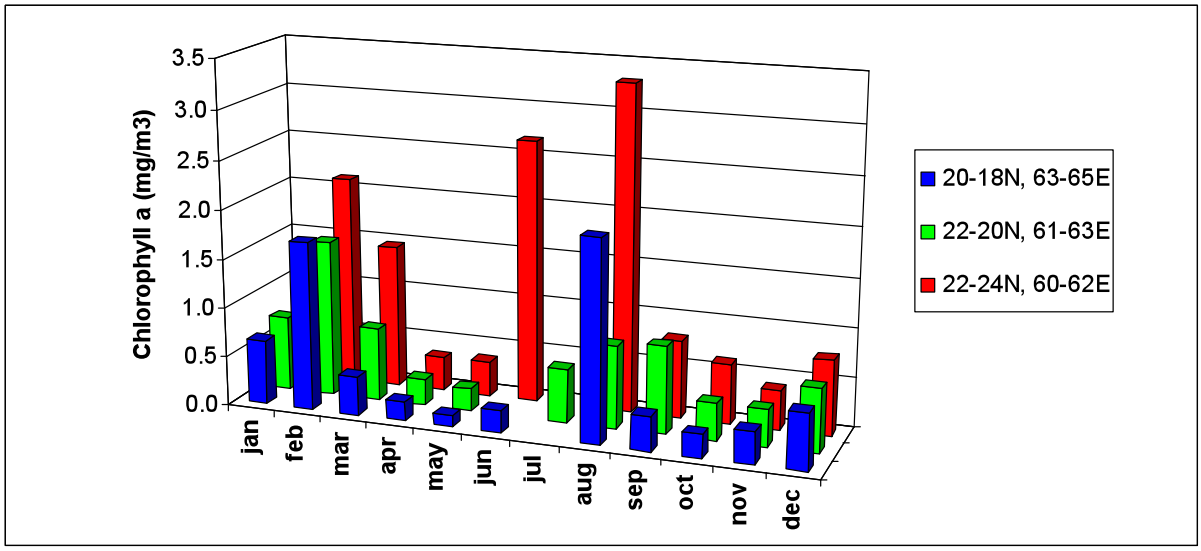

Figure 4 - Monthly changes of chlorophyll a (mg m^{-3}) in the three regions (2^{o} quadrates) along the track of a cyclone Gonu.

All three time series showed a well pronounced seasonal cycle of chlorophyll *a*, with peak concentration in August and February due to summer and winter monsoons. In the north-western quadrate (22-24°N/60-62°E) corresponding to the end of track the third well developed peak was observed. It matched the month of June -the time of cyclone passage. The chlorophyll *a* concentration in June 2007 in this region was 1.2 times less than the concentration featuring the summer monsoon of the same year.

The seasonal changes observed in the cyclone-affected region (north-western quadrate, 22-24°N/60-62°E) in 2007 were compared to the seasonal changes for the previous years- in 2005 and 2003 (Figure 5).

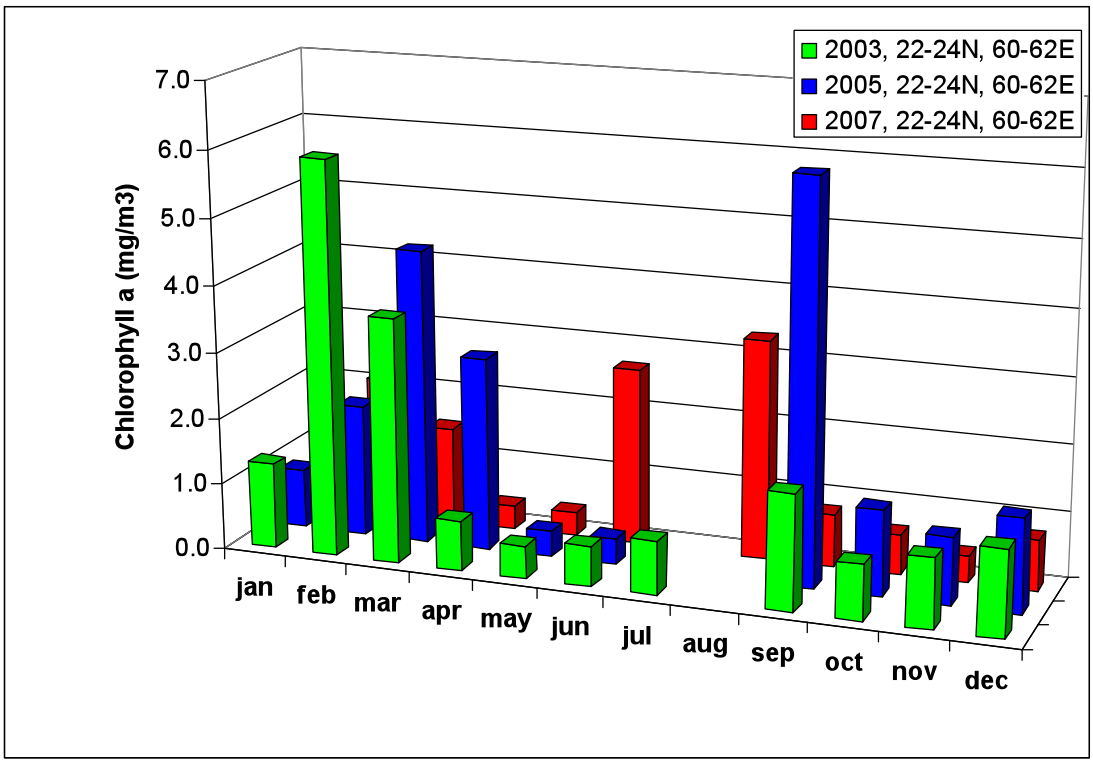

Figure 5 - Monthly changes of chlorophyll a (mg m^{-3}) in 2007 compared to 2005 and 2003 (22-24°N, 60-62°E).

None of these changes have exhibited peaks in June however. The two most developed peaks occurred during the times of the summer and winter monsoons.

Chlorophyll a and the other tropical cyclones

One of the issues aroused by the data on the productivity of Gonu was the hypothesis that the footprint left by a cyclone passing through a region could gradually depend on a speed of this passage. In order to seek the relationship between the translation speed of a cyclone and the concentration of chlorophyll *a* after its passage, data on 29 tropical cyclones reported for the Atlantic, Pacific and Indian Oceans were assembled (Table 1).

In this data set, the maximal wind speed varied from 20 to 72 m s^{-1}. The translation speed has been changing in a range of about one order of magnitude (1-12 m s^{-1}). Variation of the sea surface temperature gradient (characterizing the difference before and after cyclone passage) was in a range from 0.3 to 6.0 ^{o}C. The chlorophyll ratio (comparing the concentration of chlorophyll *a* after the passage of a cyclone to the concentration before the passage of a cyclone) varied from 1 to 32.

The data assembled enabled us to come up with a general pattern of the relationship featuring the chlorophyll ratio as a function of the translation speed of the cyclone that passed through the region (Figure 6).

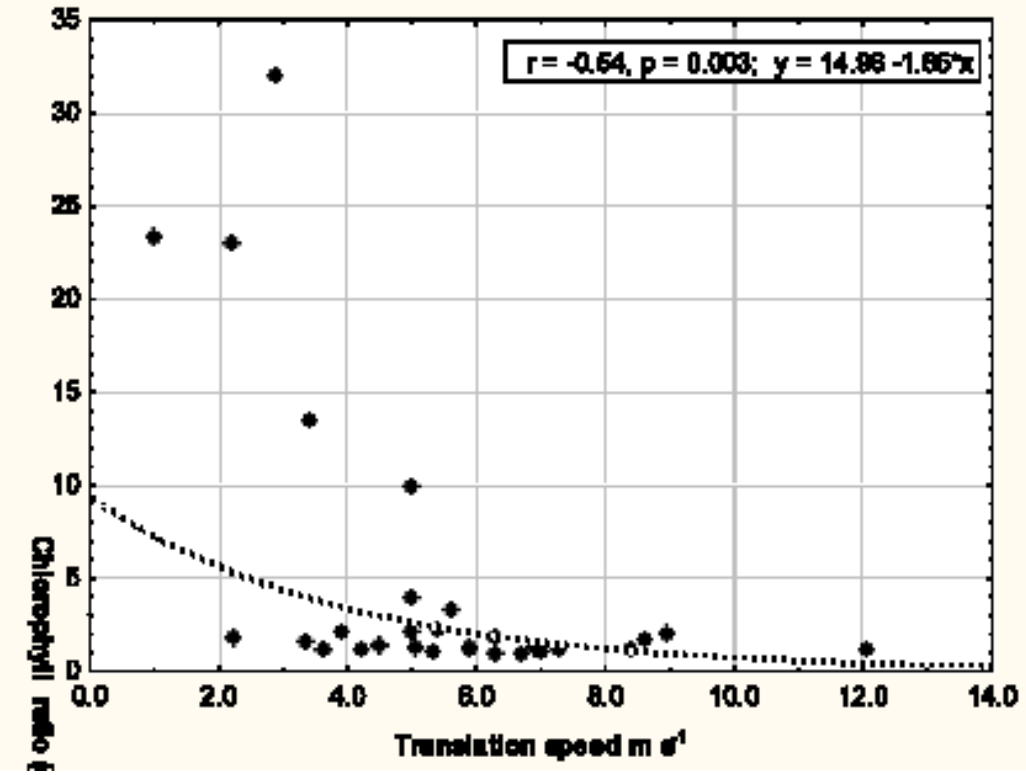

Figure 6 - The relationship between the chlorophyll ratio and the translation speed of a cyclone based on data for 29 cyclones (Table 1).

Table 1 - Some basic characteristics of the cyclones.

Cyclone Name	Ocean	Region	Month	Year	Max.Wind speed	Translation speed	Gradient SST	Chlorophyll *a*, ratio	Key references
					$m\ s^{-1}$	$m\ s^{-1}$	before/after	after/before	
Bonnie	Atlantic Ocean	North Carolina	Aug	1998	51	5.0	2.1	1.3	Babin et al, 2004; http://www.nhc.noaa.gov
Danielle	Atlantic Ocean	North-west Atlantic	Aug	1998	45	5.9	1.2	1.2	Babin et al, 2004; http://www.nhc.noaa.gov
Cindy	Atlantic Ocean	Gulf of Mexico	Jul	1999	63	4.2	2.6	1.2	Babin et al, 2004; http://www.nhc.noaa.gov
Dennis	Atlantic Ocean	North Carolina	Aug	1999	47	3.6	1.1	1.2	Babin et al, 2004; http://www.nhc.noaa.gov
Floyd	Atlantic Ocean	North-west Atlantic	Sep	1999	69	5.9	1.6	1.2	Babin et al, 2004; http://www.nhc.noaa.gov
Gert	Atlantic Ocean	Central north Atlantic	Sep	1999	63	4.5	2	1.4	Babin et al, 2004; http://www.nhc.noaa.gov
Jose	Atlantic Ocean	Virgin Islands	Oct	1999	34	7.0	0.5	1.1	Babin et al, 2004; http://www.nhc.noaa.gov
Alberto	Atlantic Ocean	Bermuda Islands	Aug	2000	38	7.3	0.9	1.1	Babin et al, 2004; http://www.nhc.noaa.gov
Florence	Atlantic Ocean	Bermuda Islands	Sep	2000	34	3.4	0.8	1.6	Babin et al, 2004; http://www.nhc.noaa.gov
Isaac	Atlantic Ocean	Cape Verde Islands	Sep	2000	58	9.0	2.1	2.0	Babin et al, 2004; http://www.nhc.noaa.gov
Michael	Atlantic Ocean	North-west Atlantic	Oct	2000	34	2.2	1.8	1.8	Babin et al, 2004; http://www.nhc.noaa.gov
Erin	Atlantic Ocean	Bermuda Islands	Sep	2001	47	5.3	0.3	1.1	Babin et al, 2004; http://www.nhc.noaa.gov
Michelle	Atlantic Ocean	Cuba	Oct	2001	38	12.0	2.6	1.2	Babin et al, 2004; http://www.nhc.noaa.gov
Fabian	Atlantic Ocean	Sargasso Sea	Sep	2003	64	8.6	3	1.7	Son et al, 2007; Black and Dickey, 2008
Felix	Atlantic Ocean	Sargasso Sea	Aug	2005	38	6.9	3.5	1.3	Black and Dickey, 2008
Nate	Atlantic Ocean	Sargasso Sea	Sep	2005	20	6.7	3	1.0	Black and Dickey, 2008
Harvey	Atlantic Ocean	Sargasso Sea	Aug	2005	26	6.3	2.5	1.0	Black and Dickey, 2008
Katrina	Atlantic Ocean	Gulf of Mexico	Aug	2005	72	3.4	4	13.5	Gierach et al, 2009; Gierach and Subrahmanyam, 2007

Ivan	Atlantic Ocean	Gulf of Mexico	Sep	2004	62	5.4	5	2.3	Walker et al, 2005; Stone et al, 2005
Barry	Atlantic Ocean	Gulf of Mexico	Aug	2001	31	5.0		10.0	Yuan et al, 2004
Georges	Atlantic Ocean	Gulf of Mexico	Sep	1998	48	5.0	4.5	2.1	Vukovich et al.
Gonu	Indian Ocean	Arabian Sea	Jun	2007	70	5.0	2	4.0	Piontkovski and Al-Azri, 2009
Orissa	Indian Ocean	Arabian Sea	Oct	1999	70	3.9		2.2	Patra et al, 2007; Madhu et al, 2002; Rao et al, 2007
01A	Indian Ocean	Arabian Sea	May	2001	38	1.0		23.3	Subrahmanyam et al, 2002, 2005; http://www.class.noaa
01B	Indian Ocean	Bay of Bengal	May	2003	28	2.2	4.8	23.0	Smitha et al, 2006
Herb	Pacific Ocean	China Sea	Jul	1996	53	8.4	3	1.2	Shiah et al, 2000; Wu and Kuo, 1999
Kai-Tak	Pacific Ocean	China Sea	Jul	2000	46	2.9	6	32.0	Lin et al, 2000; Zhao et al, 2008
Tim	Pacific Ocean	China Sea	Jul	1994	64	6.3	4	1.8	Chang et al., 1996; http://agora.ex.nii.ac.jp
Fred	Pacific Ocean	China Sea	Aug	1994	67	5.6		3.3	Chang et al., 1997

The relationship indicated an exponential increase in the chlorophyll ratio with a decrease of the translation speed of a cyclone (r= -0.54, p= 0.003). The fast moving cyclones produce minimal or no effect on the chlorophyll field (the chlorophyll ratio =1), whereas the slow moving cyclones (with a translation speed ≤ 3 m s^{-1}) tend to leave well developed phytoplankton blooms in which the chlorophyll *a* concentration exceeds (10 to 30 fold) the one before the cyclone passage.

Besides the translation speed, we analyzed the gradient of the sea surface temperature as an other "ecologically significant factor" which could affect the footprint left in the chlorophyll field by the passed cyclone (Figure 7).

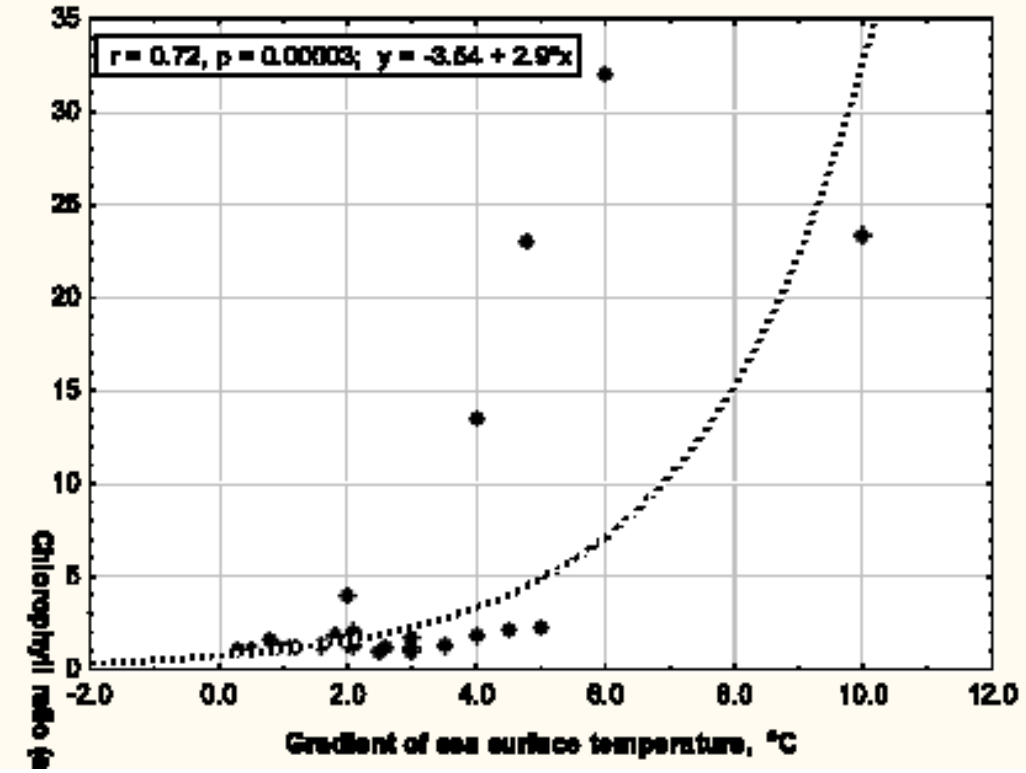

Figure 7 - The relationship between the chlorophyll ratio and the gradient of sea surface temperature for 29 cyclones (Table 1).

It turned out, the chlorophyll ratio increases exponentially with an increase of the sea surface temperature gradient (characterizing the difference in temperature before and after the cyclone passage). The correlation between both parameters was fairly high (r=0.72; p=0.00003).

The relationships found between the chlorophyll ratio versus the translation speed of cyclones, and the chlorophyll ratio versus the sea surface temperature gradient, both might be represented in the form of a more generalized graph (Figure 8).

The three-dimensional graph enables one to determine the range of translation speeds and sea surface temperature gradients in which the chlorophyll field (featured by the chlorophyll ratio) exhibits maximal response to the passed cyclones.

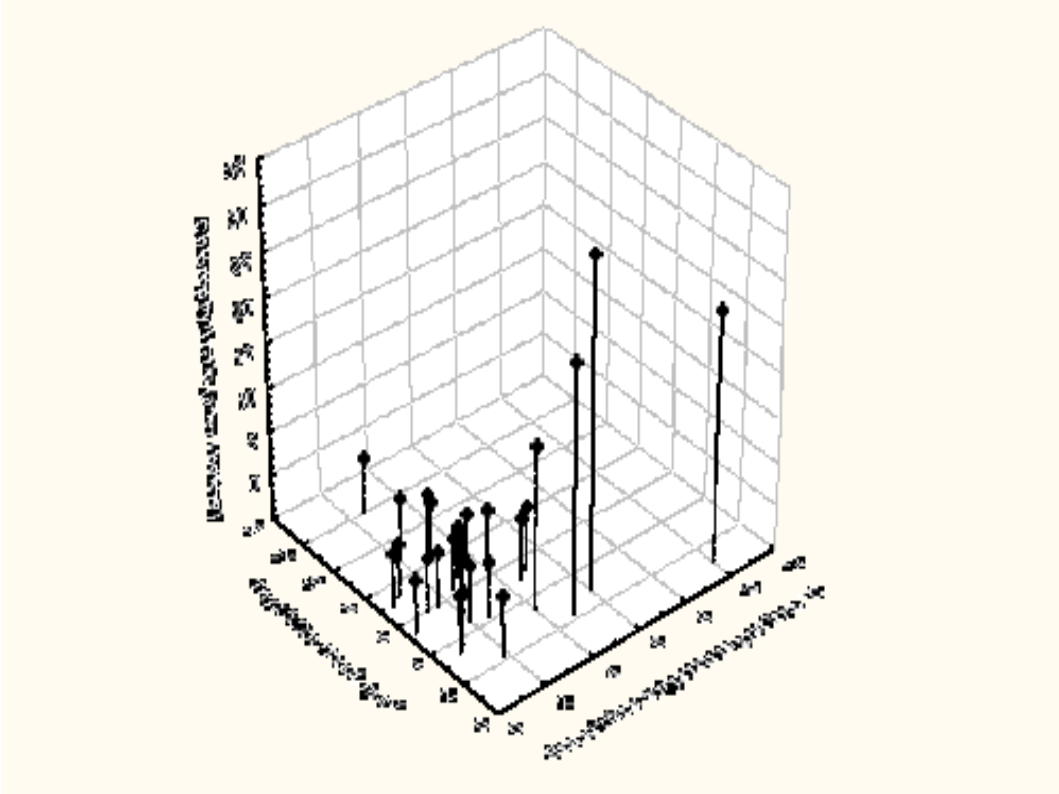

Figure 8 - Three dimensional presentation of the chlorophyll ratio as the function of the translation speed and the gradient of sea surface temperature (for 29 cyclones).

3. DISCUSSION

Chlorophyll a and hurricane Gonu

The zones of cyclonic varticity are coupled with the winds around the centre of the cyclone. This coupling leads to the surface Ekman divergence underneath the central part as well as geostrophic convergence at the edge of the cyclone (Subrahmanyam et al, 2005; Shiah et al, 2000). Also, the wind field of a tropical cyclone leads to localized mixing of the upper layer causing depleted temperature (Sriver and Huber 2007). In case of Gonu (super cyclone activity), sea surface temperature images showed that an entire north-western part of the Arabian Sea was occupied by waters with depleted temperature. This range of temperature is usually observed over the coastal upwelling area of Oman. The scale of the event has corresponded to the scale of the cyclone-as it has been seen in the field of wind from the QuikScat satellite data (http://www.nasa.gov/multimedia/imagegallery/image_feature_841.html).

The temperature drop observed over the region was about 1.5-2^{o}C, which is close to that reported for the case of cyclone passage in the south-western Bay of Bengal in 2000 (Ali et al 2006), but less than the averaged drop of temperature (2.6^{o}C) observed for the other 28 cyclones listed in Table 1.

Mixing of the upper layer leads to the injection of nutrients into this layer and subsequent enhancement of the chlorophyll *a* concentration –the indicator of phytoplankton bloom. However, significant cloud cover in the cyclone region usually does not allow one to come up with daily resolution in the chlorophyll imagery. The 5 day composite used in our study of Gonu showed an enhanced concentration of chlorophyll *a* in the final part of the cyclone track only. This zone of enhanced concentration had a form of the local filament, i.e. it did not match the scale of the depleted temperature zone. Being smaller in size, the phytoplankton bloom was stretched longitudinally, between 61-62^{o}E, hence appearing mainly to the right of a cyclone. Similar location of the cyclone-induced phytoplankton bloom was reported for the typhoon Damrey in the South China Sea (Zheng and Tang, 2007) and a cyclone 01A in the eastern Arabian Sea (Subrahmanyam et al

2002). Maximal gradients of sea surface temperature are tend to be located to the right of the track where the upwelling induced by the passing cyclone affect the upper 200m layer most of all (Price, 1981; Brooks, 1983; Brink, 1989).

Overall, interpretation of the influence of Gonu on phytoplankton productivity is fairly difficult, due to the passage of this cyclone through the biologically productive waters affected by Omani and Iranian coastal upwellings. The chlorophyll field (Figure 2) showed filaments of enhanced concentration (of about 2.7 mg m^{-3}) stretched out from the coastal regions towards the open ocean. However, the analysis of the seasonal changes revealed the month of June-2007 value as the only anomaly in the seasonal cycle, in comparison to the other years. Plus, this anomaly coincided spatially with the track of Gonu, when it picked up the strength of the super cyclone.

Due to the monthly resolution in the time series derived, we could notice that the persistence of the peak concentration induced by the passage of Gonu did not exceed one month. In comparison to the other regions and cases, local increase of the chlorophyll *a* attributed to the passage of tropical cyclones fits the time range from several days to one month (Babin et al 2004; Lin et al 2003; Subrahmanyam et al 2002). The development of cyclone-induced chlorophyll peaks was reported to lag the passage of the cyclone from 3 to 6 days (Lin et al 2003; Subrahmanyam et al 2002; Zheng and Tang 2007; Walker et al 2005).

Patterns of physical stratification of water masses under the cyclone track affect parameters of phytoplankton bloom. Following the passage of a tropical cyclone in the Bay of Bengal by the SeaWiFS records, Patra et al (2007) have noticed that due to strong stratification, enhanced production occurred only in small patches even under the influence of the Orissa Super Cyclone, which exhibited wind speed of up to 140 knots. As far as the Gonu track is concerned, the cyclone motion towards the Omani coast has been in fact the motion from stratified oligotrophic waters (in the central Arabian Sea) towards the productive ones, (in the north-eastern part of the sea). This might be one of the reasons why an actual response of chlorophyll concentration (i.e. the June peak) was observed in the most western part of the track.

Comparing the magnitude of the chlorophyll *a* concentration presumably induced by Gonu with the maximal concentration observed over the seasonal cycle (Figs. 4 and 5), one could notice that "the Gonu-induced concentration" was less the observed in August 2007 during summer upwelling. On the other hand, "the Gonu-induced concentration" has exceeded the concentration observed during the 2007 winter upwelling (with its peak in February). With a remark to the interannual variability (Figure 4), one could treat the Gonu-induced bloom to be less pronounced (by the magnitude of chlorophyll concentration) compared to the blooms induced by Omani seasonal upwelling in summer.

Among the other reasons of moderate chlorophyll concentration induced by Gonu, its high translation speed should be taken into account. Upwelling-induced injection of nutrients and enhanced vertical mixing could take place at a certain (low) translation speed of tropical cyclones (Price 1981). For instance, typhoons "Kai-Tak" and "Damrey", which had induced intensive (over 10 fold increase) phytoplankton blooms in the South China Sea, had a translation speed of 0-1.4 and 3.7 m s^{-1} correspondently (Zheng and Tang 2007). Cyclone Gonu had much higher translation speed (about 5 m s^{-1}) which did not allow a huge phytoplankton bloom to develop, under the greatest part of a cyclone track.

A survey of chemical and biological parameters in the continental shelf of the south East China Sea, northwest of Taiwan conducted shortly after the passage of tropical cyclone Herb in the summer-1996 has indicated typical oligotrophic waters in the study region. After the cyclone passage, all values of chemical and biological parameters were much greater than those derived from normal summer periods (Shiah et al 2000). This study has demonstrated that the whole shelf ecosystem could become more productive after the cyclone event. Checking for the same event in regards to Gonu, we compared (over the years) the summer concentration of chlorophyll *a* (from July through September) averaged within a rectangular (21-23^{o}N/59-60^{o}E) covering a major part of the Omani coastal upwelling. No differences were found. Over the five consecutive years (from 2004

through 2007) the average concentration in 2006 and 2007 could be attributed to the lowest ones.

Chlorophyll a and the other tropical cyclones

Rao et al (2007) used a three-dimensional model to study the impact of the Orissa super cyclone (originated in the Bay of Bengal in 1999). The forcing mechanism in the model was the wind stress derived from satellite data. The model predicted a maximum sea surface temperature drop (of about 6.0^{o}C) which depended on translation speed. It was concluded that the speed of the cyclone (which determines its resident time over the ocean) has an overwhelming influence on sea-surface cooling. We have shown that, the magnitude of chlorophyll increase after cyclone passage exponentially depends on the translation speed of this cyclone. On the other hand, the magnitude of chlorophyll increase exponentially depends on the gradient of sea surface temperature (which is the temperature difference before and after the cyclone passage).

The range of the sea surface cooling induced by cyclone passage (summarized in Table 1) could be gradually affected by the thermohaline stratification of the water masses. In regions of weak stratification, the decrease of sea surface temperature could be pronounced much more than in highly stratified waters (Gopalakrishna et al, 1993; Subrahmanyam et al, 2005; Vinaychandran et al, 2002). In the Indian Ocean, it takes about one to two weeks for revival of sea surface temperature to "normal" state after the cyclone passage (Gopalakrishna et al, 1993; Subrahmanyam et al, 2005).

In terms of the differences in productivity of the slow moving versus fast moving cyclones, the impact time seems to be the major factor because the injection of nutrients into the upper layers due to mixing is positively related to the duration of cyclonic impact on sea surface. In the South China Sea for instance, the weak slow-moving typhoon Kai-Tak has induced phytoplankton bloom with higher chlorophyll *a* concentration in comparison to the strong but fast-moving typhoon Ling-Ling (Zhao et al, 2008).

Among the factors affecting plankton blooms induced by tropical cyclones the impact of atmospheric precipitation is still poorly understood. Heavy rainfall (typical attribute of tropical cyclones) could act as the factor suppressing the enhancement of cyclone productivity due to formation of a low salinity zone along the track. In this zone, the salinity could be as low as 18-20 ppt (Subrahmanyam et al, 2005). Heavy precipitation could also produce an effect of abnormal cooling of sea surface temperature. This masks the cooling due to the divergence underneath the cyclone centre (Subrahmanyam et al, 2005).

Conclusion

The concentration of the chlorophyll *a* along the track of tropical cyclone Gonu exceeded the background concentration in the adjacent regions. The enhanced concentration was observed over the final (western) part of the track, corresponding to a super cyclone phase. The persistence of the enhanced concentration induced by the passage of Gonu did not exceed one month and did not reach the concentration range typical for the Omani coastal upwelling in summer, which is the season of the highest concentration of the chlorophyll *a* due to the south-west monsoon.

Data analysis on 29 tropical cyclones ocean wide, has shown that the magnitude of chlorophyll concentration increase after cyclone passage depends (exponentially and negatively) on the translation speed of this cyclone. On the other hand, the magnitude of chlorophyll concentration increase after cyclone passage depends (exponentially and positively) on the sea surface gradient (which is the difference of sea surface temperature before and after the cyclone passage).

References

Ali, M.M., Smitha, A., and Rao, K.H., 2006, A study on cyclone induced productivity in south-western Bay of Bengal during November-December 2000 using MODIS (SST and chlorophyll-a) and altimeter sea surface height observations, Indian Journal of Marine Science, 35, 153-160.

Babin, S., Carton, J.A., Dickey, T.D., et al, 2004, Satellite evidence of hurricane-induced phytoplankton blooms in an oceanic desert, Journal of Geophysical Research, 109, C03043, doi:10.1029/2003JC001938.

Badarinath, K.V.S., Kharol, S.K., Prasad, K.V., Kaskaoutis, D.G., and Kambezidis, H.D., 2008, Variation in aerosol properties over Hyderabad, India during intense cyclonic conditions, International Journal of Remote Sensing, 29,15, 4575–4597.

Black, W.J., and Dickey, T.D., 2008, Observations and analyses of upper ocean responses to tropical storms and hurricanes in the vicinity of Bermuda, Journal of Geophysical Research,113, C08009, doi:10.1029/2007JC004358.

Brink, K.H., 1989, Observations of the response of thermocline currents to a hurricane, Journal of Physical Oceanography, 19, 1017-1022.

Brooks, D.A., 1983, The wake of hurricane Allen in the western Gulf of Mexico, Journal of Physical Oceanography, 13, 117-129.

Chang, J., Chung, C-C., and Gong, G-C., 1996, Influences of cyclones on chlorophyll a concentration and Synechococcus abundance in a subtropical western Pacific coastal ecosystem, Marine Ecology Progress Series, 140, 199-205.

Gierach, M. M., and Subrahmanyam, B., 2007, Satellite data analysis of the upper ocean response to hurricanes Katrina and Rita (2005) in the Gulf of Mexico, IEEE Geoscience Remote Sensing Letters, 4, 132-136.

Gierach, M. M., Subrahmanyam, B., and Thoppil, P.G., 2009, Physical and biological responses to Hurricane Katrina (2005) in a 1/25° nested Gulf of Mexico HYCOM, Journal of Marine Systems, 78, 1, 168-179.

Gopalakrishna, V.V., Murty, V.S.N, Sarma, M.S.S., and Sastry, J.S., 1993, Thermal response of the upper layers of Bay of Bengal to forcing of a severe cyclonic storm: a case study, Indian Journal of Marine Science, 22, 8-11.

Gray, W.M., 1968, Global view of the origin of tropical disturbances and storms, Monthly Weather Review, 96, 669-700.

Gray, W.M., 1985, Technical document, WMO TD No.72, *WMO, Geneva, Switzerland* 1**,** 3–19.

Joint Typhoon Warning Centre, 2007, November 11 Tropical Cyclone Formation Alert, ftp://ftp.met.fsu.edu/pub/weather/tropical/GuamStuff/2007111021-WTIO.PGTW, Retrieved 2007-11-15.

Kokhanovsky, A.A., and Von Hoyningen-Huene, W., 2004, Optical properties of a hurricane, Atmospheric Research, 69, 165–183.

Lin, I., Liu, W.T., Wu, C.C., et al., 2003, New evidence for enhanced ocean primary production triggered by tropical cyclone, Geophysical Research Letters, 30, 13, 1718, doi:10.1029/2003GL017141.

Madhu, N.V., Maheswaran, P.A., Jyothibabu, et al, 2002, Enhanced biological production off Chennai triggered by October 1999 super cyclone (Orissa), Current Science, 82,12, 1472 - 1479.

McBride, J.L., 1995, Tropical cyclone formation. In: Global Perspectives on Tropical Cyclones. R.Elsberry (Ed.), Geneva, World Meteorological Organization.

Padgett, G., 2008, Monthly global tropical cyclone summary, http://www.typhoon2000.ph/garyp_mgtcs/jun07sum.txt (2008). Retrieved 16 September 2008.

Patra, P.K., Kumar, M.D., Mahowald, N., et al., 2007, Atmospheric deposition and surface stratification as controls of contrasting chlorophyll abundance in the North Indian Ocean, Journal of Geophysical Research, C, Oceans 112, 5, C05029.

Pielke, R.A., Lansea, Jr. C., Mayfield, M., et al, 2005, Hurricanes and global warming, Bulletin of American Meteorological Society, 86, 11, 1571–1575.

Piontkovski, S.A., and Al-Azri, A., 2009, Influence of a tropical cyclone GONU on phytoplankton biomass (chlorophyll a) in the Arabian Sea, In: Indian Ocean Tropical Cyclones and Climate Change. Charabi Yassine (Ed.). Springer, 285pp.

Price, J.F., 1981, Upper ocean response to a hurricane. Journal of Physical Oceanography, 11,153-175.

Rahman, P., 2007, Cyclone Death Toll Up to 3,100 in Bangladesh, May Rise, Associated Press, http://news.nationalgeographic.com/news/2007/11/071119-AP-bangladesh-cyclone.html., Retrieved 2007-11-20.

Rao, A.D., Dash http://www.bioone.org/doi/abs/10.2112/05-0517.1 - aff2#aff2, S., Babu, S.V.http://www.bioone.org/doi/abs/10.2112/05-0517.1 - aff1#aff1, et al, 2007, Numerical Modeling of Cyclone's Impact on the Ocean—A Case Study of the Orissa Super Cyclone, Journal of Coastal Research, 23, 5, 1245-1250.

Shiah, F.K., Chung, S.W., Kao, S.J, et al., 2000, Biological and hydrographical responses to tropical cyclones (typhoons) in the continental shelf of the Taiwan Strait, Continental and Shelf Research, 20, 2029–2044.

Smitha, A., Rao, K.H, and Sengupta, D., 2006, Effect of May 2003 tropical cyclone on physical and biological processes in the Bay of Bengal, International Journal of Remote Sensing, 27, 5301-5314.

Sriver, R.L., and Huber, M., 2007, Observational evidence for an ocean heat pump induced by tropical cyclones, Nature, 447, 577-580.

Stone, G.W., Walker, N.D., Hsu, S.A., et.al, 2005, Hurricane Ivan's impact along the northern Gulf of Mexico, EOS, 86, 48, 497-508.

Subrahmanyam, B., Rao, K.H, Rao, S.N., et al., 2002, Influence of a tropical cyclone on chlorophyll-a concentration in the Arabian Sea, Geophysical Research Letters, 29, 1-22.

Subrahmanyam, B, Murty, V.S.N., Sharp, R.J., et al., 2005, Air-sea coupling during the tropical cyclones in the Indian Ocean: a case study using satellite observations, Pure and Applied Geophysics, 162, 1643-1672.

Zhao, H., Tang, D., and Wang, Y., 2008, Comparison of phytoplankton blooms triggered by two typhoons with different intensities and translation speeds in the South China Sea, Marine Ecology Progress Series, 365, 57-65.

Zheng, G.M., and Tang, D., 2007, Offshore and nearshore chlorophyll increases induced by typhoon winds and subsequent terrestrial rainwater runoff. Marine Ecology Progress Series, 333, 61-74.

Vinaychandran, P.N., Murty, V.S.N., and Babu, R.V., 2002, Observations of Barrier layer formation in the Bay of Bengal during Southwest Monsoon, Journal of Geophysical Research, 107, 8018, doi:10.1029/2001JC000831.SRF 19-1to SRF 19-9.

Vukovich, F.M., Müller-Karger, F., and Nababan, B., 2009, Hurricane Impacts on the Northeastern Gulf of Mexico as seen with the NOAA AVHRR and SeaWiFS, http://imars.usf.edu/~hu/scratch/dennis/hurricane_paper_final_2.doc. Retrieved 20.10.2009.

Yuan, J., Miller, R.L., Powell, R.T., and Dagg, M.J., 2004, Storm-induced injection of the Messissipi River plume into the open Gulf of Mexico, Geophysical Research Letters, 31. L09312, doi: 10.1029/2003GL019335.

Walker, N.D., Leben, R.R., and Balasubramanian, S., 2005, Hurricane-forced upwelling and chlorophyll a enhancement within cold-core cyclones in the Gulf of Mexico, Geophysical Research Letters, 32, L18610, doi:10.1029/2005GL023716.

Wu, C., and Kuo, Y., 1999, Typhoons affecting Taiwan: current understanding and future challenges. Bulletin of American Meteorological Society, 80, 1, 67-80.

EFFECT OF TROPICAL CYCLONES ON AGRICULTURE AND SOCIO-ECONOMIC CONDITIONS OF RURAL PEOPLE IN BANGLADESH

Md. Toriqul Islam, Md. Zakaria Hossain, Masaaki Ishida and Toshinori Sakai
Graduate School of Bioresources, Mie University,
1577 Kurimamachiya-cho, Tsu-city, Mie 51408507, Japan

Abstract

This paper depicts the results of recent studies on severity and countermeasures of tropical cyclones of Bangladesh based on the field visits to cyclone site, collected data and information on damages and deaths of peoples during field visits, necessary data related to tropical cyclones obtained from available publications and news paper information reported in the recent years and previously. The effect of the tropical cyclones in terms of death of peoples, damages, flood surge heights, wind speed and radius of the severe storm are analyzed and given in various charts and diagrams. Data of 37 years since 1970 when the country was going to born are analyzed and depicted. It is found that in 2007, Bangladesh again witnessed unprecedented tropical cyclone called as “Sidr” causes enormous disruptions, damages and remarkable number of death of peoples. It is revealed that the coast of the Bay of Bengal is particularly vulnerable to tropical cyclones where at least sixteen major cyclones including four severe cyclonic storms occurred that killed over four hundred thousand people especially after the Bhola cyclone. It is observed that the return period of the destructive cyclones decrease gradually indicating that the country is more vulnerable to devastating cyclones in the recent years.

Keywords

Bay of Bengal, Bangladesh, Tropical Cyclones, Severity, Agriculture, Socio-Economic Condition, Rural Peoples

INTRODUCTION

Bangladesh is a country vulnerable to cyclones associated with tidal surge particularly in pre-monsoon months of April-May and post-monsoon months of October-November. The country is also susceptible to flood associated with heavy rain and snow melts on the eroded materials from the south and southern slopes of Himalaya Mountains during the monsoon season (June to September). Within 37 years, the Bay of Bengal has witnessed many major cyclones causing enormous disruptions, damages and remarkable number of death of peoples. The cyclones occurred in the year of 1970 (Bhola), 1991 (Tropical), 1999 (Orissa) and 2007 (Sidr) are some of the examples. The 1970 Bhola cyclone was a devastating cyclone that struck on November 12, 1970 (Islam, 2006). It was the deadliest tropical cyclone ever recorded, and one of the deadliest natural disasters in modern times. More than 250,000 people lost their lives in the storm, primarily as a result of the storm surge that flooded much of the low-lying islands of the Ganges Delta. This cyclone was the sixth cyclonic storm of the 1970 North Indian Ocean cyclone season, and was also the most powerful, reaching a strength equivalent to a Category 3 hurricane. This cyclone formed over the central Bay of Bengal on November 8 and travelled north, intensifying as it did so. It reached its peak with winds of 185 km/h (115 mph) on November 12, and made landfall on the coast of East Pakistan that night. The storm surge devastated many of the offshore islands, wiping out villages and destroying crops throughout the region. The city of Thana, Tazumuddin, was the most severely affected, with over 45% of the population of 167,000 killed by the storm (Paul and Rahman, 2006).

The cyclone which struck Bangladesh on the night of 29-30, April, 1991 was particularly severe causing widespread damage, killing 138,882 people (Bern, et al 1993). There has been massive damage to life line systems as well as private properties. Total loss has been estimated at US$2.07 billion dollars for all sectors. Cyclone on 18th October, ’99 hit on the eastern cost of India along the Bay of Bengal affecting the coastal districts of Ganjam, Puri, Jagatsinghpur, Khurda, Gajapati and Balasore. Subsequently, the State was hit by a Super Cyclone on 29th October, ’99 with winds of more than 250 km/h, tidal waves rising 20 feet high and torrential rains. The Super Cyclone and its aftermath caused "severe" damage in the districts of Jagatsinghpur, Balsore,

Cuttack, Puri, Nayagarh, Jajpur Kendrapada, Bhadrak and Khurda and "moderate" damage in the districts of Mayurbhanj, Dhenkanal and Keonjhar (BWDB. 1998). In 2007, Bangladesh suffered a natural disaster like the cyclone Sidr of November 15, an unusually powerful storm that triggered giant waves up to 30ft (7m) high and killed more than 10,000 people in the south western coastal belt of Bangladesh covering the districts of Bagerhat, Barisal, Patuakhali, Pirozepur, Khulna and Satkhira. Even five days after the calamity, in village after village along the battered roads of the coastal districts, the survivors of the storm, their cheeks hollow and eyes sunken from hunger wait in vain for relief to come. True, natural disasters are a universal reality.

But in modern times, it is the preparedness that counts. Damage can be minimized, rehabilitation can be effective, but only if a nation has an organized disaster management plan. Unhappily, Bangladesh does not. Accompanied by 260 km/h ravaging winds and sea surge as high as 30ft that swept about 20 km inland, a grade 5 hurricane, the highest level possible, devastated 23 districts in the south western part of Bangladesh at midnight on November 15, 2007 (EU, 1998). The country is yet to fully repair many of the damages done to her infrastructure due to devastating flood occurred in the same year just three months ago (Hossain and Sakai, 2008). Agricultural infrastructures such as farm structures, irrigation structures, dairy, poultry, fisheries, shelter, sanitation, drinking water, electricity supplies, transportation services including both land and water transports are in great danger in the region of Bay of Bengal where natural disasters occur frequently. Some destruction due to devastating Sidr in term of damages of houses, flooding, fallout and uprooted of trees is shown in Figure1. In view of the above objectives, a comparative study of the major cyclones those struck Bangladesh in the last four decades especially just before and after the independence of Bangladesh. Along with the severities, this paper also reports some countermeasures of tropical cyclones of Bangladesh taken by the government of the country. Data collected during the field visits to cyclone site, information on damages and deaths of peoples published in technical literature and news papers are analyzed and demonstrated. Along with the damages of previous cyclones, the disruptions, damages and death of peoples occurred in the year 2007 are illustrated in various charts for better comparison. The return period of destructive cyclones, frequency, warning system of the weather broadcasting centre and the countermeasures taken by the government of the country are depicted in this paper. Damages of agricultural engineering infrastructures such as rural roads, embankments, water sanitation, shelters and food security are also discussed.

Figure 1 - Severities and damages of Sidr, 2007 (Daily Inquilab), (a. uprooted, b. death, c. flooded, d. fallout, e. ship destruction, f. house damaged).

1. PHYSICAL FACTS, CYCLONES PATH AND SEVERITIES

The path of the four severe cyclones along with the physical facts of Bangladesh is shown in Figure 2. It should be noted that Bangladesh extends between 21o and 27o North latitude and 88o and 92.5o East longitude. The Bay of Bengal is in the south side of the country. The total area is 144,000 sq km and size of population is around 15 million (2007). Per capita income is around US$ 550, one of the lowest in the world. The coastal land of Bangladesh (710 km long) is of recent origin formed out of the process of sedimentation. Most parts of the area are, therefore, low lying which can be subject to inundation even under ordinary circumstances of tides. A tidal surge accompanied by a cyclone storm makes the situation alarming which is further exacerbated by the triangular shape of the Bay of Bengal (Figure 2). The wide shallow continental shelf is conducive to amplification of surges causing wide spread flooding. The country has been subjected to frequent natural disasters in many forms, particularly cyclonic storms and tidal surges. From 1970 to 2007, four major cyclone storms and tidal surges have been reported. These indicate that Bangladesh is prone to frequent destructive tropical cyclones associated with tidal surge. The low-lying coastal areas are particularly vulnerable, thus placing these population, infrastructure, agriculture, livestock and economic development in a high-risk situation. During the 1991 cyclone, the cyclonic storm was detected as a low pressure area over the Southeast Bay and adjoining Andaman Sea on 23 April. Finally, the cyclone of hurricane intensity crossed the Chittagong coast a little north of Chittagong at 2 a. m. of 30 April, 1991 that killed some 143,000 people in Bangladesh. The aspects of the detection of the cyclone, its monitoring and prediction and weakness of warning and special weather bulletins have been reflected upon. Most of the worst affected thanas are either off-shore islands or coastal thanas. The less affected thanas are mostly located inside and further from the coast. The 2007 cyclone Sidr smashed into the country's southern coastline late on Thursday midnight of November 15 with 250km/h (155 m/h) winds that whipped up a five meter tidal surge and swept about 20 km inland, a grade 5 hurricanes, the highest level possible, devastated 23 districts in the south western part of Bangladesh. Gigantic walls of water smashed into the coastline, washing away everything in their path. The backwash dragged hundreds of people into the sea, bodies were towards the shoreline -- twisted, bloated and broken -- washing up from the overflowing creeks and ponds around the villages. Death and its nauseating stench were everywhere.

Figure 2 - Physical facts and path of severe tropical cyclones in Bangladesh.

2. RESULTS AND DISCUSSION

2.1 Wind Speed and Storm Surge

In order to understand the severity of storm of the tropical cyclones in Bangladesh, a comparative study of the maximum wind speed and storm surge of major cyclones those struck in Bay of Bengal during the last four decades is depicted in Figsures 3 and 4. The high power of the storm was mainly due to the higher wind speed which is apparent from Figure 3 for all the cases after 1970. In 1970 that is known as Bhola cyclone, though the wind speed was not as high as of the recent cyclones that can be found in 1991, 1998 and 2007, however, the number of casualties was severe at that time. The wind speed of Bhola cyclone was nearly 227 km/h whereas the others were over 230 km/h such as 257, 237 and 247 km/h for the cyclones occurred in the year of 1991, 1999 and 2007, respectively. The storm surge, on the other hand, was recorded as 7.8, 8.8, 8.1 and 8.4 m for the cyclones occurred in the year of 1991, 1999 and 2007, respectively, as shown in Figure 4. The radius of the major cyclones is shown in Figure 5.

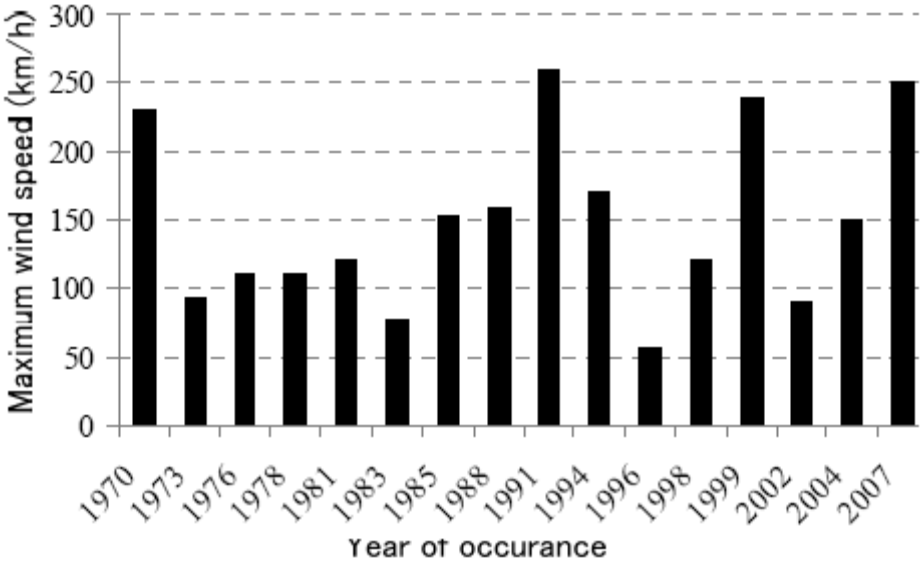

Figure 3 - Wind Speed during the major cyclones in Bangladesh.

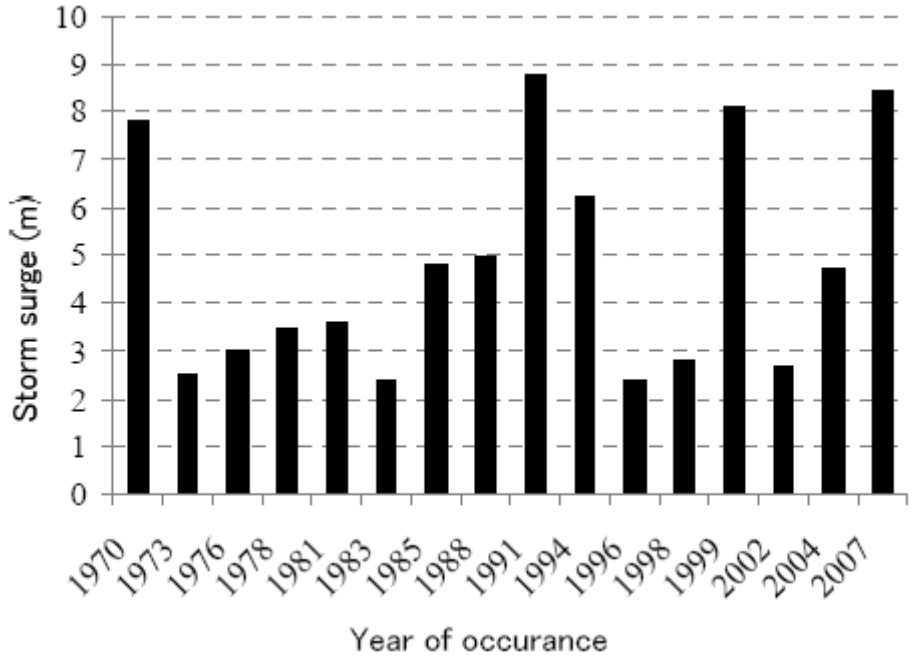

Figure 4 - Flood surge height during the major cyclones in Bangladesh.

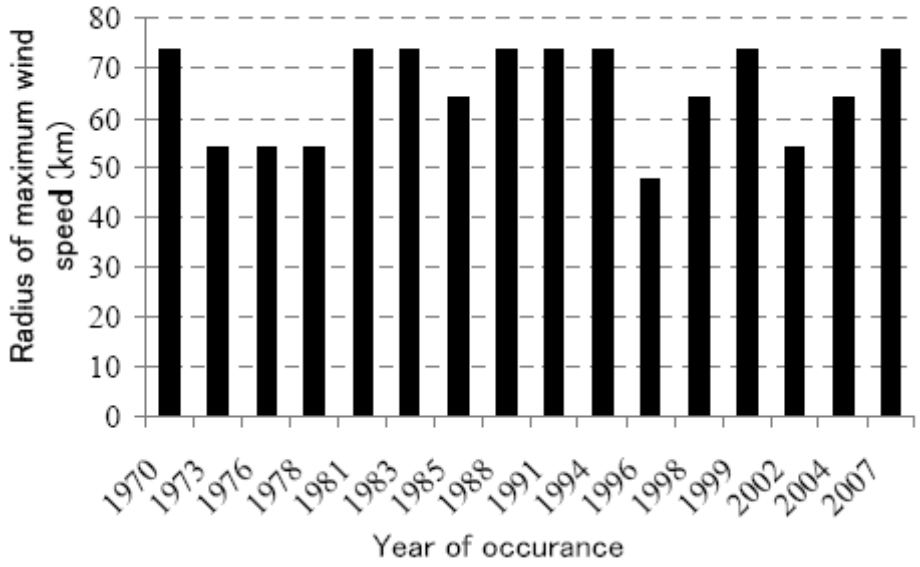

Figure 5 - Maximum radius of major cyclones.

2.2 Number of death of people and damages

The number of death of people and the damages due to major cyclones in Bangladesh are given in Figure 6 as the line graphs for the sake of clarification of the ferocious devastation brought to Bangladesh by the cyclones in just 37 years. Although the wind speed and tidal surge was lower for the 1970 Bhola cyclone, than the recent ones, the number of death of people was extremely higher at that time. It was estimated that more than 250000 people was died during the 1970 Bhola cyclone. It was saying that this was the deadliest one in the earth in its history. On the other hand, the 1991 cyclone was also other deadliest tropical cyclones on record that struck greater Chittagong with strong winds and storm surge, killing at least 140000 people and leaving as many as one crore people homeless and destroying 10 lake homes. The damage of property was estimated at 1.8 billion US dollar in 1991. The damage in 1999 and 2007 is noted as 4.2 and 5.3 billion US dollar. A large number of boats and smaller ships ran aground. Bangladesh Navy and Air Force were also heavily hit. BNS Isha Khan Naval Base was flooded, with heavy damage to the ships. Most of the fighter planes of the Air Force were also damaged. Comparison between the death of people and the damages in Figure 6 in terms of money in US$ during the past four major cyclones notices that the number of death of people is getting to decrease although the damages of the properties increases in the recent years. This clearly indicates the awareness and preparedness of the people in the coastal region, improvement of weather broadcasting system and countermeasures taken by the government of the country. However, these measures could not be considered enough yet and more action need to be taken to minimize the death and damages of the peoples, their homes, cattle, agriculture, forestry and fisheries, as well as its environment, bio-diversity, Sundarbans (world largest mangrove) and wildlife.

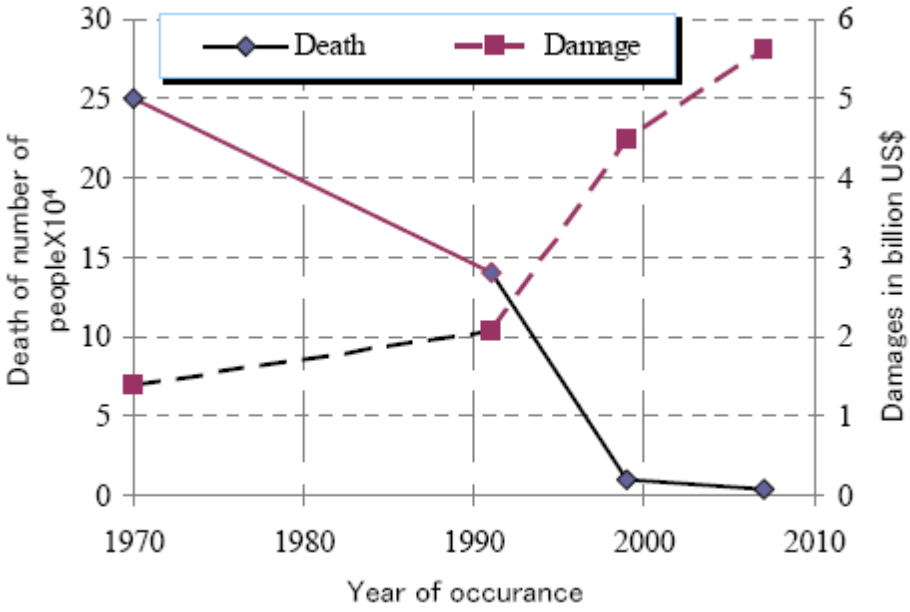

Figure 6 - Number of death of people and damages of severe cyclonic storms in Bangladesh.

2.3 Sidr's Victims and Rehabilitation

There were a lot of Sidr victims not only in the coastal region but also in the regions neighbouring the path of Sidr as it passes on the capital of the country. An example of some of the Sidr victims from the union-3 in Sharonkhola in Bagerhat is shown in Figure 7. Victims are living on a road in makeshift houses as their locality was torn up by the devastating cyclone on November 15. Rehabilitation programme for Sidraffected areas has been undertaken by the local authorities along with the government of the country and NGOs. This included economic rehabilitation, infrastructure development, disaster preparedness programmes and climate adaptation programmes to strengthen the region's defense against future natural disasters.

Figure 7 - Scores of Sidr victims in Bagerhat living on a road (Daily Inquilab).

2.4 Countermeasures

The government has taken a number of countermeasures to prevent the lives of the peoples in the coastal regions especially after the Great Bhola Cyclone of 1970. An example of concrete cyclone shelters that was built in the cyclone prone area is shown in Figure 8. The construction of cyclone shelters was accelerated after the 1991 cyclone. This process is continued till to date and further reinforced after the recent cyclones. Bangladesh now has over 2500 multi-purpose cyclone shelters some of it is used as primary schools also. The recent warning system in Bangladesh is fairly effective at notifying the population of an approaching cyclone. Earlier many residents were chosen not to evacuate to the shelters, since most of them are in poor condition with minimum or no maintenance at all. But now-a-days, peoples of the country are aware and showing much more response to the weather information than earlier that saves many lives in 2007.Along with the government action, the NGOs also have devised cyclone preparedness programmes, building shelters, organizing simulated cyclone evacuation exercises and educating villagers in the most exposed areas on how to flee. Efficient early warning systems and the widespread use of mobile phones meant that this time even people in remote regions were aware of the impending disaster. On-time information had reduced the extent of the destruction. Before the 1999 cyclone, weak technological strength and the lack of practical know-how were the main obstacles to implementing the strategy in the country.

But, recently information and communication technology, especially mobile phones and internet facilities along with the improvement of weather broadcasting technology greatly adds to an effective disaster management along with global T.V. channels and web sites. This involved preparing, warning, supporting and rebuilding the society before occurrence of the Sidr. However, a slight variation of landfall timing was observed. While there was a lot to cover in terms of accurately predicting, it was not clear where exactly the centre of the cyclone and when it was going to make landfall and what would be its intensity and impact. The major challenge was to convert this information into a timely evacuation plan. On mid-day of Wednesday 14th November, 2007 many people were evacuated to the cyclone shelters because of the cyclone warning of Bangladesh Meteorological Department. The Storm Centre of BMD in its bulletin forecasted that Cyclone Sidr would make landfall by noon. According to the Disaster Management Bureau, when the people who took shelter saw that cyclone had still not come, they thought it would not materialize and left the cyclone shelters for their homes. Many of these people felt victim to the fury of the cyclone. BMD came under heavy criticism for having forecasted landfall ahead of time.

Figure 8 - Shelter in coastal area of Bangladesh to save peoples from cyclones.

2.5 Agricultural and socio economic conditions

Food Security:

According to UN, more than 1.6 million acres of cropland was reportedly damaged. The main crop damaged was rice that was under cultivation during this Aman season. Unlike many other regions in Bangladesh, the area affected has a single harvest during the months of November thru January. Thus the timing of the cyclone was particularly harmful, in that many of the crops were at or nearly ready for harvest. A quarter of ready-to-harvest crops have been destroyed. Many households lost their food stocks as a result of severe damage to housing. Large numbers of cattle, buffalos, goats and poultry have been killed. The government of Bangladesh estimated that nearly 382,000 livestock animals were killed; the large majority of these were believed to be cattle. The UN assessment team members witnessed many animal carcasses floating in the rivers or washed up on the river banks. Livestock losses represent not only a loss of critical household assets, with an associated loss to wealth and income, but also a loss in milk production for own consumption. In coastal areas fish were a key source of food and animal protein. During the near term period fish consumption in the diet was declined, as catches were reduced due to either damage to boats and nets etc., and/or the unavailability of labour which was diverted to other critical activities such as housing repairs and reconstruction. Fish production from household ponds and shrimp fisheries was also declined, as many ponds and shrimp cultivation areas were badly damaged and littered with storm wreckage and debris. Many small shops selling food in worst affected areas were severely damaged due to strong winds and falling trees. Food prices were already high prior to the storm due to high international food prices and earlier flood related losses, prices were high further after cyclone.

Physical access to food markets has been disrupted in some of the worst affected areas; however most of the trees blocking roads and thereby hindering the transport of food to market areas have been cleared, and so food availability in the markets was not a major concern. Where housing damages were particularly bad, household kitchens and cooking areas had been badly affected, with serious implications for the ability to cook and utilize food. Although the affected population was able to salvage some possessions, many people were unable to cook due to missing utensils.

Shelter:

Housing damages were the most visible and tangible damages associated with cyclone. For worst affected areas UN assessment team members witnessed numerous cases of flattened, overturned or sideways leaning household structures. Piles of damaged housing and construction materials were common within the hardest hit residential areas. The total number of houses damaged was nearly 1.2 million, approximately 30% of those were reported as fully damaged, and the remaining 70% partially damaged. Approximately 697400 houses were damaged within only five districts. In many Upazilas more than half of thatched-roof homes, primarily inhabited by the extreme poor, were completely destroyed. A high proportion of wood-framed houses with corrugated iron roofs had been destroyed or severely damaged in coastal areas. Less extensive damage was observed at locations further in land or north of the coast.

Water and Sanitation:

Damage to sanitation facilities and infrastructure was significant. For some of the worst affected areas, one estimate puts the percentage of slab latrines damaged or destroyed as high as 70%. The affected population was vulnerable to outbreaks of diarrhea and other hygiene-related diseases. Drinking water sources in many communities had been contaminated by saline and debris. Power outages had affected water supplies in areas with piped water.

Transport:

There was widespread damage to transport and communications networks. Rural roads, and many of the embankments protecting such roads, were extensively damaged. Most of the road damage was associated with the tidal surges in coastal areas. Large uprooted trees on roadsides also account for some of the damages, as trees were uprooted segments of tarmac or earthen roads became cracked or fragmented. Damage to transport infrastructure in coastal and inland

waterways had occurred. Numerous ferries, and associated landing and loading areas damaged. In more than a few cases, the storm surge was so strong that medium to large sized ferries were actually lifted clear out of the water and beached on neighbouring land.

Conclusions

The paper analyzes the extent and severity of tropical cyclone in Bangladesh and its countermeasures taken by the government of the country along with the NGOs'. There were four deadliest storms since 1970 in the Bay of Bengal and Sidr was one of the fiercest cyclones that had hit the region of Bangladesh in just 37 years since 1970. For a poor country like Bangladesh, a natural disaster always means a huge death toll, displacement and inconceivable destruction. Sidr 2007 was as devastating as the earlier ones, however, it has taken far fewer lives than 1991's Cyclone, which killed at least 138,000 people, and the 1970 cyclone in Bhola, which left as many as above 250,000 people dead and is considered the deadliest cyclone, and one of the worst natural disasters, in human history. Nonetheless, Sidr 2007 is one of the deadliest one causing thousands of people dead, millions of acres of cropland washed down by the sweeping ocean-surge, one third of Sundarban, a world natural heritage, utterly torn down, and substantial infrastructural damages have caused combined losses of assets and agricultural production.

After the shattering cyclone of 1991, around 2,500 cyclone shelters and 200 flood shelters were constructed in the coastal regions, but experts opine that additional 2000 shelters are badly needed. In Patenga, Chittagong, the coast has been heavily protected with concrete levees. In addition, forestation has been initiated in the coastal regions to create a green belt. About 3,931 km long coastal embankment to protect coastal land from inundation by tidal waves and storm-surges, and drainage channels of total length of 4,774 km have so far been constructed, but lack of maintenance has rendered them almost ineffective. A comprehensive Cyclone Preparedness Programme (CPP) is jointly planned, operated and managed by the Ministry of Disaster Management and Relief (MDMR) and the Bangladesh Red Crescent Society (BRCS), and a volunteer force of more than 32,000 has been trained to help in warning and evacuation in the coastal areas.

References

Islam, T. 2006. *Integrated Approach to Cyclone Wind Analysis and disaster planning for the Benladesh coast*,Ph.D. Dissertation, Texas Tech University, December.

Paul, A., and Rahman, M. 2006. *Cyclone Mitigation Perspectives in the Islands of Bangladesh: A Case of Sandwip and Hatia Islands*, Coastal Management, 34, Issue 2 April, pp.199-215.

Bern, C., Sniezek, J., Mathbor, G. M., Siddiqi, M. S., Ronsmans, C., Chowdhury, A. M., Choudhury, A. E., Islam, K., Bennish, M., and Noji, E. 1993. *Risk factors for mortality in the Bangladesh cyclone of 1991*, Bulletin of the World Health Organization, 71(1), pp.73-78.

BWDB. 1998. *DHV, Meghna Estuary Study, Draft Master Plan*, Volume 1, Main Report, for BWDB, Dhaka. EU (European Community). 1998. *Cyclone Shelter Preparatory Study (CPSP*), Stage I, Feasibility Study, Draft Final Report, Vol. 3.

Hossain, M.Z. and Sakai, T. *Extent and Severity of Flood Embankments in Bangladesh*, Agricultural Engineering International, the CIGR Ejournal. Manuscript LW 08 004. Vol. X. UN (United Nation), 2007. *Cyclone Sidr United Nations Rapid Initial Assessment Report*, With a Focus on 9 Worst Affected Districts, 22 November.

M.Z. Hossain, M.T. Islam, T. Sakai and M. Ishida. *Impact of Tropical Cyclones on Rural Infrastructures in Bangladesh*, Agricultural Engineering International: the CIGR Ejournal. Invited Overview No. 2, Vol. X. April, 2008.

World Weather Research Programme (WWRP)
Report Series

Sixth WMO International Workshop on Tropical Cyclones (IWTC-VI), San Jose, Costa Rica, 21-30 November 2006 (WMO TD No. 1383**) (WWRP 2007 - 1).**

Third WMO International Verification Workshop Emphasizing Training Aspects, ECMWF, Reading, UK, 29 January - 2 February 2007) (WMO TD No. 1391) **(WWRP 2007 - 2).**

WMO International Training Workshop on Tropical Cyclone Disaster Reduction (Guangzhou, China, 26 - 31 March 2007) (WMO TD No. 1392) **(WWRP 2007 - 3)**.

Report of the WMO/CAS Working Group on Tropical Meteorology Research (Guangzhou, China, 22-24 March 2007) (WMO TD No. 1393) **(WWRP 2007 - 4).**

Report of the First Session of the Joint Scientific Committee (JSC) for the World Weather Research Programme (WWRP), (Geneva, Switzerland, 23-25 April 2007) (WMO TD No. 1412) **(WWRP 2007 – 5).**

Report of the CAS Working Group on Tropical Meteorology Research (Shenzhen, China, 12-16 December 2005) (WMO TD No. 1414) **(WWRP 2007 – 6).**

Preprints of Abstracts of Papers for the Fourth WMO International Workshop on Monsoons (IWM-IV) (Beijing, China, 20-25 October 2008) (WMO TD No. 1446) **(WWRP 2008 – 1).**

Proceedings of the Fourth WMO International Workshop on Monsoons (IWM-IV) (Beijing, China, 20-25 October 2008) (WMO TD No. 1447) **(WWRP 2008 – 2).**

WMO Training Workshop on Operational Monsoon Research and Forecast Issues – Lecture Notes, Beijing, China, 24-25 October 2008 (WMO TD No. 1453**) (WWRP 2008 – 3).**

Expert Meeting to Evaluate Skill of Tropical Cyclone Seasonal Forecasts (Boulder, Colorado, USA, 24-25 April 2008) (WMO TD No. 1455) **(WWRP 2008 – 4).**

Recommendations for the Verification and Intercomparison of QPFS and PQPFS from Operational NWP Models – Revision 2 - October 2008 (WMO TD No. 1485) **(WWRP 2009 - 1).**

Strategic Plan for the Implementation of WMO's World Weather Research Programme (WWRP): 2009-2017 (WMO TD No. 1505) **(WWRP 2009 – 2).**

4th WMO International Verification Methods Workshop, Helsinki, Finland, 8-10 June 2009 (WMO TD No. 1540) **(WWRP 2010-1)**